

# **PDE3A Signalling in Blood Platelets**

**Robert Law**

**PhD Medical Sciences**

**The University of Hull and the University of York**

**Hull York Medical School**

**April 2016**



## Abstract

Cyclic 3', 5' adenosine monophosphate (cAMP) signalling downstream of prostacyclin (PGI<sub>2</sub>) is a key inhibitory pathway in blood platelets. This pathway is dynamically regulated by phosphodiesterase 3A (PDE3A), which hydrolyses cAMP into metabolically inactive AMP. Although PDE3A is an established drug target in anti-platelet therapies, the molecular mechanisms that underlie its function in platelets remain unclear. Therefore, the major aim of this study was to further explore PDE3A signalling in human platelets. Using a combination of cell fractionation and immunoblotting we identified two PDE3A splice variants in platelets, PDE3A1 and PDE3A2, that were differentially localised within the cell. PDE3A1 was located in the membrane fraction, whereas PDE3A2 was primarily located in the cytosolic fraction. Treatment of platelets with PGI<sub>2</sub> induced a transient phosphorylation of PDE3A2 at Ser<sup>312</sup> in a PKA dependent manner. In contrast, no phosphorylation of PDE3A1 was detected. The phosphorylation of PDE3A2 was associated with increased PDE3A enzymatic activity, which suggested that cAMP signalling activated only the cytosolic form of the enzyme. In many cells, A-kinase anchoring proteins (AKAPs) orchestrate a coordinated response between PKA and its effector proteins. The phosphorylation and activation of PDE3A2 in response to PGI<sub>2</sub> was blunted by a cell permeable peptide inhibitor of PKA-AKAP interactions suggesting that PKA-mediated activation of PDE3A2 was dependent on an AKAP. Using a cAMP-pull down approach to enrich cAMP binding proteins combined with immunoblotting, we confirmed the presence of two AKAP7 isoforms (δ and γ) in platelets. Additionally, we found that AKAP7δ co-precipitated with PDE3A2 and possessed associated PDE3A activity. Furthermore, AKAP7 also possessed PKA activity, which was a result of its

constitutive association with PKA-II. Critically, immunoprecipitated PDE3A was found to be co-associated with both PKA-II and AKAP7 $\delta$ . The findings in this thesis suggest that blood platelets express multiple differentially-regulated PDE3A splice variants, of which PDE3A2 is regulated by PKA-II within a novel cytosolic AKAP7 $\delta$  facilitated signalling complex. The selective inhibition of PDE3A splice variants and/or pharmacological disruption of PDE3A signalosomes may provide safer and more specific ways of controlling pathological platelet activation.

## **Publications**

ABURIMA, A., WRAITH, K.S., RASLAN, Z., LAW, R., MAGWENZI, S. & NASEEM, K.M. 2014. cAMP signaling regulates platelet myosin light chain (MLC) phosphorylation and shape change through targeting the RhoA- Rho kinase-MLC phosphatase signaling pathway. *Blood*, 122, 487850.

LAW., R., RASLAN, Z., ABURIMA, A., KLUSMANN, E., TASKEN, K., NASEEM, K. 2016. Protein kinase A regulates platelet phosphodiesterase 3A through an A-kinase anchoring protein dependent manner. (*Manuscript in preparation*).

## **Oral presentations**

LAW. R. 2015. Protein kinase A regulates platelet phosphodiesterase 3A through an A-kinase anchoring protein dependent manner. 2015. *Hull York Medical School research conference, Hull, UK.*

## **Poster presentations**

LAW., R., RASLAN, Z., ABURIMA, A., KLUSMANN, E., TASKEN, K., NASEEM, K. 2015. Protein kinase A regulates platelet phosphodiesterase 3A through an A-kinase anchoring protein dependent manner. 2015. *16th UK Platelet Group Meeting, Leicester, UK.*

LAW., R., RASLAN, Z., ABURIMA, A., KLUSMANN, E., TASKEN, K., NASEEM, K. 2015. Protein kinase A regulates platelet phosphodiesterase 3A through an A-kinase anchoring protein dependent manner. *Gordon research conference, Cell Biology of Megakaryocytes & Platelets, Tuscany, Italy.*

## Table of contents

<b>Abstract</b> .....	<b>i</b>
<b>Publications</b> .....	<b>iii</b>
<b>Oral presentations</b> .....	<b>iii</b>
<b>Table of contents</b> .....	<b>iv</b>
<b>Table of figures</b> .....	<b>x</b>
<b>Table of tables</b> .....	<b>xiii</b>
<b>Author's declaration</b> .....	<b>xviii</b>
<b>Acknowledgements</b> .....	<b>xix</b>
<b>1 Introduction</b> .....	<b>1</b>
1.1 General introduction .....	1
1.2 Platelet formation .....	2
1.3 Platelet ultra-structure .....	2
1.3.1 Platelet membrane .....	3
1.3.2 Platelet cytoskeleton.....	4
1.3.3 Platelet organelles and granules .....	4
1.4 Haemostatic function of blood platelets.....	5
1.4.1 Platelet adhesion .....	5
1.4.2 Platelet activation .....	8
1.4.3 Amplification of the platelet haemostatic plug .....	13
1.4.4 Platelet aggregation.....	14
1.4.5 Thrombus consolidation .....	15
1.5 Platelet regulation.....	16
1.5.1 Cyclic AMP signalling .....	16
1.5.2 Cyclic GMP signalling.....	19

1.5.3	Protein kinase A and G protein targets.....	21
1.6	Platelet phosphodiesterases .....	27
1.6.1	PDE2A.....	27
1.6.2	PDE3A.....	29
1.6.3	PDE5 .....	32
1.6.4	PDE2A and PDE3A cross-talk.....	34
1.7	Co-ordination of cyclic nucleotide signalling.....	34
1.7.1	Compartmentalisation of cAMP and cGMP by PDEs .....	35
1.7.2	A and G-kinase anchoring proteins .....	37
1.8	Aims of the study.....	41
<b>2</b>	<b>Materials and methods.....</b>	<b>43</b>
2.1	Materials.....	43
2.1.1	Pharmacological agonists, inhibitors and peptides.....	43
2.2	Preparation of washed platelets from whole blood.....	44
2.3	Platelet counting.....	45
2.4	Measurement of Platelet aggregation .....	45
2.5	Methods for examination of intracellular protein function .....	48
2.5.1	Whole cell sample preparation .....	48
2.5.2	Sub-cellular fractionation of platelets.....	48
2.5.3	Quantification of sample protein concentration .....	49
2.5.4	Immunoprecipitation .....	50
2.5.5	Co-immunoprecipitation of associated proteins.....	51
2.5.6	Enrichment of cAMP binding proteins using cAMP linked agarose beads. ....	53
2.6	Sodium dodecyl sulphate-polyacrylamide gel electrophoresis.....	54

2.7	Immunoblotting .....	57
2.7.1	Stripping PVDF membranes and re-probing .....	60
2.8	cAMP immunoassay.....	62
2.9	Phosphodiesterase activity assay .....	63
2.10	Protein kinase A activity assay .....	66
2.11	Proximity ligation assay.....	66
2.12	MEG-01 cell culture .....	67
2.12.1	MEG-01 cell thawing.....	67
2.12.2	MEG-01 cell counting and assessment .....	68
2.12.3	MEG-01 cell maintenance and differentiation.....	68
2.13	MEG-01 FACS analysis .....	69
2.14	Statistical analysis .....	70
<b>3</b>	<b>Characterisation of platelet and megakaryocyte phosphodiesterases....</b>	<b>71</b>
3.1	Introduction.....	71
3.2	PGI <sub>2</sub> inhibits platelet activation .....	73
3.3	Platelet PDE isoform expression.....	75
3.3.1	Human platelets express PDE2A, PDE3A and PDE5.....	75
3.3.2	Platelet PDE isoforms are differentially localised within the cell.....	77
3.3.3	Characterisation of platelet PDE3A splice variants .....	79
3.4	Characterisation of platelet responses to PDE inhibition .....	81
3.5	The activity of PDEs in platelets.....	84
3.5.1	The activity of purified PDE1 .....	84
3.5.2	PDE activity assay optimisation for use in human platelets .....	86
3.5.3	Characterisation of PDE2A, PDE3A and PDE5 activity in platelets ....	88
3.6	PDE enzymes in the megakaryocytic cell line MEG-01 .....	90

3.6.1	MEG-01 cells express the megakaryocyte marker CD41.....	90
3.6.2	MEG-01 cells exhibit megakaryocyte morphology .....	92
3.6.3	MEG-01 signalling responses to PGI <sub>2</sub> and the nitric oxide donor GSNO.. .....	94
3.6.4	Characterisation of PDE isoform expression in MEG-01 cells .....	96
3.7	Discussion .....	98
<b>4</b>	<b>PKA-mediated regulation of PDE3A .....</b>	<b>104</b>
4.1	Introduction.....	104
4.2	PGI <sub>2</sub> elevates intracellular platelet cAMP concentrations.....	106
4.2.1	PGI <sub>2</sub> and forskolin elevate cAMP levels in a dose dependent manner..... .....	106
4.2.2	PGI <sub>2</sub> elevates cAMP in a time dependent manner.....	109
4.3	PGI <sub>2</sub> increases PKA substrate phosphorylation in platelets.....	111
4.4	Spatiotemporal dynamics of PKA substrate phosphorylation in platelets	114
4.5	PDE3A inhibition enhances the cAMP/PKA signalling response to PGI <sub>2</sub>	117
4.5.1	PDE3A inhibition increase cAMP levels in PGI <sub>2</sub> stimulated platelets	117
4.5.2	PDE3A inhibition potentiates PKA activity in PGI <sub>2</sub> stimulated platelets..... .....	119
4.6	Optimisation of anti-phospho PDE3A Ser <sup>312</sup> antibody.....	121
4.7	Analysis of alternative serine phosphorylation sites on PDE3A.....	123
4.8	Characterisation of PDE3A phosphorylation and activity in response to PGI <sub>2</sub> ..... .....	125
4.8.1	PDE3A phosphorylation and activity in response to PGI <sub>2</sub> .....	125
4.8.2	Temporal profile of PDE3A phosphorylation and activity in response to PGI <sub>2</sub> ..... .....	127

4.9	Characterisation of PDE3A phosphorylation and activity in response to PKA activating agents .....	129
4.10	PDE3A phosphorylation correlates with PDE3A hydrolytic activity .....	131
4.11	PDE3A splice variant PDE3A2 is phosphorylated by PKA at Ser <sup>312</sup> .....	133
4.12	Discussion .....	135
<b>5</b>	<b>Investigating PDE3A signalosomes .....</b>	<b>144</b>
5.1	Introduction.....	144
5.2	AKAP disruption blunts PDE3A phosphorylation and activity .....	146
5.3	Characterising the effect of AKAP disruption on platelet cAMP responses.....	149
5.4	PKA type II is associated with PDE3A .....	151
5.5	Human platelets express AKAP7 .....	153
5.5.1	Immunoblotting AKAP7 in human and mouse platelets .....	153
5.5.2	Enrichment of cAMP binding proteins in human platelets .....	155
5.5.3	cAMP pull - down of PKA type II and AKAP7 .....	157
5.5.4	Immunoprecipitation of AKAP7 from platelets .....	159
5.6	AKAP7 harbours co-associated PKA activity .....	161
5.7	AKAP7 is associated with PKA type II in platelets .....	163
5.8	Characterising the platelet PDE3A signalosome.....	165
5.8.1	Co-immunoprecipitation of PDE3A signalling partners.....	165
5.8.2	Reverse co-immunoprecipitation of PDE3A signalling partners .....	167
5.8.3	PKA type II and AKAP7 associated PDE3A activity .....	169
5.8.4	Subcellular localisation of the PDE3A signalosome .....	171
5.9	PDE3A specifically regulates multiple platelet PKA substrates.....	173
5.10	Discussion .....	175

<b>6 Discussion .....</b>	<b>183</b>
6.1 Future direction .....	189
<b>References.....</b>	<b>191</b>

## Table of figures

### 1 Introduction

1.1 Morphology of resting and activated platelets .....	3
1.2 Mechanisms of platelet adhesion .....	8
1.3 Platelet effectors and receptors .....	12
1.4 cAMP-mediated activation of PKA.....	19
1.5 Structure of human PDE2A.....	29
1.6 PDE3A splice variants.....	30
1.7 Regulation of cyclic nucleotide signalling pathways in human platelets.....	33
1.8 Compartmentalisation of cAMP in cardiac myocytes by PDEs.....	36
1.9 AKAP signalling .....	39

### 2 Methods

2.1 Turbidimetric platelet aggregation.....	47
2.2 Co-immunoprecipitation procedure .....	53
2.3 Analysis of proteins using SDS-PAGE and immunoblotting.....	59
2.4 cAMP immunoassay procedure .....	63
2.5 PDE activity assay procedure.....	65

### 3 Characterisation of platelet and megakaryocyte phosphodiesterases

3.1 Washed platelet aggregation response to PGI <sub>2</sub> .....	74
3.2 Analysis of phosphodiesterase isoform expression in human platelets .....	76
3.3 Subcellular PDE expression in human platelets.....	78
3.4 PDE3A splice variants .....	80
3.5 Characterisation of PDE inhibitory effects on platelet aggregation .....	83
3.6 PDE1 dose response and time course of cAMP Hydrolysis.....	85
3.7 Optimisation of PDE activity assay to measure platelet PDE3A activity .....	87

3.8	Quantification of platelet PDE isoform activity .....	89
3.9	CD41 expression in MEG-01 cells .....	91
3.10	Brightfield microscopy of MEG-01 cell morphology and culture flask adhesion.....	93
3.11	PKA signalling in MEG-01 cells .....	95
3.12	MEG-01 expression of PDE isoforms and cyclic nucleotide signalling proteins.....	97
<b>4</b>	<b>PKA-mediated regulation of PDE3A</b>	
4.1	cAMP and dose response to PGI <sub>2</sub> and forskolin stimulation.....	108
4.2	cAMP time profile to PGI <sub>2</sub> stimulation.....	110
4.3	PKA substrate phosphorylation in response to PGI <sub>2</sub> .....	113
4.4	Spatiotemporal profile PKA substrate phosphorylation in platelet fractions .....	116
4.5	cAMP signalling responses to PGI <sub>2</sub> and PDE3A inhibition .....	118
4.6	PKA substrate phosphorylation in response to PDE3A inhibition .....	120
4.7	Anti-phospho PDE3A Ser <sup>312</sup> antibody optimisation.....	122
4.8	Immunoblot analysis of PDE3A phosphorylation .....	124
4.9	PDE3A phosphorylation and activity in response to PGI <sub>2</sub> concentration range.....	126
4.10	PDE3A phosphorylation and activity time profile in response to PGI <sub>2</sub> ....	128
4.11	PDE3A phosphorylation and activity in response to PKA activating agents .....	130
4.12	PDE3A phosphorylation and activity in response to calf intestinal phosphatase incubation .....	132

4.13 PDE3A splice variant analysis for Ser <sup>312</sup> phosphorylation in response to PGI <sub>2</sub> .....	134
---	-----

## **5 Investigating PDE3A signalosomes**

5.1 Effect of AKAP disruption on PDE3A2 phosphorylation and total PDE3A activity .....	148
5.2 Effect of AKAP disruption on platelet cAMP levels .....	150
5.3 Analysis of PKA association with PDE3A in platelets .....	152
5.4 Immunoblotting AKAP7 expression in human and mouse platelets .....	154
5.5 cAMP pull down of human platelet proteins .....	156
5.6 cAMP pull down of AKAP7.....	158
5.7 AKAP7 immunoprecipitation .....	160
5.8 Analysis of associated PKA activity in AKAP7 Immunoprecipitates.....	162
5.9 Proximity ligation analysis of AKAP7 and PKA type II association.....	164
5.10 Co-immunoprecipitation of PKA RII, PKAc and AKAP7 with PDE3A.....	166
5.11 Co-immunoprecipitation of PKA RII, PKAc and AKAP7 with PDE3A .....	168
5.12 Analysing co-associated PDE3A activity in PKA RII and AKAP7 immunoprecipitates.....	170
5.13 Subcellular localisation of PDE3A2 Ser <sup>312</sup> phosphorylation and signalosome proteins.....	172
5.14 Immunoblotting PDE3A co-associated PKA substrates in platelet fractions.....	174

## **6 Discussion**

6.1 Revised model of PDE3A signalling in platelets as proposed by data in this study.....	190
---	-----

## **Table of tables**

### **1 Introduction**

1.1 PKA and PKG platelet substrates .....	26
1.2 AKAP expression in human platelets .....	40

### **2 Methods**

2.1 Reagents required for Buffer 1 and 2 .....	56
2.2 Reagents required for two 18-10% polyacrylamide gradient gels .....	56
2.3 Reagents required for two 10% polyacrylamide gels .....	56
2.4 Reagent required for two resolving gels.....	56
2.5 Antibodies used in experimentation.....	61

## Abbreviations

ABP	Actin-binding protein
AC	Adenylyl cyclase
ACD	Acid-citrate dextrose
ADP	Adenosine diphosphate
AKAP	A-kinase anchoring protein
ATP	Adenosine triphosphate
BSA	Bovine serum albumin
CRP	Collagen related peptide
cAMP	Cyclic adenosine monophosphate
cGMP	Cyclic guanosine monophosphate
COX	Cyclooxygenase
DAG	Diacylglycerol
DNA	Deoxyribonucleic acid
DTS	Dense tubular system
DTT	Dithiothreitol
ECL	Enhanced chemiluminescence
EDTA	Ethylenediaminetetraacetic acid
EGTA	Ethyleneglycoltetraacetic acid
EHNA	Erythro-9-(2-hydroxy-2-nonyl)adenine
EIA	Enzyme immunoassay
eNOS	Endothelial nitric oxide synthase
FACS	Fluorescence-activated cell sorter
FBS	Fetal bovine serum
GAP	GTPase activating protein

GDP	Guanosine diphosphate
GP	Glycoprotein
GPCR	G protein-coupled receptor
GKAP	G-kinase anchoring protein
GSNO	S-nitrosoglutathione
GTP	Guanosine triphosphate
HEPES	N-(2-Hydroxyethyl) piperazine-N'-(2ethanesulfonic acid)
HRP	Horseradish peroxidase
HSP	Heat shock protein
HT31	AKAP St-Ht31 Inhibitor Peptide
IBMX	1-Methyl-3-isobutylxanthine
IgG	Immunoglobulin G
iNOS	Inducible nitric oxide synthase
IP <sub>3</sub>	Inositol triphosphate
IRAG	IP <sub>3</sub> receptor-associated cGKI substrate protein
ITAM	Immunoreceptor tyrosine-based activation motif
LASP	LIM and SH3 domain protein
MAPK	P38 mitogen activated protein kinase
MEG	Megakaryocyte
MLC	Myosin light chain
MLCK	Myosin light chain kinase
MLCP	Myosin light chain phosphatase
NO	Nitric oxide
OCS	Open canicular system
PAGE	Polyacrylamide gel electrophoresis

PAR	Protease-activated receptor
PDE	Phosphodiesterase
PG	Prostaglandin
PGI <sub>2</sub>	Prostacyclin
PKA	Protein kinase A
PKB	Protein kinase B
PKC	Protein kinase C
PKG	Protein kinase G
PLA <sub>2</sub>	Phospholipase A <sub>2</sub>
PLC	Phospholipase C
PMA	Phorbol 12-myristate 13-acetate
PPP	Platelet poor plasma
PRP	Platelet rich plasma
PVDF	Polyvinylidene fluoride
RIAD	RI anchoring disruptor peptide
ROCK	RhoA/Rho-associated kinase
SDS	Sodium dodecyl sulphate
SOCE	Orai1 store operated Ca <sup>2+</sup> entry
sCG	Soluble guanylyl cyclase
TEMED	N,N,N',N'-tetramethylethylenediamine
TP	Thromboxane A <sub>2</sub> receptor
TPO	Thrombopoietin
TRPC	Transient receptor potential canonical
TBS	Tris-buffered saline
TXA <sub>2</sub>	Thromboxane A <sub>2</sub>

VASP	Vasodilator-stimulated phosphoprotein
VEGF	Vascular endothelial growth factor
vWF	von Willebrand factor
WHO	World Health Organisation
WPs	Washed platelets

## **Author's declaration**

I confirm that this work is original and that if any passage(s) or diagram(s) have been copied from academic papers, books, the internet or any other sources these are clearly identified by the use of quotation marks and the reference(s) is fully cited. I certify that, other than where indicated, this is my own work and does not breach the regulations of HYMS, the University of Hull or the University of York regarding plagiarism or academic conduct in examinations. I have read the HYMS Code of Practice on Academic Misconduct, and state that this piece of work is my own and does not contain any unacknowledged work from any other sources.

## **Acknowledgements**

First and foremost, I would like to thank Prof. Khalid Naseem for the opportunity to work on this PhD. I have benefited greatly from his excellent guidance and supervision throughout my time at the HYMS, for which I will always be thankful. I would like to thank my TAP panel members, Dr. Roger Sturmey and Dr. Simon Hart for their advice and input throughout this project. I would also like to take this opportunity to thank all the support staff at HYMS, in particularly Helen Proctor and Dr. Sian Leech-Mills, who work hard every day to make our research possible. This project would also not of been possible without our blood donors who selflessly donate to our research group come rain or shine. I would like to say thank you to all my colleagues, Dr. Ahmed Aburima, Dr. Zaher Raslan, Dr. Simba Magwenzie, Dr. Katie Wraith, Dr. Benjamin Spurgeon, Dr. Sreemoti Banerjee, Dr. Martin Berger, Dr. Jennifer Rossington, Casey Woodward, Arti Trivedi, Kochar Walladbegi, Miriayi Abibula, Constantine Simintiras, Pooja Joshi and Robert Atkinson for their endless support, friendship and scientific input. I would also like to say a special thank you to Dr. Simon Calaminus and Muhammed Yusuf for their help and expertise concerning my work with megakaryocytes. I would like to thank my bachelor project supervisor Dr. Alistair Corbett for his advice and excellent teaching, which first inspired me to pursue a PhD. I would also like to thank Rosita, Karim and Andrea, who have selflessly supported me throughout the final stages of my PhD. Lastly, I would like to thank my family. To Jane, Brian and Amanda, I could never ask for a more encouraging, wonderful and loving family.

# 1 Introduction

## 1.1 General introduction

Haemostasis is an essential physiological process that prevents blood loss, maintains the fluidity of blood and removes haemostatic plugs following vascular repair. This process requires intricate interplay between vascular endothelium, platelets and the coagulation cascade (Versteeg et al., 2013). In healthy blood vessels a single layer of endothelial cells, termed the endothelium, lines the vessel wall. This layer serves first as an anti-thrombogenic surface and second as a physical barrier to separate blood from thrombogenic factors, which lie beneath its surface. Platelets circulate in close proximity to the endothelium, attributed to the forces of laminar blood flow. Here they are maintained in a quiescent state by the actions of endothelium-derived prostacyclin ( $\text{PGI}_2$ ) and nitric oxide (NO) (Schwarz et al., 2001). Exposure of the subendothelium through vessel trauma initiates immediate platelet adhesion, activation and aggregation to form a haemostatic plug in concert with the coagulation cascade. Thrombus size is tightly regulated by neighbouring endothelial cells that secrete anti-thrombogenic  $\text{PGI}_2$  and NO into the local environment (Clemetson, 2012). However, pathological conditions that comprise endothelial function and platelet sensitivity to endogenous inhibition can lead to uncontrolled thrombus development and growth (Gps and Ruggeri, 2002). The occlusion of blood flow under this circumstance can result in serious cardiovascular events such as a stroke or myocardial infarction. Therefore, improving our understanding of the mechanisms that underlie endothelial inhibition of platelet activation may lead to the identification of novel therapeutic targets for the treatment of pathological thrombosis. This chapter will review blood platelet

function, with a particular focus on the regulation of endogenous platelet inhibition by phosphodiesterase (PDE) enzymes.

### 1.2 Platelet formation

Platelets are small anucleate discoid cells that circulate in the blood alongside erythrocytes and lymphocytes. These cells function primarily as regulators of haemostasis, but also play secondary roles in innate immunity and angiogenesis (Kisucka et al., 2006; Von Hundelshausen and Weber, 2007). Platelets derive from long cytoplasm extensions of highly specialised megakaryocyte cells that reside primarily in the bone marrow (Pease, 1956). Platelet production is predominantly driven by thrombopoietin (TPO) that signals through the cMpl receptor present on the megakaryocyte surface (Kaushansky, 2006). This process constantly renews the entire platelet population, measured at roughly one trillion platelets in adults, every 8-10 days (Harker and Finch, 1969).

### 1.3 Platelet ultra-structure

Quiescent platelets are 2.0 to 5.0 $\mu\text{m}$  in diameter and 0.5 $\mu\text{m}$  in thickness with a mean volume of 6-10 femtolitres (Hartwig and Italiano, 2003). Platelets contain a number of distinguishable features including the open canicular system (OCS), the dense tubular system (DTS), an actin-based cytoskeleton, a peripheral band of microtubules and numerous organelles including alpha and dense granules (Thon and Italiano, 2012). Upon activation, platelets undergo a series of morphological changes that involve the extension of membrane projections termed filopodia and lamellipodia, which aid adhesion and aggregation at the site of vascular damage (Hartwig, 1992) (Figure 1.1).

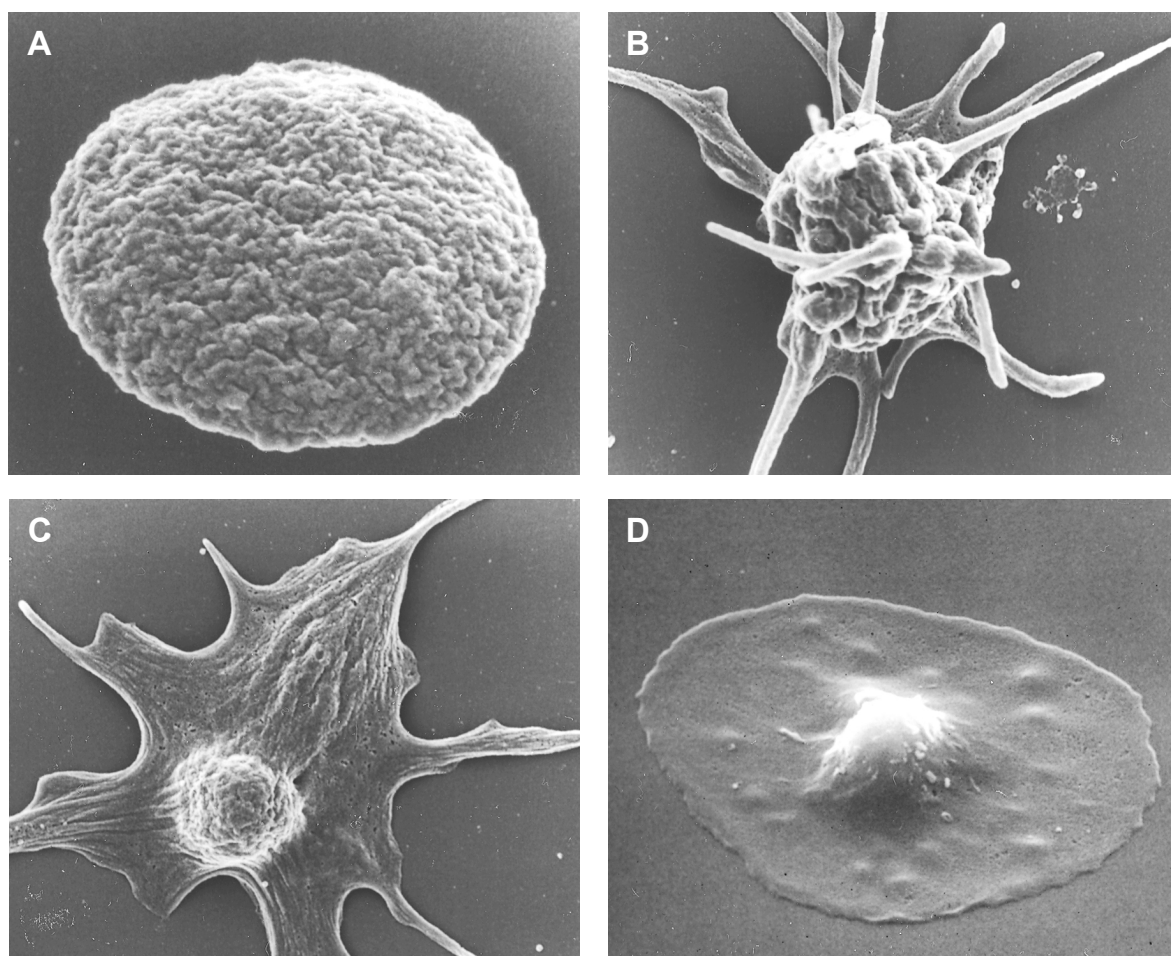


**Figure 1.1 Morphology of resting and activated platelets.** Electron microscopy images of platelet morphology. (A) The discoid shape of a resting platelet with wrinkled surfaces representing membrane invaginations. (B) Early stages of platelet activation with extended filopodia projections. (C) Joining of filopodia extensions with lamellipodia to form a (D) fully spread platelet (White, 2007).

### 1.3.1 Platelet membrane

The platelet membrane is composed of phospholipid bilayer embedded with cholesterol, glycolipids and glycoproteins. The membrane itself is covered with tiny folds and small openings to the surface-connected OCS. The OCS is a semi-selective channel system that runs throughout the platelet, allowing the passage of small molecules (Escobar and White, 1991). The plasma membrane also contains

cholesterol-rich lipid rafts that play important roles in signalling and intracellular trafficking (Bodin et al., 2003).

### **1.3.2 Platelet cytoskeleton**

The discoid shape of the platelet is maintained by an internal circumferential coil of microtubules. In addition to the coil is a supportive cytoskeleton composed of actin filaments and associated proteins. This cytoskeletal system can reorganise upon platelet activation, drastically changing the shape of the platelet (Escobar et al., 1986) (Figure 1.1).

### **1.3.3 Platelet organelles and granules**

Platelets contain relatively few organelles, namely lysosomes that sequester degradative enzymes, energy storing glycosomes and mitochondria required for energy metabolism (White, 2007). Located in the platelet cytoplasm is the DTS, constructed from residual sections of endoplasmic reticulum to form a closed-channel network that functions as an intracellular calcium store, positioned in close proximity to the OCS (Van Nispen Tot Pannerden et al., 2010). Calcium release from the DTS is an essential requirement for platelet activation (Varga-Szabo et al., 2009). Specific to the platelet, are internally packaged granules that are released at the site of vascular injury. Alpha granules are most abundant, 50-80 per platelet, and contain a plethora of adhesive proteins including vWF, stored in its potent form, and fibrinogen (Blair and Flaumenhaft, 2009). Dense granules, named after their electron dense matrix, are fewer in number and contain different prothrombotic factors namely the potent platelet agonist ADP and ATP (McNicol and Israels, 1999). Platelet degranulation plays an essential role in the

haemostatic response to vascular damage by recruiting platelets from the circulation to the nascent haemostatic plug and activating platelets.

### 1.4 Haemostatic function of blood platelets

The primary function of platelets is to arrest blood loss in the event of haemorrhage. This protective role can be divided into four phases: platelet adhesion, activation, amplification and aggregation.

#### 1.4.1 Platelet adhesion

In healthy blood vessels, platelets circulate quiescently in close proximity to the endothelium. Vascular damage exposes the subendothelial matrix, which contains several platelet adhesive macromolecules, including collagen, laminin and fibronectin. Stable adhesion of platelets to the subendothelial matrix is a coordinated process involving tethering, rolling, activation and secure adhesion. Initial platelet tethering is dependent on local rheological shear conditions. Under low shear ( $<1000\text{s}^{-1}$ ), typically within veins and large arteries, platelets adhere to the subendothelial matrix through the interaction between exposed collagen and the platelet receptors glycoprotein VI (GPVI) and integrin  $\alpha_2\beta_1$ . However in small arteries and the microvasculature, which are subject to high shear rates ( $>1000\text{s}^{-1}$ ), platelet adhesion to collagen is indirect and dependent on the interaction between immobilized vWF and glycoprotein Iba (GPIb) (Ruggeri and Mendolicchio, 2007).

### **1.4.1.1 Direct collagen binding**

Subendothelial fibrillar collagen is a highly thrombogenic surface that supports platelet adhesion through both indirect and direct mechanisms. Platelets express several direct collagen receptors, most notably GPVI and integrin  $\alpha_2\beta_1$ , in addition to GPIb and integrin  $\alpha_{IIb}\beta_3$  that interact with collagen indirectly via vWF (Varga-Szabo et al., 2008).

GPVI is the major collagen receptor expressed on the platelet surface (Kehrel et al., 1998). This platelet exclusive type I transmembrane receptor associates with the Fc receptor-gamma (FcR gamma) chain, which possesses an immunoreceptor tyrosine-based activation motif (ITAM). Collagen binding to the GPVI receptor results in tyrosine phosphorylation of the ITAM, triggering platelet activating tyrosine kinase signalling cascades (Moroi and Jung, 2004). However, GPVI on its own is unable to support stable platelet adhesion due to its low affinity for collagen and functions primarily as an activatory receptor (Nieswandt et al., 2001). It is thought that GPVI works in concert with integrin receptors to provide the platelet with adhesive capacity. Of particular relevance is integrin  $\alpha_2\beta_1$ , which also acts as a collagen receptor. Like other integrins, platelet activation by GPVI increases the affinity of integrin  $\alpha_2\beta_1$  for collagen, termed inside-out signalling, leading to stable adhesion and spreading (Jung and Moroi, 2000). These complementary roles of GPVI and integrin  $\alpha_2\beta_1$  simultaneously strengthen platelet adhesion to the subendothelial matrix and stimulate platelet activatory signalling cascades.

### **1.4.1.2 Indirect collagen binding**

The central mediator of platelet adhesion under high shear conditions is the multimeric glycoprotein vWF, which is found in endothelial Weibel Palade bodies, platelet alpha granules and blood plasma. vWF contains both binding sites for collagen and the platelet receptors GPIb and integrin  $\alpha_{IIb}\beta_3$  (Ruggeri, 2003). Exposure of collagen results in immediate binding of vWF via its collagen binding A1 and A3 domains (Hoylaerts et al., 1997; Lankhof et al., 1996). In this state, VWF recruits platelets from the circulation through the binding of GPIb and integrin  $\alpha_{IIb}\beta_3$ . However in healthy vessels, vWF does not normally interact with platelets due to the cryptic nature of the platelet binding sites that are only unveiled when vWF is immobilised (Ulrichs et al., 2006). GPIb exists as part of GPIb-V-IX signalling complex that stimulates granule release and integrin receptor activation through tyrosine kinase signalling pathways when bound to immobilised vWF (Clemetson, 2012). The precise mechanisms by which GPIb initiates tyrosine kinase signalling remain undefined, but there is good evidence that it is similar to GPVI (Gibbins, 2004).

The final phase in platelet adhesion is the activation and binding of several integrin receptors, the most abundant of which is integrin  $\alpha_{IIb}\beta_3$ . Although in its activated form integrin  $\alpha_{IIb}\beta_3$  mediates adhesion of platelets to immobilised vWF, it is also considered the most important receptor in platelet aggregation (Ma et al., 2007). Due to the fast on and off rate of GPIb and integrin  $\alpha_{IIb}\beta_3$  binding to vWF, stable adhesion of the growing thrombus requires both direct and indirect platelet binding to collagen (Moroi et al., 1996). Outside-in signalling induced by ligation of integrin  $\alpha_{IIb}\beta_3$  is thought to be a driving force behind stable platelet adhesion and platelet spreading (Li et al., 2010).

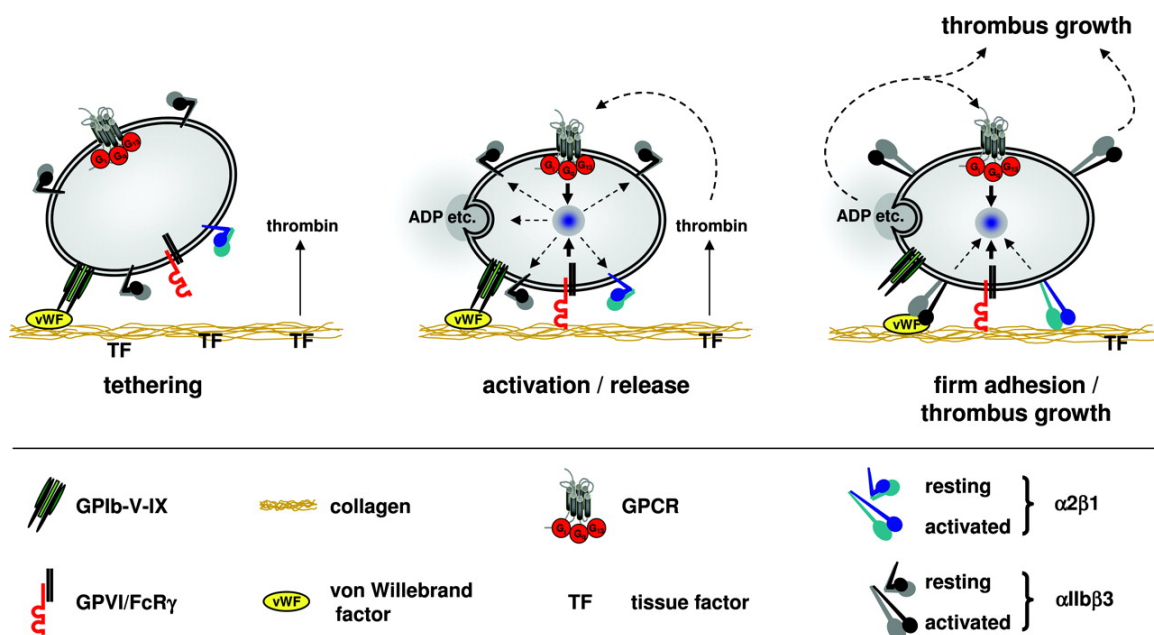


**Figure 1.2. Mechanisms of platelet adhesion.** Initially tethering of platelets to the subendothelium is mediated by actions of GPIb with collagen-immobilised vWF. Integrin  $\alpha_2\beta_1$  and GPVI bind directly to collagen and activate Integrin  $\alpha_{IIb}\beta_3$  and granule release for firm adhesion. At the same time, tissue factor is released from the subendothelium that triggers the formation of thrombin via the coagulation cascade. Thrombin not only amplifies the mechanisms of platelet activation but converts integrin  $\alpha_{IIb}\beta_3$  bound fibrinogen into supporting fibrin strands that strengthen the newly formed haemostatic plug (Sachs and Nieswandt, 2007).

#### 1.4.2 Platelet activation

Platelet activation in response to thrombotic stimuli is a coordinated process involving several signalling cascades, including tyrosine kinase signalling, G-protein coupled receptor (GPCR) signalling and inside-out activation of integrin receptors (Broos et al., 2011).

### **1.4.2.1 Tyrosine kinase signalling**

GPVI is thought to initiate tyrosine kinase signalling through the binding of collagen and subsequent tyrosine phosphorylation of the associated FcR $\gamma$ -chain. In its phosphorylated form, FcR $\gamma$ -chain recruits the tyrosine kinase Syk, which in turn activates phospholipase C $\gamma$ 2 (PLC $\gamma$ 2). PLC $\gamma$ 2 functions to hydrolyse phosphatidylinositol 4,5 bisphosphate into inositol 1,4,5 trisphosphate (IP $_3$ ) and diacylglycerol (DAG) (Watson et al., 2005). When formed, IP $_3$  releases Ca $^{2+}$  from the DTS intracellular calcium store through binding to the IP $_3$  receptor calcium channel. Elevations in platelet Ca $^{2+}$  levels triggers several mechanisms of platelet activation including reorganisation of the actin cytoskeleton necessary for shape change, granule release and integrin receptor activation (Varga-Szabo et al., 2009). In addition to the actions of IP $_3$ , membrane-bound DAG functions together with Ca $^{2+}$  to activate protein kinase C (PKC), a major positive regulator of platelet activation (Harper and Poole, 2010).

### **1.4.2.2 G-protein coupled receptor signalling**

There are a number of G-protein coupled receptors expressed on the platelet surface that operate both activatory and inhibitory signalling cascades. These receptors transduce the effects of soluble agonists released or generated after initial platelet activation and include, adenosine diphosphate (ADP), thrombin and thromboxane A $_2$  (TXA $_2$ ). ADP, released from platelet dense granules, signals through two GPCRs: P2Y $_1$  and P2Y $_{12}$ . P2Y $_1$  is a G $\alpha_q$  coupled GPCR that activates platelets through calcium mobilisation from the DTS (Jin et al., 1998). The P2Y $_{12}$  receptor is coupled to the inhibition of adenylyl cyclase through G $\alpha_i$  (Ohlmann et al., 1995). In its activated state, adenylyl cyclase synthesises the secondary

messenger cyclic adenosine monophosphate (cAMP) from adenosine triphosphate (ATP); cAMP-stimulated signalling cascades are a powerful mechanism of platelet inhibition (Raslan and Naseem, 2014). Therefore, P2Y<sub>12</sub> ligation of ADP reduces the stimuli threshold required for platelet activation and aggregation. The co-activation of both P2Y<sub>1</sub> and P2Y<sub>12</sub> is required for ADP-induced platelet activation and aggregation, elegantly demonstrated in platelet function studies Hechler and colleagues using P2Y<sub>1</sub> and P2Y<sub>12</sub> selective inhibitors (Hechler et al., 1998).

Similar to ADP, TXA<sub>2</sub> functions as a positive feedback regulator of platelet activation. TXA<sub>2</sub> production is initiated by elevations in Ca<sup>2+</sup> levels, which result in the phosphorylation and subsequent activation of phospholipase A<sub>2</sub> (PLA<sub>2</sub>) by P38 mitogen activated protein kinase (MAPK). Activated PLA<sub>2</sub> cleaves arachidonic acid from phospholipids, which is then transformed by COX-1 into the thromboxane synthase substrate PGH<sub>2</sub>. Following TXA<sub>2</sub> production from PGH<sub>2</sub> by thromboxane synthase, TXA<sub>2</sub> is released into the haemostatic environment where upon it binds to its receptor (Samuelsson et al., 1978). The TXA<sub>2</sub> receptor (TP) is a Gα<sub>q</sub> and Gα<sub>12</sub>/Gα<sub>13</sub> coupled receptor that activates platelets through calcium release from the DTS (Thomas et al., 1998). However, the actions of TXA<sub>2</sub> are locally restricted due to its short half-life (FitzGerald et al., 1983).

Thrombin, the main effector of the coagulation cascade, is formed when circulating coagulation factors contact tissue factor exposed from vascular damage (Coughlin, 2000) and then subsequently on the platelet surface. The main function of thrombin is to convert circulating fibrinogen into fibrin monomers that polymerise to form fibrin; the structural mesh of thrombi. However in addition to this function, thrombin also serves as a potent platelet agonist through ligation of protease-activated receptors (PAR), which are coupled to Gα<sub>q</sub>, Gα<sub>12</sub>/Gα<sub>13</sub> and Gα<sub>i</sub>

(Offermanns, 2006). Of the four PAR receptors, human platelets express PAR1 and PAR4. Ligation of these receptors by thrombin forms a distinct mechanism that involves the cleavage of the PAR receptor N-terminus to form a new N-terminus, which by refolding acts as a ligand to the receptor (Vu et al., 1991). Ligation and activation of PAR receptors stimulates platelet shape, change granule release and integrin activation. Studies have shown that activation of either PAR receptor by thrombin is sufficient to activate platelets (Kahn et al., 1999). In conjunction, the effects of ADP, TXA<sub>2</sub> and thrombin on their GPCRs are to activate and recruit platelets to the site of injury.

#### **1.4.2.3 Activation of integrin $\alpha_{IIb}\beta_3$**

The final stage in platelet activation is the aggregation of adjacent platelets through activation and crosslinking of integrin  $\alpha_{IIb}\beta_3$  by fibrinogen (Kulkarni et al., 2000). Under resting conditions, integrin  $\alpha_{IIb}\beta_3$  is maintained in an inactive conformation, functioning as a low-affinity receptor vWF and fibrinogen (Savage and Ruggeri, 1991). Both inside-out and outside-in signaling cascades can increase the affinity of integrin  $\alpha_{IIb}\beta_3$  for these ligands. GPVI and GPIb are important initiators of integrin  $\alpha_{IIb}\beta_3$  activation through inside-out signalling. As previously discussed, ligation of collagen to these receptors triggers PLC $\gamma$ 2 to hydrolyze PIP<sub>2</sub> into IP<sub>3</sub> and DAG. IP<sub>3</sub> releases Ca<sup>2+</sup> from the DTS intracellular calcium store whilst membrane-bound DAG functions together with Ca<sup>2+</sup> to activate protein kinase C (PKC) (Harper and Poole, 2010). Both of these mediators, Ca<sup>2+</sup> and activated PKC, increase the affinity of integrin  $\alpha_{IIb}\beta_3$  for vWF and fibrinogen (Ma et al., 2007). In contrast, outside-in signaling results from fibrinogen binding to integrin  $\alpha_{IIb}\beta_3$ , which promotes receptor clustering and a

ligand induced conformational change to the receptors cytoplasmic tail. This event results in the activation of Syk, which in turn activates PLC $\gamma$ 2 leading to subsequent platelet activation (Li et al., 2010). In its activated state, integrin  $\alpha_{IIb}\beta_3$  forms molecular bridges between platelets through fibrinogen binding. These bridges play an essential role in haemostatic plug formation by facilitating platelet interaction, aggregation and providing thrombus support.

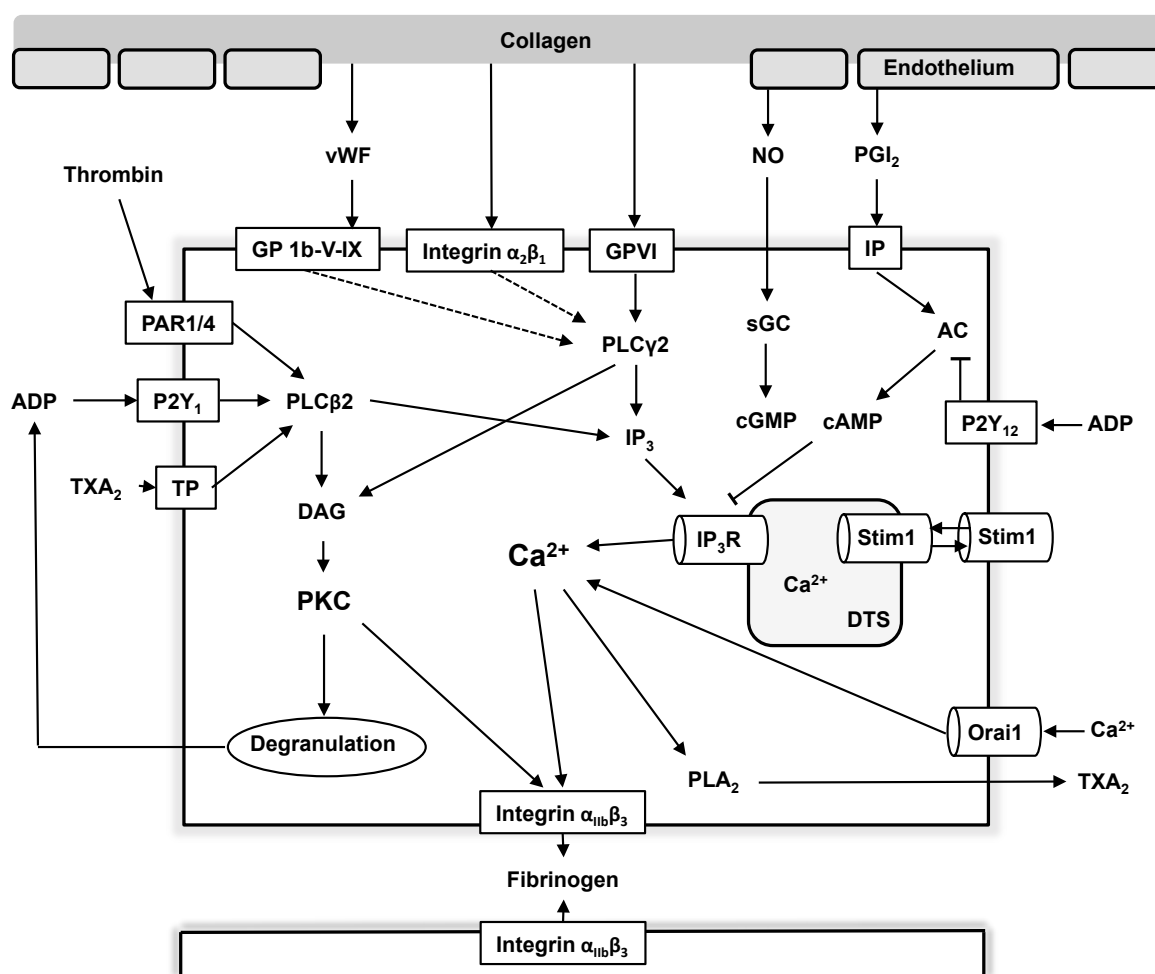


**Figure 1.3. Platelet effectors and receptors.** Schematic representation of platelet agonists, receptors and intracellular signalling cascades that mediate platelet activation. Figure adapted from (Broos et al., 2011).

### 1.4.3 Amplification of the platelet haemostatic plug

The adhesion and activation of platelets triggers the release of platelet alpha and dense granular contents into the local environment, which not only activate and recruit platelets from the circulation but promote platelet activation in an autocrine manner (Broos et al., 2011). This process can drastically advance thrombus formation and, therefore, is highly regulated by pro and anti-thrombotic stimuli. As previously described, the most abundant granule in platelets is the alpha granule, which contains a heterogeneous content of bio-active molecules (Blair and Flaumenhaft, 2009). Among these molecules is vWF, stored in its more potent form, and fibrinogen (Gralnick et al., 1985). Once released into the extracellular environment, these agents activate platelets through outside-in signalling cascades and promote platelet aggregation via cross-linkage of integrin  $\alpha_{IIb}\beta_3$  and GPIb (Canobbio et al., 2004; Shattil and Newman, 2004). In addition to adhesive molecules, alpha granules contain several coagulation factors to promote secondary haemostasis and the formation of clot stabilising fibrin. Alpha granules also function as reserves for adhesion receptors, namely GPVI, GPIb and integrin  $\alpha_{IIb}\beta_3$  (Berger et al., 1996). These receptors are transferred to the platelet surface when the granule membranes fuse with the plasma membrane or OCS for content release (Flaumenhaft, 2003).

Dense granules are less in number but equally important in amplifying platelet activation through release of the potent platelet agonist ADP and adenosine triphosphate (ATP) (Nurden and Nurden, 2008). As previously discussed, ADP activates platelets through the ligation of the P2Y<sub>1</sub> GPCR that initiates calcium mobilisation from the DTS and ligation of P2Y<sub>12</sub> GPCR, which plays an important role as a co-stimulatory receptor by impeding inhibitory adenylyl cyclase/cAMP-

dependant signalling cascades, thereby reducing the threshold for platelet activation. ATP, on the other hand, binds to the ligand-gated cation channel P<sub>2</sub>X<sub>1</sub> that results in an influx of calcium into the platelet, in turn stimulating further granule release and cytoskeletal rearrangement (Oury et al., 2006). However the influx of calcium is not sustained due to rapid desensitisation of the P<sub>2</sub>X<sub>1</sub> receptor (Rolf et al., 2001).

#### **1.4.4 Platelet aggregation**

Platelet aggregation is the binding together of platelets to form a fibrinogen-rich thrombus at the site of vascular injury. This complex and dynamic process involves the interplay between several platelet ligands, notably fibrinogen and vWF, and receptors such as GPIb and integrin  $\alpha_{IIb}\beta_3$  (Broos et al., 2011). Like platelet adhesion, the mechanisms of platelet aggregation are dependent on local rheological shear conditions. Recently reviews have categorised platelet aggregation into three distinct mechanisms (Jackson, 2007). Under low shear rates  $<1000s^{-1}$ , typically found within large arteries and veins, platelet aggregation is predominantly mediated by integrin  $\alpha_{IIb}\beta_3$  and fibrinogen. Direct platelet-to-platelet interactions are supported by integrin  $\alpha_{IIb}\beta_3$  molecular bridges that are formed through fibrinogen binding. Although this mechanism has been shown to function independently of vWF binding by GPIb *in vitro* (Savage et al., 1998), *in vivo* mouse studies have shown vWF is a requirement for platelet aggregation under low shear, possibly by binding integrin  $\alpha_{IIb}\beta_3$  (Bergmeier et al., 2008). At higher shear rates between  $1000s^{-1}$  and  $10,000s^{-1}$ , usually experienced within small arteries and the microvasculature platelet adhesion is mediated by the actions of GPIb and integrin  $\alpha_{IIb}\beta_3$  with vWF and fibrinogen. Platelets that are

immobilised onto the surface of the thrombus project thin membrane tethers. These dynamic structures extend from platelet to platelet adhesion contacts under the influence of high shear rates, attaching platelets to the thrombus long enough for more sustained platelet-platelet interactions (Nesbitt et al., 2009). Blocking of integrin  $\alpha_{IIb}\beta_3$  does not hinder tether formation, therefore, it is thought their formation is dependent on vWF binding to GPIb (Dopheide et al., 2002). However, integrin  $\alpha_{IIb}\beta_3$  activation and binding is a prerequisite for the formation of stable aggregates (Ma et al., 2007).

At shear rates greater than  $10,000s^{-1}$ , found within stenotic arteries, platelet adhesion to soluble vWF can occur independently of vessel trauma and platelet activation (Ruggeri, 2007). Under these extreme conditions, platelets bind to vWF exclusively through GPIb (Ruggeri et al., 2006). These vWF bound platelet aggregates are then cleared from the circulation, consequently lowering levels of endogenous multimeric vWF and impeding normal haemostasis (Hollestelle et al., 2011).

#### **1.4.5 Thrombus consolidation**

The end product of platelet aggregation is a fibrinogen-rich thrombus consisting of platelets cross-linked together via vWF and fibrinogen binding to integrin  $\alpha_{IIb}\beta_3$ . These linkages are strengthened through thrombin-mediated conversion of integrin  $\alpha_{IIb}\beta_3$  bound fibrinogen into fibrin to form a supportive mesh. Thrombus formation is completed by integrin driven clot retraction, a cytoskeletal process channeled through fibrin bound integrin  $\alpha_{IIb}\beta_3$  (Brass et al., 2005). The resulting haemostatic structure enables protection against blood loss whilst withstanding the shear forces of blood flow within the vasculature.

**1.5 Platelet regulation**

Spontaneous thrombus formation and uncontrolled thrombus growth can result in the occlusion of vital blood flow and tissue death. There are numerous pathological conditions that predispose the circulatory system to these morbid events. Healthy blood vessels possess a number of protective mechanisms that prevent inappropriate platelet activation and regulate thrombus size. Firstly, platelet agonists are only generated at sites of vascular injury with agonists sequestered inside platelet granules and contained within the subendothelial matrix under normal conditions (Chen and López, 2005). Agonists that are free within the circulation are quickly removed and neutralised by endothelial cells through the CD39/ecto-ADPase pathway thereby localising the haemostatic response (Marcus et al., 1997). In addition to agonist removal, the endothelium also synthesises and releases the anti-thrombotic factors PGI<sub>2</sub> and NO into the immediate environment of circulating platelets (M. W. Radomski et al., 1987; Weiss and Turitto, 1979). These important platelet inhibitors signal through cyclic nucleotide signalling cascades that result in the inhibition of virtually every known mechanism of platelet activation (Schwarz et al., 2001). The following sections will describe both PGI<sub>2</sub> and NO signalling in platelets and the mechanisms of pathway regulation.

**1.5.1 Cyclic AMP signalling****1.5.1.1 Prostacyclin**

Prostacyclin is synthesised in endothelial cells from the phospholipid metabolite arachidonic acid in a two-step process. Arachidonic acid is first metabolised by

cyclooxygenase (COX) and 5-lipoxygenase to produce prostaglandin G<sub>2</sub> (PGG<sub>2</sub>), which is then further metabolised into PGH<sub>2</sub> and finally converted into PGI<sub>2</sub> by the enzyme prostacyclin synthase (Weksler et al., 1977). Once secreted from the endothelium, PGI<sub>2</sub> binds to the G $\alpha_s$  coupled IP receptor, expressed on the platelet surface (Armstrong, 1996). Upon ligand binding, the IP receptor undergoes a conformational change that results in the detachment of G $\alpha_s$ , through GDP exchange with GTP, which then activates the integral membrane glycoprotein adenylyl cyclase (AC). Following signal propagation, G $\alpha_s$  bound GTP is hydrolyzed back to GDP, prompting reattachment of G $\alpha_s$  to the IP receptor.

#### ***1.5.1.2 Adenylyl cyclase and cyclic AMP***

Adenylyl cyclases are a ubiquitously expressed group of transmembrane proteins that catalyse the formation of cAMP. Platelets express the adenylyl cyclase isoform ADCY6 and potentially ADCY3 and ADCY5 (Burkhart et al., 2012). Upon stimulation by G $\alpha_s$ , adenylyl cyclase hydrolyses ATP to form the ubiquitous secondary messenger cAMP. Elevations in platelets cAMP levels are a powerful mechanism of platelet inhibition (Sim et al., 2016). Adenylyl cyclase activity can also be inhibited by the actions of G $\alpha_i$ , consequently lowering cAMP levels and the threshold for activation. The platelet agonists thrombin and ADP both signal in this manner (Offermanns, 2006). Thrombin binds to its PAR1 G $\alpha_i$  linked receptor whereas ADP binds to the G $\alpha_i$  linked P2Y<sub>12</sub> receptor, as previously discussed in section 1.4.2.2. The inhibitory actions of cAMP are mediated by protein kinase A (PKA), the foremost effector of cAMP signalling in platelets (Raslan and Naseem, 2014).

### 1.5.1.3 Protein kinase A

PKA is a heterotetrameric kinase constructed from a regulatory subunit dimer (RI $\alpha$ , RI $\beta$ , RII $\alpha$ , RII $\beta$ ) and two catalytic subunits (C $\alpha$ , C $\beta$ ) (Skalhegg and Tasken, 2000). Differential expression of PKA regulatory and catalytic subunits gives rise to a number of different PKA permutations with each combination having distinct biochemical properties and cell-specific expression, further contributing to diversity and specificity in cAMP signalling (Taskén and Aandahl, 2004). Proteomic studies have shown the expression of two PKA isoenzymes in platelets, type I and type II, that are categorised according to their regulatory subunit (Burkhart et al., 2012). Furthermore, recent studies have identified differential localisation of PKA isoenzymes in platelets, with PKA type I targeted towards the plasma membrane and PKA type II present in the platelet cytosol (Raslan et al., 2015b).

Each of the PKA regulatory domains has two cAMP binding sites, termed A and B. When PKA is inactive, only the B sites are available for cAMP binding. Binding of cAMP to the B sites enhances cAMP binding to the A sites. Occupation of both A and B sites on each PKA regulatory domain by cAMP triggers a conformational change that drives the dissociation of the catalytic subunits (Figure 1.4) (Kopperud et al., 2002). The free catalytic subunits go on to phosphorylate specific intracellular platelet proteins at a conserved consensus sequence (-Arg-Arg-X-Ser/Thr-X) (Ubersax and Ferrell Jr, 2007). These specific PKA substrates play functionally important roles in the mechanisms of platelet activation. PKA phosphorylation is a mechanism by which the substrates function can be modified during stimulation of cAMP/PKA signalling in order to preserve platelets in a quiescent state, and in some cases, reverse transient platelet activation (Smolenski, 2012). To date, over 100 different PKA-regulated proteins have been

identified in platelets with the majority still requiring characterisation (Beck et al., 2014).

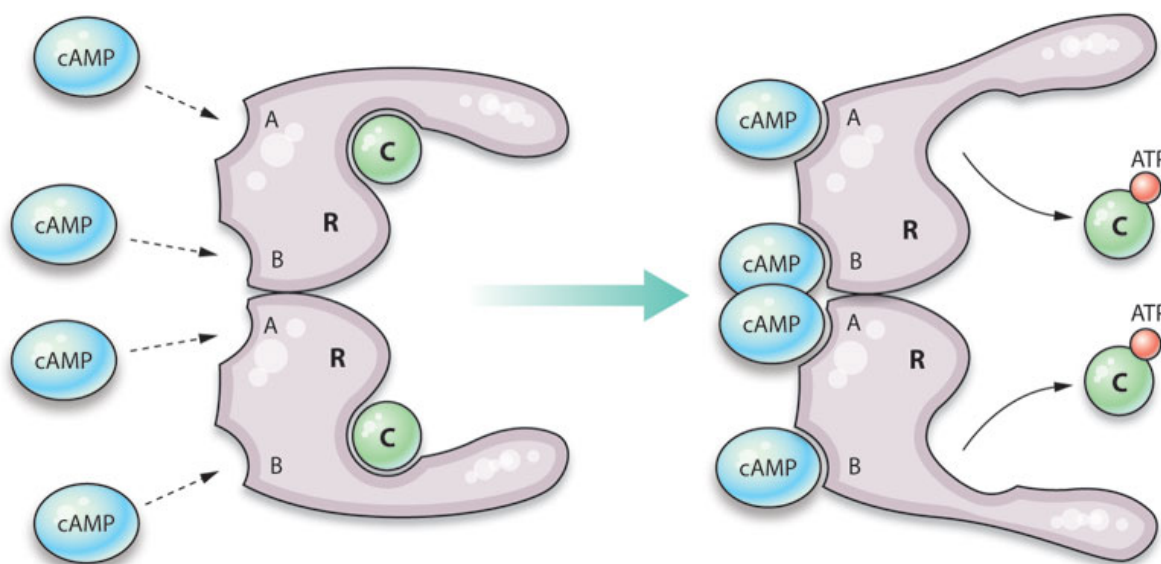


**Figure 1.4 cAMP-mediated activation of PKA.** Inactive PKA exists as a tetramer constructed from two regulatory subunits and two catalytic subunits. Binding of two cAMP molecules to each regulatory subunit initiates the disassociation of the catalytic subunits, which then bind to ATP and go on to phosphorylate a range of proteins, at specific serine and threonine residues, that play central roles in the mechanisms of platelet activation (Murray, 2008).

## 1.5.2 Cyclic GMP signalling

### 1.5.2.1 Nitric oxide

Endothelium-derived NO regulates platelet activity through cGMP-dependent signalling cascades, in addition to acting as a modulator of vascular tone (Gkaliagkousi et al., 2007; Naseem and Riba, 2008). This soluble gas has a relatively short half-life of 6-30 seconds and is continually synthesised from the

amino acid L-arginine via a two-step oxidation of L-arginine into L-citrulline by endothelial nitric oxide synthase (eNOS, NOS3) (Palmer et al., 1988). A variety of stimuli have been shown to increase the activity of eNOS, including ATP, vascular endothelial growth factor (VEGF), bradykinin and laminar shear stress (Sessa, 2004). Although eNOS is established the main source of vascular NO, small quantities of inducible NOS (iNOS) have been identified in endothelial cells (Cristina de Assis et al., 2002; Gross et al., 1991). Once released from the endothelium, NO readily diffuses through the plasma membrane of circulating platelets, where it activates soluble guanylyl cyclase (sGC) to produce cGMP (Schmidt et al., 1993).

### ***1.5.2.2 Guanylyl cyclase and cyclic GMP***

Guanylyl cyclases are a group of enzymes that when catalytically active convert GTP to cGMP. To date, only the soluble form of guanylyl cyclase (sGC, NO-sensitive GC) and not the membrane-bound form is expressed in platelets, located in the platelet cytoplasm (Dangel et al., 2010). sGC is a heterodimeric haemoprotein constructed from two subunits, termed  $\alpha$  and  $\beta$ , which dimerise and catalyse the formation of cGMP from GTP in response to NO stimulation (Harteneck et al., 1990). In this way, sGC acts as an intracellular receptor for NO. The binding of NO to the haem moiety of sGC leads to a 200-fold increase in the production of cGMP (Friebe and Koesling, 2003). Once synthesised, cGMP goes on to activate protein kinase G (PKG), the central effector molecule of cGMP signalling, and potentiate cAMP signalling through inhibition of regulatory phosphodiesterase 3A. Initial studies by Zhang and collaborators using platelet-specific sGC knock mice reported a stimulatory role of soluble guanylyl cyclase in

platelets, as opposed to an inhibitory role as stated in the literature (Zhang et al., 2011). However, this contradictory report has since been refuted by other investigations using the same knockout models (Gambaryan et al., 2012; Rukoyatkina et al., 2011).

### **1.5.2.3 Protein kinase G**

There are two families of PKG, soluble PKG type I and membrane-bound PKG type II, that are the products of two separate genes (*prkg1* and *prkg2*) (Francis et al., 2010). Both are homodimeric kinases containing an N-terminal dimerization domain, a regulatory domain and a catalytic domain (Francis et al., 2010). PKG type I exists as two splice variants, PKG type I $\alpha$  and PKG type I $\beta$ , differing in tissue expression, N-terminal structure and cGMP affinity (Massberg et al., 1999). In platelets, PKG type I $\beta$  has been identified as the main intracellular receptor for cGMP (Eigenthaler et al., 1992). Knockout mouse studies have shown that platelets lacking PKG type I platelets are unresponsive to NO (Massberg et al., 1999). The mechanism of PKG type I $\beta$  activation is comparable to that of PKA, with the release of the catalytic subunits triggered by cGMP binding to four sites on the regulatory domains (Francis and Corbin, 1999). The activated catalytic subunits are then free to selectively phosphorylate an array of functionally important platelet proteins to effectuate platelet inhibition (Schwarz et al., 2001).

### **1.5.3 Protein kinase A and G protein targets**

Cyclic nucleotide signalling targets and restrains multiple mechanisms of platelet activation including platelet receptor signalling, calcium mobilisation and cytoskeletal reorganisation (Aburima et al., 2013; Chaloux et al., 2007; Chen and

Stracher, 1989; El-Daher et al., 2000; Horstrup et al., 1994; Manganello et al., 1999; Walsh et al., 2000). Many of the proteins targeted by cyclic nucleotide signalling are dually regulated by both PKA and PKG while some proteins are regulated in a kinase specific manner (summarised in table 1.1) (Smolenski, 2012). In comparison to other cell types, human platelets contain particularly high concentrations of both PKA type I and II and PKG type I $\beta$ , highlighting the functional importance of protein phosphorylation in regulating platelet inhibition (Eigenthaler et al., 1992). Proteomic studies have suggested hundreds of potential PKA-regulated platelet proteins, although only a selection of these substrates have been validated (Beck et al., 2014). The following section briefly describes the currently characterised PKA/PKG protein targets and their roles in platelet function.

### ***1.5.3.1 Receptor signalling events***

Platelet activation at sites of vascular damage is a concerted process that requires a multitude of receptors that link platelet agonists to intracellular signalling cascades. Many of these receptors are targeted and regulated by PKA and PKG. As previously described, GPIIb $\beta$  is a subunit of the GPIIb-V-IX signalling complex that stimulates granule release and integrin receptor activation through tyrosine kinase signalling pathways when bound to immobilised vWF (Gibbins, 2004). GPIIb $\beta$  is phosphorylated by PKA at Ser<sup>166</sup>, resulting in a reduced vWF binding and vWF mediated platelet agglutination (Bodnar et al., 2002; Raslan et al., 2015b).

The actions of TXA<sub>2</sub>, the potent and short-lived platelet agonist, are also thought to be regulated by cyclic nucleotide signalling. Although not yet demonstrated in

human platelets, investigations using human embryonic kidney (HEK)-239 cells have suggested that the TP $\alpha$  TXA<sub>2</sub> receptor, expressed on the platelet surface, is desensitised in response to both PKA phosphorylation at Ser<sup>229</sup> and PKG phosphorylation at Ser<sup>331</sup> (Reid and Kinsella, 2003). In platelets, PKA has also been shown to phosphorylate the G-protein G $\alpha_{13}$ , employed by both TXA<sub>2</sub> and thrombin receptors to transmit intracellular platelet-activating signals (Offermanns, 2006). Phosphorylation of G $\alpha_{13}$  has been shown to block signal transmission thus blunting the platelet response to these potent agonists (Manganello et al., 1999). In addition to direct desensitisation of platelet surface receptors, small GTPases that act as molecular switches in regulating platelet function, cycling between an inactive GDP-bound state and an active GTP-bound state, are also targeted by cyclic nucleotide signalling. The GTPase Rap1b is thought to play a prominent role in the activation of integrin  $\alpha_{IIb}\beta_3$ . Both PKA and PKG have been shown to phosphorylate Rap1b (Schultess et al., 2005; Siess et al., 1990). However, the exact role of this phosphorylation event in platelets remains to be proven (Subramanian et al., 2013). Another small GTPase targeted by PKA and PKG is RhoA. In platelets, activation of RhoA leads to the formation of a RhoA/Rho-associated kinase (ROCK) complex that inactivates myosin light chain phosphatase (MLCP), resulting in phosphorylation of myosin light chain (MLC) and platelet shape change. Phosphorylation of RhoA by PKA has been shown to prevent the formation of the RhoA/ROCK complex and, therefore, restrains platelet shape change (Aburima et al., 2013).

### **1.5.3.2 Calcium mobilization**

Elevations in intracellular  $\text{Ca}^{2+}$  concentrations are an essential mechanism of platelet activation. Both  $\text{PGI}_2$  and NO are potent inhibitors of increases in intracellular  $\text{Ca}^{2+}$  levels (Geiger et al., 1994; Trepakova et al., 1999). Calcium influx occurs through  $\text{IP}_3$  facilitated release of  $\text{Ca}^{2+}$  from intracellular stores and  $\text{Ca}^{2+}$  entry through the plasma membrane mediated by Orai1 store-operated  $\text{Ca}^{2+}$  entry (SOCE), transient receptor potential canonical 6 (TRPC6) and  $\text{P2X}_1$  channels (Varga-Szabo et al., 2009). Platelets are known to express all three  $\text{IP}_3$  receptors, which are phosphorylated by both PKA and PKG at yet unidentified sites, which is thought to inhibit calcium release (El-Daher et al., 2000). Additionally, a type I  $\text{IP}_3$  receptor-associated protein termed  $\text{IP}_3$  receptor-associated cGKI substrate protein (IRAG) has also been shown to be phosphorylated by PKG at Ser<sup>664</sup> and Ser<sup>667</sup>, linked to inhibition of calcium release from the DTS (Antl et al., 2007). However the role that PKA and PKG play in regulating the influx of  $\text{Ca}^{2+}$  across the plasma membrane still requires elucidation, with TRPC6 identified as a PKA substrate (Hassock et al., 2002).

### **1.5.3.3 Cytoskeletal reorganisation**

The actin cytoskeleton required for platelet shape change is a major target for regulation by cAMP and cGMP-dependant signalling cascades. Over the past decades a plethora PKA and PKG substrates that are associate with the remodelling of the platelet actin cytoskeleton have been identified, including Vasodilator-stimulated phosphoprotein (VASP), LIM and SH3 domain protein (LASP), heat shock protein 27 (HSP27), filamin-A (actin binding protein) and caldesmon (Butt et al., 2003, 2001, 1994; Chen and Stracher, 1989; Hettasch and

Sellers, 1991). Phosphorylation of VASP at Ser<sup>157</sup> by PKA and Ser<sup>239</sup> by PKG reduces actin bundling and the formation of focal adhesion points *in vitro* (Galler et al., 2006; Harbeck et al., 2000). LASP is phosphorylated by PKA and PKG at Ser<sup>146</sup>, which results in reduced binding affinity of LASP to F-actin *in vitro* (Butt et al., 2003). Actin polymerisation is reduced *in vitro* through the phosphorylation of HSP27 by PKG at Thr<sup>143</sup> (Butt et al., 2001). Filamin A is required for contraction of the platelet cytoskeleton and PKA phosphorylation on Ser<sup>2152</sup> stabilises the resting platelet cytoskeleton (Chen and Stracher, 1989). It is clear, however, that many of these observations require repeating *in vivo* as opposed to *in vitro*, in order to fully understand their significance in platelet function.

Table 1.1 PKA and PKG platelet substrates

Confirmed platelet substrate	Molecular mass (kDa)	PKA	PKG	Function of phosphorylation
Caldesmon	82	✓		Unknown (Hettasch and Sellers, 1991)
Filamin-A (actin binding protein)	250	✓		Stabilisation of platelet cytoskeleton (Chen and Stracher, 1989)
G-protein $\alpha_{13}$ subunit	44	✓		Inhibition of TXA <sub>2</sub> signalling (Manganello et al., 1999)
GPIIb $\beta$	24	✓		Inhibition vWF binding (Bodnar et al., 2002; Fox and Berndt, 1989)
GSK-3 $\alpha$	51	✓		Unknown (Beck et al., 2014)
Heat shock protein 27 (HSP27)	27		✓	Inhibition of actin polymerisation (Butt et al., 2001)
IP <sub>3</sub> receptor	260	✓	✓	Inhibition of calcium mobilisation (Cavallini et al., 1996)
IP <sub>3</sub> receptor associated cGMP kinase substrate (IRAG)	98		✓	Inhibition of calcium mobilisation (Antl et al., 2007)
LASP	40	✓		Inhibition of actin polymerisation (Beck et al., 2014)
Phosphodiesterase 3A (PDE3A)	110	✓		Enhanced cAMP hydrolysis (Hunter et al., 2009)
Phosphodiesterase 5 (PDE5)	100		✓	Enhanced cGMP hydrolysis (Mullershausen et al., 2003)
Rap1b	22	✓	✓	Unknown (Subramanian et al., 2013)
RhoA	22	✓	✓	Inhibition of Rho kinase signalling (Aburima et al., 2013)
TRPC6	106	✓		Unknown (Hassock et al., 2002)
Vasodilator-stimulated phosphoprotein (VASP)	46/50	✓	✓	Stabilisation of platelet cytoskeleton (Galler et al., 2006)

## 1.6 Platelet phosphodiesterases

Platelet cyclic nucleotide concentrations are regulated in space and time by the hydrolysing actions of PDE enzymes. There are currently eleven PDE family members defined in the literature, which selectively and non-selectively convert cAMP and cGMP into inactive 5' nucleotide metabolites through the hydrolysis of the 3'-phosphodiester bond. Early studies investigating platelet PDEs identified three distinct peaks of enzymatic activity in platelet lysates using DEAE-cellulose chromatography (Hidaka and Asano, 1976). Using a combination of PDE inhibitors and hydrolytic activity measurements, Hidaka and Asano were able to characterise these enzymatic peaks as PDE2A, cAMP-specific PDE3A and cGMP-specific PDE5 (Hidaka and Asano, 1976). These three PDE isoforms differ in structure, selectivity, cellular distribution, regulation and sensitivity to inhibitors (Bender and Beavo, 2006).

### 1.6.1 PDE2A

Initially named the cGMP-stimulated PDE, due to the ability of cGMP to increase the enzyme's catalytic activity, PDE2A hydrolyses both cAMP and cGMP at similar maximal rates (Haslam et al., 1999). The PDE2A gene gives rise to three splice variants, PDE2A1, PDE2A2 and PDE2A3, with PDE2A3 containing a unique N-terminal sequence that facilitates membrane localisation (Rosman et al., 1997). However, the individual expression of these splice variants in human platelets remains to be investigated.

PDE2A exists as a homodimer constructed from two 105kDa subunits that each possess two N-terminal regulatory GAF domains, GAF-A and GAF-B, and a C-

terminal catalytic domain, connected together by two long  $\alpha$ -helices LH1 and LH2 (Figure 1.5) (Pandit et al., 2009). The GAF domains, so called after the molecules in which they were first identified (cGMP-specific phosphodiesterases, Adenylyl cyclases and FhlA), specifically bind cGMP in a non-catalytic manner. Interestingly, these GAF domains are structurally similar yet perform entirely different functions, with cGMP binding to GAF-A inducing PDE2A subunit dimerization and cGMP binding to GAF-B prompting movement of structural H-loops that further unveil the PDE2A catalytic domains, thereby improving cGMP access and increasing PDE2A catalytic activity (Martinez et al., 2002; Pandit et al., 2009).

The availability of PDE2A specific inhibitors as research tools, including erythro-9-(2-hydroxy-3-nonyl)adenine (EHNA) and BAY 60-7550, have increased our understanding of PDE2A function in various cell types (Bender and Beavo, 2006). In platelets, PDE2A regulates both cAMP and cGMP-dependent signalling cascades due to its dual specificity. However, the expression of PDE2A in platelets is low in comparison to that of PDE3A and PDE5, as confirmed by genomic and proteomic studies, with less than 300 copies estimated per platelet (Burkhart et al., 2012). Although inhibition of PDE2A alone leads to increased levels of cAMP, interestingly there is little effect on platelet function (Manns et al., 2002). It is thought that PDE2A functions instead as limiting mechanism of NO induced cAMP accumulation that arises from cGMP-mediated inhibition of PDE3A (Dickinson et al., 1997).

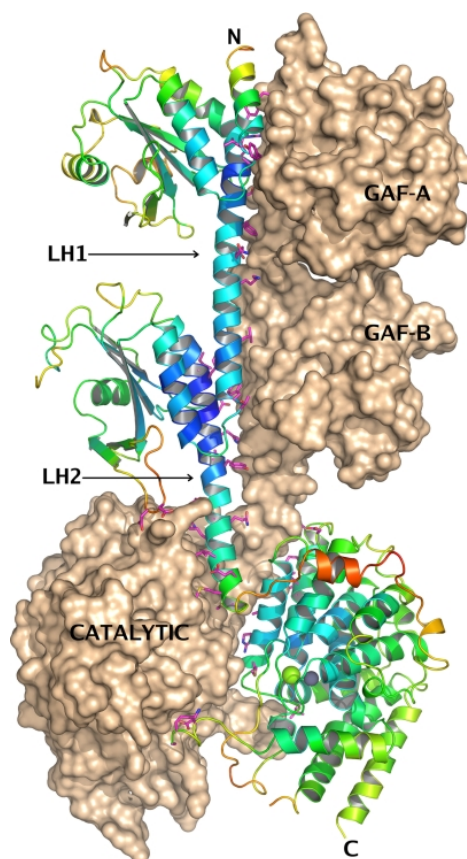


**Figure 1.5. Structure of human PDE2A.** Computer generated model of PDE2A subunit structure detailing both cGMP binding GAF domains, the catalytic subunit and the  $\alpha$ -helices that link them together (Pandit et al., 2009)

### 1.6.2 PDE3A

PDE3A, also known as the cGMP-inhibited PDE, has similar affinities for both cAMP and cGMP, but due to a low hydrolysis rate of cGMP, PDE3A preferentially hydrolyses cAMP (Schwarz et al., 2001). There are three splice variants that are alternatively transcribed from the PDE3A gene, PDE3A1, PDE3A2 and PDE3A3, which in other cell types, differ in catalytic activity, subcellular localisation and regulation (Hambleton et al., 2005; Vandeput et al., 2013). In terms of structure, all three PDE3A splice variants share a conserved catalytic domain but differ in a

common N-terminal sequence on PDE3A2 and PDE3A1, which contains PKA and PKC phosphorylation sites, and a unique N-terminal membrane localisation domain on PDE3A1 (Figure 1.6) (Wechsler, 2002). The expression of these three PDE3A splice variants in platelets is an exciting research area that remains to be explored.

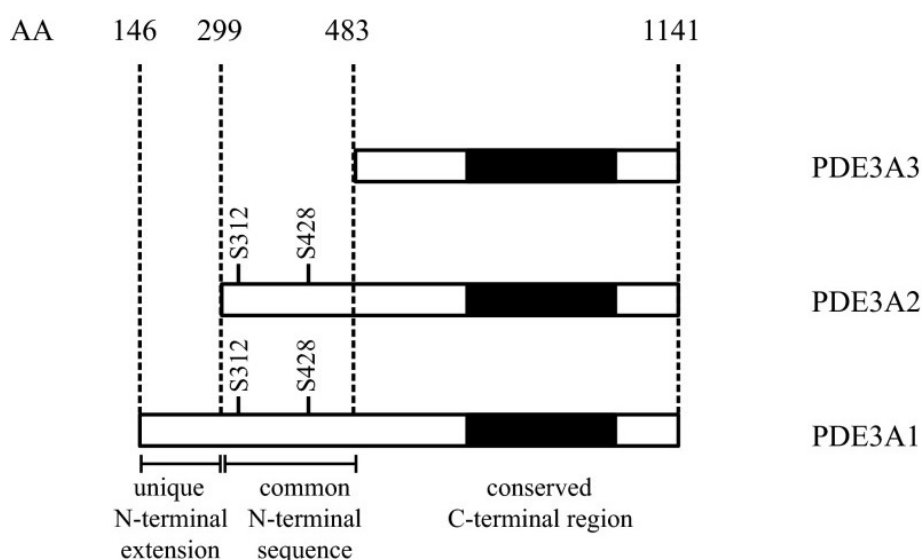


**Figure 1.6. PDE3A splice variants.** Diagram detailing PDE3A splice variant structure with established phosphorylation sites (Vandeput et al., 2013)

The importance of PDE3A in regulating endogenous platelet inhibition through the breakdown of cAMP is well documented. Studies by Manns and colleagues have shown that selective inhibition of platelet PDE3A with cilostazol elevates resting cAMP levels (Manns et al., 2002). Furthermore, recent studies have also shown that selective inhibition of PDE3A with milrinone potentiates cAMP elevations in response to PGI<sub>2</sub> (Roberts et al., 2010). In regards to platelet function, PDE3A

inhibition has been shown to restrain thrombin-induced aggregation, intracellular calcium release, integrin activation and granule secretion (Feijge et al., 2004; Manns et al., 2002; Sim et al., 2016; Sun et al., 2007). Moreover, this powerful inhibitory effect of PDE3A inhibition on platelet activation has been elegantly demonstrated in mouse knockout studies with the absence of PDE3A expression conferring a cardioprotective phenotype (Sun et al., 2007). The protective effect of PDE3A inhibition against pathological thrombosis is such that PDE3A inhibitors, including cilostazol and milrinone, have been used for the treatment and prevention of ischaemic cardiovascular disease (Gresele et al., 2011).

Early studies investigating PDE3A activity in human platelets revealed that phosphorylation of PDE3A under PGI<sub>2</sub> stimulated conditions increases the enzyme's hydrolytic activity (Grant et al., 1988; Macphee et al., 1988). More recent platelet studies have identified five PKC phosphorylation sites on the PDE3A common N-terminal sequence, with one site at Ser<sup>312</sup> also phosphorylated by PKA (Hunter et al., 2009; Pozuelo Rubio et al., 2005). It is thought that PKC phosphorylation of PDE3A facilitates agonist-induced platelet activation via increased cAMP breakdown, whereas PKA phosphorylation of PDE3A in response to PGI<sub>2</sub> forms a negative feedback loop that regulates cAMP elevations (Hunter et al., 2009). PKB has also been shown to phosphorylate and activate PDE3A, however, this has been disputed by recent studies and is yet to be reported in other cell types (Elbatarny and Maurice, 2005; Hunter et al., 2009; Vandeput et al., 2013; Zhang and Colman, 2007).

### 1.6.3 PDE5

The most highly expressed PDE isoform in platelets is the cGMP-specific PDE isoform PDE5 (Burkhart et al., 2012). Similar to PDE2A and PDE3A, alternative splicing of the PDE5 gene gives rise to three splice PDE5 variants, PDE5A1, PDE5A2 and PDE5A3, however, it is unknown which variants are expressed in platelets (Lin et al., 2002). PDE5 exists as a homodimer with each subunit comprised of a regulatory domain containing two GAF domains, GAF-A and GAF-B, and at least, one phosphorylation site at Ser<sup>92</sup> near the N-terminal and a catalytic domain at the C-terminal (Fink et al., 1999). The GAF-A domain of PDE5 adopts a similar function to the GAF-B domain of PDE2A, by allosterically binding cGMP, whereas cGMP binding to the GAF-B domain of PDE5A contributes to PDE5 subunit dimerization (Sopory et al., 2003; Zoraghi et al., 2005).

In platelets and other cell types, PDE5 hydrolytic activity is increased through allosteric binding of cGMP to the GAF-A domain paralleled with PKG phosphorylation of Ser<sup>92</sup> (Corbin et al., 2000; Mullershausen et al., 2003). It is thought that PKG phosphorylation of PDE5 acts a memory switch for PDE5 activation which in turn leads to prolonged feedback regulation of NO/cGMP inhibitory signalling (Mullershausen et al., 2004). PDE5 inhibitors have gained notoriety as successful treatments for erectile dysfunction. In platelets, selective PDE5 inhibition with sildenafil has been shown to potentiate the inhibitory effect of NO on platelet aggregation in response to collagen through blockade of cGMP metabolism (Gudmundsdóttir et al., 2005). However, PDE5 inhibition with sildenafil has only been shown to induce a minor inhibitory effect on platelet aggregation in response to ADP and collagen (Berkels et al., 2001; Halcox et al., 2002). These studies suggest that cGMP production is low under resting conditions and that

PDE5 functions mainly as a regulator of cGMP elevations. Although a wide selection of specific PDE5 inhibitors and have been developed, including zaprinast, avanafil, sildenafil, vardenafil and tadalafil, only Dipyridamole is currently used in anti-platelet therapies (Gresele et al., 2011).

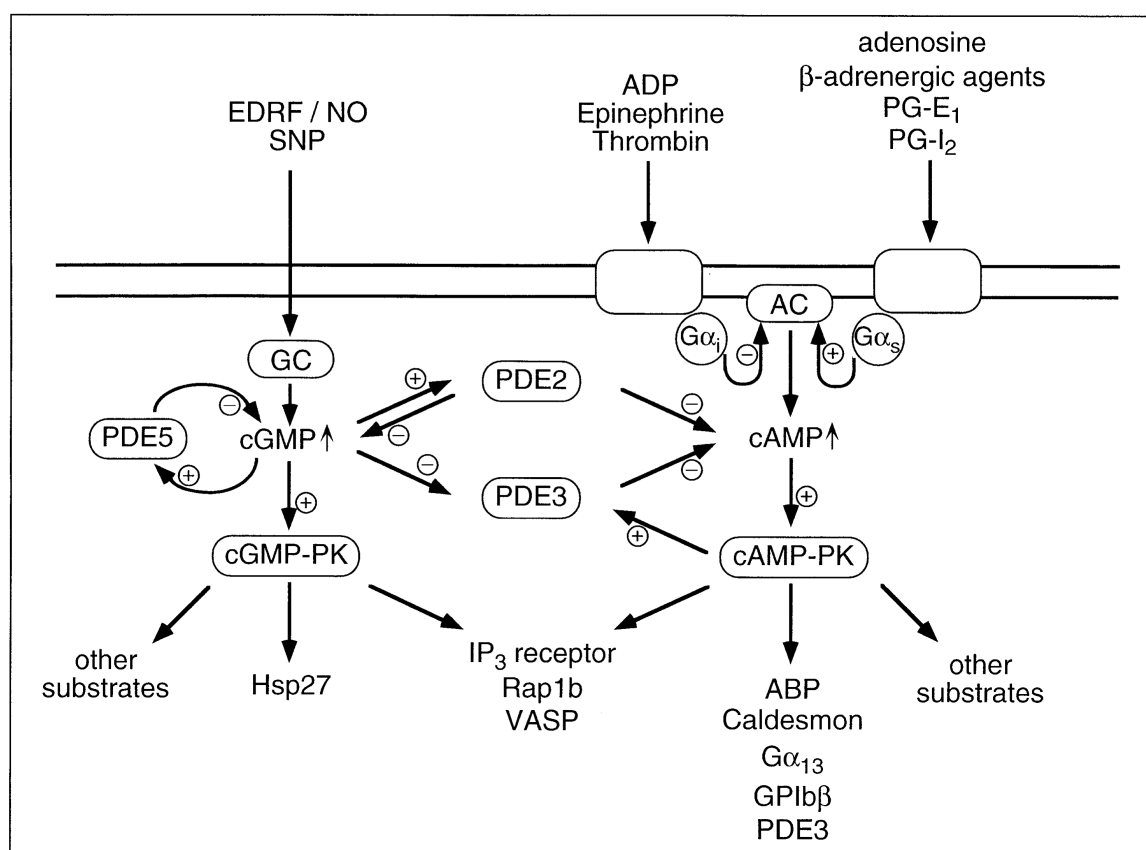


**Figure 1.7. Regulation of cyclic nucleotide signalling pathways in human platelets.** Schematic representation of cAMP and cGMP-dependent signalling cascade regulation by PDEs in human platelets (Schwarz et al., 2001)

#### 1.6.4 PDE2A and PDE3A cross-talk

It is well established that pharmacological inhibition of PDE3A potentiates elevations in cAMP and thus endogenous platelet inhibition (Feijge et al., 2004; Manns et al., 2002; Sim et al., 2016). There is also good evidence that this mechanism, to some degree, occurs physiologically in the human platelet. Studies have shown that stimulation of platelets with NO results not only in the accumulation of cGMP but also cAMP (Maurice and Haslam, 1990). These NO-stimulated elevations in cAMP are thought to occur through cGMP-mediated inhibition of PDE3A (Maurice and Haslam, 1990). This mechanism of endogenous cGMP-mediated PDE3A inhibition is thought to account, in part, for the observed synergistic effect of PGI<sub>2</sub> and NO on platelet inhibition (Haslam et al., 1999; M. W. Radomski et al., 1987a). Studies by Dickinson and colleagues suggested that under these PDE3A-inhibited conditions, PDE2A functions as a regulator of cAMP elevations, as cGMP is a known stimulator of PDE2A activity and treatment of platelets with EHNA greatly potentiates the synergistic effect that exists between PGI<sub>2</sub> and NO (Dickinson et al., 1997).

#### 1.7 Co-ordination of cyclic nucleotide signalling

The complexity of cyclic nucleotide signalling in platelets is evident. It is becoming apparent that there are two main mechanisms that tightly control the specificity of cAMP and cGMP signalling cascades. The first being compartmentalisation of cyclic nucleotide concentrations into discrete subcellular domains by PDEs, and second, the scaffolding of domain-specific functional multiprotein signalling complexes by A and G-kinase anchoring proteins (AKAPs and GKAPs) (Lefkimmatis and Zaccolo, 2014).

### 1.7.1 Compartmentalisation of cAMP and cGMP by PDEs

As the only known mechanism for cyclic nucleotide degradation, PDEs are critical in regulating cAMP and cGMP-dependent signalling cascades. Due to their hydrophilic nature, cyclic nucleotides are highly diffusible molecules (Nikolaev et al., 2004). It would, therefore, be expected that cellular diffusion of cAMP and cGMP would result in simultaneous activation of all corresponding effector molecules, including PKA and PKG, throughout the cell. However, there are now numerous studies that show concentrations of cyclic nucleotides are instead organised into discrete microdomains, which are regulated in space and time by PDEs (Castro et al., 2006; Conti et al., 2013; Zaccolo and Pozzan, 2002) (Figure 1.8). Localised to these domains are various cAMP and cGMP-signalling components that work within multi-protein complexes to perform specific cellular functions (Baillie et al., 2005). Although this concept is not yet established in platelets, there are several lines of supporting evidence (Raslan et al., 2015a). Early studies by El-Daher demonstrated that both PKA and PKG isoforms are differentially localised within platelets and in approximation to known substrates (El-Daher et al., 2000, 1996). These data are supported by platelet genomic and proteomic studies that have identified multiple AKAPs and GKAPs responsible for targeting PKA and PKG containing signalosomes to these distinct subcellular locations (Burkhart et al., 2012; Margarucci et al., 2011; Rowley et al., 2011). Furthermore, selective inhibition of either PDE2A or PDE3A, which both hydrolyse cAMP, in platelets leads to dissimilar functional outcomes, suggesting the presence of differentially regulated cAMP pools (Manns et al., 2002). However, even in light of these studies, the concept of PDEs regulating domain specific cAMP and cGMP compartments in platelets is still unknown.

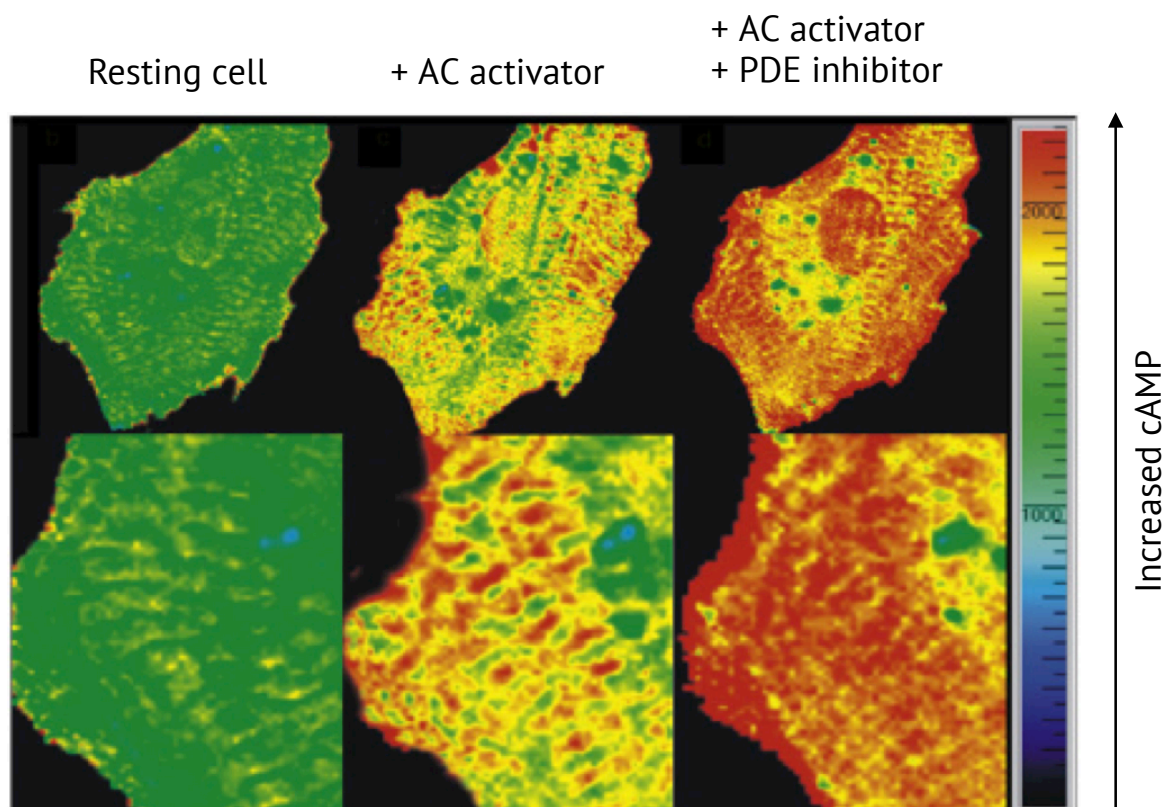


**Figure 1.8. Compartmentalisation of cAMP in cardiac myocytes by PDEs.** FRET analysis of cAMP localisation in cardiac myocytes treated with the adenylyl cyclase activator forskolin ( $25\mu\text{M}$ ) and the non-selective PDE inhibitor IBMX ( $10\mu\text{M}$ ). Under resting conditions cAMP concentrations within the myocyte are low. Treatment with the adenylyl cyclase activator forskolin stimulates AC to synthesise cAMP, which is visually compartmentalised into discrete pools within the cell. The organisation of these pools is disrupted in the presence of the non-selective PDE inhibitor IBMX (Houslay, 2010; Zaccolo and Pozzan, 2002).

### 1.7.2 A and G-kinase anchoring proteins

In many cell types, AKAPs and GKAPs target PKA and PKG, respectively, to specific subcellular locations often scaffolding the kinases with specific substrates and regulating enzymes, including PDEs, to form functional signalosomes (Michel and Scott, 2002). Currently, the majority of scientific attention has been directed towards AKAPs with over 50 different family members, including splice variants, so far identified (Jarnaess and Taskén, 2007).

Each AKAP possesses a unique targeting domain that directs PKA to a distinct subcellular location and a highly homologous 14-18 amino acid long amphipathic helix which binds both PKA type I and type II by interacting with the PKA regulatory subunit docking and dimerization domain (D/D domain) (Figure 1.4) (Carr et al., 1991). Although AKAPs can bind both PKA isoforms, the majority of identified AKAPs bind to PKA type II with higher affinity than that of PKA type I (Pidoux and Taskén, 2010). Our understanding of AKAP function has been greatly aided with the development of cell-permeable disruptor peptides that inhibit the interaction between AKAPs and PKA (Calejo and Taskén, 2015). AKAP scaffolded complexes have been shown to play important functional roles in reproduction, immune function, cardiovascular function and metabolism (Taskén and Aandahl, 2004).

The role of AKAPs in co-ordinating platelet cyclic nucleotide signalling cascades is a newly emerging field in platelet biology. Platelets are thought to express up to 16 different AKAPs (Burkhart et al., 2012; Margarucci et al., 2011; Rowley et al., 2011) (table. 1.2). Only until very recently has the first AKAP in platelets, moesin, been characterised. It is thought that in platelets moesin functions to localise PKA

type I in proximity with GPIb to facilitate receptor phosphorylation and inhibition of vWF binding (Raslan et al., 2015b). It will be of great interest in future studies to further explore the role of AKAPs in platelet function.

Although much less is known of GKAPs, initial studies by Ngan and colleagues have identified G-KAPs in rat aorta, brain and intestine using protein overlay techniques (Vo et al., 1998). GKAPs possess the ability to bind both PKG type I and type II at a regulatory region located close the GKAP N-terminal (Vo et al., 1998). Currently, only a very small number GKAPs are recognised, which in part is due to low expression levels and lack of GKAP specific molecular tools (Corradini et al., 2015). At this point in time, proteins identified as GKAPS are GKAP1, huntingtin-associated protein 1 (HAP1), vimentin and myosin (Corradini et al., 2015; MacMillan-Crow and Lincoln, 1994; Vo et al., 1998). Both myosin (myosin class 3, 4, 5A, 6, 9 and 18A) and vimentin are expressed in platelets, as confirmed by genomic and proteomic studies, however, their functional role in regards to PKG anchoring remains to be determined (Burkhart et al., 2012; Rowley et al., 2011).

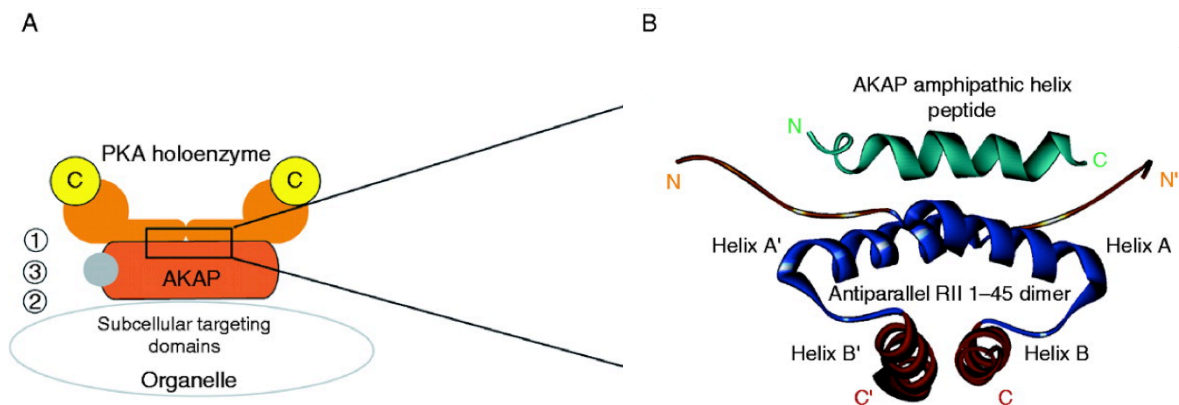


**Figure 1.9. AKAP signalling.** (A) Illustration detailing: (1) AKAP binding of PKA through interaction with the D/D domain on the PKA regulatory subunits, (2) the unique subcellular targeting domain that directs AKAP scaffolded signalling complexes to discrete locations within the cell and (3) additional binding sites on the AKAP for PKA substrates, PDEs and phosphatases. (B) Computer generated diagram representing the structure of PKA type II in association with the amphipathic helix of an AKAP (Pidoux and Taskén, 2010).

**Table 1.2 AKAP expression in human platelets**

<b>AKAP</b>	<b>Full AKAP name</b>	<b>Also known as</b>	<b>Genomic name</b>
AKAP1	A-kinase anchoring protein 1	D-AKAP1, AKAP84, S-AKAP84, AKAP121, AKAP140, AKAP149	AKAP1
AKAP10	A-kinase anchoring protein 10		AKAP10
AKAP11	A-kinase anchoring protein 11	AKAP220	AKAP11
AKAP13	A-kinase anchoring protein 13	AKAP-lbc, Brx, proto-Lbc, Onco-Lbc	AKAP13
AKAP2	A-kinase anchoring protein 2		AKAP2
AKAP7	A-kinase anchoring protein 7	AKAP18, AKAP15	AKAP7
AKAP9	A-kinase anchoring protein 9	CG-NAP, Yotiao, Hyperion, AKAP350, AKAP450, AKAP120	AKAP9
BIG1	ADP ribosylation factor guanine nucleotide exchange factor 1		ARFGEF1
BIG2	ADP ribosylation factor guanine nucleotide exchange factor 2		ARFGEF2
Ezrin	Ezrin	AKAP78	EZR
Map2	Microtubule-associated protein 2		Map2
Moesin	Membrane-Organizing Extension Spike Protein	Epididymis Luminal Protein 70, HEL70	MSN
Neurobeachin	Neurobeachin		NBEA
Rab32	Ras-related protein 32		Rab32
smAKAP	Small membrane A-kinase anchoring protein		C2orf88
WAVE-1	WAS protein family member 1		WASF1

## 1.8 Aims of the study

In flowing blood, platelets circulate in a quiescent state continuously scanning the integrity of the endothelial layer. Adhesion of platelets to sites of vascular injury is essential for haemostasis, but if uncontrolled may lead to serious cardiovascular events such as myocardial infarction and stroke. In healthy blood vessels, inappropriate platelet activation and thrombus size are regulated by endothelium-derived PGI<sub>2</sub> and NO. These inhibitory agents regulate most aspects of platelet function through cAMP and cGMP-dependant signalling cascades (Schwarz et al., 2001). However, the tight spatiotemporal regulation of these cascades that allow PGI<sub>2</sub> and NO to facilitate haemostasis while inhibit thrombosis is unclear.

A major regulator of intracellular cAMP and cGMP concentrations are PDEs, which hydrolyse cAMP and cGMP into inactive metabolites (Haslam et al., 1999). In platelets, PDE3A is the leading regulator of cAMP concentrations, to such a degree that PDE3A knockout mice display a thrombus-protective phenotype and PDE3A inhibitors are used in anti-platelet therapies (Maurice et al., 2014; Sun et al., 2007). New and exciting research in other cell types has emerged, detailing alternatively regulated PDE3A splice variants and previously unknown PDE3A signalosomes (Vandeput et al., 2013). Despite this, the mechanisms of PDE3A signalling in platelets remain largely unexplored.

The aim of this study was to investigate PDE3A signalling in human platelets with a particular focus on PDE3A regulation and protein interactions. This aim will be achieved by:

1. Characterising all three PDE isoforms in terms of expression, subcellular localisation and activity in platelets and examining their presence in megakaryocytes.
2. Investigating PDE3A phosphorylation and regulation by PKA and determine its specificity, in terms of PDE3A splice variants.
3. Exploring the role of AKAPs in the interaction and association of PKA and PDE3A in platelets.

## 2 Materials and methods

### 2.1 Materials

DC protein assay kit II, dual colour ladder, Trans-blot Turbo™ polyvinylidene difluoride (PVDF) transfer Packs, 30% bis-acrylamide solution were obtained from Bio-Rad Laboratories Ltd. (Hertfordshire, UK). Biotinylated protein ladder was obtained from Cell Signalling Technology (Hertfordshire, UK). Phosphodiesterase activity assay was obtained from Enzo life sciences (Exeter, UK). Amersham cAMP biotrack enzyme immunoassay (EIA) system, fetal bovine serum (FBS) and L-glutamine were obtained from GE Healthcare Life Sciences (Buckinghamshire, UK). PKA activity assay was obtained from Promega (Southampton, UK). Crosslink co-immunoprecipitation kit and RPMI 1640 medium were obtained from ThermoFisher scientific (Renfrew, UK). All other general reagents and kits were purchased from Sigma-Aldrich Company Ltd. (Dorset, UK). All antibodies are listed in table 2.5.

#### 2.1.1 Pharmacological agonists, inhibitors and peptides

8- (4- chlorophenylthio)adenosine- 3', 5'- cyclic monophosphate (8-CPT-cAMP) and 8-CPT-cAMP RP isomer (RP-8-CPT-cAMP) were obtained from Biolog Life Science (Bremen, Germany). Collagen was obtained from Bio/Data Corporation, (Horsham, USA). 1-methyl-3-isobutylxanthine (IBMX), erythro-9-(2-hydroxy-2-nonyl)adenine (EHNA), and prostacyclin (PGI<sub>2</sub>) were obtained from Cayman Chemical Company (Cambridge, UK). AKAP St-Ht31 Inhibitor Peptide (HT31) and HT31 control peptide were obtained from Promega (Southampton, UK). Forskolin, S-Nitrosoglutathione (GSNO), KT5720, phosphatase inhibitor cocktail, phorbol 12-

myristate 13-acetate (PMA) and protease inhibitor cocktail were obtained from Sigma-Aldrich Company Ltd. (Dorset, UK). Milrinone and zaprinast were obtained from Tocris Bioscience (Bristol, UK). RI anchoring disruptor peptide (RIAD) and scrambled RI anchoring disruptor peptide were a kind gift from Prof K Tasken, Centre for Molecular Medicine (Oslo, Norway).

### **2.2 Preparation of washed platelets from whole blood**

In order to preserve cyclic nucleotide signalling pathways, washed platelets (WPs) were prepared using the establish pH method (Mustard et al., 1989) in the absence of PGI<sub>2</sub>. Experiments were approved by the Ethics Committee at the Hull York Medical School. Venous blood was drawn from consented and drug-free healthy volunteers using a 21-gauge butterfly needle into filtered acid-citrate-dextrose (ACD) (2.9mM citric acid, 113.8mM dextrose, 72.6mM sodium chloride, 29.9mM sodium citrate, pH 6.4) at a ratio of 1:5. ACD prevents platelet activation during centrifugation steps by lowering the pH of platelet rich plasma to 6.4. The first 2ml of drawn blood was discarded to exclude artificially activated platelets. Whole blood was placed into 50ml falcon tubes and centrifuged at 200xg for 20 minutes at 20°C. The top platelet rich plasma (PRP) layer was carefully transferred to 15ml falcon tubes using a plastic transfer pipette and treated with citric acid (0.3M) at a ratio of 1:50, followed by centrifugation at 800g for 12 minutes at 20°C. The resultant platelet poor plasma (PPP) was discarded and the platelet pellet gently resuspended in 5ml of wash buffer (36µM citric acid, 10µM EDTA, 5µM glucose, 5µM potassium chloride, 90µM sodium chloride, pH 6.5) and centrifuged at 800xg for 12 minutes at 20°C. The wash buffer was discarded and the platelet pellet gently resuspended in ≤1ml of modified Tyrode's buffer (5.6mM dextrose,

5mM HEPES, 0.5mM magnesium chloride, 2.7mM potassium chloride, 150mM sodium chloride, 7mM sodium bicarbonate, 0.55mM sodium phosphate monobasic, pH 7.4). In some instances, 0.1 mM EGTA was added to washed platelets in order to prevent platelet aggregation during experimentation.

### **2.3 Platelet counting**

Washed platelets were counted using a Beckman Coulter Z1 Particle Counter. This electronic device counts cells by measuring the electrical resistance of cells as they are passed through a microchannel. Washed platelets (5 $\mu$ l) were suspended in 10mls of Beckman Coulter Isotone II diluent within a Beckman Coulter Accuvette. The Accuvette was placed within the Beckman Coulter Z1 Particle Counter and automatically counted for platelets, displayed as platelets per millilitre: proportional to the washed platelet Accuvette sample.

### **2.4 Measurement of Platelet aggregation**

Turbidimetric platelet aggregation, first described by Born in 1962, is a technique based on the change in light transmission between uniformly disturbed resting platelets and platelet aggregates within suspension (Born et al., 1962). Changes in light transmission through a platelet suspension are proportional to the level of platelet aggregation within the suspension and can be measured using a photocell. As can be seen in figure 2.1, platelets first undergo shape change where light transmission is briefly reduced, followed by two stages of aggregation, including the primary phase which is reversible, followed by the secondary phase which is irreversible and results from the release of secondary mediators from platelets.

In this study, washed platelets (250 $\mu$ l;  $2.5 \times 10^8$  platelets/ml) were incubated at 37° with stirring at 800rpm for 1 minute to allow for temperature equilibration. Washed platelets were subsequently stimulated with agonists and platelet aggregation measured for 5 minutes using a multi-channel Chronolog aggregometer. For each sample, the aggregometer was calibrated using resting platelets for 0% aggregation and modified Tyrode's buffer as 100% aggregation. Aggregation was expressed as percentage increase in light transmission through the platelet sample, relative to the light transmission through non-stimulated platelets. In some instances, washed platelets were pre-incubated with inhibitors at 37° prior to stimulation.

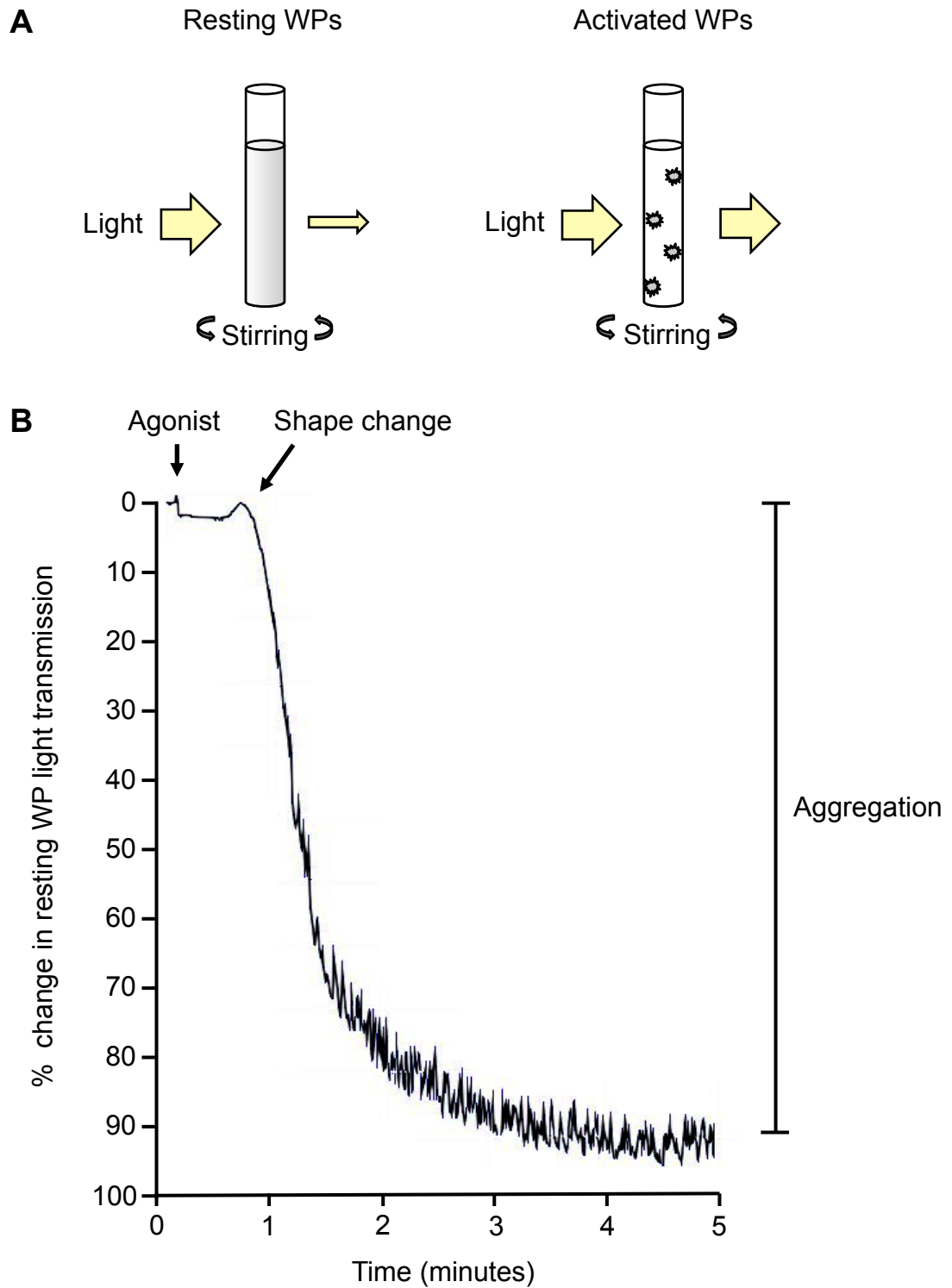


**Figure 2.1 Turbidimetric platelet aggregation.** (A) Diagram of the measurement of platelet aggregation (B) Representative aggregation trace of WPs stimulated with collagen (5 $\mu$ g/ml).

## 2.5 Methods for examination of intracellular protein function

The next series of methods describes the different strategies employed to examine intracellular protein signalling and function, prior to analysis by SDS-PAGE and immunoblotting.

### 2.5.1 Whole cell sample preparation

For standard immunoblotting samples, washed platelets ( $5 \times 10^8/\text{ml}$ ) were incubated at  $37^\circ$  with stirring at 800rpm. Following 1 minute temperature equilibration, washed platelets were stimulated with agonists and inhibitors for selected time periods. Platelet samples were immediately lysed in 2x Laemmli buffer (20% glycerol (v/v), 10% 2-mercaptoethanol (v/v), 4% SDS (w/v), 50mM Tris base) and heated for 5 minutes at  $95^\circ$ .  $10\mu\text{l}$  of washed platelets ( $5 \times 10^8/\text{ml}$ ) were suspended in 2x lysis buffer (150mM sodium chloride, 10mM Tris base, 10% Igepal (v/v), 1mM EDTA, 1mM EGTA, 1:200 phosphatase inhibitor cocktail (v/v), protease inhibitor cocktail 1:100 (v/v)) for future protein quantification. Samples were stored at  $-20^\circ\text{C}$  until use.

### 2.5.2 Sub-cellular fractionation of platelets

Sub-cellular fractionation separates cells into their membrane and cytosolic constituents. Here liquid nitrogen is used to lyse the cells, through rupturing of the plasma membrane, followed by high-speed ultracentrifugation to sediment the plasma and cellular membranes from the cytosol (Castle, 2004). Washed platelets ( $400\mu\text{l}$  of  $7 \times 10^8/\text{ml}$ ) were incubated at  $37^\circ$  with stirring at 800rpm. Following 1 minute temperature equilibration, washed platelets were stimulated with agonists and inhibitors for selected time intervals then immediately diluted in 2x

fractionation buffer (4mM HEPES, 320mM sucrose, 0.5mM sodium orthovanadate, 1:200 phosphatase inhibitor cocktail (v/v), protease inhibitor cocktail 1:100 (v/v)) and submerged in liquid nitrogen. After 10 seconds, samples were thawed in luke warm water and then re-submerged in liquid nitrogen, repeated for 6 cycles. Lysates were then centrifuged at 1000g for 5 minutes at 4°C to sediment any whole platelets. The supernatant was removed and transferred into 1.5ml ultracentrifugation tubes that were spun at 30,000xg for 60 minutes at 4°C using a Beckman Coulter Optima MAX-XP ultracentrifuge. Following the spin, the cytosolic supernatant was carefully removed and the resulting membrane pellet was resuspended in 200µl of ice-cold fractionation buffer. Aliquots (10µl) of each fraction were then analysed for protein content. Finally, fractions were either prepared for SDS-PAGE analysis as in section 2.5.2 or stored at -80 °C until use in immunoprecipitation experiments.

### **2.5.3 Quantification of sample protein concentration**

The protein concentration of platelet lysates was quantified using a Bio-Rad DC Bradford assay kit. In this system, sample proteins react with a copper tartrate solution in an alkaline environment. The copper treated proteins reduce a Folin reagent, by removal of 1-3 oxygen atoms, changing its colour from yellow to blue. The intensity of the blue colour directly correlates with the protein concentration of the sample, which can then be quantified by measuring absorbance at 750nm.

The initial 1.5mg/ml BSA solution was diluted with lysis buffer to produce the following concentrations: 1.2mg/ml, 0.9mg/ml, 0.6mg/ml, 0.3mg/ml, and 0mg/ml. BSA samples (5µl) or platelet lysate (5µl) were added to a 96 well plate in triplicate. Solution A was then prepared from 1ml reagent A and 20ul reagent S,

mixed in an Eppendorf tube. To each well, 25 $\mu$ l of solution A and 200 $\mu$ l of solution B were added using a multichannel pipette. The plate was then placed on a gentle shake for 15 minutes at room temperature and absorbance read at 750nm using a TECAN infinite M200 microplate reader. The BSA standard curve was produced by plotting absorbance against protein concentration. The protein concentration of the platelet lysate was then plotted on the curve and protein concentration noted.

### 2.5.4 Immunoprecipitation

Immunoprecipitation (IP) is the technique of precipitating specific proteins from a cell lysate using specific antibodies (Cullen and Schwartz, 1976). A primary antibody is conjugated to highly porous sepharose beads coated with protein A or protein G. Cell lysates are then incubated with the beads to allow the conjugated primary antibody to bind to the protein of interest. The beads, the bound protein of interest and associated proteins are isolated from the lysate using centrifugation. Proteins are then removed from the beads with the addition of Laemmli buffer and sample boiling.

In this study, the protein A/G sepharose beads were selected, dependent on the species of primary antibody used for immunoprecipitation. The selected beads were pelleted by centrifugation at 1000 $g$  for 1 minute and ethanol containing supernatant removed. The bead pellet was re-suspended in TBS-Tween at a ratio of 3:1 (w/v) and centrifuged again at 1000 $g$  for 1 minute, repeated twice. The beads were then re-suspended in TBS-Tween at a ratio of 1:1 (w/v).

Platelet samples were prepared as in section 2.5, lysed in lysis buffer and immediately placed on ice. The protein concentration of each sample was then

measured using a Bio-Rad DC Bradford assay kit, as described in section 2.5.2. Platelet lysates (500µg-1mg) were first incubated with 25µl of washed beads for 1 hour at 4°C with gentle rotation, to remove any proteins that non-specifically bound to the sepharose bead support. The samples were then centrifuged at 1500xg for 1 minute. The supernatant lysate was removed and incubated with 1-5µg of primary antibody per sample overnight at 4°C with gentle rotating. Following incubation, 25µl of washed beads were added to each sample and incubated at 4°C for 1 hour with gentle rotating. The samples were then centrifuged at 1500xg for 1 minute. The supernatant was carefully removed and stored at -20°C for analysis using SDS-PAGE and immunoblotting. The bead pellet was re-suspended and washed with 100µl of TBS-tween (150mM sodium chloride, 20mM Tris base, 1% (v/v) Tween-20, pH 7.6) with gentle inversion, followed by centrifugation at 5000rpm for 1 minute, repeated twice. After the third wash cycle, the bead pellet was re-suspended in Laemmli buffer (50µl) ready for analysis by Sodium dodecyl sulphate-polyacrylamide gel electrophoresis (SDS-PAGE) and immunoblotting.

### **2.5.5 Co-immunoprecipitation of associated proteins**

Co-immunoprecipitation is an extension of the immunoprecipitation technique that purifies the primary protein target with other proteins that associate to the target through native interactions in the sample solution. In this study, we used a commercial co-immunoprecipitation system developed by ThermoFisher scientific. This system substitutes sepharose beads with an amine-reactive resin that covalently couples the primary antibody. Once the protein of interest has been immobilised onto the resin, the resin is isolated and the protein removed using an

elution buffer. The antibody-coupled resin can then be washed and re-used for multiple experiments, saving both time and money (Figure 2.2). The system also minimises the handling and mixing of samples by using spin columns and collection tubes for the co-immunoprecipitation procedure. Additionally, there is no elution of the primary antibody, therefore, samples are free from antibody heavy and light chains that can often mask protein bands in standard immunoprecipitation experiments.

First, 50µl of resin slurry was added to a spin column and washed three times with 200µl of coupling buffer using centrifugation at 1000xg for 1 minute. Primary antibody (5-10µg), coupling buffer (200µl) and sodium cyanoborohydride (3µl) solution were added to the resin, which was slowly rotated for 2 hours at room temperature. The resin was then washed three times with 200µl of coupling buffer, followed by washing with 200µl of quenching buffer. Sodium cyanoborohydride (3µl) and quenching buffer (200µl) were then added to the resin, which was rotated slowly at room temperature for 15 minutes. The resin was then washed six times with 150µl of wash buffer. Platelet lysates (500-1000µg) were added to the resin containing spin columns and incubated at 4°C overnight with gentle rotation. The resin-immobilised protein complexes were then eluted from the resin using 50µl of elution buffer and collected in a sample tube using centrifugation at 1000xg for 1 minute. The eluted proteins were then prepared for SDS-PAGE analysis with the addition of 1mM Dithiothreitol (DTT) and a 5x lane marker.

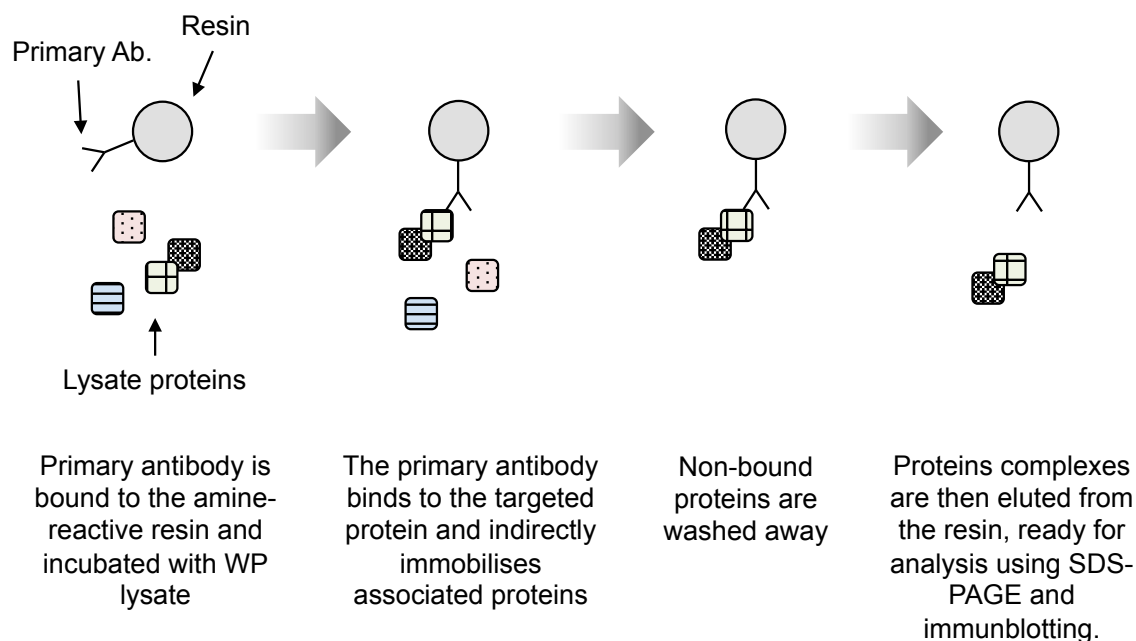


**Figure 2.2. Co-immunoprecipitation procedure.** Schematic representing the amine-reactive resin based co-immunoprecipitation system.

### 2.5.6 Enrichment of cAMP binding proteins using cAMP linked agarose beads

The cAMP agarose pull-down assay is a technique used to enrich cAMP binding proteins from cell lysates (Wang et al., 2001). In this assay, cell lysates are incubated with cAMP coated agarose beads. Proteins that directly or indirectly bind cAMP are immobilised onto the beads, namely PKA type I, PKA type II, AKAPs and PKA substrates. These beads are then isolated using centrifugation and washing in TBS-Tween. The cAMP-bound proteins are then eluted from the beads and prepared for SDS-PAGE and immunoblotting analysis with the addition of Laemmli buffer.

In this assay, platelet samples were prepared as in section 2.5, lysed in lysis buffer and immediately placed on ice. The protein concentration of each sample was

then measured using a Bio-Rad DC Bradford assay kit, as described in section 2.5.2. cAMP coated beads were pelleted by centrifugation at 1000xg for 1 minute and suspension supernatant removed. The bead pellet was re-suspended in lysis buffer at a ratio of 3:1 (w/v) and centrifuged again at 1000xg for 1 minute, repeated twice. The beads were then re-suspended in lysis buffer at a ratio of 1:1 (w/v). Using an automatic pipette with a wide tip, 50µl of beads were added to 1mg of sample lysate and incubated with gentle rotation overnight at 4°C. Samples were then centrifuged at 1500xg for 1 minute. The supernatant was carefully removed and stored at -20°C for analysis using SDS-PAGE and immunoblotting. The bead pellet was re-suspended and washed with 100µl of TBS-Tween with gentle inversion, followed by centrifugation at 1500xg for 1 minute, repeated twice. After the third wash cycle, the bead pellet was re-suspended in Laemmli buffer (50µl) ready for analysis by sodium dodecyl sulphate-polyacrylamide gel electrophoresis (SDS-PAGE) and immunoblotting.

### **2.6 Sodium dodecyl sulphate-polyacrylamide gel electrophoresis**

SDS-PAGE is a technique for separating proteins by molecular weight and charge using electrophoresis and a polyacrylamide gel support.

First, Laemmli buffer is used to lyse cells, denature proteins and apply a negative charge to each protein through the chemical action of SDS (Laemmli, 1970). The platelet proteins are further denatured by the presence of 2-mercaptoethanol, which breaks disulphide bonds. These fully denatured protein samples, existing in a primary conformation, can be then be loaded into porous polyacrylamide gels assembled from long chains of acrylamide molecules cross-linked by N, N-methylene bis-acrylamide (bis). The percentage of acrylamide used in the gels

construction is proportional to its molecular pore size. Application of an electrical current to the gel causes the negatively charged proteins to migrate through the gel pores. Protein migration is directly determined by charge and molecular weight. The separated protein can then be transferred to a PVDF membrane for immunoblotting or stained for direct protein visualisation.

In this study, 10% and 18-10% gradient 1.5mm thick resolving acrylamide gels were used for electrophoresis (tables 2.2 and 2.3). After 1 hour setting time, a 3% acrylamide stacking gel was added, with well-forming combs, and left to set for 30 minutes (table 2.4). The constructed gels were placed into a Bio-Rad\Mini Protean 3 cell electrophoresis tank and immersed in running buffer (192mM glycine, 25mM Tris base, 0.1% SDS (w/v)). Platelet samples were then loaded into individual wells; 20µg for whole cell samples and 50µl for IP samples. Each gel was also loaded with 10µl of biotinylated marker. A constant voltage of 120V was applied across the gel using a Bio-Rad power pack 300 for 2 hours.

**Table 2.1: Reagents required for Buffer 1 and 2**

Reagent	Buffer 1	Buffer 2
SDS	(0.4% w/v)	(0.4% w/v)
Tris base	1.5M	0.5M

**Table 2.2: Reagents required for two 18-10% polyacrylamide gradient gels**

Reagent	18%	10%
Acrylamide	1.961ml	1.182ml
Distilled water	0.708ml	1.418ml
Buffer 1	0.886ml	0.886ml
Ammonium persulphate (10% w/v)	18 $\mu$ l	18 $\mu$ l
TEMED	2 $\mu$ l	2 $\mu$ l

**Table 2.3: Reagents required for two 10% polyacrylamide gels**

Reagent	10%
Acrylamide	6.4ml
Distilled water	5.3ml
Buffer 1	4ml
Ammonium persulphate (10% w/v)	75 $\mu$ l
TEMED	5.3 $\mu$ l

**Table 2.4: Reagent required for two stacking gels**

Reagent	3%
Acrylamide	0.75ml
Distilled water	4.87ml
Buffer 2	1.87ml
Ammonium persulphate (10% w/v)	75 $\mu$ l
TEMED	10 $\mu$ l

## 2.7 Immunoblotting

Immunoblotting enables the identification of proteins through the ability of antibodies to recognise specific protein epitopes. Following SDS-PAGE, proteins are electrophoretically transferred and immobilised onto polyvinylidene difluoride (PVDF) membranes based on hydrophobic interactions that occur between the membrane and proteins. The PVDF membranes are then probed with primary antibodies that bind to proteins via specific epitopes (table 2.5). A secondary antibody, which recognises and binds to the primary antibody, is then added to the membrane. The secondary antibody is conjugated to a detection molecule, usually either HRP (horseradish peroxidase) enzymes or fluorescence emitting dyes. In the case of HRP, the addition of  $H_2O_2$  and luminol to the HRP enzyme results in the emission of light (428 nm), which can be detected by photographic films. In the case of fluorescence emitting dyes, the signal is detected using an electronic imaging system. In this study, HRP was used as the detection method for the majority of immunoblots, however towards the latter end of the study fluorescence emitting dyes were used in conjunction with the Odyssey<sup>TM</sup> CLx electronic imaging system.

Gels were removed from the electrophoresis tank and placed within a Trans-blot Turbo<sup>TM</sup> mini PVDF transfer pack. The transfer pack was then inserted into a Bio-Rad Trans-blot Turbo<sup>TM</sup> transfer system for 10 minutes. After transfer, the gel was discarded and PVDF membranes placed in blocking buffer (20ml per membrane) containing either 5% (w/v) bovine serum albumin (BSA) or 10% (w/v) powdered milk in TBS-tween for 30 minutes, to reduce non-specific antibody binding. Blocked membranes were incubated with the primary antibody diluted in TBS-

tween containing 2% BSA (w/v) overnight with mild shaking. Following incubation, membranes were washed twice for 10 minutes in TBS-tween with mild shaking.

In the case of HRP detection, the HRP-conjugated secondary antibody was diluted in 10ml TBS-tween at 1/10000 (v/v) containing 1/2000 (v/v) anti-biotin and then added to the membranes for 1 hour with mild shaking. Membranes were washed six times for 10 minutes each in TBS-tween with mild shaking. ECL 1 (100mM Tris base, 250mM luminol, 90mM p-coumaric acid) and ECL 2 (100mM Tris base, 30% H<sub>2</sub>O<sub>2</sub> (v/v)) at a ratio of 1:1 (v/v) were then applied to the membranes. After 90 seconds incubation in the dark with mild shaking, membranes were placed into an exposure cassette. The cassette was transported to a specially prepared dark room where X-ray film was exposed to the membrane for 60 seconds and then developed in Kodak developer and Kodak fixer solutions.

In the case of fluorescent dye detection, fluorescent dye-conjugated secondary antibodies were diluted in 10ml TBS-tween 1/15000 (v/v) and added to the membranes for 1 hour with mild shaking, protected from the light. Membranes were then washed six times for 10 minutes each in TBS-tween, protected from the light, and then imaged using the Odyssey<sup>TM</sup> CLx electronic imaging system from LI-COR. Resulting files were saved onto a memory stick for subsequent data analysis.

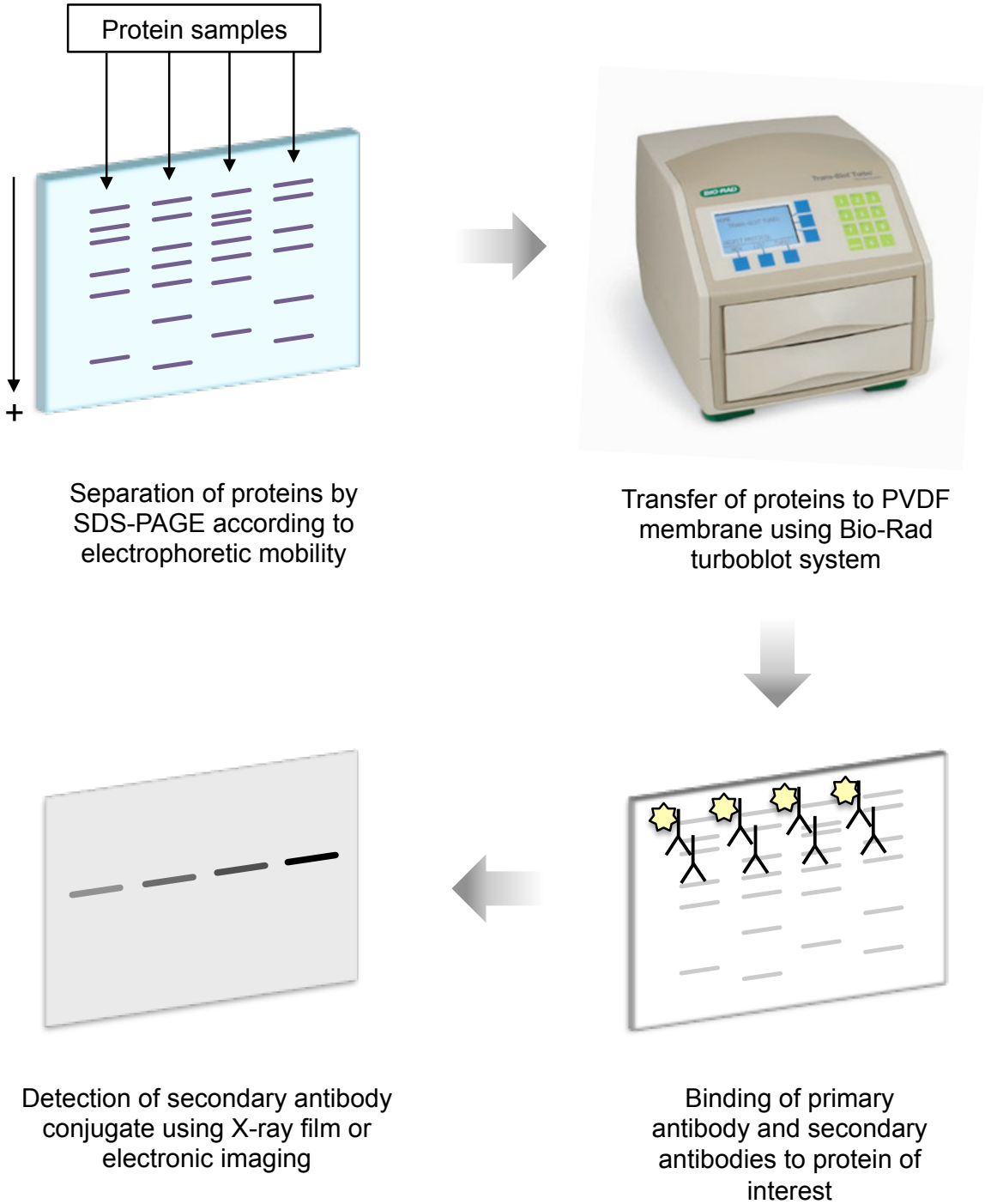


**Figure 2.3. Analysis of proteins using SDS-PAGE and immunoblotting.** This schematic describes the analysis of denatured sample proteins using SDS-PAGE and immunoblotting.

**2.7.1 Stripping PVDF membranes and re-probing**

Membrane stripping describes the removal of primary and secondary antibodies from a PVDF membrane while leaving the immobilised cellular proteins attached. The membrane can then be re-probed with primary antibodies for additional proteins of interest. This technique enables multiple immunoblots from one membrane. Following signal detection, membranes were washed twice in TBS-tween for 15 minutes. Membranes were then washed in stripping buffer (0.2M glycine, 1g SDS (w/v), 1% TBS -tween (v/v)) heated to 50°C for two 15 minute washes. The stripping buffer was removed with two 5 minute washes in TBS-tween. Membranes were blocked with either BSA or milk and re-probed with a new primary antibody.

Table 2.5: Antibodies used in experimentation

Antibody target	Species	Manufacturer	Experimental concentrations
Goat IgG	Rabbit	Santa Cruz Biotechnology	1:10,000 (v/v) IB
CD41	Mouse	Abd serotec	1:100 (v/v) FC
Mouse IgG	Sheep	Amersham	1:10,000 (v/v) IB
PDE2A	Goat	Santa Cruz Biotechnology	1:1000 (v/v) IB
PDE3A	Sheep	MRC-PPU reagents	1:1000 (v/v) IB 1:300 (w/w) IP
PDE3A Ser <sup>312</sup>	Sheep	MRC-PPU reagents	1:250 (v/v) IB
PDE3A Ser <sup>428</sup>	Sheep	MRC-PPU reagents	1:250 (v/v) IB
PDE3A Ser <sup>465</sup>	Sheep	MRC-PPU reagents	1:250 (v/v) IB
PDE5	Rabbit	Santa Cruz Biotechnology	1:1000 (v/v) IB
Phospho-PKA substrate	Rabbit	Cell Signalling Technology	1:1000 (v/v) IB
PKA catalytic subunit	Mouse	Cell Signalling Technology	1:1000 (v/v) IB
PKA RI	Mouse	Cell Signalling Technology	1:1000 (v/v) IB
PKA RII	Mouse	Cell Signalling Technology	1:1000 (v/v) IB
PKG	Rabbit	Enzo life sciences	1:1000 (v/v) IB
Rabbit IgG	Goat	Amersham	1:10,000 (v/v) IB
sGC $\alpha$	Rabbit	Sigma-Aldrich Company Ltd	1:1000 (v/v) IB
sGC $\beta$	Rabbit	Sigma-Aldrich Company Ltd	1:1000 (v/v) IB
Sheep IgG	Rabbit	Upstate Technology	1:10,000 (v/v) IB
SLP-76	Sheep	Upstate Technology	1:1000 (v/v) IB
VASP Ser <sup>157</sup>	Rabbit	Cell Signalling Technology	1:1000 (v/v) IB
VASP Ser <sup>239</sup>	Rabbit	Cell Signalling Technology	1:1000 (v/v) IB
$\beta_3$	Rabbit	Santa Cruz Biotechnology (USA)	1:1000 (v/v) IB
$\beta$ -tubulin	Mouse	Millipore	1:1000 (v/v) IB

## 2.8 cAMP immunoassay

In this study, a commercially available cAMP enzyme immunoassay (EIA) from GE Healthcare was used to quantify platelet intracellular cAMP concentrations. We selected this assay from a number of competitors as it was sensitive enough for platelets (25 – 6400 cAMP fmol/well), non-radioactive and comparatively fast with experiments completed in 12 hours. This system measures cAMP through the competition between cAMP in a platelet sample and a fixed quantity of peroxidase-labelled cAMP, for a limited number of binding sites on a cAMP-specific antibody coated inside a well. The bound peroxidase-labelled cAMP is then visualised using a H<sub>2</sub>O<sub>2</sub> containing enzyme substrate and absorbance read at 630nm as a measure of platelet sample cAMP concentrations (Figure 2.4).

Washed platelets ( $2 \times 10^8$ /ml) were stimulated with agonists and inhibitors for selected time intervals and lysed with 10x lysis buffer 1A (2.5% dodecyl trimethylammonium in assay buffer). Next, 100µl of each sample was diluted in 100µl of antiserum solution and then added to the wells of a 96 well plate in duplicate, as per manufacturer's instructions, alongside non-specific binding and blank controls. The plate was incubated for exactly 2 hours at 4°C with gentle shaking. After incubation, 50µl of cAMP-peroxidase conjugate was then added to each well and incubated for 1 hour at 4°C with gentle shaking. Next, the wells were washed with 400µl of wash buffer, repeated four times. To each well, 150µl of the H<sub>2</sub>O<sub>2</sub> containing enzyme substrate was added, resulting in the development of a blue colour that was read at 630nm using a TECAN Infinite™ M200 microplate reader. The readings were then plotted against an AMP stand curve as a measurement of platelet intracellular cAMP concentrations and adjusted for cell count.

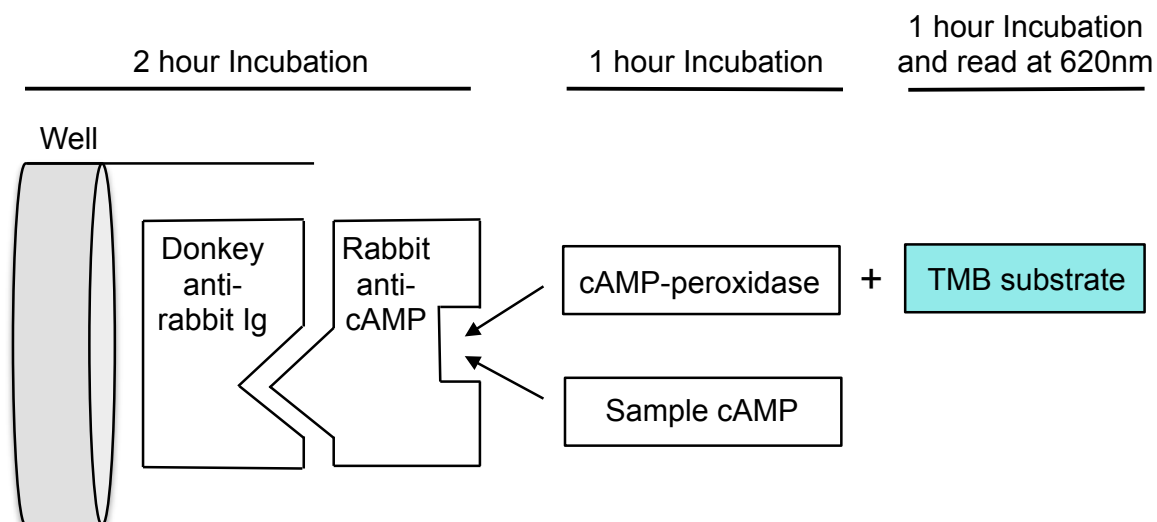


**Figure 2.4. cAMP immunoassay procedure.** Schematic representation of the cAMP enzyme immunoassay procedure.

## 2.9 Phosphodiesterase activity assay

To measure intracellular PDE activity we used a commercially available non-radioactive colorimetric assay developed by ENZO life sciences. The basis of this assay is the hydrolysis of cAMP or cGMP into 5'AMP and 5'GMP by PDEs. These 5'nucleotides, 5'AMP and 5'GMP, are then cleaved into a nucleoside and phosphate by 5'nucleotidase, harvested from snake venom. The phosphate is then detected by a BIOMOL GREEN<sup>TM</sup> reagent that changes colour from a pale yellow to strong green. The colour change is read using a microplate reader set at 620nm, as a measure of PDE activity. In our experiments, PDEs were purified for use in the assay using immunoprecipitation, as phosphates free within lysate samples caused high background readings.

Washed platelets ( $5 \times 10^8$ /ml) were stimulated with agonists and inhibitors for selected time intervals, lysed in 2x PDE extraction buffer (150mM sodium chloride,

50mM HEPES, 20% glycerol (v/v), 10% Igepal (v/v), 1mM, EDTA, 1:200 phosphatase inhibitor cocktail (v/v), protease inhibitor cocktail 1:100 (v/v)) and immediately placed on ice. The protein content of each sample was then calculated using a Bio-Rad DC Bradford assay kit, as described in section 2.5.2. Exactly 25µl of protein A or G beads, dependent on the PDE primary antibody selected, and 1µg of the primary anti-PDE antibody were then added to each lysate containing 500µg of protein. Alongside the anti-PDE antibody containing samples, an IgG (1µg) control sample was also created to account for background phosphates. Samples were incubated for 3 hours with slow rotation at 4°C. The beads were then centrifuged at 1000xg and washed in 250µl of ice-cold assay buffer supplemented with 1:200 phosphatase inhibitor cocktail (v/v), protease inhibitor cocktail 1:100 (v/v). This washing step was repeated three times to ensure removal any non-specifically bound proteins. The beads were then incubated with 30µl of assay buffer, 10µl of 5'-nucleotidase and 10µl of cAMP (0.5mM) or cGMP (0.5mM) substrate, specifically in that order so the reaction begins with the final addition of cAMP/cGMP substrate. PDE inhibitors were added directly to reaction vessels, as the inhibitors would wash off during the immunoprecipitation procedure. Following the addition cAMP/cGMP, reaction vessels were slowly rotated at 37°C for 1 hour. Reaction vessels were then centrifuged for 1 minute at 1000xg to sediment the beads, and the resulting supernatant (50µl) transferred to a 96 well plate containing 100µl of BIOMOL GREEN reagent, which terminated the reaction. The 96 well plates were gently rotated at room temperature to allow the green colour, representing PDE activity, to develop. The 96 well plate was then read at 620nm using a TECAN infinite

M200 microplate reader. The readings were plotted against a 5'AMP/GMP stand curve as a measurement of PDE activity.

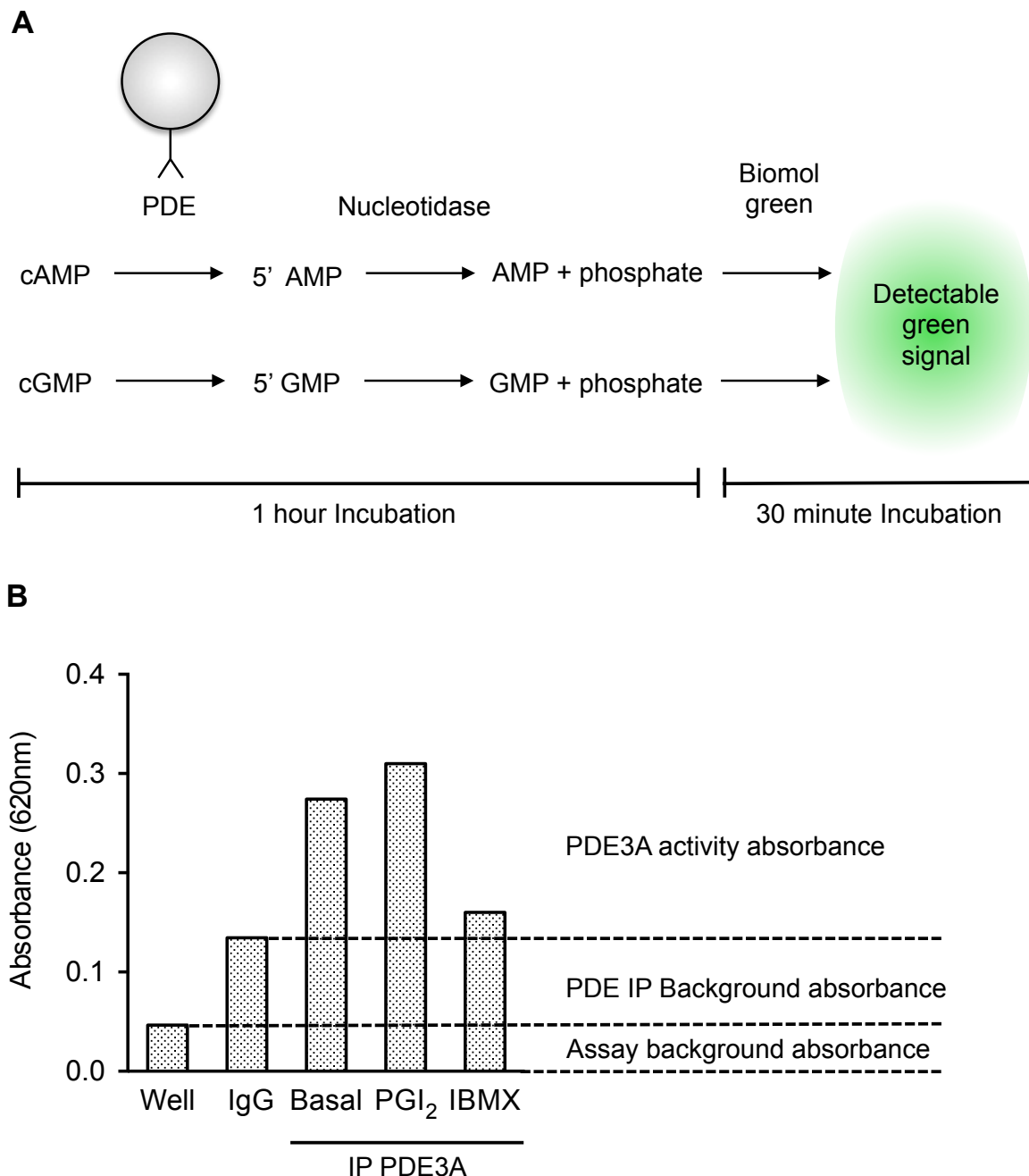


**Figure 2.5. PDE activity assay procedure.** (A) Schematic representation of the PDE activity assay procedure. (B) Graph representing the data from one PDE3A activity assay experiment.

**2.10 Protein kinase A activity assay**

In this study, associated PKA activity was measured using a non-radioactive kit from Promega. Briefly, protein immunoprecipitates are incubated with cAMP to activate associated PKA and release its catalytic subunits. The catalytic subunit containing supernatant is then incubated with a brightly coloured, fluorescent and highly specific synthetic PKA substrate kemptide (Macala et al., 1998). Kemptide phosphorylation by the PKA catalytic subunits changes its net charge from +1 to -1. Phosphorylated and non-phosphorylated kemptide can then be readily separated by electrophoresis on an agarose gel. The band representing phosphorylated (negatively charged) kemptide is then excised and solubilised. PKA activity is quantified by measuring the absorbance of the solubilized phosphorylated kemptide at 570nm, following manufactures protocol. In this thesis, PKA activity experiments were carried out by Dr. Zaher Raslan.

**2.11 Proximity ligation assay**

Protein-to-protein interactions were examined *ex vivo* using a Duolink™ proximity ligation assay from Sigma-Aldrich. This assay utilises both antibody and DNA properties to detect, quantify and obtain the cellular localisation of specific protein interactions within a single experiment (Gullberg et al., 2003). In this system, washed platelets are first fixed, permeabilised and mounted onto poly-L-lysine-coated coverslips. The fixed platelets are then incubated with two primary antibodies raised from different species that are specific to the proteins of interest. Following antigen recognition, two species-specific secondary antibodies called PLA probes are then added to the platelets, with each probe conjugated to a unique short DNA sequence. Two additional DNA strands called connector

oligonucleotides are introduced alongside the PLA probes. Close proximity of the proteins of interest, within 30-40nm, brings together the two unique short DNA strands, which are then ligated together with the connector oligonucleotides through the addition of a reaction mixture to form a single stranded DNA circle. Following formation of the DNA circle, DNA polymerase present in the reaction mixture produces a long DNA sequence through rolling circle amplification on the DNA circle. This sequence is then recognised by fluorescently labelled DNA probes resulting in a specific detectable signal that can be analysed using microscopy. In this thesis, platelets were also counterstained with a fluorescent lectin to visualise the cells. Proximity ligation experiments were carried out by Dr. Zaher Raslan.

### **2.12 MEG-01 cell culture**

MEG-01 cells are a megakaryocyte-like cell line used to study human megakaryocyte cells, proplatelet formation and platelet release. The cells derive from the bone marrow of a 55-year-old Japanese male with chronic myelogenous leukaemia (Ogura et al., 1985). In this study, we used MEG-01 cells to examine PDE isoform expression and cAMP signalling pathways in megakaryocytes.

#### **2.12.1 MEG-01 cell thawing**

A frozen vial of MEG-01 cells was taken from liquid nitrogen storage and thawed in a water bath set at 37°C. The contents of the vial were then gently pipetted into a 20ml universal tube containing 5ml of reconstituted RPMI medium (500ml RPMI 1640 medium, 50ml fetal bovine serum (FBS), 5ml L-glutamine fortified with

penicillin and streptomycin). The tubes were then centrifuged at 1000g for 5 minutes at 20°C to harvest the cells. The supernatant was then carefully removed and the cell pellet suspended in 1ml of reconstituted RPMI medium. Cells were stained with Trypan blue and then counted with a haemocytometer for viability and cell number. Trypan blue is a vital stain that selectively colours dead cells blue based on the principle that living cells possess intact membranes that exclude the dye (Strober, 2001).

### 2.12.2 MEG-01 cell counting and assessment

An equal volume of MEG-01 cell suspension was mixed with Trypan blue, typically 20µl of cell suspension with 20µl Trypan blue. The mix of MEG-01 cells and Trypan blue was then gently pipetted, avoiding any air bubbles, underneath a cover slip resting on a haemocytometer slide. Non-stained cells were then counted under a microscope using the 10x objective lens and then calculated for cells/ml with the following equation:

$$\text{Cells/ml} = \left( \frac{\text{Average viable cell count in 5 large}}{\text{haemocytometer squares}} \right) \times \text{dilution factor} \times 10^4$$

### 2.12.3 MEG-01 cell maintenance and differentiation

Having counted for viable cells, MEG-01 cells were pipetted into a T75 culture flask containing 15ml of reconstituted RPMI medium at a cell count  $\leq 2 \times 10^5$  cells/ml. Cell containing flasks were then incubated at 37°C, 5% CO<sub>2</sub> for 2-3 days. Following incubation, flasks were taken out the incubator and viewed for cell confluency. If cells were sufficiently confluent, then the culture medium and cells

were extracted into a 20ml universal tube using a pipette. Tubes were then centrifuged at 1000xg to pellet the cells. The supernatant medium was carefully removed using a pipette and MEG-01 cells suspended in 5ml of fresh reconstituted RPMI medium. The cells were then counted, as described in section 2.13.2. Cells were then pipetted into 20ml of fresh reconstituted RPMI medium at a count of  $2-4 \times 10^5$  cells/ml and then incubated at 37°C, 5% CO<sub>2</sub> for 2-3 days. The extra MEG-01 cells produced in the incubation cycle were then used immediately for experimentation. Phorbol diesters can be used to differentiate MEG-01 cells into more mature megakaryocyte-like cells exhibiting megakaryocyte morphology, ultrastructure and functional changes (Ogura et al., 1988). In these experiments, cultures were stimulated with phorbol-12-myristate-13-acetate (PMA; 100nM) and incubated at 37°C 5% CO<sub>2</sub> for 24 hours, prior to use.

### **2.13 MEG-01 FACS analysis**

FACS (fluorescence-activated cell sorting) analysis is a technique used to measure various individual cell characteristics within a population. In this method, a flow cytometer machine hydrodynamically focuses cells from a loaded sample into a single stream, which is then passed through several lasers beams. As cells move through the lasers, the flow cytometer analyses the cells for granularity, measured by the scattering of light, and size, measured by forward scattered light. In addition to these characteristics, any pre-incubated fluorescent antibodies present on the cell surface are excited by the lasers to produce detectable signals. These signals are then read by the flow cytometer. These data can then be analysed using specially designed software.

MEG-01 cells (100 $\mu$ l of  $2 \times 10^5$  cells/ml) were added to sample tubes containing 5 $\mu$ l of FITC conjugated CD41 antibody or IgG control antibody. The sample tubes were gently mixed and incubated in the dark for 20 minutes. MEG-01 cells were then fixed with 0.5ml of formyl saline (0.2%, v/v) for 30 minutes at room temperature. Using a BD LSR Fortessa<sup>TM</sup>, fixed MEG-01 cells were analysed for CD41 expression, with 10,000 events being recorded for each sample.

### 2.14 Statistical analysis

Data expressed as mean  $\pm$  SEM, were compared using Students t-test and one-way ANOVA. Statistical tests were performed using GraphPad Prism 6 (GraphPad Software, La Jolla, CA). Significance was accepted at  $P < 0.05$ .

## 3 Characterisation of platelet and megakaryocyte phosphodiesterases

### 3.1 Introduction

Blood platelets are critical in preventing haemorrhage in the event of vessel trauma. Under physiological conditions, platelets circulate in a quiescent state maintained by the endothelium-derived anti-thrombotic factors prostacyclin (PGI<sub>2</sub>) and nitric oxide (NO) (Jin et al., 2005). These endogenous platelet inhibitors exert their effects through cyclic nucleotide signalling cascades. Ligation of PGI<sub>2</sub> to the Gs-protein coupled IP receptor, present on the platelet surface, results in activation of transmembrane adenylyl cyclases and the synthesis of cAMP from adenosine triphosphate (ATP). NO diffuses through the platelet membrane and activates cytosolic soluble guanylyl cyclase to synthesise cGMP from guanosine triphosphate (GTP). Elevations in cAMP and cGMP concentrations lead to the activation of localised protein kinase A (PKA) and protein kinase G (PKG), respectively. These serine-threonine kinases phosphorylate proteins that regulate and inhibit key mechanisms of platelet activation (Schwarz et al., 2001).

Cyclic nucleotide signalling is a highly organised cellular process tightly regulated in space and time by phosphodiesterases (PDEs) (Zaccolo and Pozzan, 2002). These enzymes hydrolyse cyclic nucleotides into inactive 5'AMP and 5'GMP metabolites. Platelets express three PDE isoforms: phosphodiesterase 2A (PDE2A), cAMP-specific phosphodiesterase 3A (PDE3A) and cGMP-specific phosphodiesterase 5 (PDE5). The hydrolytic activity of these enzymes can be

influenced through cyclic nucleotide binding and protein phosphorylation, however, these mechanisms are poorly understood in platelets.

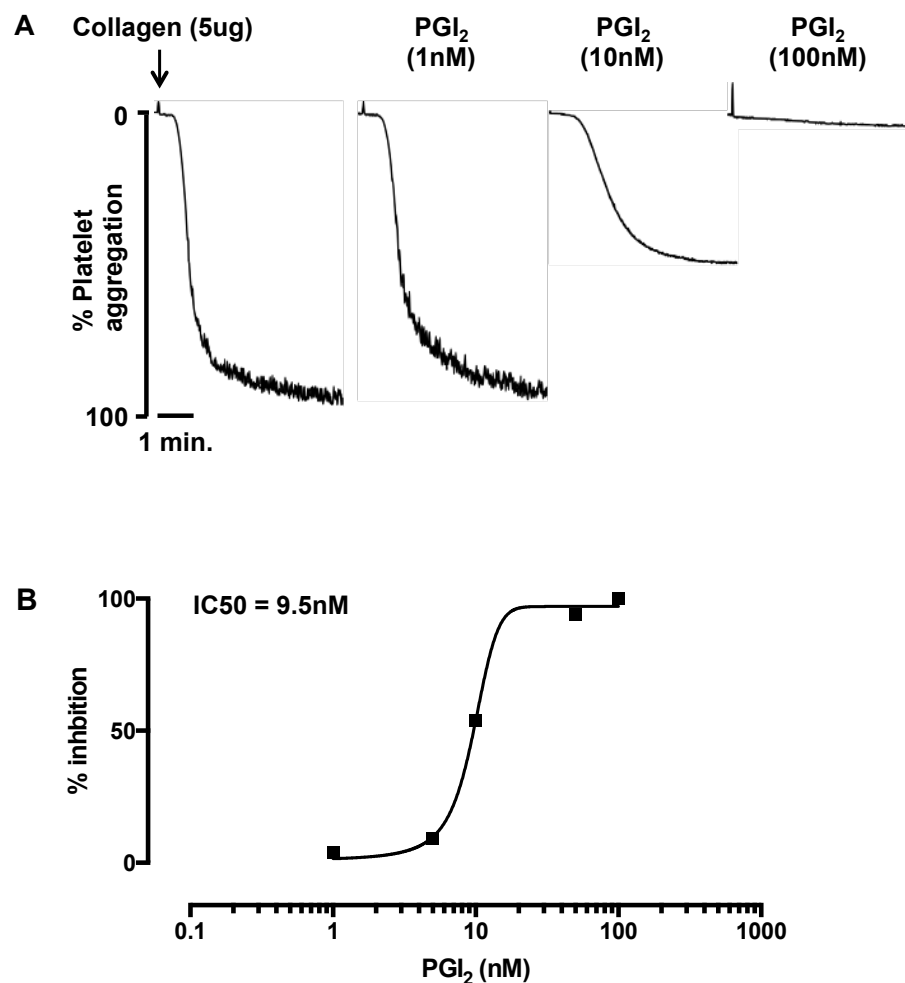
The major aim of this study is to understand PDE3A signalling in human platelets. In this first chapter, we aimed to characterise all three platelet PDE isoforms in terms of expression, subcellular localisation and activity in platelets and explored their presence in the established MEG-01 megakaryocyte cell line.

More specifically the objectives were to:

- Characterise the expression and subcellular localisation of PDE2A, PDE3A and PDE5 in platelets.
- Optimise a PDE activity assay that can successfully measure platelet PDE activity.
- Explore PDEs and cyclic nucleotide signalling in the MEG-01 megakaryocyte cell line.

### 3.2 PGI<sub>2</sub> inhibits platelet activation

In order to preserve cyclic nucleotide signalling pathways, washed platelets were prepared using the established pH method (Mustard et al., 1989). This method of platelet isolation avoids unwanted platelet activation during centrifugation steps by lowering the pH of PRP to 6.4. To validate our platelet preparation protocol we examined the functionality of both activatory and inhibitory pathways using light transmission aggregometry (LTA) (Figure 3.1). Washed platelets were stimulated with collagen (5µg/ml) for 5 minutes, which induced an aggregation response of 96%. This response was similar to other studies where platelets had been isolated using different methods (Radomski et al., 1988; Vargas et al., 1982). We next preincubated washed platelets for 1 minute with a PGI<sub>2</sub> concentration range and measured their functional response to collagen. The collagen response was inhibited by PGI<sub>2</sub> in a dose dependent manner with full platelet inhibition at 100nM and an IC<sub>50</sub> value of 9.5nM. These data are comparable to studies performed by Aburima and colleagues, in which thrombin-induced platelet shape change was inhibited in a dose dependent manner by prostaglandin (PGE<sub>1</sub>) (Aburima et al., 2013).



**3.1. Washed platelet aggregation responses to PGI<sub>2</sub>.** WP ( $2.5 \times 10^8$  platelets/ml) were stimulated with collagen ( $5 \mu\text{g/ml}$ ) in the presence and absence of PGI<sub>2</sub> (2 min. incubation). Aggregation traces were recorded for 5 minutes with stirring (1000rpm) at 37°. (A) Shown are representative aggregation traces generated by aggroLink software (B) Data presented as dose response curve of 1 experiment.

### 3.3 Platelet PDE isoform expression

Having confirmed that washed platelets are functionally responsive to collagen and PGI<sub>2</sub>, we next sought to characterise platelet PDE expression and determine their subcellular localisation (Figure 3.2). To achieve this, we used PDE isoform-specific antibodies in combination with SDS-PAGE and immunoblotting to search for PDE2A, PDE3A and PDE5 expression in whole platelet lysates and platelet lysates separated into membrane and cytosolic fractions.

#### 3.3.1 Human platelets express PDE2A, PDE3A and PDE5

First, washed platelet lysates were immunoblotted for PDE2A, PDE3A and PDE5 expression. Increasing amounts of platelet lysates were separated by SDS-PAGE and immunoblotted for PDE isoforms. We detected protein bands for PDE2A, PDE3A and PDE5A. The apparent molecular weights of these PDE protein bands were approximately 105kDa, 110kDa and 100kDa for PDE2A, PDE3A and PDE5, respectively. Furthermore, the molecular weights of the PDE protein bands matched the PDE protein bands from positive control tissues that were established in the literature to express the same isoforms; brain lysate for PDE2A, heart lysate for PDE3A and smooth muscle lysate for PDE5 (Bender and Beavo, 2006). However, the band signal for the positive controls was relatively weak in comparison to the platelet lysates. This could be attributed to the preparation and age of these lysates as they were obtained from collaborative labs at an adjusted protein concentration of 1mg/ml. The bottom panel shows  $\beta$ -tubulin as evidence for equal loading. These data confirm that human platelets express PDE2A, PDE3A and PDE5.

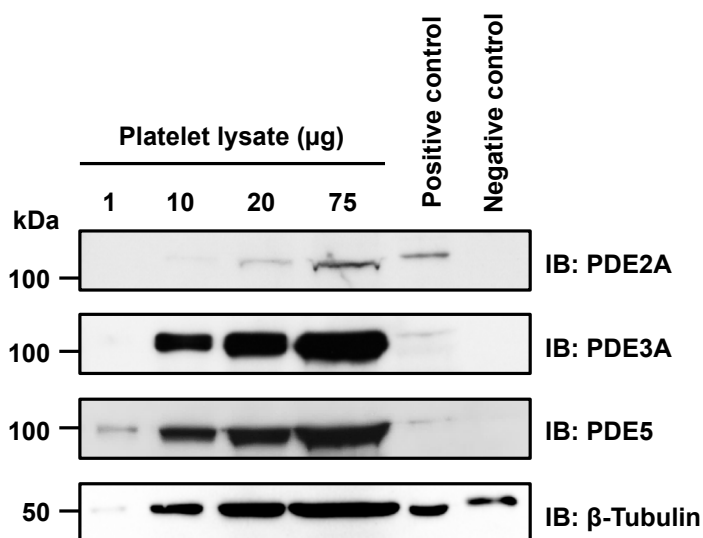


**Figure 3.2. Analysis of phosphodiesterase isoform expression in human platelets.** WP ( $5 \times 10^8$  cells/ml) lysates were immunoblotted for PDE2A, PDE3A and PDE5 with  $\beta$ -tubulin as a loading control. Brain, heart and smooth muscle lysates were used as positive controls and lung, heart and macrophage lysates were used as negative controls for PDE2A, PDE3A and PDE5 respectively. Immunoblot membranes were stripped and reprobbed for  $\beta$ -tubulin as a protein loading control. Data representative of 3 independent experiments.

### 3.3.2 Platelet PDE isoforms are differentially localised within the cell

We next sought to determine the subcellular localisation of these PDE isoforms in platelets. A well-established method for examining protein localisation in cells is cellular fractionation, in which cells are snap frozen, lysed and centrifuged into their membrane and cytosolic protein fractions (Castle, 2004). The fractions are then analysed for protein expression using SDS-PAGE and immunoblotting. We employed this technique to examine PDE isoform expression in platelet membrane and cytosolic fractions (Figure 3.3). In the top panel, we detected PDE2A expression primarily in platelet membrane fraction at 105kDa. We also detected a non-specific band with a molecular weight of 140kDa. This band may represent a protein that has degraded during the fractionation process, unmasking an epitope that was non-specifically recognised by the anti-PDE2A antibody. The second panel shows PDE3A expression detected in the membrane and cytosolic fractions at slightly different molecular weights, between 100kDa and 115kDa. Membrane localised PDE3A was expressed at high levels when compared to the expression of PDE3A in the cytosol. This comparable low expression of cytosolic PDE3A made it difficult to detect its representative protein band at 10 $\mu$ g without over exposing the bands representing membrane localised PDE3A. PDE5 expression in the middle panel was detected as equally expressed between the cytosol and membrane fractions. The lower panels show expression of the cytosolic protein SLP-76 and membrane protein  $\beta_3$  to ensure successful separation of platelet fractions (Kim et al., 2009; Silverman et al., 2006). Together these data reveal that PDE2A, PDE3A and PDE5 are differentially localised within human platelets.

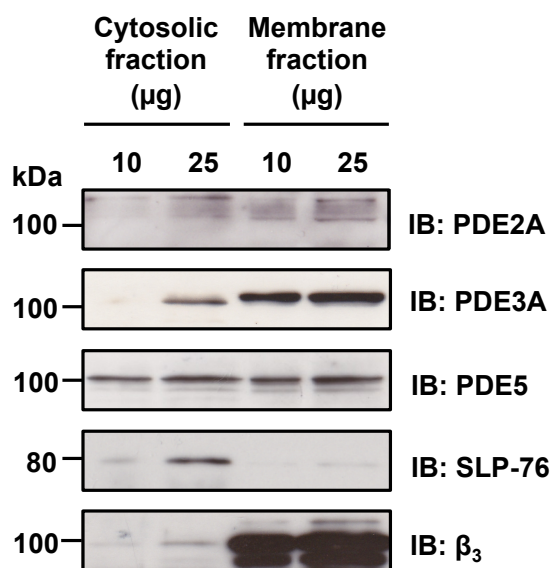


**Figure 3.3. Subcellular PDE expression in human platelets.** WP ( $7 \times 10^8$  cells/ml) lysates were fractionated into cytosolic and membrane fractions using centrifugation and immunoblotted for PDE2A, PDE3A and PDE5. Immunoblot membranes were stripped and re-probed for cytosolic protein SLP-76 and membrane protein  $\beta_3$  as fraction controls. Data representative of 3 independent experiments.

### 3.3.3 Characterisation of platelet PDE3A splice variants

Splice variants of PDE3A have been identified in heart cells, differing in molecular mass, subcellular localisation and regulation (Vandeput et al., 2013; Wechsler, 2002). We investigated the expression of PDE3A splice variants in platelets using a combination of molecular techniques (Figure 3.4). In these experiments polyacrylamide gels were set at an increased run time and lower temperature to further separate platelet proteins and increase band definition, enabling greater visualisation of potential PDE3A splice variants.

First, PDE3A was purified from platelet lysates using immunoprecipitation and analysed by SDS-PAGE and immunoblotting. Immunoblot analysis of separated PDE3A Immunoprecipitates resulted in two distinct PDE3A bands detected at 100kDa and 115kD. Next, we cross-validated our MRC-PPU anti-PDE3A antibody, targeted to the conserved region of PDE3A, with an antibody obtained from Santa Cruz, targeted towards the PDE3A C-terminus, to ensure that our immunoblotting signal was specific for PDE3A. The PDE3A doublet band was observed in immunoblot experiments using both PDE3A antibodies with a weaker signal generated using the Santa Cruz antibody. Lastly, platelet cytosolic and membrane fractions were immunoblotted for localisation of potential PDE3A splice variants. Under fractionation conditions, the top PDE3A band was localised specifically to the platelet membrane fraction and lower band to primarily the cytosol with a trace in the membrane. These data suggest the presence of two PDE3A splice variants of 100kDa and 115kDa, and that they may be differentially localised under basal conditions.

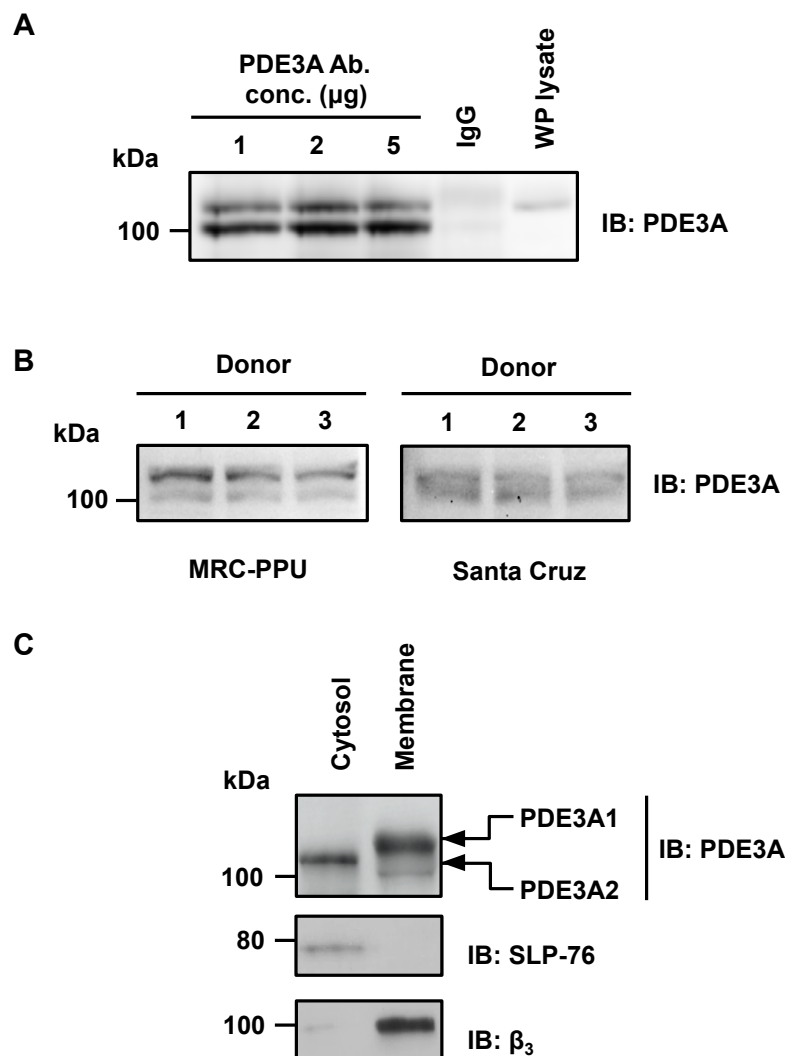


**Figure 3.4. PDE3A splice variants.** (A) PDE3A was immunoprecipitated from washed platelet lysates (500µg) and immunoblotted for total PDE3A. (B) WP ( $5 \times 10^8$  cells/ml) lysates were immunoblotted for PDE3A (C) WP lysates ( $7 \times 10^8$  cells/ml) were fractionated using ultra centrifugation and immunoblotted for PDE3A. Immunoblot membranes were stripped and re-probed for the membrane protein  $\beta_3$  and cytosolic protein SLP-76 as fraction controls. All polyacrylamide gels were run for an extended period of time of 4 hours at  $4^\circ\text{C}$  to promote increased protein band separation. (A, C) data representative of 3 independent experiments (B) data representative of 1 independent experiment.

### 3.4 Characterisation of platelet responses to PDE inhibition

Having examined platelet PDE isoform expression, we next measured role of PDE isoforms, using a range of inhibitors, in platelet aggregation (Figure 3.5). Due to the spectrum of important functional roles PDEs play in the human body, a number of isoform-specific PDE inhibitors have been developed for use in research and clinical settings (Lugnier, 2006). Here, washed platelets were treated with either an isoform-specific or non-selective PDE inhibitor for 20 minutes. We then examined the effects of these inhibitors on collagen-induced aggregation and on the inhibition of collagen-induced aggregation by PGI<sub>2</sub> and NO.

Stimulation with collagen (5µg/ml) induced maximal platelet aggregation at 89±3% light transmission (LT), reduced to 52±2% in the presence of PGI<sub>2</sub> (10nM) ( $p<0.01$ ). Treatment of washed platelets with the PDE2A inhibitor erythro-9-(2-hydroxy-3-nonyl)adenine (EHNA) (20µM) significantly reduced collagen-induced platelet aggregation to 62±2% LT ( $p<0.01$ ). This inhibitory response was marginally increased to 46±4% when used synergistically with PGI<sub>2</sub>. These data show that inhibition of PDE2A can blunt platelet activation in response to collagen, however, PDE2A inhibition did not synergise with PGI<sub>2</sub>. Treatment with the PDE3A inhibitor milrinone (10µM) reduced collagen-induced platelet aggregation to 30±4% LT ( $p<0.01$ ). This inhibitory effect of milrinone was significantly more potent than that of EHNA ( $p<0.01$ ), supporting previous reports that milrinone exerts a greater inhibitory effect on platelet activation when compared to the effect of EHNA (Manns et al., 2002). When milrinone was used synergistically with PGI<sub>2</sub>, the inhibitory effect of PGI<sub>2</sub> on collagen-induced platelet activation was significantly potentiated to near maximal platelet inhibition at 5±1% LT ( $p<0.01$ ). These findings

show that inhibition of PDE3A can strongly enhance the effects of PGI<sub>2</sub>. Treatment of washed platelets with GSNO reduced collagen-induced platelet aggregation to 37±4% LT ( $p<0.01$ ), whereas inhibition of PDE5 with zaprinast (10µM) had little effect on platelet aggregation at 80±8% LT. However when used synergistically, zaprinast significantly potentiated the inhibitory effect of GSNO on collagen-induced platelet aggregation at 16±1% LT ( $p<0.05$ ). These data suggest the PDE5 does not exert much influence on basal cGMP levels but instead regulates cGMP elevations in response to activation of the cGMP signalling pathway. Inhibition of all platelet PDE isoforms with IBMX (10µM) completely inhibited collagen-induced platelet aggregation to 6±2% LT ( $p<0.01$ ). Data from this experiment shows that inhibition of PDE isoforms can modify platelet functional responses to endogenous platelet inhibitors and collagen.

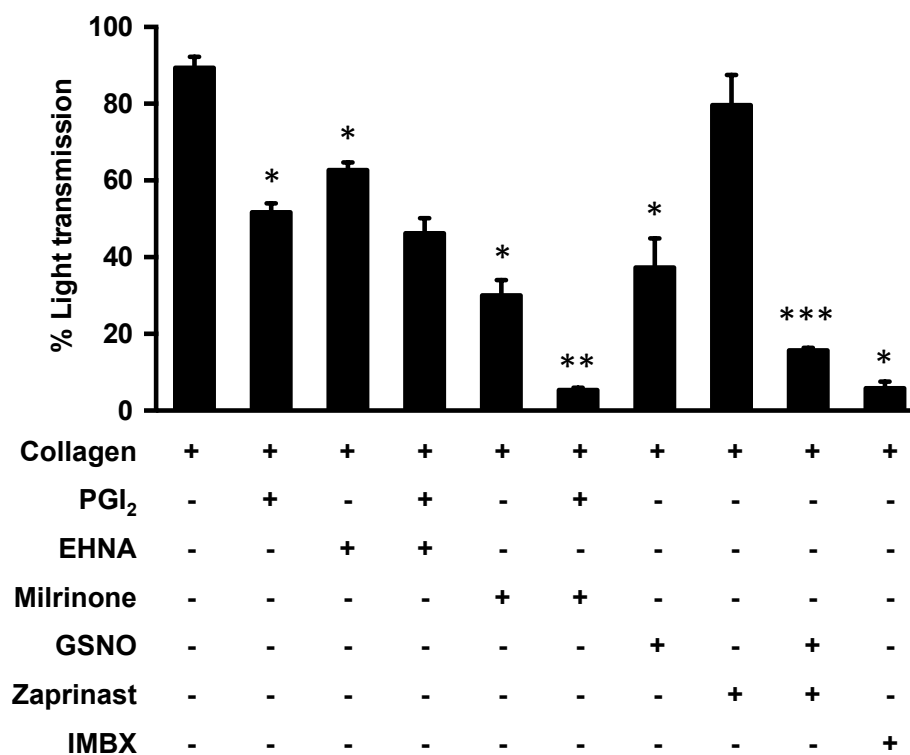


**Figure 3.5. Characterisation of PDE inhibitory effects on platelet aggregation.** WP ( $2.5 \times 10^8$  platelets/ml) were incubated with the PDE inhibitors milrinone ( $10 \mu\text{M}$ ), EHNA ( $20 \mu\text{M}$ ), ( $10 \mu\text{M}$ ,) and IBMX ( $10 \mu\text{M}$ ) for 20 minutes prior to stimulation with collagen ( $5 \mu\text{g/ml}$ ) in the presence and absence of PGI<sub>2</sub> ( $10 \text{nM}$ , 2 minute incubation) or GSNO ( $50 \mu\text{M}$ , 2 minutes). Aggregation traces were recorded for 5 minutes with stirring ( $1000 \text{rpm}$ ) at  $37^\circ$ . Data are from 3 independent experiments represented as means  $\pm$  SEM. \* $P < 0.01$  compared with collagen. \*\* $P < 0.01$  compared with collagen + PGI<sub>2</sub>. \*\*\* $P < 0.05$  compared with collagen + GSNO.

### 3.5 The activity of PDEs in platelets

In the next set of experiments, we wished to confirm PDE activity in human platelets. The traditional method for measuring PDE activity is a two-step radiometric assay. This assay detects PDE activity by direct binding of radiolabeled cyclic nucleotide hydrolysis products, either AMP or GMP, to specially prepared resin. The immobilised radioactive hydrolysis products are then quantified using scintillation counting (Thompson and Appleman, 1971). There are alternative methods of measuring PDE activity available based on multiple step enzyme systems, luminescence and colorimetric changes. In this thesis, we used a commercially available colorimetric assay that quantifies PDE activity using a reagent that changes colour when in the presence of the phosphate produced from the cleavage of either 5'-AMP or 5'-GMP by 5'-nucleotidase. This assay first required optimization before platelet PDE activity could be quantified.

#### 3.5.1 The activity of purified PDE1

The first optimization step was to quantify the activity of commercially purified PDE1 (Figure 3.6). Although absent in platelets, PDE1 is ubiquitously expressed throughout the human body with the ability to hydrolyse both cAMP and cGMP (Bender and Beavo, 2006). With this assay, we observed that PDE1 hydrolysed cAMP in a concentration and time-dependent manner. Data from this experiment shows that this assay system can successfully quantify PDE activity.

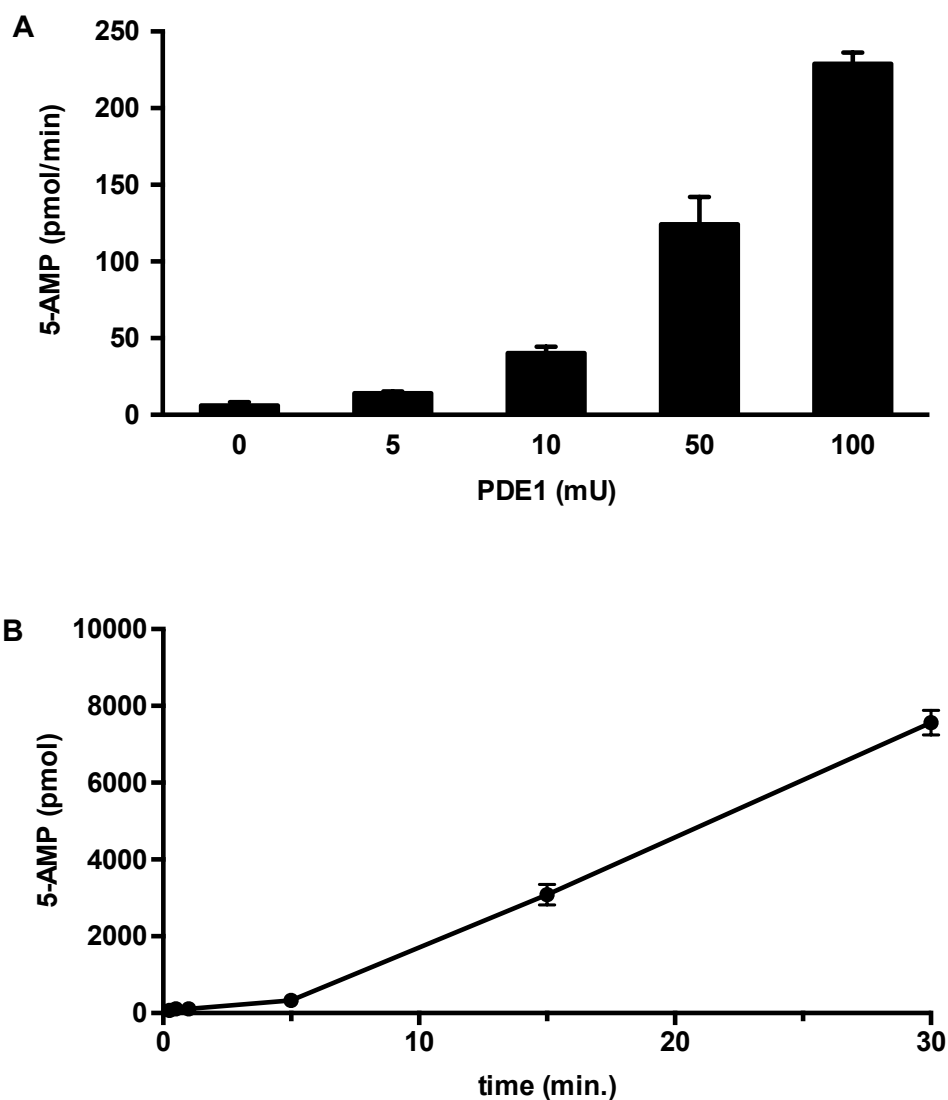


**Figure 3.6. PDE1 dose response and time course of cAMP hydrolysis.** (A) Duplicate PDE1 enzyme samples at selected concentrations were incubated with cAMP (200 $\mu$ M) and 5'-nucleotidase (50 kU/well) at 30°C for 30 minutes (B) PDE1 enzyme (100mU) was incubated with cAMP (200 $\mu$ M) and 5'-nucleotidase (50 kU/well) at 30°C for selected time intervals. Reactions were terminated by addition of 100 $\mu$ l of BIOMOL® GREEN and read at 620nm after 30 minutes. Absorbance at OD620nm was converted to pmol of 5'-AMP using a standard curve. Shown are graphs for 3 independent experiments expressed as means  $\pm$  SEM.

### 3.5.2 PDE activity assay optimisation for use in human platelets

Next, we tested the assay using human platelets to see if we could successfully quantify platelet cAMP-specific PDE activity (Figure 3.7). Three different assay inputs were prepared including platelet rich plasma (PRP) lysates, washed platelet lysates and PDE3A immunoprecipitated from platelet lysates.

In basal PRP lysates and basal washed platelet lysates, we detected cAMP hydrolysis rates of  $2602 \pm 54$  pmol/h 5-AMP and  $2605 \pm 10$  pmol/h 5-AMP, respectively. However, these readings did not change in the presence of  $\text{PGI}_2$  (100nM) or IBMX (10 $\mu$ M), suggesting that these data were an artefact of intracellular platelet phosphates in both PRP and washed platelet samples. The Biomol green reagent in this assay is a highly sensitive phosphate detection solution that quantifies PDE activity by measuring the phosphate product from the cleavage of 5'-nucleotides, the output of cyclic nucleotide hydrolysis, in the assay system. Any external phosphates from labware and reagent solutions or, in this case samples, greatly increases background absorbance. In immunoprecipitated PDE3A samples a basal activity of  $1949 \pm 66$  pmol/h 5-AMP over an IgG reading of  $1139 \pm 28$  pmol/h 5-AMP was recorded (\* $P < 0.01$ ). Stimulation of washed platelets with  $\text{PGI}_2$  increased PDE3A hydrolysis rate to  $2551 \pm 7$  pmol/h 5-AMP over IgG (\*\* $P < 0.05$ ). In the presence of IBMX (10 $\mu$ M), added directly to reaction vessels, PDE3A activity was reduced to  $436 \pm 84$  pmol/h 5-AMP (\* $P < 0.01$ ). These data show that this assay system can successfully quantify platelet PDE3A activity, that there is significant basal activity sensitive to IBMX and that this activity can be increased by  $\text{PGI}_2$ .

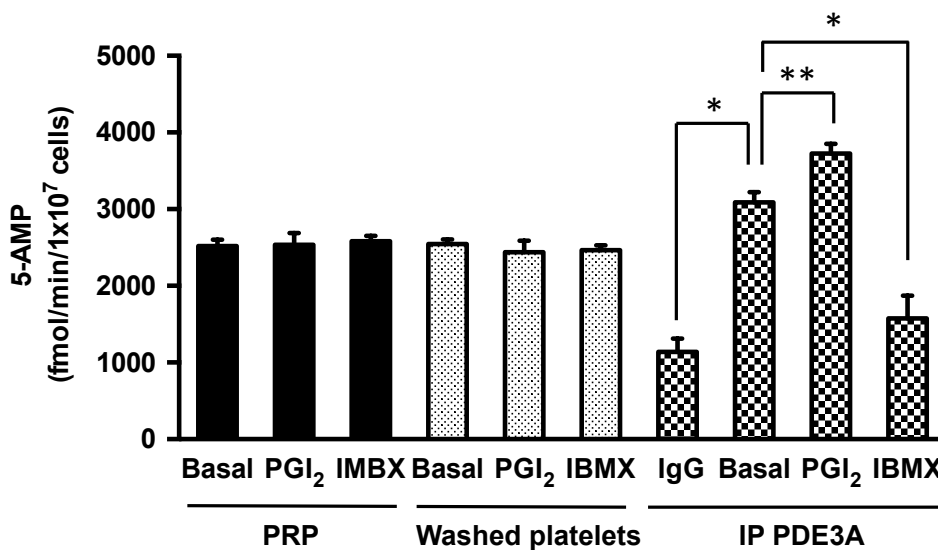


**Figure 3.7. Optimisation of PDE activity assay to measure platelet PDE3A activity.** PRP ( $5 \times 10^8$  cells/ml) and WPs ( $5 \times 10^8$  cells/ml) were stimulated with PGI<sub>2</sub> (100nM, 2 minutes) or IBMX (10 $\mu$ M, 20minutes) and lysed in PDE assay lysis buffer. PRP (5 $\mu$ l), WPs (5 $\mu$ l) and immunoprecipitated PDE3A from WPs (2 $\mu$ g antibody, 500 $\mu$ g protein) were incubated with cAMP (200 $\mu$ M) and 5'-nucleotidase (50 kU/vessel) at 30°C for 60 minutes. Reactions were terminated by addition of 100 $\mu$ l of BIOMOL® GREEN and read at 620nm after 30 minutes. Shown are representative graphs for 3 independent experiments expressed as means  $\pm$  SEM (\* $P$ <0.01, \*\* $P$ <0.05).

### 3.5.3 Characterisation of PDE2A, PDE3A and PDE5 activity in platelets

Having optimised the PDE activity assay for use in platelets, we sought to investigate the activity of all PDE isoforms using this system. This was achieved by immunoprecipitating each PDE isoform from platelets under stimulated and non-stimulated conditions and quantifying the hydrolysis of either cAMP or cGMP for PDE2A, cAMP for PDE3A and cGMP for PDE5 (Figure 3.8). These data were then plotted on the same graph to compare nucleotide hydrolyse rates between platelet PDE isoforms. PDE Immunoprecipitates used in the activity assays were analysed by SDS-PAGE and immunoblotting to confirm successful immunoprecipitation.

Our data show that PDE2A isolated from resting washed platelets had a hydrolysis rate of  $1542 \pm 155$  fmol 5-AMP/GMP/min/ $1 \times 10^7$  cells when incubated with cGMP and cAMP. PDE3A activity was increased from  $3149 \pm 161$  to  $3894 \pm 141$  fmol 5-AMP/ min/ $1 \times 10^7$  under PGI<sub>2</sub> (100nM) stimulated conditions. Stimulation of washed platelets with GSNO (50 $\mu$ M) greatly increased PDE5 activity from  $2699 \pm 139$  to  $7853 \pm 942$  fmol 5-GMP/min/ $1 \times 10^7$  cells. The activity of all PDE isoforms was inhibited by addition of IBMX (10 $\mu$ M) to reaction vessels ( $\pm$  representative of range) (Figure 3.8 A, n=2). All three PDE isoforms were successfully immunoprecipitated for use in the activity assay (Figure 3.8 B, n=1). Together these data show that platelet PDE activity varies between each isoform in resting platelets and platelets stimulated with activators of cyclic nucleotide signalling cascades.

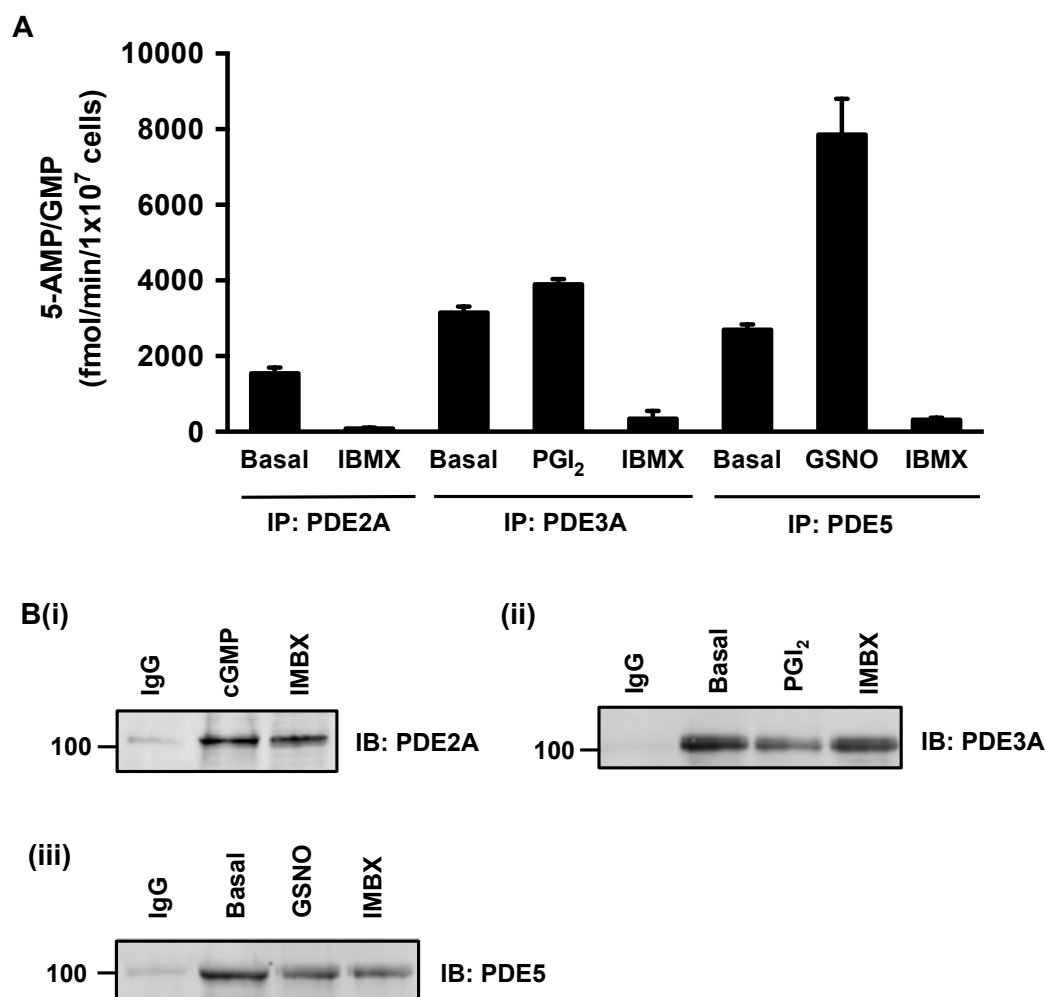


**Figure 3.8. Quantification of platelet PDE isoform activity.** (A) PDE2A, PDE3A and PDE5 were immunoprecipitated (2 $\mu$ g antibody, 500 $\mu$ g protein) from basal, PGI<sub>2</sub> (100nM, 2 min) and GSNO (50 $\mu$ M, 2 min) stimulated WPs. Immunoprecipitates were incubated with both cAMP (100 $\mu$ M) and cGMP (100 $\mu$ M) for PDE2A or cAMP (200 $\mu$ M) for PDE3A and cGMP (200 $\mu$ M) for PDE5. Reaction vessels were incubated with 5'-nucleotidase (50kU/vessel) at 30°C for 60 minutes. Reactions were terminated by addition of 100 $\mu$ l of BIOMOL® GREEN and read at 620nm after 30 minutes (B) Immunoprecipitates from activity assay were immunoblotted for PDE2A, PDE3A and PDE5. (A) Graph of 2 independent experiments represented as means $\pm$ range (B) data from 1 independent experiment.

### 3.6 PDE enzymes in the megakaryocytic cell line MEG-01

Elevations in platelet cyclic nucleotide concentrations are a key mechanism of platelet inhibition. Little is known of cyclic nucleotide signalling and its regulation by PDEs in megakaryocytes. With this in mind, we wanted to explore the presence of PDEs and cyclic nucleotide signalling pathways in megakaryocytes. To achieve this, we used the established megakaryoblastic cell line MEG-01 as a model for primary megakaryocytes in our experiments (Ogura et al., 1985). This cell line has been used extensively as a model for megakaryocyte maturation and platelet formation (Battinelli et al., 2001; Lacabartz-p.Porret et al., 2000), with capacity to differentiate morphologically, ultrastructurally and biochemically into more mature megakaryocytes when stimulated with phorbol 12-myristate 13-acetate (PMA) (Ogura et al., 1988). Before using these cells in experimentation, we wanted to validate our MEG-01 differentiation protocol with megakaryocyte surface markers and morphological studies.

#### 3.6.1 MEG-01 cells express the megakaryocyte marker CD41

CD41 (GPIIb, integrin  $\alpha$ IIb) is an integral membrane protein specifically expressed on the surface of platelets and megakaryocytes. This surface protein was used as a marker for MEG-01 cell differentiation (Figure 3.9). MEG-01 cells were stimulated with a PMA concentration range for 24 hours and analysed by FACS for CD41 expression.

Under non-stimulated conditions, 10% of MEG-01 cells expressed CD41. CD41 expression peaked at 30% with 100nM of PMA. This expression declined with higher concentrations of PMA. Consistent with the literature, these data show that

MEG-01 differentiation can be induced by PMA stimulation. The optimal PMA concentration of 100nM was selected for future experimentation.

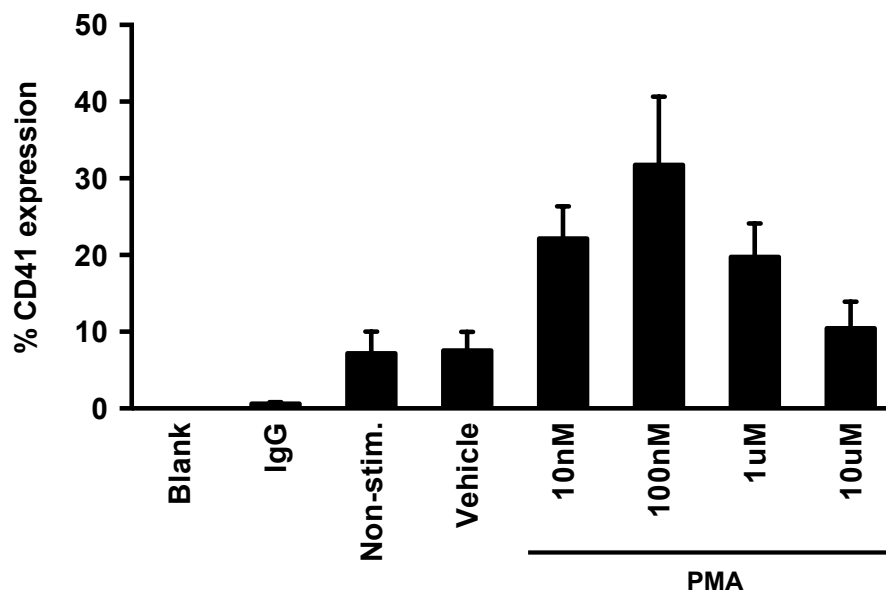


**Figure 3.9. CD41 expression in MEG-01 cells.** MEG-01 cells  $2-4 \times 10^5$  cells/ml were cultured in suspension in reconstituted RPMI 1640 medium at  $37^\circ\text{C}$ , 5%  $\text{CO}_2$ . Once confluent, MEG-01 cells were stimulated with PMA at different concentrations for 24 hours at  $37^\circ\text{C}$ , 5%  $\text{CO}_2$ . Cells were then analysed for CD41 expression using fluorescence-activated cell sorting (FACS). Shown is a representative graph of 3 independent experiments represented as means  $\pm$  SEM.

**3.6.2 MEG-01 cells exhibit megakaryocyte morphology**

Following the confirmation of MEG-01 CD41 expression, we sought to visually assess the morphology of these cells under non-stimulated and PMA stimulated conditions (Figure 3.10). Under non-stimulated conditions, MEG-01 cells were high in number, uniformly spherical and grouped into small clusters (Figure 3.10, Ai). These cells were easily washed off the tissue culture plates (Figure 3.10, Bi). Stimulation with PMA resulted in low numbers of differentiated MEG-01 cells displaying larger more granular cell bodies with long projections and membrane buddings (Figure 3.10, Aii). These differentiated cells tightly adhered to culture flasks with spread-like morphology (Figure 3.10, Bii). The results of this experiment show that PMA can induce the differentiation of MEG-01 cells into mature megakaryocytes.

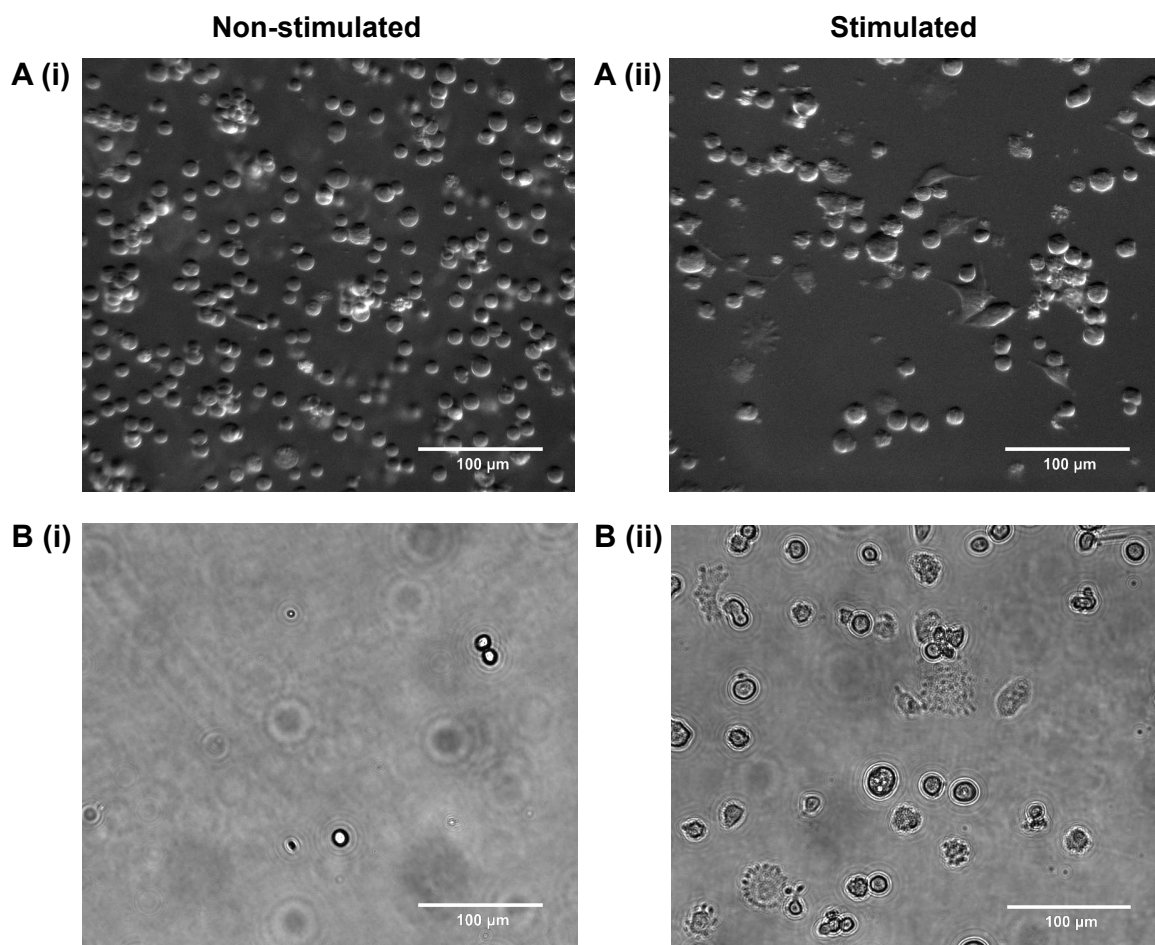


**Figure 3.10. Brightfield microscopy of MEG-01 cell morphology and culture flask adhesion.** (A) Non-stimulated (i) and PMA stimulated (ii) MEG-01 cells were visualised for morphological changes using light microscopy. (B) Non-stimulated (i) and PMA-stimulated (ii) MEG-01 culture flasks were gently washed with PBS and analysed for adherent MEG-01 cells using light microscopy. Shown are representative images of 2 independent experiments.

### 3.6.3 MEG-01 signalling responses to PGI<sub>2</sub> and the nitric oxide donor GSNO

Next, the ability of these cells to respond to cyclic nucleotide elevating agents was examined (Figure 3.11). An established marker of cyclic nucleotide signalling events is PKA substrate phosphorylation. MEG-01 cells were stimulated with the adenylyl cyclase activator forskolin (10 $\mu$ M), PGI<sub>2</sub> (100nM) and GSNO (50 $\mu$ M), and analysed for phosphorylation of vasodilator-stimulated phosphoprotein (VASP) and PKA substrate phosphorylation using SDS-PAGE and immunoblotting.

Non-differentiated MEG-01 cells responded to forskolin and PGI<sub>2</sub> with increases in VASP Ser<sup>157</sup>, Ser<sup>239</sup> and PKA substrate phosphorylation. In contrast, GSNO stimulation reduced PKA substrate phosphorylation to below basal levels. In differentiated MEG-01 cells, we detected VASP Ser<sup>157</sup> phosphorylation under basal conditions. This was attributed to the activation of PKC by PMA used to differentiate the MEG-01 cells, which is known to phosphorylate VASP Ser<sup>157</sup>. Stimulation with forskolin and PGI<sub>2</sub> increased VASP Ser<sup>239</sup> phosphorylation and surprisingly reduced PKA substrate phosphorylation. GSNO stimulation inhibited VASP Ser<sup>157</sup>, Ser<sup>239</sup> and PKA substrate phosphorylation. The PKA substrate profiles of MEG-01 cells were not comparable to those in human platelets. Data from this experiment shows that MEG-01 cells respond to cyclic nucleotide elevators.

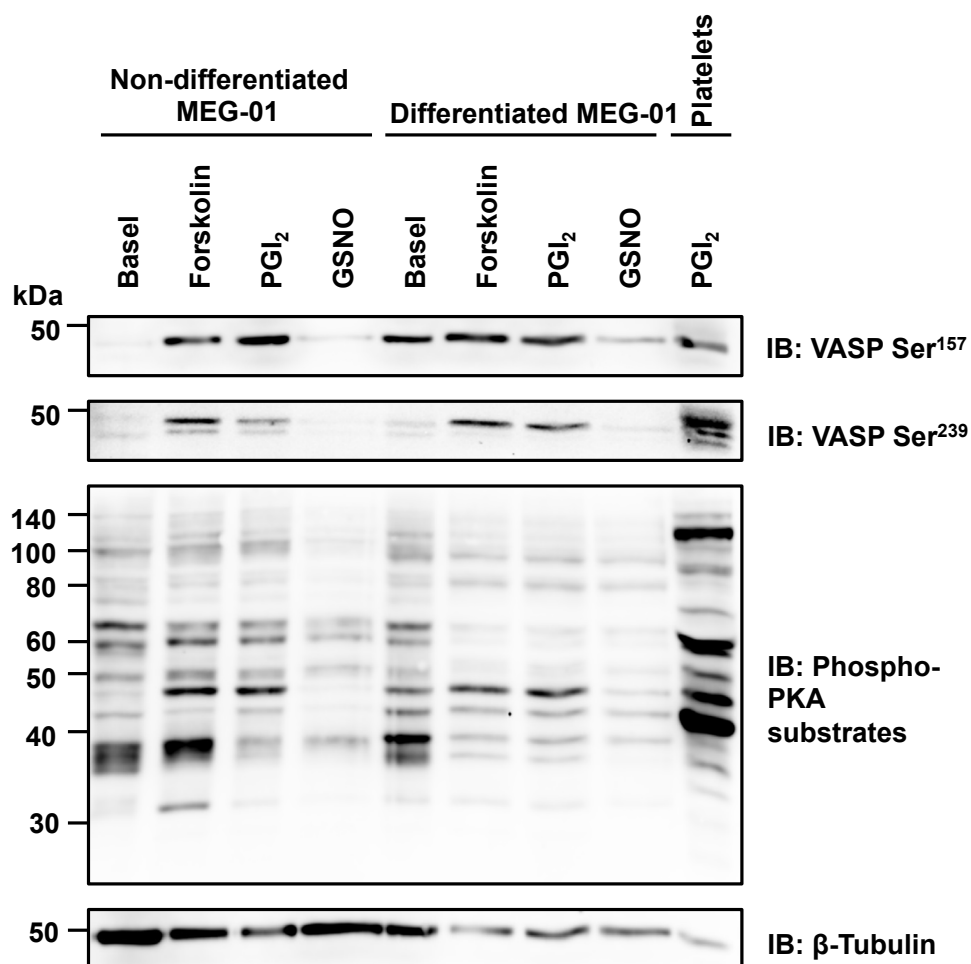


**Figure 3.11. PKA signalling in MEG-01 cells.** Non-differentiated and PMA-differentiated MEG-01 cells ( $2 \times 10^5$  cells/ml) were stimulated with forskolin ( $10 \mu\text{M}$ , 5 min), PGI<sub>2</sub> ( $100 \text{ nM}$ , 2 min) and GSNO ( $50 \mu\text{M}$ , 2 min) and immunoblotted for VASP Ser<sup>157</sup>, VASP Ser<sup>239</sup> and phosphorylated PKA substrates. WPs ( $5 \times 10^8$  cells/ml) stimulated with PGI<sub>2</sub> ( $100 \text{ nM}$ , 2 min) were immunoblotted with the same antibodies for cell comparison. β-tubulin was immunoblotted as a protein loading control. Data of one experiment.

### 3.6.4 Characterisation of PDE isoform expression in MEG-01 cells

Having validated our MEG-01 differentiation protocol and visualised MEG-01 cyclic nucleotide signalling events, we investigated the expression of phosphodiesterase isoforms and cyclic nucleotide signalling proteins (Figure 3.12). MEG-01 lysates were analysed for PDE2A, PDE3A, PDE5, PKA catalytic subunit (PKAc), PKA regulatory subunits type 1 (PKA RI) and 2 (PKA RII), soluble guanylyl cyclase  $\alpha$  (sGC $\alpha$ ) and  $\beta$  (sGC $\beta$ ), and protein kinase G (PKG) using SDS-PAGE and immunoblotting.

In non-differentiated MEG-01 cells, we detected low expression of PDE2A and PDE3A. Interestingly, no expression of PDE5 was detected. All cAMP and cGMP cyclic signalling proteins were detected with low expression of both sGC isoforms and high expression PKG when compared with platelets. In contrast, differentiated MEG-01 cells expressed low levels of PDE5 with no expression of PDE2A or PDE3A, yet displayed similar expression of cAMP and cGMP cyclic signalling proteins when compared to non-differentiated MEG-01 cells. Together these data show that differentiated MEG-01 cells express PDE5 alongside other cyclic nucleotide signalling proteins but are absent in PDE2A or PDE3A.

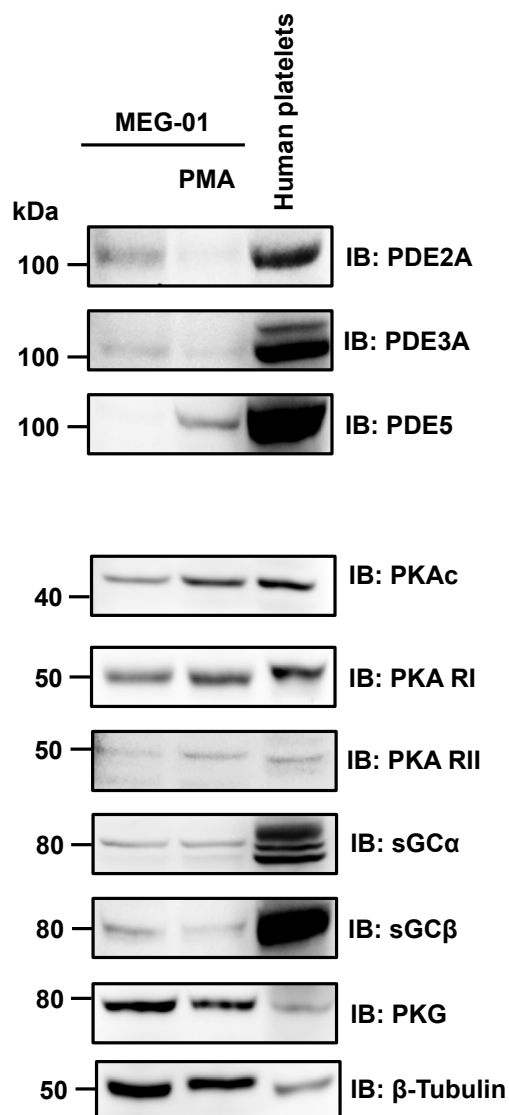


**Figure 3.12. MEG-01 expression of PDE isoforms and cyclic nucleotide signalling proteins.** Non-differentiated and differentiated MEG-01 lysates (20 $\mu$ g protein) were immunoblotted for expression of the PDE isoforms PDE2A, PDE3A, PDE5 and cyclic nucleotide signalling proteins PKAc, PKA RI, PKA RII, sGC, sGC, and PKG.  $\beta$ -tubulin was immunoblotted as a protein loading control. Data representative of three independent experiments.

### 3.7 Discussion

The first important study of platelet PDEs was that of Hidaka and Asano, who observed three distinct peaks of PDE activity in platelet lysates (Hidaka and Asano, 1976). We now know these three peaks of activity to represent the PDE isoforms PDE2A, PDE3A and PDE5, confirmed by inhibitor and proteomic studies (Burkhart et al., 2012; Haslam et al., 1999). These isoforms directly regulate platelet cyclic nucleotide concentrations in space and time, and thus platelet responses to endogenous inhibition. Recently, in other cell types, there have been exciting advances in our understanding of PDE3A signalling in terms of PDE3A splice variants, regulation, cellular localisation and protein interactions. However, PDE3A signalling in platelets is still poorly understood, yet its importance is well documented. For instance, inhibition of PDE3A is known to suppress agonist-induced platelet aggregation in concentration dependent manner (Manns et al., 2002). Deletion of PDE3A in mice results in a cardioprotective phenotype against collagen-induced thrombosis (Sun et al., 2007). Furthermore, the PDE3A inhibitors cilostazol and milrinone are currently used clinically as antiplatelet therapies (Gresele et al., 2011). The overarching aim of this thesis was to improve our understanding of PDE3A signalling in platelets.

In this chapter, we sought to characterise all three PDE isoforms in platelets and megakaryocytes. The first step in this process was to validate our platelet preparation, ensuring that platelets isolated from healthy volunteers were responsive to activatory and inhibitory stimuli. Data from figure 3.1 shows that platelets isolated by the pH method aggregated normally in response to collagen. Pre-treatment with PGI<sub>2</sub> inhibited collagen-induced platelet aggregation by 50% at

9.5nM, concurrent with previous studies (M. W. Radomski et al., 1987b; Weiss and Turitto, 1979). An important initial step was to confirm the expression of all three PDE isoforms in platelets. We detected the expression PDE2A, PDE3A and PDE5 with a weak signal for PDE2A. Compiled data sources put the ratio of platelet PDE expression at 1.00:0.17:0.04 for PDE5:PDE3A:PDE2A, which may account for the weak PDE2A signal (Burkhart et al., 2012). Current evidence strongly supports that cyclic nucleotide signalling is highly compartmentalised into discrete pools that are regulated in space and time by anchored PDEs (Lefkimmiatis and Zaccolo, 2014; Zaccolo and Pozzan, 2002), although it is unclear if this exists in platelets. With this in mind, we looked at the subcellular localisation of PDE2A, PDE3A and PDE5 to see if these enzymes were differentially localised within platelets. We showed that PDE2A and PDE3A were primarily localised to the platelet membrane fraction whereas PDE5 was equally localised between both the platelet membrane and cytosol. Interestingly, PDE3A localised to the membrane had a slightly greater mass than that of cytosolic PDE3A. Similar studies in cardiac myocytes have identified three differently localised PDE3A splice variants, PDE3A1, PDE3A2 and PDE3A3 (Hambleton et al., 2005; Wechsler, 2002). Excitingly, recent research has shown that these PDE3A splice variants are differently regulated (Vandeput et al., 2013). Thus, we investigated the possibility the presence of PDE3A splice variants in platelets. Due to the small differences in splice variant molecular weight, we ran our polyacrylamide gels for an extended time to further separate PDE3A proteins. For the first time, we suggest that platelets express the PDE3A splice variants PDE3A1 and PDE3A2, with molecular weights and subcellular localisation profiles similar to that in cardiac myocytes (Faiyaz Ahmad et al., 2015). Mass spectrometry could be used to further strengthen this observation.

In order to assess the functional significance of PDEs on platelet function, specific and non-specific PDE inhibitors were used in platelets stimulated with PGI<sub>2</sub> and the nitric oxide donor GSNO. Data from these experiments showed that inhibition of PDE2A activity elicits a minor inhibitory effect on platelet activation. In contrast, the inhibition of PDE3A induces a much stronger inhibitory effect, which is potentiated by PGI<sub>2</sub>. These data agree with earlier reports that inhibition of PDE3A has a direct effect on platelet inhibition in contrast to PDE2A inhibition that has relatively little effect (Manns et al., 2002). For PDE2A and PDE3A inhibition alone to induce platelet inhibition, adenylyl cyclase must retain some activity under non-stimulatory conditions. This is supported by studies that show adenylyl cyclase 6 is basally active in other cell types (Pieroni et al., 1995). In contrast, inhibition of PDE5 has little effect on platelet aggregation, yet greatly potentiated the inhibitory effect of NO. These data suggest that soluble guanylyl cyclase has no basal activity and under NO-stimulated conditions PDE5 plays an important role in regulating cGMP levels. Comparable platelet responses have been observed in other research teams using the PDE5 inhibitor Sildenafil and NO donor sodium nitroprusside (Wilson et al., 2008)

It was important in this work to establish a method measuring PDE hydrolytic activity in platelets. Traditionally, PDE activity is measured using a two-step radiometric assay that detects PDE activity by quantifying radiolabeled cyclic nucleotide hydrolysis products, either AMP or GMP, with a scintillation counter (Thompson and Appleman, 1971). Although scintillation counting is considered the “gold” standard for measuring PDE activity in cells, we sought to use an alternative safer method. For this study, we optimised a colourimetric assay, which quantified PDE activity using a reagent that changes colour when in the presence of either

the PDE hydrolysis products AMP or GMP. A major limitation of this assay was that it did not work in platelet lysates. This was due to background platelet phosphates reacting with the assay colour-changing reagent, which resulted in artificially high readings of PDE activity. As a consequence, all PDE isoforms were purified by immunoprecipitation for use in the assay. Findings showed that basal PDE2A hydrolysed cGMP and cAMP at a rate of 1542 fmol AMP/GMP/min/ $1 \times 10^7$  cells. Basal PDE3A activity was the highest out of all three PDE isoforms tested, with a hydrolysis rate of 3149 fmol AMP/min/ $1 \times 10^7$  cells. This activity was increased to 3894 fmol AMP/min/ $1 \times 10^7$  cells, upon stimulation with  $\text{PGI}_2$ . These data are in agreement with early reports that stimulation of platelets with  $\text{PGI}_2$  increases PDE3A catalytic activity (Grant et al., 1988; Macphee et al., 1988). Stimulation of platelets with GSNO increased PDE5 basal activity from 2699 GMP/min/ $1 \times 10^7$  cells to 7853 GMP/min/ $1 \times 10^7$  cells. However, the basal activities of PDE2A and PDE5 should be interpreted with caution, as cGMP added to the reaction vessel is known to increase their hydrolytic activity (Martins et al., 1982; Mullershausen et al., 2003). Together, these data suggest that PDE3A and PDE5 function as negative feedback regulators of  $\text{PGI}_2$  and GSNO signalling, as stimulation of these signalling cascades increases PDE hydrolytic activity. Other platelet research groups have suggested this negative feedback model of platelet inhibition (Macphee et al., 1988; Wilson et al., 2008). It would be of interest in future work to examine localised PDE activity within platelet fractions, to support the exciting concept of PDE regulated cyclic nucleotide compartments within platelets (Conti et al., 2013).

It is thought that cyclic nucleotide signalling in megakaryocytes plays important roles in thrombopoiesis (Begonja et al., 2013). Current evidence suggests that

cAMP signalling promotes megakaryocyte differentiation and suppresses platelet production, whereas cGMP signalling has no effect on megakaryocyte development but strongly promotes platelet production (Begonja et al., 2013). However, the regulation of these pathways by PDEs remains relatively unknown. To investigate this, the megakaryoblastic cell line MEG-01 was used as a model for primary megakaryocytes. Differentiation of these cells with phorbol esters induced megakaryocyte CD41 receptor expression, megakaryocyte-like morphological changes and adhesion to plastic surfaces, as described in previous studies (Ogura et al., 1988).

We have shown that MEG-01 cells are responsive to  $\text{PGI}_2$  and GSNO stimulation using markers of PKA activity in both non-differentiated and differentiated states. Interestingly, PDE expression in MEG-01 cells changed substantially upon differentiation into mature megakaryocytes. In a non-differentiated highly proliferative state, MEG-01 cells expressed PDE2A and PDE3A, whereupon differentiation only PDE5 was expressed. A possible explanation of these data can be offered by the current understanding of cyclic nucleotide signalling megakaryocytes, which suggests cAMP promotes megakaryocyte differentiation and cGMP promotes platelet production (Begonja et al., 2013). In highly proliferative MEG-01 cells, the cellular energy and resources for proliferation must be preserved through down-regulation of cell differentiation. This is shown in figure 3.10 (A), which demonstrates the featureless discoid shape of unstimulated proliferative MEG-01 cells. In this case, down-regulation of cAMP signalling pathways that promote differentiation through the up-regulation of cAMP hydrolysing PDE expression, PDE2A and PDE3A, would be of great benefit to the cell. In contrast, the down-regulation of PDE2A and PDE3A and consequent up-regulation of cAMP signalling

would help drive the cell differentiation process in PMA stimulation MEG-01 cells. However this does not explain the expression of PDE5 in differentiated MEG-01 cells, as cGMP signalling is thought to promote platelet formation. Clearly, further investigations are required to tease apart the role PDEs play in megakaryocyte cyclic nucleotide signalling.

In conclusion, data in this chapter has described the characteristics of all three platelet PDE isoforms and explored their expression in megakaryocytes. We have demonstrated that PDE2A, PDE3A and PDE5 are differentially localised between the platelet membrane and cytosol, and provided evidence for the expression of two platelet PDE3A splice variants. Furthermore, we have optimised an assay that can quantify PDE hydrolytic activity in both resting and stimulated platelets. These data provide the experimental foundation for successive chapters examining PDE3A regulation and protein interactions.

## 4 PKA-mediated regulation of PDE3A

### 4.1 Introduction

Cyclic AMP signalling downstream of prostacyclin (PGI<sub>2</sub>) is a key inhibitory pathway in blood platelets. The main effector of cAMP signalling in platelets is protein kinase A (PKA), a heterotetramer kinase constructed from a regulatory subunit dimer and two catalytic subunits. There are two PKA isoenzymes, type I and type II, both of which are expressed in platelets (Burkhart et al., 2012). Binding of cAMP to the PKA regulatory subunits triggers the disassociation of two PKA catalytic subunits that go on to phosphorylate over 100 different platelet proteins (Beck et al., 2014). Together, these phosphorylation events are thought to underlie the inhibition of platelet activatory signalling pathways, ultimately preserving platelets in their quiescent state, and in some cases reversal of transient platelet activation (Schwarz et al., 2001).

There are numerous studies identifying these substrates and deciphering the effect PKA-mediated phosphorylation has on their function (Smolenski, 2012). One of these identified substrates is PDE3A, the main regulator of platelet cAMP levels. Phosphorylation of PDE3A is thought to contribute to enzyme regulation since hydrolytic activity increases upon phosphorylation. This was proposed to form a negative feedback loop for cAMP signalling (Grant et al., 1988; Macphee et al., 1988). It has also been suggested that PDE3A phosphorylation influences the enzymes interaction with multi-protein complexes and proteins that regulate its function (Faiyaz Ahmad et al., 2015). Studies by Vandeput and colleagues showed that PDE3A splice variants in cardiac myocytes are differentially phosphorylated

and regulated by PKA (Vandeput et al., 2013). To date, there is only one PKA-specific PDE3A phosphorylation site that has been identified in platelets at Ser<sup>312</sup> (Hunter et al., 2009). This chapter aims to fully characterise PDE3A phosphorylation by PKA and determine its specificity, in terms of PDE3A splice variants.

More specifically the objectives were to:

- Characterise the effect of PGI<sub>2</sub> on platelet cAMP levels and PKA activity.
- Characterise PDE3A phosphorylation and activity in response to PKA activation.
- Identify the specificity of PDE3A phosphorylation by PKA.

## 4.2 PGI<sub>2</sub> elevates intracellular platelet cAMP concentrations

PGI<sub>2</sub> exerts its platelet inhibitory effect through ligation of the Gs-protein coupled IP receptor and subsequent activation of adenylyl cyclase (AC) to synthesise cAMP (Siegl et al., 1979; Tateson et al., 1977). In this first experiment, we wanted to characterise the platelet cAMP signalling response to PGI<sub>2</sub> and the adenylyl cyclase activator forskolin (Figures 4.1 and 4.2). Synthesised from the Indian Coleus plant (*Coleus forskohlii*), forskolin is a direct activator of AC isoforms 1-8, but not of 9, used extensively in research to raise levels of cAMP through a receptor-independent manner (Seamon et al., 1981). Forskolin activates AC by binding to the AC catalytic heterodimer within a highly conserved hydrophobic pocket (Tang and Hurley, 1998). We investigated intracellular cAMP responses using a commercially available cAMP enzyme immunoassay. This assay is based on the competition between the cAMP present in a platelet sample and a fixed quantity of peroxidase-labeled cAMP for a limited number of binding sites on a cAMP-specific antibody. Here, cAMP levels were measured in washed platelets stimulated with both PGI<sub>2</sub> and forskolin concentration ranges and two PGI<sub>2</sub> time profiles (10nM, 100nM).

### 4.2.1 PGI<sub>2</sub> and forskolin elevate cAMP levels in a dose dependent manner

Washed platelets maintained a basal cAMP level of 130±32 fmol cAMP/1x10<sup>7</sup> cells (Figure 4.1 A). Upon stimulation with a low concentration of PGI<sub>2</sub> (10nM), cAMP levels increased to 653±111 fmol cAMP/1x10<sup>7</sup> cells ( $p<0.05$ ), whereas stimulation with a high concentration of PGI<sub>2</sub> (1µM) increased cAMP levels to 2556±260 fmol cAMP/1x10<sup>7</sup> cells after 1 minute ( $p<0.01$ ). Elevations in cAMP appeared to plateau

at  $\sim 2500$  fmol cAMP/ $1 \times 10^7$  cells when washed platelets were stimulated with PGI<sub>2</sub> concentrations greater than 50nM. Stimulation of washed platelets with forskolin (10 $\mu$ M) raised cAMP levels to 1217 fmol cAMP/ $1 \times 10^7$  cells from a resting concentration of 241 fmol cAMP/ $1 \times 10^7$  cells after 5 minutes (Figure 4.1 B). cAMP levels reached a high of 2993 fmol cAMP/ $1 \times 10^7$  cells with 100 $\mu$ M of forskolin. These data show that PGI<sub>2</sub> increases platelet cAMP levels in a dose-dependent manner.

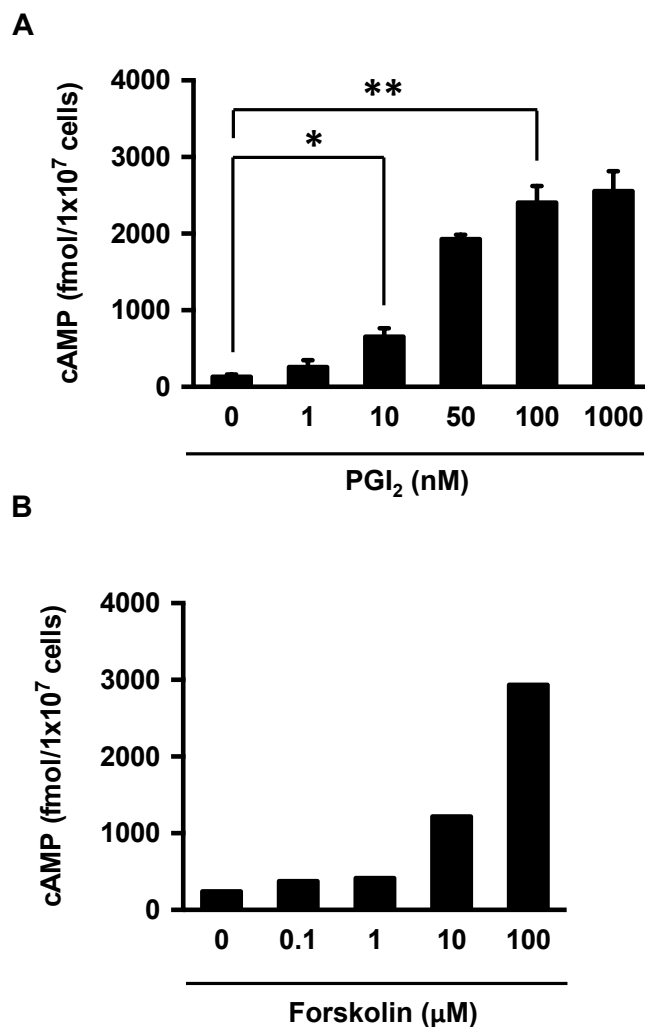


**Figure 4.1. cAMP and dose response to PGI<sub>2</sub> and forskolin stimulation.** WP ( $1.8 \times 10^8$  platelets/ml) were stimulated with a (A) PGI<sub>2</sub> concentration range (1nM, 10nM, 50nM, 100nM, 1000nM) for 1 minute and (B) Forskolin concentration range (0.1μM, 1μM, 10μM, 100μM) for 5 minutes. Intracellular cAMP concentrations were measured at selected time intervals using a commercially available cAMP enzyme immunoassay system (GE healthcare). (A) Data representative of 3 independent experiments expressed as means  $\pm$  SEM (\* $P < 0.05$ , \*\* $P < 0.01$ ). (B) Data of 1 experiment.

#### 4.2.2 PGI<sub>2</sub> elevates cAMP in a time dependent manner

Stimulation of washed platelets with PGI<sub>2</sub> (100nM) lead to a rapid increase in cAMP levels within 1 minute, peaking at  $2874 \pm 125$  fmol cAMP/ $1 \times 10^7$  cells, after 5 minutes ( $*P < 0.01$ ) (Figure 4.2). After 15 minutes, cAMP levels remained elevated at  $2043 \pm 308$  fmol cAMP/ $1 \times 10^7$  cells, however following 60 minutes stimulation cAMP levels had significantly reduced to  $1204 \pm 443$  fmol cAMP/ $1 \times 10^7$  cells, in comparison to the cAMP peak at 5 minutes ( $*P < 0.01$ ). In contrast, stimulation with PGI<sub>2</sub> (10nM) resulted in a more gradual increase in cAMP levels, yet levels also peaked after 5 minutes at  $2552 \pm 190$  fmol cAMP/ $1 \times 10^7$  cells ( $*P < 0.01$ ). After 15 minutes, cAMP levels had significantly reduced to near basal levels at  $498 \pm 191$  fmol cAMP/ $1 \times 10^7$  cells ( $*P < 0.01$ ). These data show that PGI<sub>2</sub> increases platelet cAMP levels in a time and dose-dependent manner.

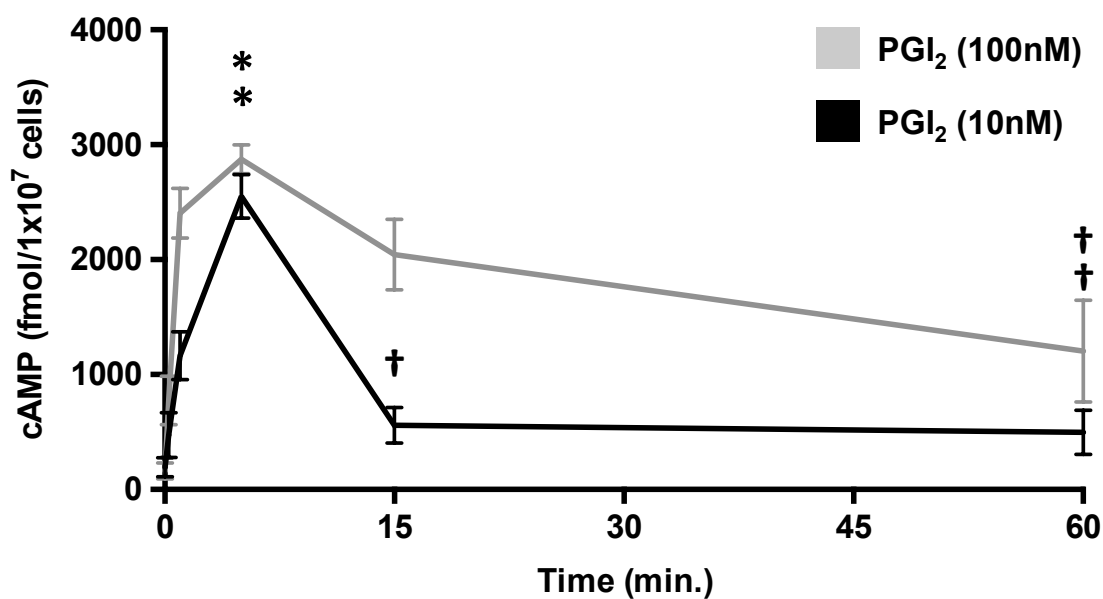


**Figure 4.2. cAMP time profile to PGI<sub>2</sub> stimulation.** WP ( $1.8 \times 10^8$  platelets/ml) were stimulated with a PGI<sub>2</sub> time profile (10nM and 100nM for 15s, 1min, 5min, 15min, 60min). Intracellular cAMP concentrations were measured at selected time intervals using a commercially available cAMP enzymeimmunoassay system (GE healthcare). Data representative of 3 independent experiments expressed as means  $\pm$  SEM (\* $P < 0.01$  when compared with basal and † when compared with 5 minutes).

### 4.3 PGI<sub>2</sub> increases PKA substrate phosphorylation in platelets

The foremost effector of cAMP signalling is PKA, which restrains platelet activation through the phosphorylation of numerous proteins that modulate multiple aspects of platelet activation (Raslan and Naseem, 2014). We wanted to examine the activity of PKA in response to PGI<sub>2</sub>. A sensitive marker of PKA activity is the phosphorylation of platelet proteins by PKA. These phosphorylation events can be visualised using an antibody that recognises PKA phosphorylation consensus sequences (-Arg-Arg-X-Ser/Thr-X) on platelet proteins (Ubersax and Ferrell Jr, 2007).

Here, platelets were stimulated with increasing concentrations of PGI<sub>2</sub> (1-100nM) and analysed for PKA phosphorylation events using an anti-phospho-PKA-substrate antibody on platelet proteins separated by SDS-PAGE (Figure 4.3). Under basal conditions, we detected 13 distinct PKA phosphorylation bands with a band at 40kDa strongly phosphorylated. This resting profile was maintained at 1nM PGI<sub>2</sub> stimulation with the 40kDa reducing in phosphorylation. Upon stimulation with PGI<sub>2</sub> concentrations  $\geq 10$ nM, we detected 18 phosphorylated bands, with strong phosphorylation events at 55kDa and 45kDa. To ensure these events were PKA-specific, platelets were incubated with cell permeable PKA inhibitors RP cAMP (500 $\mu$ M, 20 min) and KT5720 (10 $\mu$ M, 20 min). These agents, inhibit PKA through the competitive antagonism of cAMP binding sites on the PKA regulatory subunits and the adenosine triphosphate (ATP) binding sites on the PKA catalytic subunits, respectively (Dostmann, 1995; Kase et al., 1987). Inhibition of PKA greatly reduced the PKA substrate profile to 3 moderately phosphorylated bands. Of the 17 characterised platelet PKA substrates in the

literature (table 1.1), we were able to match 8 to the phospho-PKA substrate profile, according to approximate molecular weight. However we detected many unidentified PKA substrates, consistent with phosphoproteomic studies (Beck et al., 2014). It would be of interest in the future to identify these bands with mass spectrometry. Data from this experiment shows that PGI<sub>2</sub> increases PKA activity at concentrations  $\geq 10$ nM.

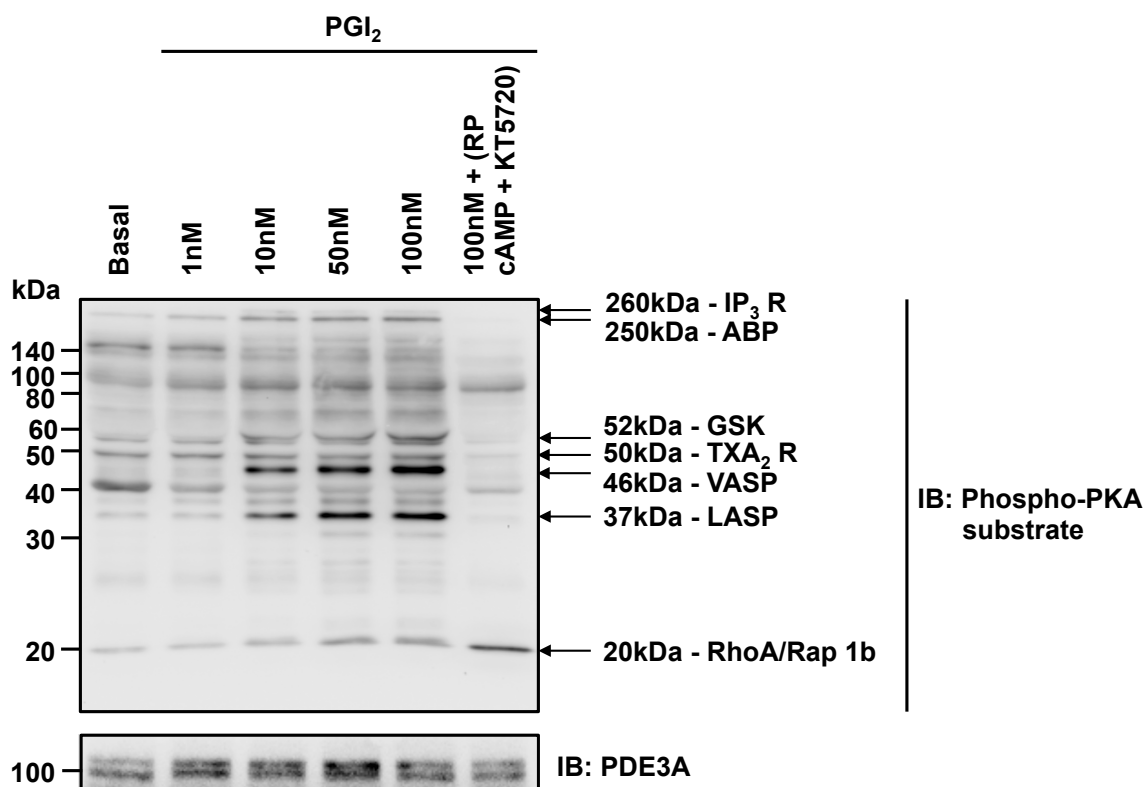


**Figure 4.3. PKA substrate phosphorylation in response to PGI<sub>2</sub>.** WP ( $5 \times 10^8$  platelets/ml) were stimulated with increasing concentrations of PGI<sub>2</sub>. In some cases, WPs were incubated with the PKA inhibitors RP cAMP (500 $\mu$ M, 20 min) and KT5720 (10 $\mu$ M, 20 min), used synergistically, prior to PGI<sub>2</sub> stimulation. Platelet lysates were immunoblotted for PKA phosphorylation events using an anti-phospho-PKA antibody. Potential PKA substrates were labelled according to molecular weights. PDE3A was immunoblotted as protein loading control. Immunoblot representative of 3 independent experiments

#### 4.4 Spatiotemporal dynamics of PKA substrate phosphorylation in platelets

Having visualised PKA phosphorylation of platelet proteins in whole platelets, we next sought to determine the spatiotemporal dynamics of these events. In this experiment, platelets were stimulated with PGI<sub>2</sub> at selected time intervals followed by centrifugation into membrane and cytosolic fractions (Figure 4.4). These fractions were then analysed for PKA phosphorylation events using an anti-phospho-PKA-substrate antibody. We wanted to detect as many PKA substrate bands as possible, as fractionation can result in low protein content of samples, so for this experiment membranes were exposed for an increased time.

In membrane fractions, we detected 7 phosphorylated substrates under basal conditions. Stimulation with PGI<sub>2</sub> (100nM) immediately increased the number of phosphorylated substrates to 15, which remained phosphorylated for approximately 15 minutes before returning to basal after 30 minutes. Interestingly, two substrates at 260kDa and 23kDa displayed a delayed phosphorylation response, where maximal phosphorylation was attained after 5 and 15 minutes, respectively. After 60 minutes, substrates had returned to a non-phosphorylated state. Furthermore, a substrate phosphorylated under basal conditions at 26kDa decreased in phosphorylation status, until no representative phospho-band was detectable at 15 minutes (Figure 4.4).

In cytosolic fractions, we detected 6 phosphorylated substrates under basal conditions. Stimulation with PGI<sub>2</sub> did not immediately increase the number of phosphorylated substrates. However, over time 5 substrates at 100kDa, 60kDa, 45kDa, 32kDa and 20kDa did gradually increase in phosphorylation status, peaking after 15 minutes. After 60 minutes the phosphorylation profile of the 5

substrates returned to basal. Unexpectedly, a new phosphorylation event at 27kda appeared following 60 minutes PGI<sub>2</sub> stimulation. This band may possibly represent a regulatory phosphatase that serves to dephosphorylate PKA substrates when activated by phosphorylation.

In this experiment, it was very difficult to keep membrane samples a consistent volume once fractionated, due to variation in protein concentrations between samples; therefore, some artificial differences in band intensity are visible. Moreover, this experiment could be improved by immunoblotting known membrane and cytosolic proteins to validate the fractionation procedure. Together these data suggest that PKA phosphorylates proteins in different cellular locations and at different time points in response to PGI<sub>2</sub>.

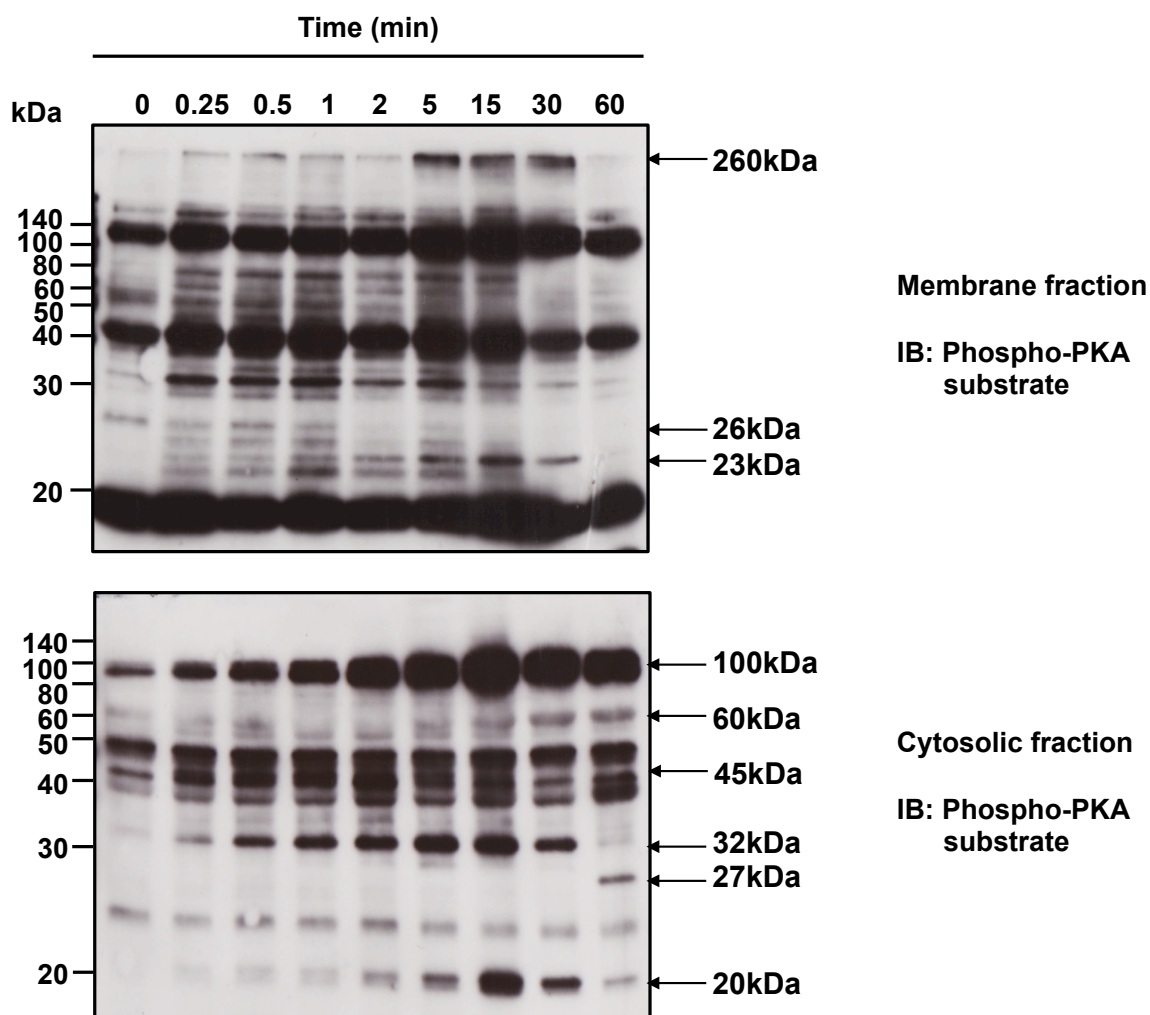


**Figure 4.4. Spatiotemporal profile PKA substrate phosphorylation in platelet fractions.** WP ( $7 \times 10^8$  platelets/ml) were stimulated with PGI<sub>2</sub> (100nM) and fractionated into cytosolic and membrane fractions at different time points using centrifugation. Fractions were immunoblotted for PKA phosphorylation events. Immunoblot representative of 3 independent experiments.

#### 4.5 PDE3A inhibition enhances the cAMP/PKA signalling response to PGI<sub>2</sub>

Having demonstrated the cAMP/PKA signalling response to PGI<sub>2</sub>, we next examined the effect of PDE3A inhibition on cAMP/PKA signalling in resting and PGI<sub>2</sub> stimulated platelets (Figures 4.5 and 4.6). Here, platelet cAMP levels and PKA substrate phosphorylation events were analysed under PGI<sub>2</sub> stimulated conditions in the presence and absence of the PDE3A inhibitor milrinone.

##### 4.5.1 PDE3A inhibition increase cAMP levels in PGI<sub>2</sub> stimulated platelets

Treatment of washed platelets with PGI<sub>2</sub> (10nM) alone elevated cAMP levels from a resting concentration of  $120 \pm 37$  fmol cAMP/ $1 \times 10^7$  cells to  $722 \pm 132$  fmol cAMP/ $1 \times 10^7$  cells ( $*P < 0.05$ ) (Figure 4.5). This signalling response was increased almost fourfold in the presence of milrinone (10 $\mu$ m, 20min) to  $2549 \pm 390$  fmol cAMP/ $1 \times 10^7$  cells ( $**P < 0.01$ ). In the absence of PGI<sub>2</sub>, milrinone alone increased cAMP levels to  $644 \pm 75$  fmol cAMP/ $1 \times 10^7$  cells ( $*P < 0.05$ ). These data show that milrinone alone elevates platelet cAMP levels in addition to potentiating cAMP elevations in response to PGI<sub>2</sub>. This finding is comparable to similar studies examining the effect of PDE3A inhibition on PGE<sub>1</sub> stimulated cAMP responses (Roberts et al., 2010).

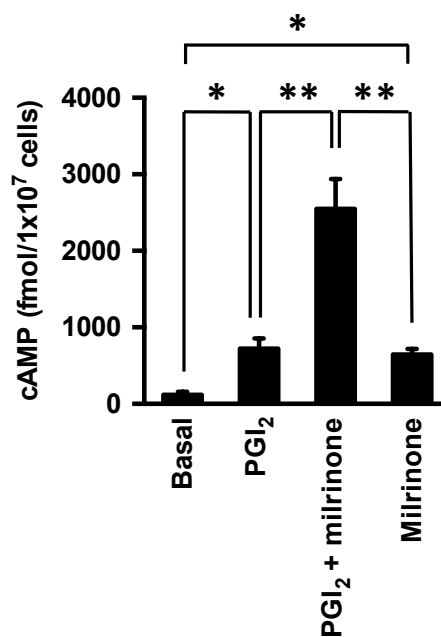


**Figure 4.5. cAMP signalling responses to PGI<sub>2</sub> and PDE3A inhibition.** WP (1.8x10<sup>8</sup> platelets/ml) were treated with PGI<sub>2</sub> (10nM, 2 min) in presence and absence of milrinone (10μM, 20 min). Intracellular cAMP concentrations were measured using a commercially available GE healthcare enzyme immunoassay kit. Data representative of 3 independent experiments expressed at means ± SEM (\*P<0.05, \*\*P<0.01).

#### 4.5.2 PDE3A inhibition potentiates PKA activity in PGI<sub>2</sub> stimulated platelets

Under resting conditions, several phosphorylated PKA substrates were detected as phosphorylated, at comparable molecular weights to previous experiments (Figure 4.6). Stimulation of washed platelets with PGI<sub>2</sub> (10nM) visibly increased substrate phosphorylation with only one band at 140kDa decreasing in phosphorylation. Pretreatment of platelets with milrinone (10µM, 20min) further potentiated the actions of PGI<sub>2</sub>, with every phosphorylation event increasing in intensity. Interestingly, the synergistic use of PGI<sub>2</sub> and milrinone also resulted in the appearance of a newly phosphorylated substrate at 24kDa. It could be suggested that this substrate resides in a subcellular location that under physiological conditions is shielded from cAMP by the actions local PDE3A. Treatment of platelets with milrinone alone increased the phosphorylation status of several substrates, eliciting an almost identical phospho-profile to PGI<sub>2</sub> stimulation. Data from this experiment shows that PDE3A inhibition alone can stimulate PKA substrate phosphorylation in addition to enhancing the effects of PGI<sub>2</sub>.

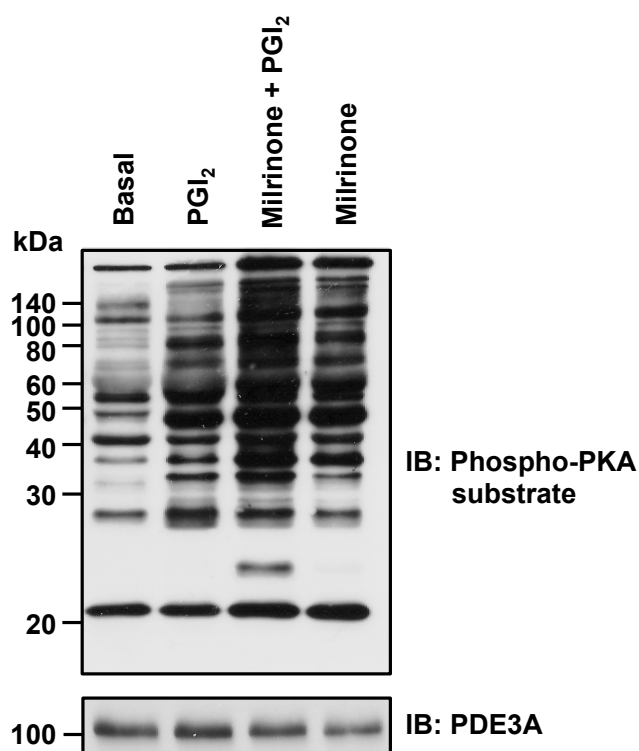


**Figure 4.6. PKA substrate phosphorylation in response to PDE3A inhibition.** WP ( $5 \times 10^8$  platelets/ml) were stimulated with PGI<sub>2</sub> (10nM, 2 min) in the presence and absence milrinone (10 $\mu$ M, 20 min). Platelet lysates were immunoblotted for PKA phosphorylation events using an anti-phospho-PKA antibody. PDE3A was immunoblotted as protein loading control. Immunoblot representative of 3 independent experiments

#### 4.6 Optimisation of anti-phospho PDE3A Ser<sup>312</sup> antibody

PDE3A was first identified as a PKA substrate by Macphee and colleagues, closely followed by Grant, Mannarino and Colman (Grant et al., 1988; Macphee et al., 1988). These initial investigations linked the PKA phosphorylation of PDE3A to the enzyme's increase in hydrolytic activity. More recently, a single PKA phosphorylation site has been identified in a study examining PKC phosphorylation and regulation of PDE3A in platelets (Hunter et al., 2009). In this next set of experiments, we characterised the PKA phosphorylation of this single PKA phosphorylation site at serine residue 312 using the same antibody from this study. However, before this antibody could be used in experimentation, the immunoblotting conditions first had to be optimised.

A variety of conditions were tested with the Ser<sup>312</sup> phospho-specific PDE3A antibody under PGI<sub>2</sub> stimulation (100nM) (Figure 4.7). Under BSA membrane blocking conditions, a very poor signal/background ratio was developed (Figure 4.7 A-D). Blocking membranes in 5% milk (v/v) yielded a much clearer background (Figure 4.7 E-H) with optimal conditions consisting of blocking membranes in 5% milk (v/v) and diluting the primary antibody in 2% milk (v/v) (Figure 4.7 G).

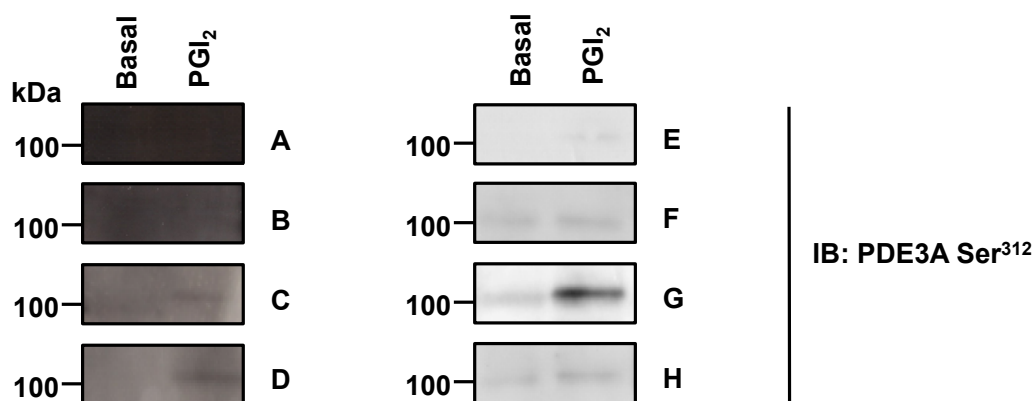


**Figure 4.7. Anti-phospho PDE3A Ser<sup>312</sup> antibody optimisation.** WP ( $5 \times 10^8$  platelets/ml) were stimulated with PGI<sub>2</sub> (100nM, 2 min) and immunoblotted for PDE3A phosphorylation at Ser<sup>312</sup>. A variety of immunoblotting conditions were used to optimise antibody signal in relation to the background signal. (A) Membrane block in 10% BSA, primary antibody diluted in 2% BSA, secondary diluted antibody in 2% BSA. (B) Membrane block in 10% BSA, primary antibody diluted in 2% BSA, secondary antibody diluted in TBS-tween, membrane washes in 2% BSA (C) Membrane block in 10% BSA, primary antibody diluted in 2% BSA, secondary antibody diluted in TBS-tween (D) Membrane block in 10% BSA, primary antibody diluted in TBS-tween, secondary antibody diluted in TBS-tween (E) Membrane block in 5% milk, primary antibody diluted in 2% milk, secondary antibody diluted in 2% milk (F) Membrane block in 5% milk, primary antibody diluted in 2% milk, secondary antibody diluted in TBS-tween, membrane washed in 2% milk (G) Membrane block in 5% milk, primary antibody diluted in 2% milk, secondary antibody diluted in TBS-tween (H) Membrane block in 5% milk, primary antibody diluted in TBS-tween, secondary antibody in TBS-tween. Representative immunoblot of 1 independent experiment.

#### 4.7 Analysis of alternative serine phosphorylation sites on PDE3A

In addition to the single PKA phosphorylation site on PDE3A at Ser<sup>312</sup>, there are also numerous protein kinase C (PKC) phosphorylation sites on PDE3A (Hunter et al., 2009). In the next experiment, we examine the phosphorylation of PDE3A in response to PGI<sub>2</sub> and the PKC activator thrombin at two of these sites, Ser<sup>428</sup> and Ser<sup>465</sup>, alongside Ser<sup>312</sup> (Figure 4.8).

Under basal conditions, no phosphorylation events were detected on PDE3A. In response to PGI<sub>2</sub> (100nM), PDE3A Ser<sup>312</sup> was phosphorylated. Thrombin (0.1U/ml) induced phosphorylation of all three serine sites. These data show that PDE3A can be phosphorylated by both PKA at Ser<sup>312</sup> and PKC at Ser<sup>428</sup>, Ser<sup>312</sup> and Ser<sup>465</sup>.

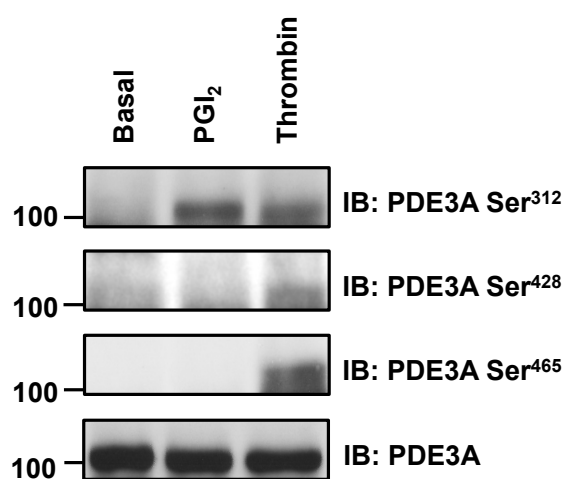


**Figure 4.8. Immunoblot analysis of PDE3A phosphorylation.** WP ( $5 \times 10^8$  platelets/ml) were stimulated with PGI<sub>2</sub> (100nM, 2 min) and thrombin (0.1U/ml, 2 min) and immunoblotted for PDE3A phosphorylation at serine sites Ser<sup>312</sup>, Ser<sup>428</sup> and Ser<sup>465</sup>. PDE3A was immunoblotted as protein loading control. Immunoblot of 1 experiment.

## 4.8 Characterisation of PDE3A phosphorylation and activity in response to PGI<sub>2</sub>

The previous results demonstrate that the phospho-specific PDE3A Ser<sup>312</sup> antibody was successfully optimised. The next series of experiments was designed to characterise the dose and temporal response of PDE3A Ser<sup>312</sup> phosphorylation and hydrolytic activity in response PGI<sub>2</sub> stimulation (Figures 4.9 and 4.10).

### 4.8.1 PDE3A phosphorylation and activity in response to PGI<sub>2</sub>

Stimulation of washed platelets with PGI<sub>2</sub> (100nM) induced a concentration dependent phosphorylation of PDE3A Ser<sup>312</sup> (\**P*<0.05) (Figure 4.9 A). This response was comparable to VASP Ser<sup>157</sup> phosphorylation, an established marker of PKA activity. PKA inhibition with RP-cAMP (500µM) and KT5720 (10µM) blocked PDE3A phosphorylation and reduced VASP Ser<sup>157</sup> phosphorylation to near basal levels. PDE3A hydrolytic activity was also increased in response to PGI<sub>2</sub> in a dose dependent manner, however, changes in PDE3A phosphorylation appeared to be more sensitive to PGI<sub>2</sub> (Figure 4.9 B).

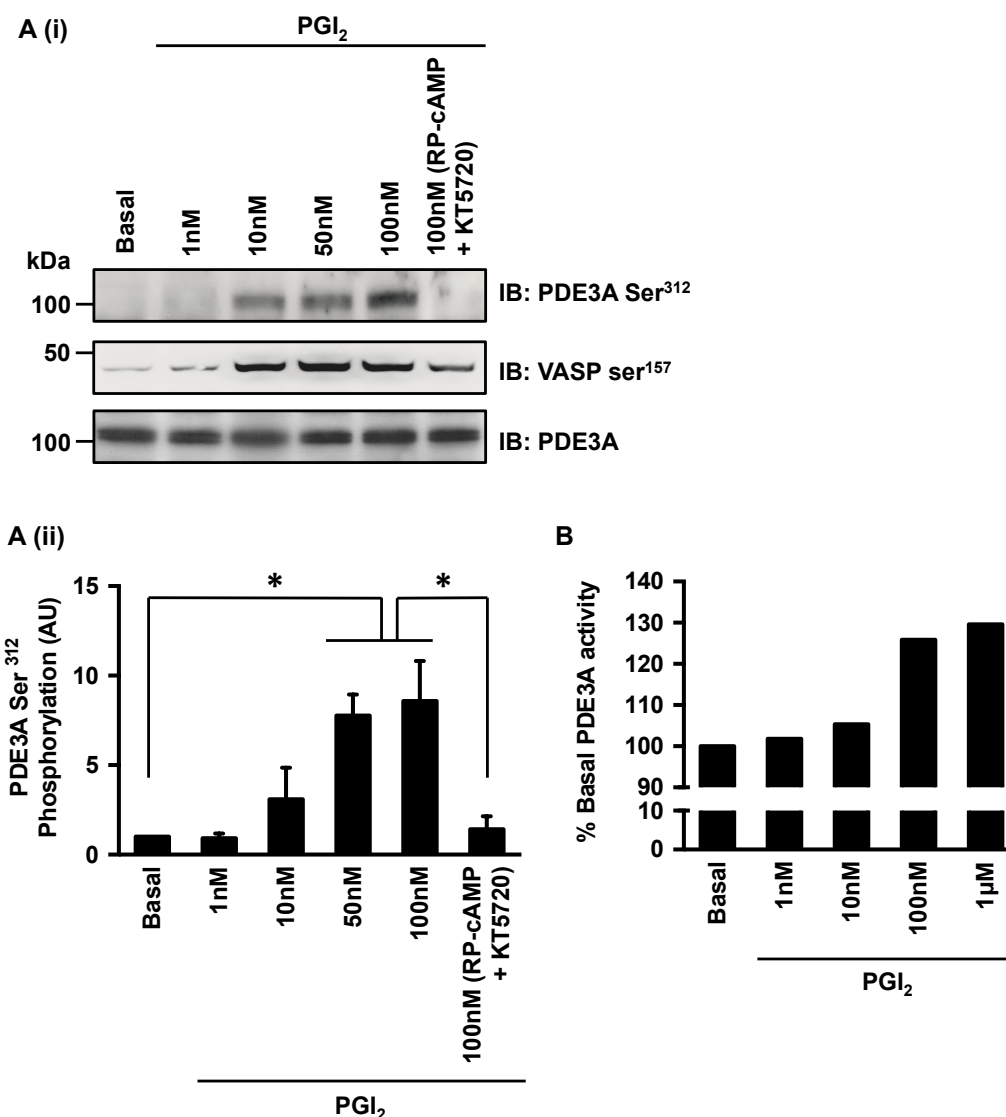


**Figure 4.9. PDE3A phosphorylation and activity in response to PGI<sub>2</sub> concentration range.** WPs ( $5 \times 10^8$  platelets/ml) were stimulated with increasing concentrations of PGI<sub>2</sub> for 1 minute. (A) In some cases, WPs were incubated with the PKA inhibitors RP cAMP ( $500 \mu\text{M}$ , 20 min) and KT5720 ( $10 \mu\text{M}$ , 20 min), used synergistically, prior to PGI<sub>2</sub> (100nM) stimulation. Platelet lysates were immunoblotted for PDE3A Ser<sup>312</sup> phosphorylation, VASP Ser<sup>157</sup> phosphorylation as a marker of PKA activity and total PDE3A as a protein loading control. (i) Representative immunoblot and (ii) quantitative analysis of 4 independent experiments expressed as means  $\pm$  SEM ( $*P < 0.05$ ). (B) PDE3A was immunoprecipitated from lysates and analysed for PDE3A activity. Data from 1 experiment.

#### 4.8.2 Temporal profile of PDE3A phosphorylation and activity in response to PGI<sub>2</sub>

Phosphorylation of PDE3A in response to PGI<sub>2</sub> was rapid and occurred within 15 seconds (Figure 4.10 A). After 15 minutes PDE3A had returned to a dephosphorylated state ( $*P < 0.05$ ). VASP Ser<sup>157</sup> phosphorylation was prolonged, remaining phosphorylated at 15 minutes. These phosphorylation events were blocked under PKA inhibiting conditions with RP-cAMP (500 $\mu$ M) and KT5720 (10 $\mu$ M). PDE3A activity peaked after 1-minute stimulation with PGI<sub>2</sub> before declining to near basal levels after 60 minutes (Figure 4.10 B). Together these data show that PDE3A is phosphorylated and activated in a PGI<sub>2</sub> dose and time dependent manner.

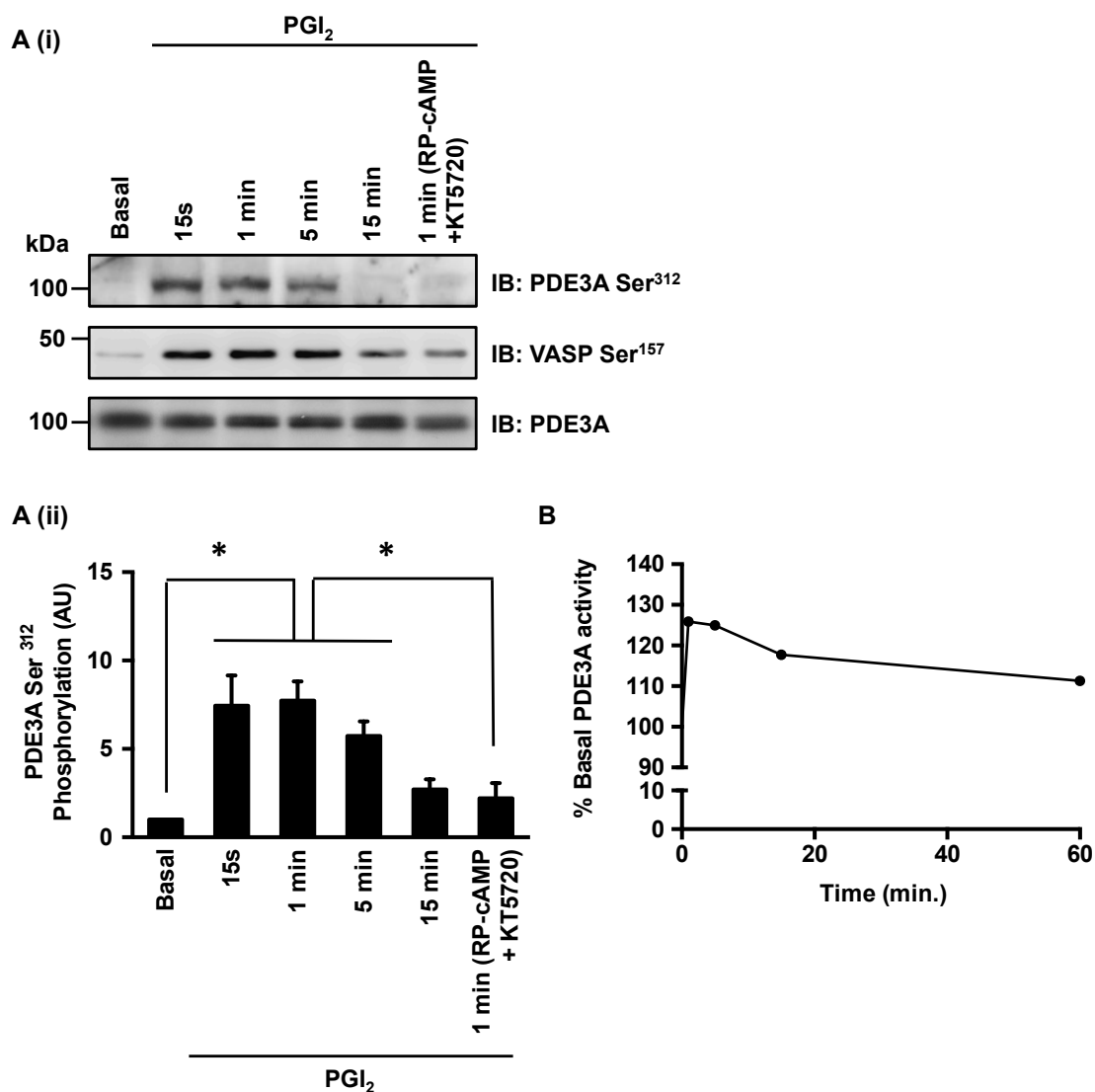


**Figure 4.10. PDE3A phosphorylation and activity time profile in response to PGI<sub>2</sub>.** WPs ( $5 \times 10^8$  platelets/ml) were stimulated with PGI<sub>2</sub> (100nM) and platelet samples extracted at select time intervals for analysis (A) In some cases, WPs were incubated with the PKA inhibitors RP cAMP (500 $\mu$ M, 20 min) and KT5720 (10 $\mu$ M, 20 min), used synergistically, prior to PGI<sub>2</sub> (1 min) stimulation. Platelet lysates were immunoblotted for PDE3A Ser<sup>312</sup> phosphorylation, VASP Ser<sup>157</sup> phosphorylation as a marker of PKA activity and total PDE3A as a protein loading control. (Ai) Representative immunoblot and (Aii) quantitative analysis of 4 independent experiments expressed as means  $\pm$  SEM ( $*P < 0.05$ ). (B) PDE3A was immunoprecipitated from lysates and analysed for PDE3A activity. Data from 1 experiment.

#### 4.9 Characterisation of PDE3A phosphorylation and activity in response to PKA activating agents

In addition to characterising PDE3A phosphorylation and activity in response to PGI<sub>2</sub>, we next investigated the effect of other PKA activating agents on these responses (Figure 4.11). This experiment was performed to validate our finding that PKA phosphorylates PDE3A Ser<sup>312</sup>, as inhibitors of PKA have been shown to non-specifically affect other kinases and signalling molecules (Murray, 2008). For this experiment, the forskolin and cAMP derivative 8-CPT-cAMP were used to indirectly and directly activate PKA, respectively. 8-CPT-cAMP is an analogue of cAMP that is cell permeable and more resistant to hydrolysis by PDEs than endogenous cAMP. In this experiment washed platelets were stimulated with PGI<sub>2</sub> (100nM), forskolin (10µM) and 8-CPT-cAMP (100µM), followed by analysis for PDE3A phosphorylation and activity.

Stimulation of washed platelets with PGI<sub>2</sub> and forskolin resulted in a 7-fold increase in PDE3A Ser<sup>312</sup> phosphorylation over basal, whereas 8-CPT-cAMP increased PDE3A Ser<sup>312</sup> phosphorylation 5-fold over basal (\*\**P*<0.01) (Figure 4.11 A). PDE3A activity was increased in response to PKA activation between 20-30% over basal, with 8-CPT-cAMP having the weakest effect (\**P*<0.05) (Figure 4.11 B). Inhibition of PKA with RP-cAMP and KT5720 reduced PGI<sub>2</sub> stimulated PDE3A phosphorylation and activity back to resting levels (\**P*<0.05). The data from this experiment shows that PKA phosphorylates PDE3A phosphorylation at Ser<sup>312</sup> in response to endogenous and exogenous PKA activating agents.

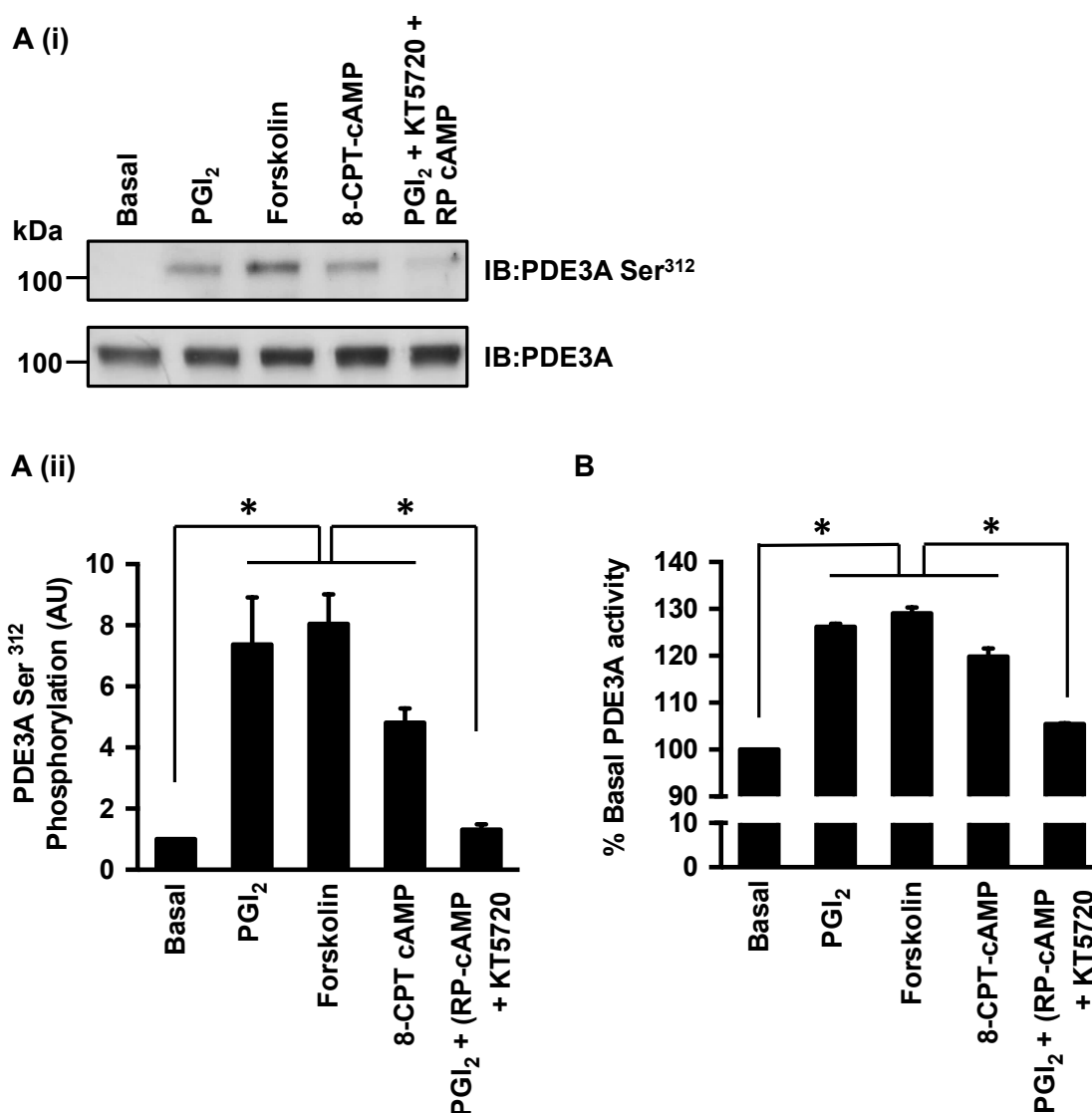


**Figure 4.11. PDE3A phosphorylation and activity in response to PKA activating agents.** WPs ( $5 \times 10^8$  platelets/ml) were stimulated with PGI<sub>2</sub> (100nM, 2 min), forskolin (10 $\mu$ M, 5 min) and 8-CPT-cAMP (100 $\mu$ M, 5min). In some cases, WPs were incubated with the PKA inhibitors RP cAMP (500 $\mu$ M, 20 min) and KT5720 (10 $\mu$ M, 20 min), used synergistically, prior to PGI<sub>2</sub> stimulation. Platelet lysates were immunoblotted for PDE3A Ser<sup>312</sup> phosphorylation and total PDE3A as a protein loading control ( $*P < 0.05$ ) (B) PDE3A was immunoprecipitated from lysates and analysed for PDE3A activity. Data representative of 3 independent experiments expressed as means  $\pm$  SEM ( $*P < 0.05$ ).

#### 4.10 PDE3A phosphorylation correlates with PDE3A hydrolytic activity

Phosphorylation represents an important mechanism of PDE regulation. Currently, 5 of the 11 PDE families expressed in humans have been recognised as kinase regulated, including the PDE3 family. The effect of phosphorylation varies between isoforms, from enzyme activation, enzyme inhibition, protein binding and localisation within cells (Omori and Kotera, 2007). In this next experiment, we sought to investigate the relationship that exists between PKA-mediated phosphorylation of PDE3A and the enzymes hydrolytic activity (Figure 4.12). To investigate this we used calf intestinal phosphatase (CIP) to dephosphorylate immunoprecipitated PDE3A following PGI<sub>2</sub> stimulation and measured the enzymes hydrolytic activity. As PDE3A activity has mirrored the enzymes phosphorylated state in previous experiments, we hypothesised that dephosphorylation of the enzyme would reduce its activity.

Stimulation of washed platelets with PGI<sub>2</sub> (100nM) resulted in PDE3A phosphorylation 8 fold over basal, which was reduced to basal levels when PDE3A was incubated with CIP (Figure 4.12 A). Incubation of PDE3A with heat inactivated CIP had no effect on PDE3A phosphorylation ( $*P<0.01$ ). Under PGI<sub>2</sub> stimulated conditions, PDE3A activity was  $27\pm 4\%$  over basal (Figure 4.12 B). This hydrolytic activity was reduced to  $4\pm 2\%$  with CIP incubation ( $**P<0.05$ ). Incubation of PDE3A with heat inactivated CIP had little effect on PDE3A activity in its phosphorylated state at  $30\pm 4\%$  ( $**P<0.05$ ). These data show that PKA phosphorylation of PDE3A directly correlates with the enzymes hydrolytic activity.

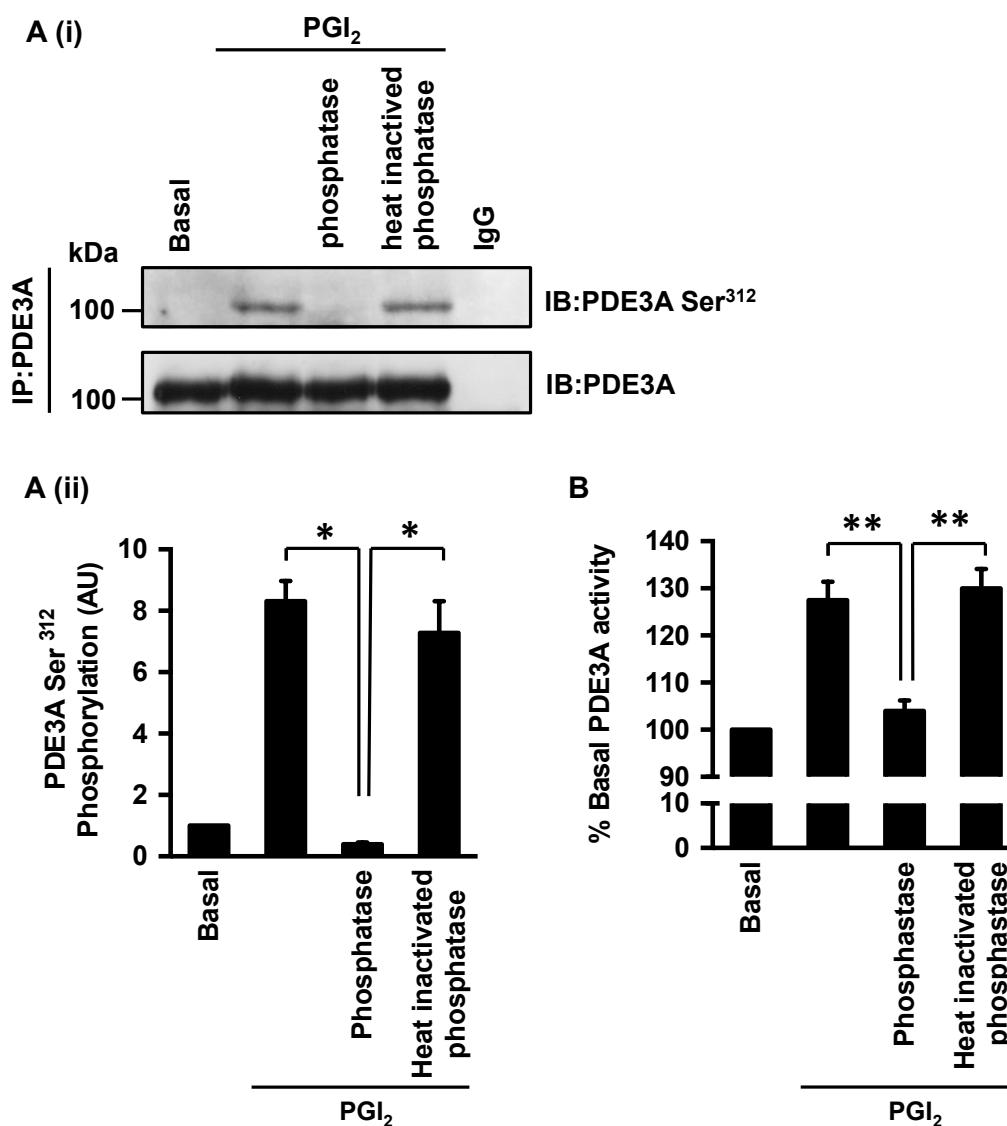


**Figure 4.12. PDE3A phosphorylation and activity in response to calf intestinal phosphatase incubation.** WPs ( $5 \times 10^8$  platelets/ml) were stimulated with PGI<sub>2</sub> (100nM) and lysed in ice-cold lysis buffer. PDE3A was immunoprecipitated from lysates, washed in phosphatase buffer and incubated 37°C for 60 minutes with 5 units of active or heat-inactivated alkaline phosphatase calf intestinal (CIP). Immunoprecipitates were then assayed for (B) PDE3A activity and immunoblotted for (A) PDE3A ser<sup>312</sup> phosphorylation and PDE3A as a control. Data representative of 3 independent experiments expressed as means  $\pm$  SEM (\* $P < 0.01$ , \*\* $P < 0.05$ ).

#### 4.11 PDE3A splice variant PDE3A2 is phosphorylated by PKA at Ser<sup>312</sup>

In the previous chapter we identified the expression of two platelet PDE3A splice variants, PDE3A1 and PDE3A2, using extended separation of PDE3A proteins by SDS-PAGE (Figure 3.4). These splice variants are identical apart from a unique N-terminal extension (NHR1) present on PDE3A1 (Wechsler, 2002). PKA and PKC phosphorylation sites are located on the common N-terminal sequence (NHR2), which similar to NHR1, is thought to facilitate PDE association with the cell membrane (Hambleton et al., 2005). As we have observed only a single band representing PDE3A Ser<sup>312</sup> phosphorylation in previous experiments, we sought to identify the PDE3A splice variant that is phosphorylated at this site. This was achieved using SDS-PAGE analysis on PGI<sub>2</sub> stimulated platelet lysates and running the protein containing polyacrylamide gel for prolonged periods at 4°C, in order to fully separate out the PDE3A splice variant proteins (Figure 4.13). We then immunoblotted for PDE3A Ser<sup>312</sup> phosphorylation, followed by blotting for total PDE3A on the same membrane. Matching the phosphorylated band to the corresponding PDE3A splice variant band confirmed which PDE3A splice variant was phosphorylated by PKA at Ser<sup>312</sup>. Using this approach PDE3A2 was putatively identified as the isoform phosphorylated by PKA at Ser<sup>312</sup> in platelets isolated from three individual donors. In the lower panel, VASP Ser<sup>157</sup> was immunoblotted as a marker of PKA activity. These data confirm that, in platelets, PDE3A splice variant PDE3A2 is phosphorylated by PKA at Ser<sup>312</sup>.

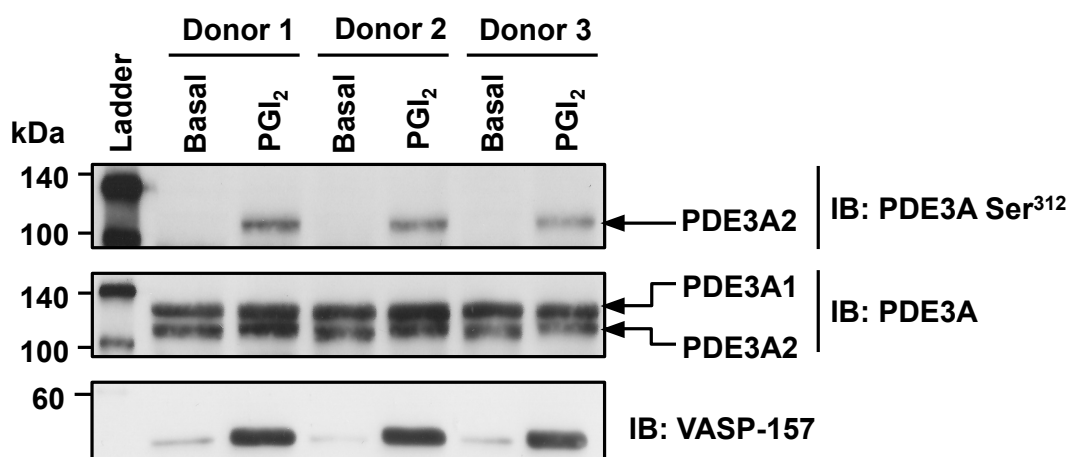


**Figure 4.13. PDE3A splice variant analysis for Ser<sup>312</sup> phosphorylation in response to PGI<sub>2</sub>.** WPs ( $5 \times 10^8$  platelets/ml) were stimulated with PGI<sub>2</sub> (100nM, 2 min) and immunoblotted for PDE3A Ser<sup>312</sup> and VASP Ser<sup>157</sup> phosphorylation. All polyacrylamide gels were run for an extended period of time of 4 hours at 4°C to promote increased protein band separation. Immunoblot membranes were stripped and probed for total PDE3A. Immunoblot of 1 experiment.

#### 4.12 Discussion

Cyclic AMP signalling represents a major inhibitory signalling pathway in platelets. This pathway requires dynamic regulation such that cAMP inhibitory signalling can be dampened to allow platelets to perform their essential haemostatic functions, but also accelerated to prevent thrombosis. Intracellular cAMP concentrations within platelets are regulated in space and time through the hydrolysing actions of PDE3A and PDE2A. The precise interplay that exists between PDE3A and PDE2A in regulating platelet cAMP concentrations is still yet to be fully understood, but what is known, is that PDE3A exerts the greatest influence on endogenous platelet inhibition (Feijge et al., 2004; Manns et al., 2002).

PDE3A hydrolysing activity can be controlled through protein phosphorylation and protein-to-protein interactions. In platelets, a single PKA phosphorylation site at on PDE3A at serine residue 312 has been identified (Hunter et al., 2009). However, it is unknown whether other PKA phosphorylation sites may also be present. It has been suggested that phosphorylation of PDE3A by PKA, the foremost effector of cAMP signalling, directly increases the enzymes hydrolytic activity thus forming a negative feedback loop to regulate cAMP signalling (Macphee et al., 1988). This chapter aimed to fully characterise PKA regulation of PDE3A and investigate its specificity in terms of PDE3A splice variants.

It was important to first examine the upstream signalling events of PKA activation, by measuring the elevation of cAMP levels in response to PGI<sub>2</sub>. Stimulation of platelets with a high dose of PGI<sub>2</sub> that fully inhibits collagen-induced platelet aggregation elicited a sharp rise in cAMP levels that was sustained after 1 hour. In contrast, a low dose of PGI<sub>2</sub> that inhibits collagen-induced platelet aggregation by

50% raised cAMP levels to the same levels as a high PGI<sub>2</sub> dose, but at a slower rate. Interestingly both PGI<sub>2</sub> doses elevated cAMP levels to the same peak concentration within 5 minutes, but cAMP levels only returned to near basal levels with a low PGI<sub>2</sub> dose. The results from this experiment agree with previous observations from Gorman, Bunting and Miller, who reported cAMP concentrations peak after 30 seconds and reduce to near basal levels after 30 minutes (Gorman et al., 1977). A possible explanation for sustained cAMP elevation in response to a high PGI<sub>2</sub> dose can be offered by the role PDEs play in the compartmentalisation of cAMP (Baillie, 2009). It could be hypothesised that highly stimulated AC produces cAMP at such a rate that PDEs at the periphery of the cAMP pool can no longer contain the response. If cAMP were to bleed out the compartment, it would be no longer subject to local PDE hydrolysis, thus, levels would remain elevated for longer.

Next we examined the overall spatiotemporal dynamics of PKA substrate phosphorylation in platelets, prior to focusing on PDE3A phosphorylation. To achieve this we used an antibody that recognises a common PKA phosphorylation consensus sequence that allows the analysis of multiple PKA phosphorylation events (White and Toker, 2013). We showed that under resting conditions a number of platelet proteins were phosphorylated by PKA, representing basal AC6 activity (Pieroni et al., 1995). PGI<sub>2</sub> increased the number of phosphorylated substrates and the intensity of the phosphorylation bands. A number of these bands appeared to match the molecular weights of previously established PKA substrates, namely the IP<sub>3</sub> receptor (IP<sub>3</sub> R), actin-binding protein (ABP), thromboxane receptor (TP receptor), vasoactive intestinal polypeptide (VASP), LIM And SH3 Protein 1 (LASP), Ras Homolog Family Member A (Rho A) and

Ras-related protein 1 (Rap 1) (table 1.1). The phosphorylation of these proteins was reduced to below basal levels with the inhibition of PKA. Comparable PKA substrate phosphorylation profiles in platelets have been reported by El-Daher and colleagues using the cAMP analogue Sp-5, 6-DCI-cBiMPS. In this study it was reported that PKA phosphorylation events peaked after 2.5 minutes and then reversed over time, demonstrating the temporal kinetics of PKA signalling (El-Daher et al., 1996). We decided to explore this concept further by examining the spatiotemporal kinetics of PKA signalling using platelet fractionation. In this experiment, immunoblots were developed for a prolonged time to identify as many PKA phosphorylation events as possible. We detected significant PKA activity in both fractions with clear temporal PKA activity. Interestingly, we detected phosphorylation events that were delayed past 1-minute PGI<sub>2</sub> stimulation, most noticeably in the cytosolic fraction, with one substrate newly phosphorylated after 30 minutes. It could be speculated that this band represents a phosphatase, in which delayed phosphorylation and activation of the phosphatase are required for its regulatory function of PKA phosphorylation events. This band may also represent a substrate that requires PKA to translocate to its location within the platelet, a cellular process that could take the platelet 30 minutes to complete. In these experiments, many detected phospho-bands again matched previously characterised PKA substrates. However, the number of phosphorylation events detected in our experiments was dwarfed by phosphoproteomic studies, which have identified over 100+ potential PKA substrates in platelets (Beck et al., 2014). This comparison clearly highlights the sensitivity threshold of immunoblotting when identifying protein phosphorylation profiles. What is clear from our experiments is that PKA signalling in human platelets is a highly complex and regulated process

with phosphorylation events appearing and disappearing at different time points and in different cellular locations. It is expected that PDE3A and PDE2A not only regulate the amplitude of the cAMP/PKA signalling response in platelets but also the duration and location. An experiment that could tease apart this role would be to examine the spatiotemporal dynamics of PKA substrate phosphorylation in the presence of PDE3A and PDE2A inhibitors. Additionally, further investigation of the PKA substrates visualised in this section of work could yield new insights into the mechanisms of cAMP-mediated platelet inhibition. A potential starting point would be to identify these bands using mass spectrometry analysis.

The main regulator of platelet cAMP/PKA signalling is PDE3A, which functions to reduce the cAMP-modulated threshold for platelet activation (Feijge et al., 2004). This role has been elegantly demonstrated in PDE3A knock-out (KO) studies that show PDE3A KO mice are protected against collagen/epinephrine-induced pulmonary thrombosis and death (Sun et al., 2007). It is highly likely that this cardioprotective effect is due to increased platelet sensitivity to PGI<sub>2</sub>. With this in mind, we showed that inhibition of PDE3A with milrinone dramatically potentiated the effect of PGI<sub>2</sub> on platelet cAMP levels by almost 4-fold. Interestingly, milrinone alone increased cAMP levels to similar levels observed with PGI<sub>2</sub> stimulation. These data were mirrored by phospho-PKA immunoblotting experiments, in which PDE3A inhibition increased PGI<sub>2</sub> stimulated PKA substrate phosphorylation. Again, in this experiment milrinone alone induced a comparable stimulatory effect as PGI<sub>2</sub> with the phosphorylation of several PKA substrates. The effect of milrinone stimulating cAMP/PKA signalling in the absence of PGI<sub>2</sub> can be attributed to the high levels of basal PDE3A activity identified in the previous chapter. It is clear from these experiments that the inhibition of this high basal PDE3A activity results

in the accumulation of newly synthesized cAMP and activation of PKA. This explanation is supported by studies that show AC6 possesses basal activity (Pieroni et al., 1995). Together these data demonstrate that PDE3A inhibition can potentiate the platelet response to PGI<sub>2</sub> and also stimulate cAMP/PKA in the absence of PGI<sub>2</sub>.

PDE3A itself has been identified as a PKA substrate, phosphorylated at Ser<sup>312</sup> (Pozuelo Rubio et al., 2005). Interestingly, in our experiments examining PKA substrate phosphorylation in platelets, we detected a very faint band at 110kDa that may represent PDE3A. Using the same antibodies as Pozuelo Rubio and colleagues, we characterised the dynamics of PDE3A phosphorylation in platelets. These antibodies required extensive optimisation to yield a clear and defined signal. Throughout this work, the antibodies became progressively weaker requiring constant attention to immunoblotting conditions. In these experiments, we confirmed that PDE3A is phosphorylated by both PKA and PKC at Ser<sup>312</sup> in addition to other sites at Ser<sup>428</sup> and Ser<sup>465</sup> solely phosphorylated by PKC. These data are in line with observations by Hunter and colleagues, who postulated PKC phosphorylation and activation of PDE3A in response to thrombotic stimuli functions to reduce cAMP levels below an inhibitory threshold (Hunter et al., 2009). This study directly disputed work by Zhang and Coleman, who showed that PDE3A is phosphorylated and activated by PKB in response to thrombin (Zhang and Colman, 2007). However, we did not examine PKB phosphorylation of PDE3A in this body of work.

We next examined the dynamics of PDE3A phosphorylation and activation in response to PGI<sub>2</sub>. Stimulation with PGI<sub>2</sub> resulted in phosphorylation of PDE3A at

Ser<sup>312</sup> in a time and dose-dependent manner. The temporal pattern of PDE3A phosphorylation was similar to that of the established PKA substrate VASP with PDE3A phosphorylation occurring immediately after 15 seconds and returning to basal after 15 minutes. This phosphorylation event was shadowed by rises in PDE3A activity. Under resting conditions, PDE3A displayed high levels of activity, as observed in the previous chapter. Stimulation with PGI<sub>2</sub> immediately increased the PDEs hydrolytic activity by approximately 30%, which reduced to near basal levels after 15 minutes. In platelets, higher levels of PDE3A activity translates as increased cAMP breakdown, thus these data demonstrate the negative feedback regulation loop of PGI<sub>2</sub> mediated platelet inhibition, first suggested by Macphee and colleagues (Macphee et al., 1988). Inhibition of PKA completely reversed PDE3A phosphorylation and markedly reduced VASP phosphorylation. However, caution must be taken when interpreting the effect of PKA inhibitors on cell function and signalling as they have been shown to non-specifically affect other kinases and signalling molecules (Murray, 2008). With this in mind, we tested other non-physiological PKA activating agents, namely the direct AC activator forskolin and cAMP analogue 8-CPT-cAMP, on PDE3A Ser<sup>312</sup> phosphorylation and activity. These agents both increased PDE3A Ser<sup>312</sup> phosphorylation and activity in addition to PGI<sub>2</sub>.

Unfortunately, these data only show the correlation between PDE3A phosphorylation and activity and do not directly identify PDE3A se<sup>312</sup> phosphorylation as the driving force behind increases in hydrolytic activity. Therefore, we investigated the role of PDE3A Ser<sup>312</sup> phosphorylation further by dephosphorylating the site *ex vivo* and examining the functional outcome. We showed that dephosphorylating PDE3A reversed the effect of PGI<sub>2</sub> increased

hydrolytic activity back to basal levels. Other research teams have reported comparable effects of PDE3A dephosphorylation on hydrolytic activity (Hunter et al., 2009; Palmer et al., 2007; Resjö et al., 1999; Zhang and Colman, 2007). However, with these findings, we can still not hold PDE3A Ser<sup>312</sup> phosphorylation accountable for regulating the enzymes activity since there could be other unidentified phosphorylation sites that affect enzyme activity. The gold standard for linking protein phosphorylation to a specific functional outcome is site-directed mutagenesis and it would be of great interest to use this technique in the future to fully establish that PDE3A phosphorylation is directly responsible for regulating the enzymes activity.

In the previous chapter, we identified the expression of two PDE3A splice variants: PDE3A1 and PDE3A2. These variants were differentially localised in the platelet, with PDE3A1 targeted to the membrane and PDE3A2 primarily localised in the cytosol. In our experiments, we detected only one Ser<sup>312</sup> phosphorylation band yet two PDE3A splice variants, which begged the question which PDE3A splice variant is phosphorylated by PKA? Recent research by Vandeput and colleagues showed that both PDE3A1 and PDE3A2 could be phosphorylated by PKA in transfected HEK239 cells, irrespective of subcellular location. In the final figure of their work, they examined the phosphorylation of these splice variants in cardiac myocytes and showed primarily membrane localised PDE3A1 is phosphorylated at Ser<sup>312</sup> by PKA (Vandeput et al., 2013). To answer this question in platelets, we used a similar technique to Vandeput and colleagues by aligning the phospho-PDE3A Ser<sup>312</sup> band to the total PDE3A band and matching them together. With this simple yet effective technique, we showed that in platelets PDE3A2 is phosphorylated by PKA at Ser<sup>312</sup> and not PDE3A1.

This difference in PDE3A regulation between cardiac myocytes and platelets may arise from differences in the functional role PDE3A plays in either cell type. In cardiac myocytes cAMP signalling directly regulates intracellular  $\text{Ca}^{2+}$  cycling, therefore cAMP elevations localised to plasma and intracellular membranes at points of  $\text{Ca}^{2+}$  entry will likely require negative-feedback regulation by PDE3A1 (Zaccolo, 2009). In contrast, cAMP signalling in platelets regulates a host of substrates many of which are cytosolic as demonstrated in our experiments. It could be suggested that these cytosolic substrates require more precise regulation by PKA and therefore in this location PDE3A2 breakdown of cAMP is also regulated by PKA. For the first time, data from these experiments reveal that there are subpopulations of PDE3A in platelets, which are differentially regulated by PKA. It would be of great interest to measure the activity of each splice variant to confirm that PKA phosphorylation of PDE3A2 is responsible for regulating specifically PDE3A2 activity. However at this present time, no PDE3A splice variant specific inhibitors are available for research. An alternative strategy could be to measure PDE3A activity solely in cytosolic platelet fractions, where PDE3A2 is the only splice variant present.

To summarise, this chapter has characterised PKA-mediated phosphorylation and activation of PDE3A in platelets. We have described the effect of  $\text{PGI}_2$  on cAMP/PKA signalling and demonstrated the potentiating effect PDE3A inhibition has on this pathway. We have also characterised the temporal profile of PDE3A phosphorylation in platelets and linked this modification event to increases in PDE3A hydrolytic activity. Finally, this chapter has provided evidence, for the first time, for the differential regulation of PDE3A splice variants in platelets. Together

these data give rise to an important question, “what are the mechanisms that facilitate and localise this interaction between PKA and PDE3A2?”

## 5 Investigating PDE3A signalosomes

### 5.1 Introduction

The platelet cAMP signalling pathway regulates multiple proteins that play key functional roles in virtually every platelet-activating mechanism. Many of these proteins are dual regulated by cAMP and cGMP with others specifically regulated by cAMP. It is clear, that the specificity of this pathway arises from tight organisation in space and time by the actions of adenylyl cyclase, PDE3A, PDE2A and A-kinase anchoring proteins (AKAPs). In many cell types, cAMP is compartmentalised in such a way that individual stimuli can engage a subset of the cAMP pathway, constrained within a defined subcellular compartment to elicit a specific response (Lefkimmatis and Zaccolo, 2014; Zaccolo and Pozzan, 2002). PKA, the main effector of cAMP signalling, is directed to these subcellular compartments by AKAPs. These anchoring proteins not only localise PKA to discrete locations within the cell but also often scaffold the kinase together with other enzymes, substrates and regulators to form multi-protein signalosomes that perform coordinated cellular functions. However AKAPs and their roles in platelet function remain fairly unexplored (Raslan et al., 2015a).

Studies in other cells have identified PDE3A as an important regulatory component of a number AKAP/PKA signalosomes (Ahmad et al., 2012). In cardiac myocytes, a novel PKA type II/AKAP7/PDE3A/PP2A/phospholamban/Serca2a signalosome has been identified, in which PDE3A modulates the basal contractility of the heart by regulating PKA phosphorylation of phospholamban and thus sarcoplasmic Ca<sup>2+</sup> movement (Beca et al., 2013). In HeLa cells, PDE3A has been

shown to localise with PKA type 1 and brefeldin A-inhibited guanine nucleotide-exchange proteins 1 and 2 (BIG1 and BIG2), which not only catalyse the activation of class 1 ADP-ribosylation factors (ARFs) by accelerating replacement of bound GDP with GTP but also possess A-kinase anchoring domains. ARFs play critical roles in vesicle transport, and it is thought that PDE3A contributes to the modulation of ARF function via regulation of PKA-mediated BIG1 and BIG2 inhibitory phosphorylation (Puxeddu et al., 2009). In these AKAP facilitated complexes, PDE3A can directly regulate PKA activity and signalosome function by hydrolysing local cAMP. There is also a multitude of signalling complexes that contain PDE3 and PKA in the literature, in which the role of AKAPs in facilitating their interaction remains to be investigated (Ahmad et al., 2012). In this next chapter, we explored the role AKAPs play in the interaction and association of PKA and PDE3A in blood platelets.

More specifically the objectives were to:

- Investigate the effect of AKAP disruption on PDE3A activity and cAMP signalling.
- Identify the AKAP that facilitates the interaction between PKA and PDE3A.
- Explore the expression of a novel PDE3A signalosome in human platelets.

## 5.2 AKAP disruption blunts PDE3A phosphorylation and activity

PKA is comprised of a regulatory dimer (RI $\alpha$ , RI $\beta$ , RII $\alpha$ , RII $\beta$ ) and two catalytic subunits (C $\alpha$ , C $\beta$ , C $\gamma$ ) (Skalhegg and Tasken, 2000). Platelets express both PKA heterotetrameric isoforms, categorised by their regulatory subunit into PKA type 1 and PKA type 2 (Burkhart et al., 2012). Molecular tools have been developed that can specifically disrupt the interaction between AKAPs and individual PKA subtypes. These tools are in the form of cell-permeable peptides that disrupt the interaction between PKA and AKAPs by blocking the PKA regulatory subunit dimerization and docking (D/D) domain required for binding to the structurally conserved AKAP amphipathic helix, also known as the A-kinase binding domain (AKB) (Dema et al., 2015). To investigate the role AKAPs play in PKA/PDE3A2 signalling, we used two different AKAP disruptor peptides, HT31 and RI-anchoring disruptor (RIAD-arg<sub>11</sub>) (Figure 5.1). HT31 interrupts PKA/AKAP interaction in an isoform-independent manner, whereas RIAD is specific to PKA type 1 (Carlson et al., 2006; Vijayaraghavan et al., 1997; Wang et al., 2006). These peptides were used alongside their scrambled (non-functioning) versions HT31-P and RIAD scrambled as experimental controls. Previous studies in platelets have shown that the control peptides do not affect platelet function (Raslan et al., 2015b).

The peptide concentrations used in this experiment were selected from previous studies examining delineation of PKA/AKP signalling in human platelets (Raslan et al., 2015a). Pre-incubation of platelets with HT31 (2 $\mu$ M) significantly blunted PKA phosphorylation of PDE3A2 Ser<sup>312</sup> and reduced total PDE3A activity by 12.42% in response to PGI<sub>2</sub> (100nM) (\* $P < 0.05$ ). In contrast, The HT31-P control peptide had a marginal blunting effect on PDE3A2 Ser<sup>312</sup> phosphorylation and only reduced

total PDE activity by a 0.43%. Pre-incubation of platelet with RIAD did not significantly reduce PDE3A Ser<sup>312</sup> phosphorylation and only increased PDE3A activity by 2.25% in response to PGI<sub>2</sub> (100nM) with RIAD scrambled inducing a similar non-significant effect on PDE3A phosphorylation and PDE3A activity, measured at an increase of 1.24%. Increasing PDE3A phosphorylation at Ser<sup>312</sup> did correlate with total PDE3A activation, however, we were not able to dissect the activity of either splice variant. As HT31 alone induced an effect on PKA/PDE3A signalling, whereas RIAD did not, these data suggest an AKAP, specific to PKA type II facilitates the regulation of PDE3A.

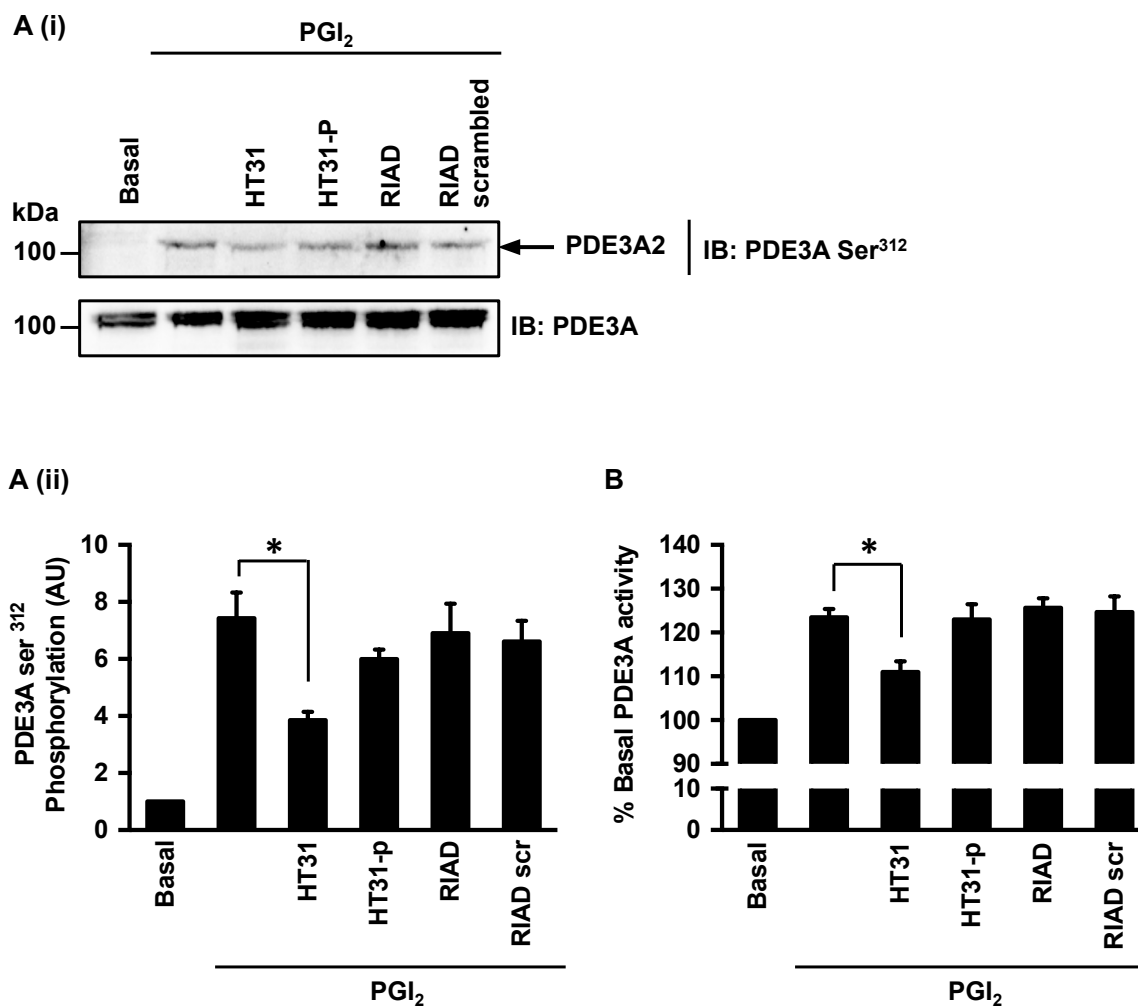


**Figure 5.1. Effect of AKAP disruption on PDE3A2 phosphorylation and total PDE3A activity.** WPs ( $5 \times 10^8$  platelets/ml) were incubated with either the non-specific AKAP disrupter peptide HT31 ( $2 \mu\text{M}$ ), the HT31 control peptide HT31-p ( $2 \mu\text{M}$ ), PKA RI specific disrupter peptide RIAD ( $2.5 \mu\text{M}$ ) or the RIAD control peptide RIAD-scr ( $2.5 \mu\text{M}$ ), for 1 hour at  $37^\circ\text{C}$ , following stimulation with  $\text{PGI}_2$  ( $100\text{nM}$ ). (A) WPs were lysed and immunoblotted for PDE3A Ser<sup>312</sup> phosphorylation and total PDE3A as a protein loading control. (i) Representative immunoblot and (ii) quantitative analysis of 3 independent experiments expressed as means  $\pm$  SEM ( $*P < 0.05$ ). (B) PDE3A was immunoprecipitated from lysates and analysed for PDE3A activity. Data representative of 3 independent experiments expressed as means  $\pm$  SEM ( $*P < 0.05$ ).

### 5.3 Characterising the effect of AKAP disruption on platelet cAMP responses

Next, we investigated the effect of AKAP disruption upstream of PKA/PDE3A signalling by quantifying cAMP levels in response to HT31 and the control peptide HT31, under PGI<sub>2</sub> stimulated conditions (Figure 5.2). In some cases, the PGI<sub>2</sub> IP receptor was antagonised with RO1138452 (RO) to confirm that the IP receptor was responsible for mediating the actions of PGI<sub>2</sub> on cAMP levels.

Resting platelets had a cAMP concentration of  $48 \pm 8$  fmol cAMP/ $1 \times 10^7$  cells, which increased to  $472 \pm 85$  fmol cAMP/ $1 \times 10^7$  cells under PGI<sub>2</sub> stimulation (10nM). This response was potentiated slightly in the presence of HT31 (2 $\mu$ M) to  $657 \pm 128$  fmol cAMP/ $1 \times 10^7$  cells, however, this increase was not statistically significant. The HT31 control peptide (2 $\mu$ M) did not have an effect on cAMP elevation with a measurement of  $494 \pm 75$  fmol cAMP/ $1 \times 10^7$  cells. The small potentiating effect of HT31 was also observed under stimulation with 50nM of PGI<sub>2</sub>, increasing PGI<sub>2</sub> (50nM) elevated cAMP levels from  $1881 \pm 150$  fmol cAMP/ $1 \times 10^7$  cells to  $2188 \pm 254$  fmol cAMP/ $1 \times 10^7$  cells. Again, this effect was not statistically significant. Antagonism of the IP receptor using RO (100 $\mu$ M) reverted the cAMP response to basal levels following stimulation with both concentrations of PGI<sub>2</sub>. These data show that disruption of PKA/AKAP interactions has a minor, yet non-significant, effect on cAMP elevations in response to PGI<sub>2</sub>.

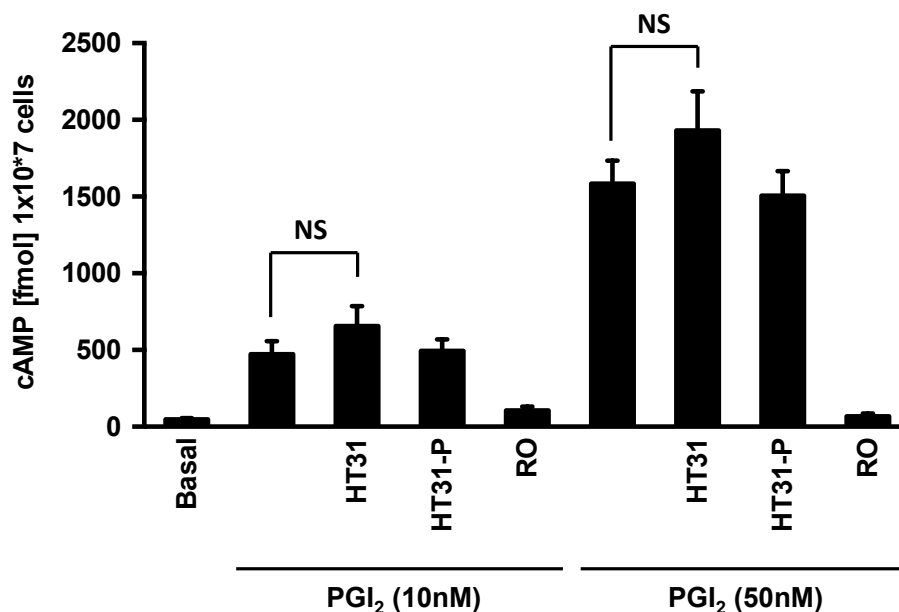


**Figure 5.2. Effect of AKAP disruption on platelet cAMP levels.** WPs ( $1.8 \times 10^8$  platelets/ml) were incubated with either the non-specific AKAP disrupter peptide HT31 ( $2 \mu\text{M}$ ), the HT31 control peptide HT31-p ( $2 \mu\text{M}$ ), PKA RI specific disrupter peptide RIAD ( $2.5 \mu\text{M}$ ) or the RIAD control peptide RIAD-scr ( $2.5 \mu\text{M}$ ), for 1 hour at  $37^\circ\text{C}$ . WPs were then stimulated with PGI<sub>2</sub> ( $10\text{nM}$  and  $50\text{nM}$  for 1min). In some cases, the PGI<sub>2</sub> IP receptor was antagonised with RO ( $100 \mu\text{M}$ , 20 min) prior to PGI<sub>2</sub> stimulation. Intracellular cAMP concentrations were measured at selected time intervals using a commercially available cAMP enzyme immunoassay system (GE healthcare). Data representative of 3 independent experiments expressed as means  $\pm$  SEM.

#### 5.4 PKA type II is associated with PDE3A

Having observed that disruption of PKA type II anchoring blunts PDE3A2 phosphorylation at Ser<sup>312</sup> and activation of total PDE3A, we wanted to further investigate this potential signalling node. In this experiment, the interaction between PKA type II with PDE3A was verified using a commercial co-immunoprecipitation kit (Figure 5.3). However, in this instance, we were not able to tailor the experiment specifically to each PDE3A splice variant, as to the best of our knowledge, there were no splice variant specific PDE3A antibodies available. The co-immunoprecipitation kit used in this experiment involved covalently binding the anti-PDE3A primary antibody to amino-link coupling resin. The resin could then be used multiple times to precipitate the PDE3A from platelet lysates using an elution buffer, providing a significant advantage both in cost and time, in comparison to conventional methods. Using this system we detected the association of PKA type II with PDE3A, in confirmation with our previous data in figure 5.1 that suggested PKA regulation of PDE3A is facilitated by a PKA type II specific AKAP. We did not detect any association of PKA type I. These data reveal for the first time that PKA type II and PDE3A are associated together in platelets. With these data in mind, we next sought to identify the AKAP responsible for orchestrating the interaction between PKA type II and PDE3A.

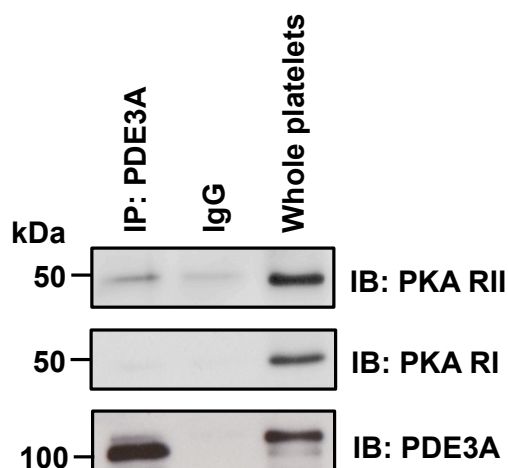


**Figure 5.3. Analysis of PKA association with PDE3A in platelets.** WP lysates (1mg protein) were incubated with anti-PDE3A antibody (5 $\mu$ g) covalently coupled to an amine-reactive resin. Following overnight incubation at 4°C, the resin, precipitated antigen and co-immunoprecipitated proteins were isolated by centrifugation. Proteins were eluted from the resin and immunoblotted for PKA type 1 and type 2 on separate membranes. PDE3A was immunoblotted to ensure successful immunoprecipitation. Immunoblot of 1 independent experiment.

## 5.5 Human platelets express AKAP7

There are currently sixteen AKAPs that have been reported as expressed by platelets in proteomic and genomic studies; AKAP1, AKAP2, AKAP7, AKAP9, AKAP10, AKAP11, AKAP13, moesin, ezrin, Rab32, BIG1, BIG2, WAVE-1 (Wiskott-Aldrich syndrome protein verprolin homologous 1), MAP2 (microtubule-associated protein 2), smAKAP (small membrane AKAP) and neurobeachin (Burkhart et al., 2012; Margarucci et al., 2011; Rowley et al., 2011). In light of the study by Beca and colleagues, in which they identified the association between PDE3A and AKAP7 $\delta$  in cardiac myocytes, we decided to investigate whether AKAP7 was the protein responsible for mediating the interaction between PKA type II and PDE3A in platelets (Beca et al., 2013). The initial step in this process was to first confirm the expression of AKAP7. This was achieved using a combination of several approaches including immunoblotting, cAMP pull-down experiments and immunoprecipitation.

### 5.5.1 Immunoblotting AKAP7 in human and mouse platelets

To immunoblot AKAP7 in human platelets, we used a commercially available anti-AKAP7 antibody that recognises all four AKAP7 splice variants, AKAP7 $\alpha$ , AKAP7 $\beta$ , AKAP7 $\gamma$  and AKAP7 $\delta$  with apparent molecular weights of 17kDa, 19kDa, 37kDa and 50kDa respectively (Johnson et al., 2012) (Figure 5.4). We detected the expression of AKAP $\delta$  at 50kDa in human platelets, which was also expressed in mouse platelets and primary megakaryocytes. A band at 100kDa was also detected in platelet lysates, believed to be non-specific as there are no

AKAP7 splice variants at this molecular weight. These data suggest that human platelets, mouse platelet and mouse megakaryocyte cells express AKAP7 $\delta$ .

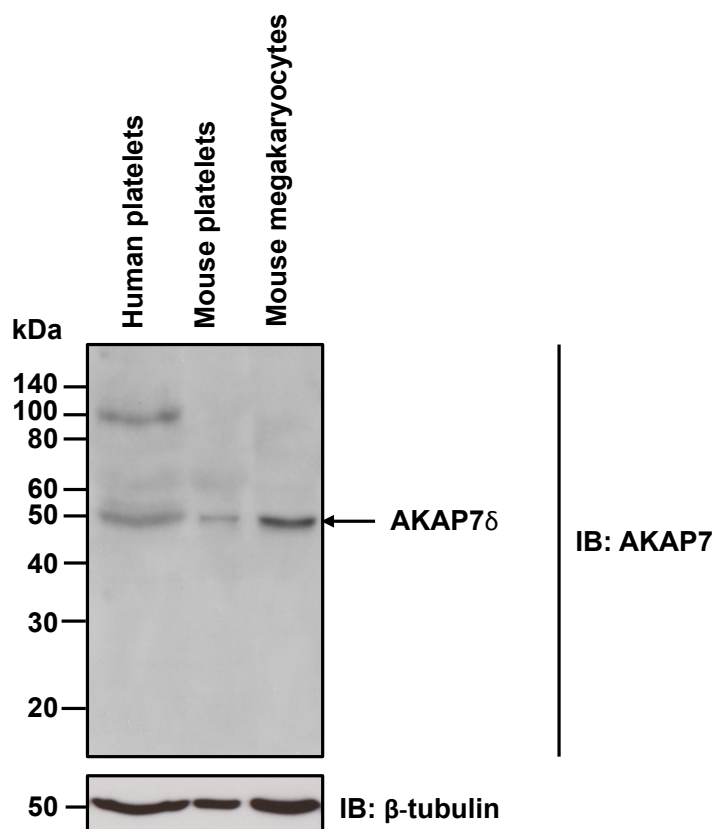


**Figure 5.4. Immunoblotting AKAP7 expression in human and mouse platelets.** Human platelet (20 $\mu$ g), mouse platelet (20 $\mu$ g) and mouse megakaryocyte (20 $\mu$ g) lysates were immunoblotted for AKAP7 expression. Immunoblot membranes were stripped and reprobbed for  $\beta$ -tubulin as a protein loading control. Immunoblot representative of 3 independent experiments.

### 5.5.2 Enrichment of cAMP binding proteins in human platelets

We next wanted to further demonstrate that the observed band at 50kDa represented AKAP7 $\delta$ . This was achieved using a cAMP agarose pull-down assay, in which cAMP-bound agarose beads are used to enrich cAMP binding proteins including PKA, AKAPs and associated PKA substrates, which are then isolated using centrifugation and wash steps (Figure 5.5). Before using this assay to confirm AKAP7 expression in human platelets, we wanted to validate our protocol by examining all the proteins that were immobilised to the cAMP-bound beads using SDS-PAGE and protein staining.

We detected multiple proteins that directly or indirectly bind to cAMP at the approximate molecular weights of 350kDa, 260kDa, 250kDa, 170kDa, 100kDa, 95kDa, 80kDa, 70kDa, 65kDa, 55kDa and 50kDa. To control for non-specific binding, platelet lysates were also incubated with agarose beads as a control, however, we detected some residual protein binding to these beads. In future experiments, we decided to omit this control step and instead saturate platelets with free cAMP to inhibit the binding of proteins to the cAMP-bound beads (Wang et al., 2001).

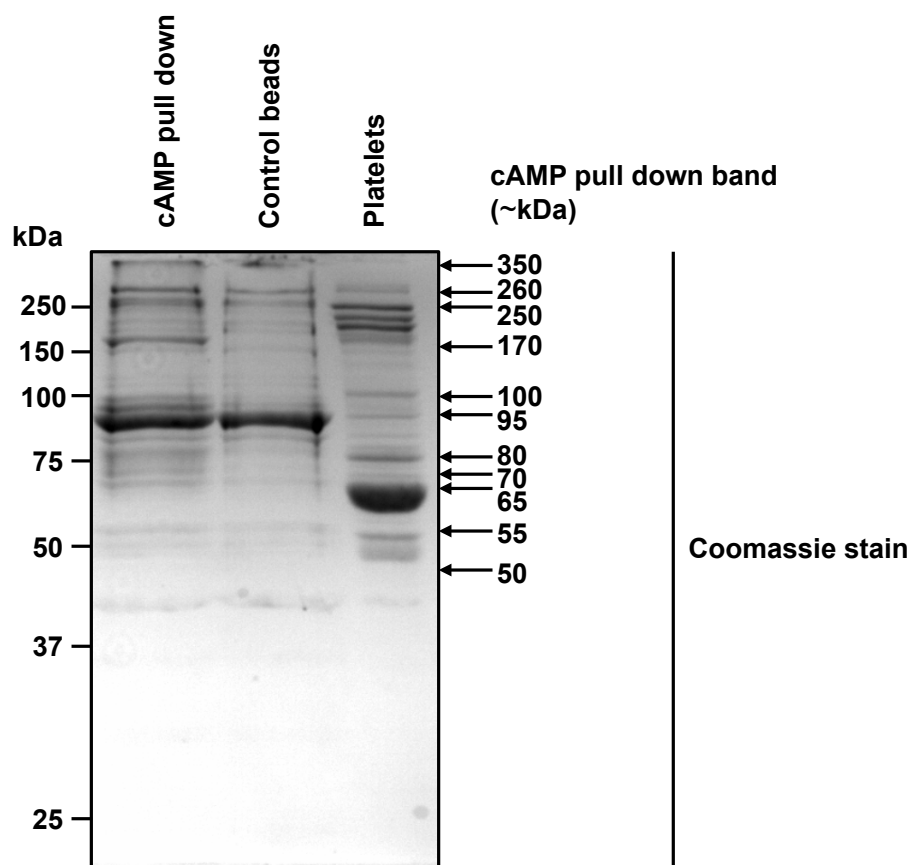


**Figure 5.5. cAMP pull down of human platelet proteins.** WP lysates (1mg protein) were incubated with cAMP bound agarose beads (25 $\mu$ l) or control agarose beads (25 $\mu$ l). Following incubation, the precipitated proteins were separated by SDS-PAGE and stained with coomassie blue to visualise proteins. Protein Bands in the cAMP pull down lane were labelled according to approximate molecular mass. Gel agarose image of 1 experiment.

### 5.5.3 cAMP pull - down of PKA type II and AKAP7

Having visualised the proteins purified using the cAMP-pull down assay, we next examined the presence of AKAP7 and PKA type II in platelets using this tool (Figure 5.6). We detected a strong signal representing PKA type II just below the 50kDa marker. Using a commercially available anti-AKAP7 antibody, we detected AKAP7 $\delta$  in the pull down at 50kDa alongside an established non-specific 60kDa band representing AKAP7 antibody binding to a protein other than AKAP7 (Henn et al., 2004). A faint band at 37kDa was also detected, which may represent AKAP7 $\gamma$  (Trotter et al., 1999).

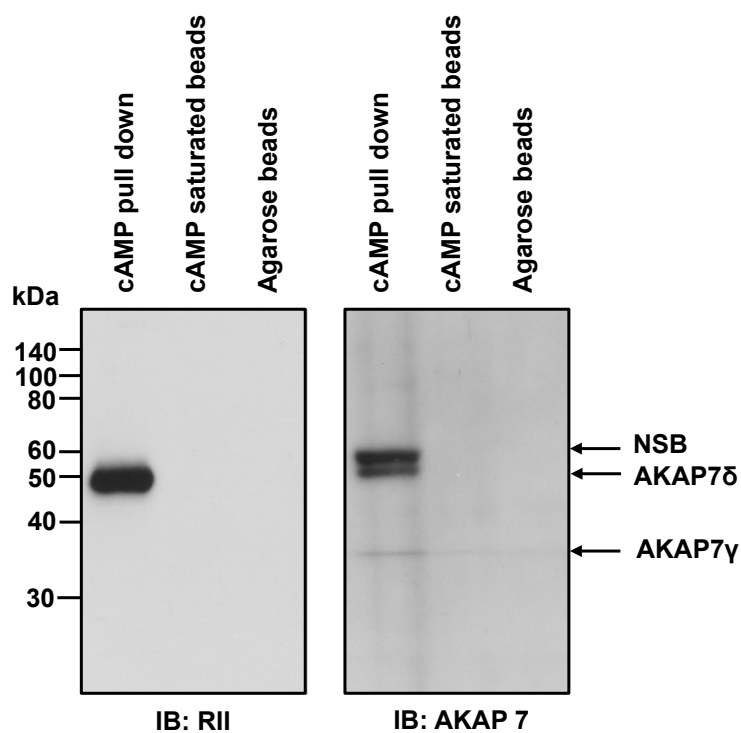


**Figure 5.6. cAMP pull down of AKAP7.** WP lysates (1mg protein) were incubated with cAMP bound agarose beads (25 $\mu$ l) +/- cAMP (50mM). Following incubation, the precipitated proteins were separated by SDS-PAGE and immunoblotted for PKA RII and AKAP7 on two separate membranes. Immunoblot representative of 3 independent experiments.

#### 5.5.4 Immunoprecipitation of AKAP7 from platelets

Throughout this study, we used a commercially available antibody to immunoblot and immunoprecipitate AKAP7. Our lab was generously given an aliquot of independently produced AKAP7 antibody from Professor Enno Klussmann (Max Delbrück Center, Berlin) (Henn et al., 2004). With this antibody, we cross-referenced the commercial AKAP7 antibody to validate its specificity (Figure 5.7). AKAP7 was immunoprecipitated using the commercially anti-AKAP7 antibody and then immunoblotted using the independent anti-AKAP7 antibody, both raised towards the conserved C-terminal region on AKAP7.

With this approach, we detected a band representing AKAP7 $\delta$  at 50kDa in human platelets. Interestingly the non-specific 60kDa was detected in the immunodepleted lysate. This experiment was only performed once as we had a limited stock of independent anti-AKAP7 antibody. The data from these experiments show that human platelet express the AKAP7 splice variant AKAP $\delta$ , and possibly AKAP7 $\gamma$ .

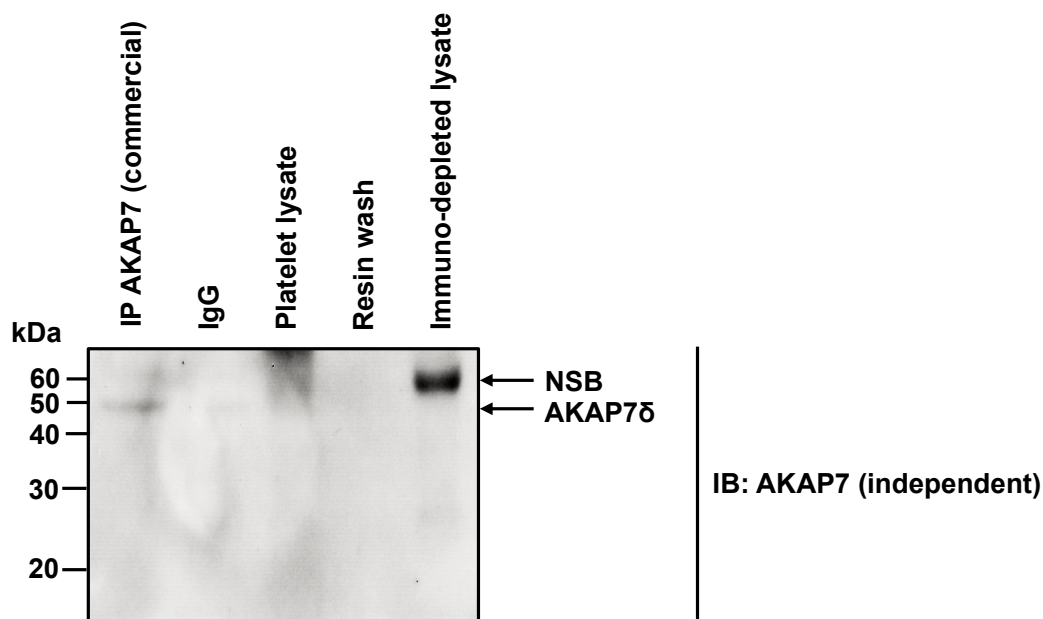


**Figure 5.7. AKAP7 immunoprecipitation.** WP lysates (1mg protein) were incubated with commercial anti-AKAP7 antibody (5 $\mu$ g) covalently coupled to an amine-reactive resin. Following overnight incubation at 4°C, the resin, precipitated antigen and co-immunoprecipitated proteins were isolated by centrifugation. Proteins were eluted from the resin using an elution buffer and immunoblotted for AKAP7 using an independently produced anti-AKAP7 antibody. The last resin wash was loaded to ensure that all non-bound proteins had been washed away. Immunoblot of 1 experiment.

## 5.6 AKAP7 harbours co-associated PKA activity

AKAP7 functions to anchor PKA to specific subcellular locations within the cell (Pidoux and Taskén, 2010). To strengthen our finding that platelets express AKAP7 and to confirm its function as a PKA-anchoring protein, we tested for PKA activity in AKAP7 immunoprecipitates (Figure 5.8). Here, we used an assay that analyses samples for the ability to phosphorylate the synthetic PKA substrate kemptide as a measure of PKA activity (Macala et al., 1998). Using this assay we detected significant PKA activity in AKAP7 immunoprecipitates,  $17\pm 3\%$  when compared to positive control. In contrast, the IgG control showed no increase in activity ( $*P<0.05$ ). These data illustrate the functionality of platelet AKAP7 as an A-kinase anchoring protein.

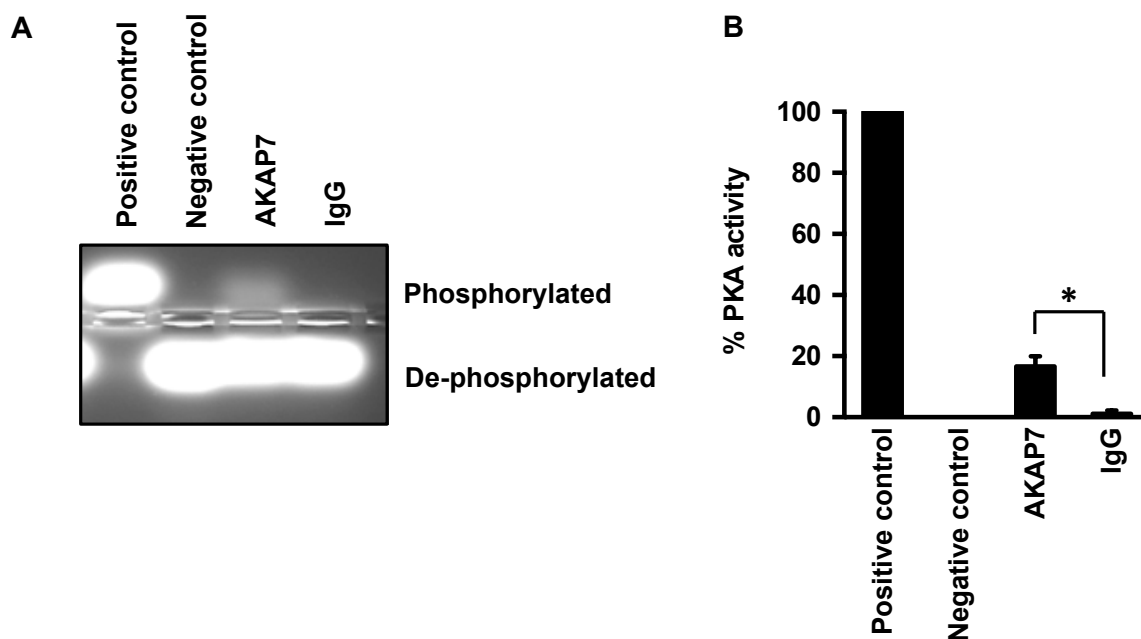


**Figure 5.8. Analysis of associated PKA activity in AKAP7 Immunoprecipitates.** AKAP7 was immunoprecipitated from washed platelet lysates (500 $\mu$ g protein) and analysed for the ability to phosphorylate the synthetic PKA substrate kemptide as a measure of associated PKA activity. The assay used a positive control of recombinant PKAc to examine enzyme activity and a negative control where recombinant PKAc was omitted. (A) Representative Gel agarose image. (B) Quantification of PKA activity expressed as % PKA activity compared with IgG representative of 3 independent experiments expressed as means  $\pm$  SEM ( $*P < 0.05$ ). This experiment was performed in conjunction with Dr Zaher Raslan.

### 5.7 AKAP7 is associated with PKA type II in platelets

In the previous experiment, we showed that platelet AKAP7 associates with PKA, although these data did not distinguish between PKA isoforms. In this next experiment, the specific association between AKAP7 and PKA type II was confirmed, and visualised *in situ*, using proximity ligation (Figure 5.9). The proximity ligation assay (PLA) utilises both antibody and DNA properties to detect the cellular localisation of a specific protein interaction within a single experiment (Gullberg et al., 2003).

Briefly, fixed and permeabilised platelets are incubated with two antigen specific primary antibodies raised from different species. Following antigen recognition, secondary antibodies called PLA probes are introduced, which are conjugated to unique short DNA sequences. Close proximity of the antigens brings together the DNA sequences, which with the addition of a reaction mixture and two long connector oligonucleotides forms a single stranded DNA circle. This DNA circle is then amplified through the actions of DNA polymerase to form a long DNA sequence that is then recognised using fluorescently labelled DNA probes.

Staining of platelets with wheat germ agglutinin (WGA) enabled the detection of multiple platelets that had been successfully immobilised on the poly-L-lysine coated coverslips. The small platelet size was evident using WGA staining with immobilised platelet presenting a resting discoid morphology. Using the PLA assay in platelets, we detected the association of AKAP7 with PKA type II, when both proteins were labelled with PLA probes. No positive signals were detected in platelets that had only AKAP7 labelled. A very faint signal was detected when PKA type II was individually labelled suggest some non-specific fluorescent DNA probe

binding. As a positive control, we visualised the association between PKA type I and PKAc. No signals were detected in samples devoid of the PLA probes or the primary antibodies. The data in this experiment shows that AKAP7 associates with PKA type II in platelets.

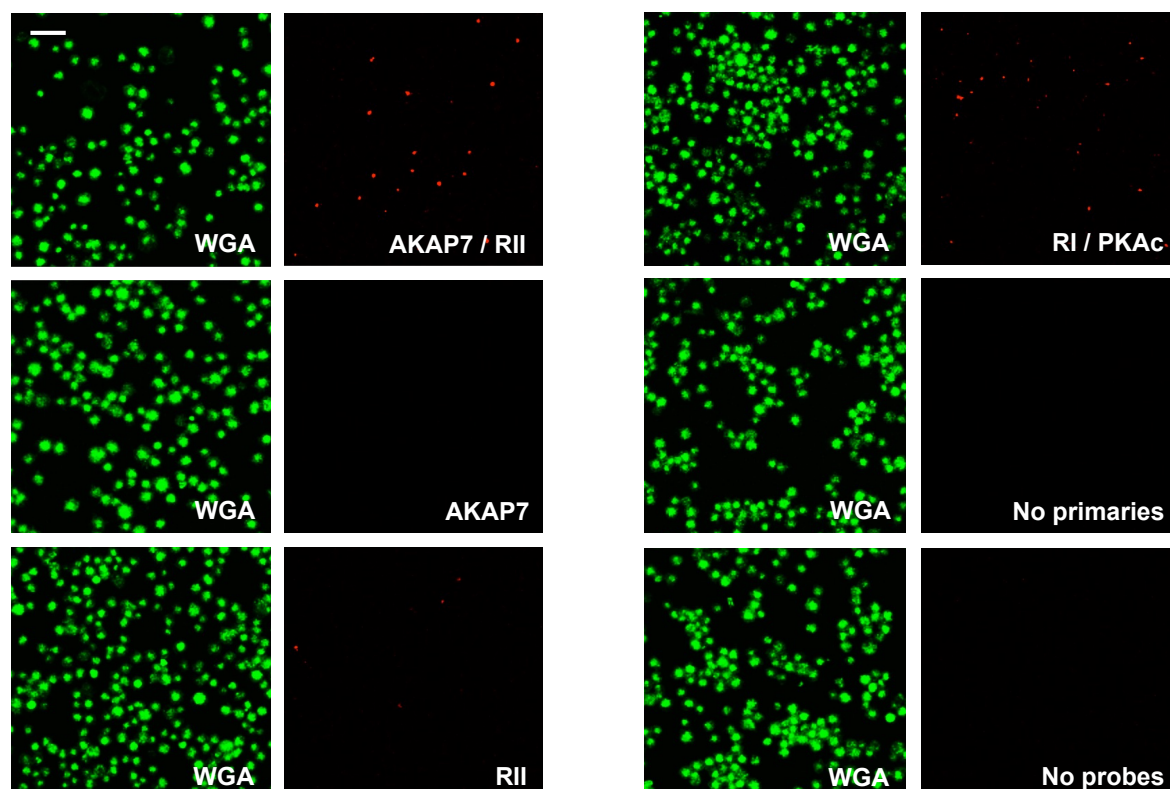


**Figure 5.9 Proximity ligation analysis of AKAP7 and PKA type II association.**

WP ( $1 \times 10^7$  platelets/ml) were fixed in 4% paraformaldehyde for 10 minutes and then washed twice with PBS. Fixed platelets were adhered on poly-L-lysine coated coverslips by centrifugation for 10min at 250g at 37°C. Platelets were then permeabilised with 0.1% Triton X-100 for 5 minutes followed by blocking with 2% BSA in PBS. Permeabilised platelets were then probed using AKAP7, PKA RII, PKA-RI and PKAc antibodies. The interactions between these proteins were then analysed using the Duolink™ proximity ligation assay, according to manufacturers instructions. Scale bar = 5µm. Images representative of 3 independent experiments. Experiment in conjunction with Dr Zaher Raslan.

## 5.8 Characterising the platelet PDE3A signalosome

In light of the previous data in this chapter and studies detailing PDE3A complexes in other cell types (Ahmad et al., 2012; Beca et al., 2013), we next explored the presence of a novel PDE3A2 signalosome in platelets that potentially contained PKA type II, PKA catalytic subunit (PKAc) and PDE3A2, scaffolded together by AKAP7. To achieve this, we used a combination of co-immunoprecipitation studies and PDE3A activity assays (Figures 5.10, 5.11 and 5.12).

### 5.8.1 Co-immunoprecipitation of PDE3A signalling partners

In this first series of experiments, we used co-immunoprecipitation to examine the association of PKA type II, PKAc and AKAP7 with total PDE3A (Figure 5.10). These interactions were examined under resting and PGI<sub>2</sub> (100nM) stimulated conditions, as recent studies have shown that phosphorylation of PDE3A can influence its interaction with signalling partners (Faiyaz Ahmad et al., 2015). Here, all co-associated proteins were immunoblotted from the same PDE3A IP experiment with samples ran on two separate gels due to the close molecular weights of AKAP7 and PKA type II when immunoblotting. In this experiment, we detected co-association of PKA type II, PKAc and AKAP7 $\delta$  with PDE3A under resting conditions. We also detected a faint AKAP7 $\delta$  band in the IgG control suggesting some non-specific binding of AKAP7 $\delta$  to the protein G coated sepharose beads. Interestingly, stimulation with PGI<sub>2</sub> did not influence the formation of this complex, however, the association of PKAc was noticeably weaker, suggesting the disassociation of PKAc. We also detected PKA type II, PKAc and AKAP7 $\delta$  expression in the immunodepleted lysates suggesting that only

a subpopulation of these proteins are in a complex with PDE3A or their interaction with PDE3A is not strong enough to withstand the mechanics of the co-immunoprecipitation procedure.

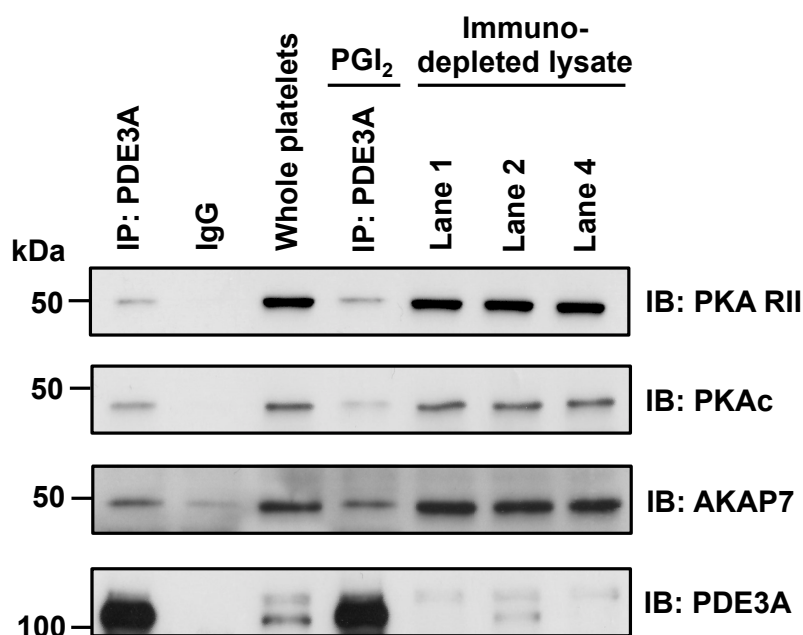


**Figure 5.10. Co-immunoprecipitation of PKA RII, PKAc and AKAP7 with PDE3A.** WPs ( $5 \times 10^8$  platelets/ml) were stimulated with PGI<sub>2</sub> (100nM) for 2 minutes and lysed in ice-cold lysis buffer. Stimulated and resting platelet lysates (1mg protein) were incubated with anti-PDE3A antibody (5 $\mu$ g) covalently coupled to amine-reactive resin. Following overnight incubation at 4°C, the resin, precipitated antigen and co-immunoprecipitated proteins were isolated by centrifugation. Proteins were eluted from the resin and immunoblotted for PKA RII, AKAP7 and PKAc. PDE3A was immunoblotted to ensure successful immunoprecipitation. Immunoblots representative of 3 independent experiments.

### 5.8.2 Reverse co-immunoprecipitation of PDE3A signalling partners

Having co-immunoprecipitated PKA type II and AKAP7 with both PDE3A splice variants, we next performed the reverse of this experiment to confirm the association of PDE3A with AKAP7 and PKA type II (Figure 5.11). In PKA type II immunoprecipitates, we detected PDE3A2, AKAP7 $\delta$ , PKAc (Figure 5.11 A). Immunoprecipitation of AKAP7 resulted in the association of PDE3A2, PKA type II, PKAc (Figure 5.11 B). In these two experiments, we detected a stronger interaction between AKAP7 $\delta$  and PKA type II, when compared to the association of PDE3A to these proteins, as AKAP7 $\delta$  and PKA type II protein bands were more intense. Interestingly, we detected minimal association of PDE3A1, represented by a faint protein band.

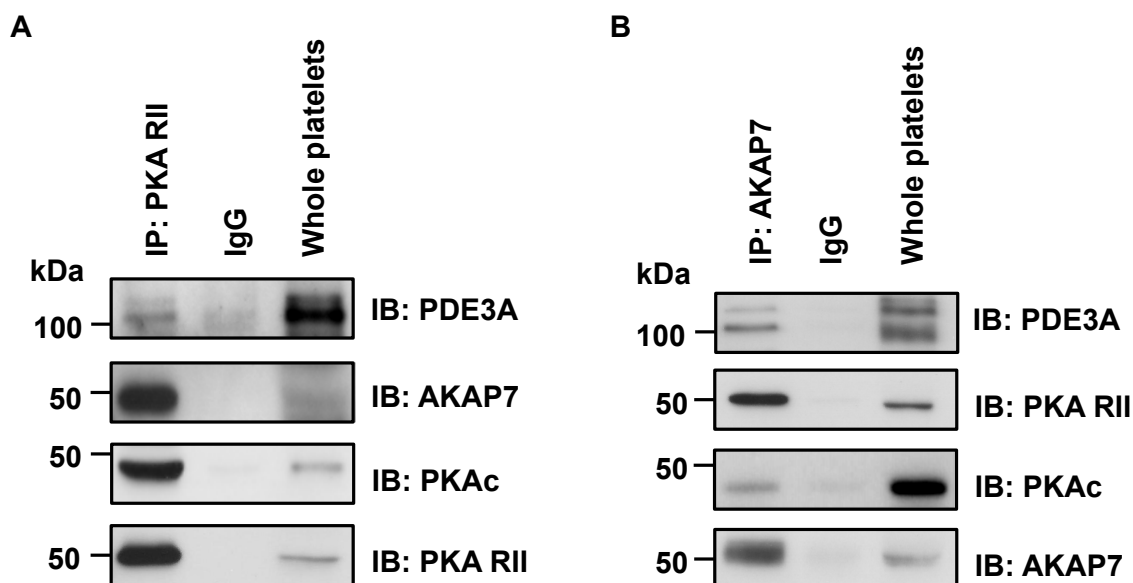


**Figure 5.11. Co-immunoprecipitation of PKA RII, AKAP7 and PKAc with PDE3A.** WPs lysates (1mg protein) were incubated with (A) anti-PKA RII antibody (5 $\mu$ g) and (B) anti-AKAP7 antibody (5 $\mu$ g) covalently coupled to amine-reactive resin. Following overnight incubation at 4°C, the resin, precipitated antigen and co-immunoprecipitated proteins were isolated by centrifugation. Proteins were eluted from the resin and immunoblotted for (A) PDE3A, AKAP7, PKAc and AKAP7 (B) PDE3A, PKA RII, PKAc and PKA. Immunoblots representative of 3 independent experiments.

### 5.8.3 PKA type II and AKAP7 associated PDE3A activity

To further strengthen our PDE3A, AKAP7 and PKA type II co-immunoprecipitation data, we measured associated total PDE3A activity in PKA type II and AKAP7 immunoprecipitates (Figure 5.12). In the first experiment, we measured the PDE3A activity of PDE3A immunoprecipitates as a control. PDE3A activity was recorded at  $3342 \pm 382$  fmol 5-AMP/min/ $1 \times 10^7$  cells, which was inhibited to  $118 \pm 57$  fmol 5-AMP/min/ $1 \times 10^7$  cells with the specific PDE3A inhibitor milrinone ( $*P < 0.01$ ). We detected PKA type II associated PDE3A activity at  $1056 \pm 77$  fmol 5-AMP/min/ $1 \times 10^7$  cells, which was reduced with milrinone to  $236 \pm 90$  5-AMP/min/ $1 \times 10^7$  cells ( $*P < 0.01$  when PKA type II is compared to PKA type II + milrinone). In AKAP7 immunoprecipitates, we detected associated PDE3A activity at  $342$  5-AMP/min/ $1 \times 10^7$  cells, which was also reduced with milrinone to  $104 \pm 19$  5-AMP/min/ $1 \times 10^7$  cells ( $**P < 0.05$  when AKAP7 is compared to AKAP7 + milrinone). These data strengthen our previous observations that describe the association of PKA RII, AKAP7 with PDE3A in human platelets.

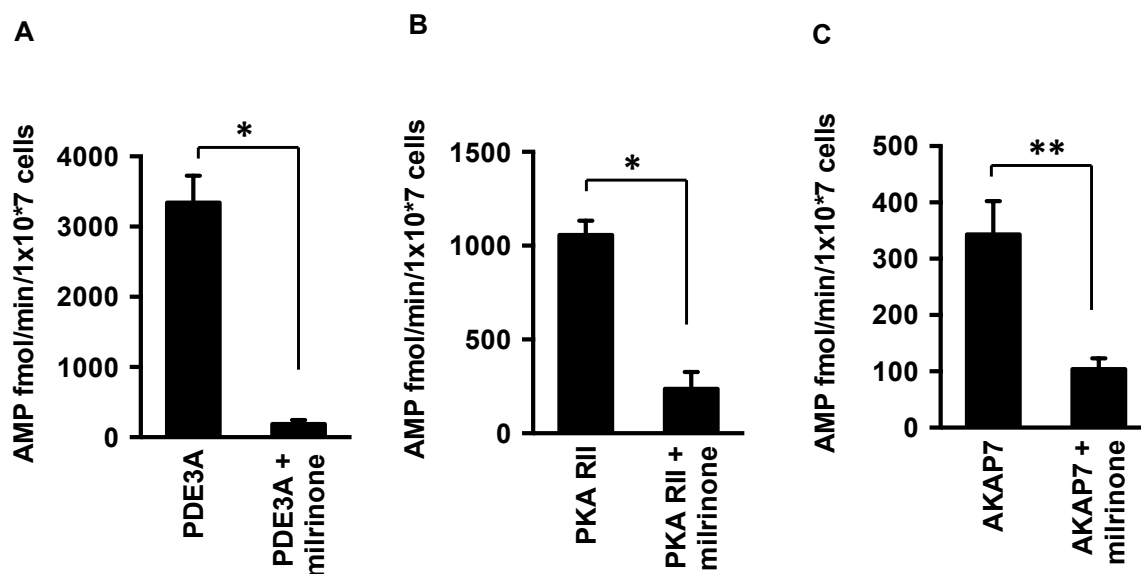


**Figure 5.12 Analysing co-associated PDE3A activity in PKA RII and AKAP7 immunoprecipitates.** (A) PDE3A (B) PKA RII and (C) AKAP7 were immunoprecipitated from washed platelet lysates (500µg protein) and analysed for PDE3A activity, in the presence and absence of Milrinone (10µM). Data representative of 3 independent experiments expressed as means ± SEM (\* $P < 0.01$ , \*\* $P < 0.05$ ).

#### 5.8.4 Subcellular localisation of the PDE3A signalosome

Having identified the protein players in the PDE3A signalosome, we next examined the subcellular localisation within the platelet (Figure 5.13). In this experiment, platelets were stimulated with PGI<sub>2</sub> and fractionated into cytosolic and membrane fractions. These fractions were then immunoblotted for PDE3A2 Ser<sup>312</sup> phosphorylation, PKA type I and type II, PDE3A and AKAP7. We detected the PDE3A2 Ser<sup>312</sup> phosphorylation solely in the platelet cytosol, alongside cytosolic expression of PKA type II and AKAP7. PDE3A2 was primarily localised to the cytosol with PDE3A1 localised to the platelet membrane. Consistent with our previous data in figure 3.3. PKA type I was expressed in both platelet fractions with the majority localised to the platelet membrane. In the lower panel,  $\beta_3$  and SLP-76 were immunoblotted as fractionation controls. Interestingly, we did not detect any movement of the signalling proteins in response to PGI<sub>2</sub>. These data, together with the experiments in figures 5.10, 5.11 and 5.12, reveal for the first time a novel platelet PDE3A signalosome constructed from PKA type II, PKAc, AKAP7 $\delta$  and PDE3A2, localised specifically in platelet cytosol.

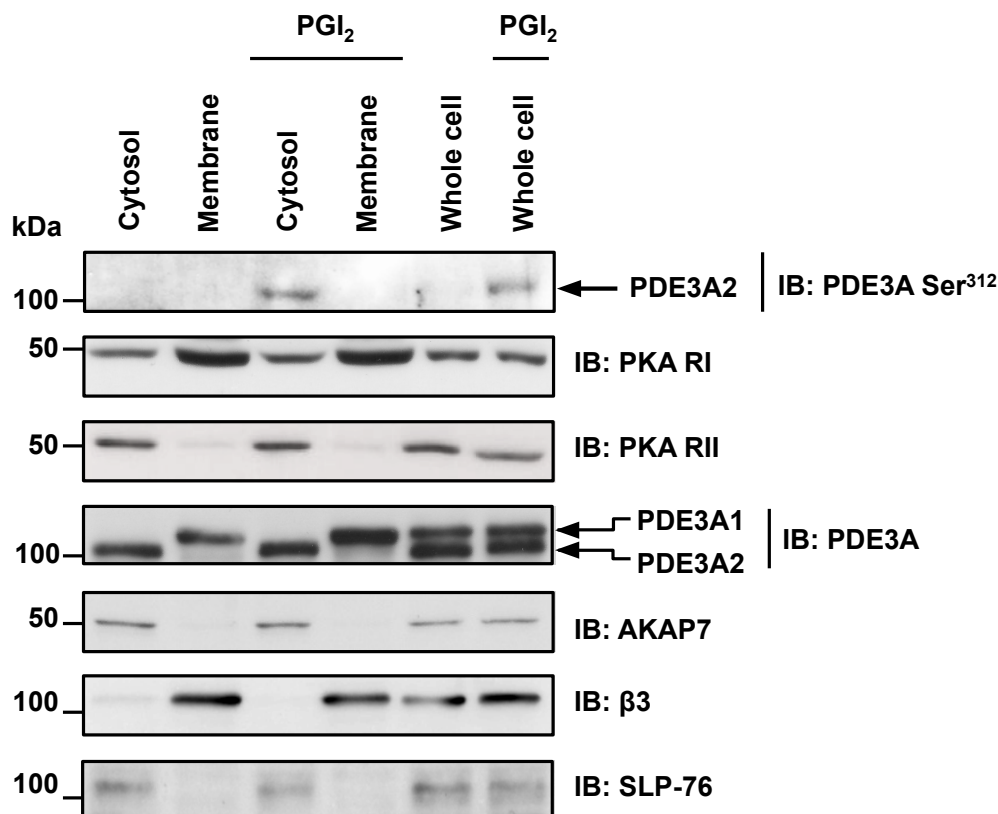


**Figure 5.13 Subcellular localisation of PDE3A2 Ser<sup>312</sup> phosphorylation and signalosome proteins.** WPs ( $7 \times 10^8$  platelets/ml) were stimulated with PGI<sub>2</sub> (100nM, 2 min), lysed using liquid nitrogen snap freezing and centrifuged into membrane and cytosolic fractions. Fractions were then immunoblotted for PDE3A Ser<sup>312</sup> phosphorylation and total PDE3A. Immunoblot membranes were stripped and reprobbed for PKA I, PKA II, AKAP7, β3 and SLP-76. Data representative of 1 independent experiment.

### 5.9 PDE3A specifically regulates multiple platelet PKA substrates

In addition to PKA and PDEs, AKAPs mediated signalling complexes often contain functionally important PKA substrates (Michel and Scott, 2002). In this next experiment, we searched for PDE3A associated PKA substrates, using combination of co-immunoprecipitation and fractionation (Figure 5.14). Here, platelets were stimulated with PGI<sub>2</sub> or the PKC activator PMA and separated into cytosolic and membrane fractions. PDE3A was then immunoprecipitated from the fractions and analysed for the co-association of PKA phosphorylated proteins. In resting platelets, we detected two basal phosphorylated PKA substrates associated with membrane localised PDE3A with molecular weights of 250kDa and 100kDa. Under PGI<sub>2</sub> stimulated conditions, we detected five PKA phosphorylation events associated with cytosolic PDE3A with molecular weights of 110kDa, 100kDa, 90kDa, 45kDa and 35kDa, indicated by arrows. Membrane localised PDE3A was associated with six phosphorylated PKA substrates with molecular weights of 250kDa, 100kDa, 95kDa, 70kDa, 60kDa and 45kDa. Surprisingly, stimulation of PMA resulted in phosphorylation of a band at 45kDa associated with cytosolic PDE3A. It would be of great interest to further examine these potential novel PDE3A signalling nodes. A clear limitation of this experiment is that the phosphorylation of the PDE3A associated PKA substrates were only examined at a single time point following PGI<sub>2</sub> stimulation. In figure 4.4, we showed a changing temporal profile of PKA substrate phosphorylation in response to PGI<sub>2</sub>. Therefore, an improvement in this experiment would be to analyse the phosphorylation of these substrates over time, which could potentially unveil new PDE3A associated PKA substrates. The data in this experiment shows for the first time that PDE3A in platelets is localised to multiple PKA substrates.

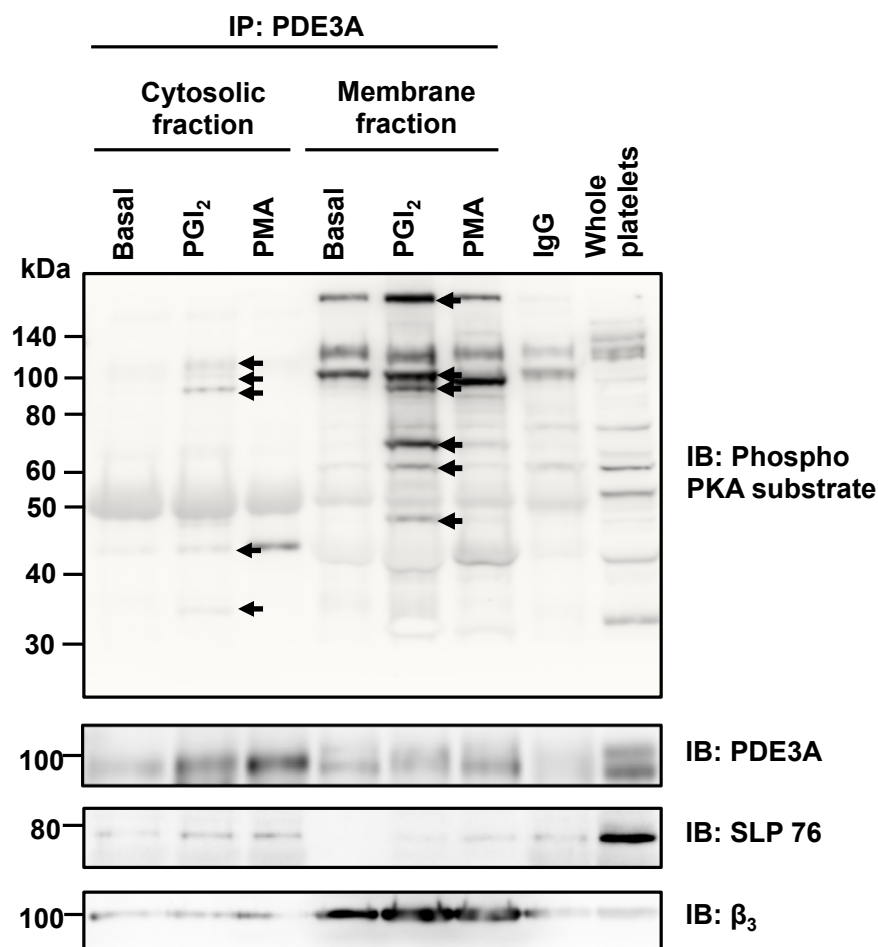


**Figure 5.14 Immunoblotting PDE3A co-associated PKA substrates in platelet fractions.** WP ( $7 \times 10^8$  platelets/ml) were stimulated with PGI<sub>2</sub> (100nM, 2 min) and PMA (0.5 $\mu$ M, 5 min), lysed using liquid nitrogen snap freezing and centrifuged into membrane and cytosolic fractions. PDE3A was immunoprecipitated from fractions (2ug antibody, 500 $\mu$ g protein) and immunoblotted for associated phospho-PKA substrates, PDE3A and the fraction control proteins SLP-76 and  $\beta_3$ . Immunoblot of 1 experiment.

### 5.10 Discussion

The phosphorylation of functionally important platelet proteins by PKA requires tight regulation in space and time in order to maintain platelets in their resting state whilst preserving their capacity for activation. In other cell types, PKA is targeted to specific cellular locations by the actions of AKAPs, which scaffold the kinase with substrates, phosphatases, and regulatory phosphodiesterases. Until very recently, AKAPs remained largely unexplored in platelets (Raslan et al., 2015b). In the previous chapter, we characterised the feedback regulation of cAMP/PKA signalling via PKA phosphorylation and activation of PDE3A. These data gave rise to an important question “what are the mechanisms that mediated this interaction?”. In the present chapter, we explored the answer to this question by examining the role AKAPs in PKA/PDE3A signalling.

Useful tools for elucidating the function of AKAPs are AKAP-disrupting peptides. These cell-permeable peptides disrupt endogenous PKA/AKAP interactions and de-localise PKA by binding to the D/D domain of the PKA regulatory subunits required for AKAP interaction (Calejo and Taskén, 2015). We examined the effects of two of these peptides, non-PKA specific HT31 and PKA type I-specific RIAD-Arg11, on PDE3A phosphorylation and activation by PKA in platelets. We showed that targeting the interaction between PKA and AKAPs with the HT31 AKAP-disruptor peptide blunted PDE3A2 phosphorylation and total PDE3A activation in response to PGI<sub>2</sub>. In contrast, PKA type I-specific AKAP-disruptor peptide RIAD induced no significant change in PDE3A2 phosphorylation and total PDE activity in response to PGI<sub>2</sub>. Therefore, these data suggest an AKAP may facilitate the interaction between PKA type II and PDE3A in platelets. This mechanism has

been identified in other cell types, in which AKAPs scaffold PDE3A and PKA together within multi-protein signalosomes. These signalosomes usually contain functionally important PKA substrates, which require tight regulation by PKA (Faiyaz Ahmad et al., 2015; Puxeddu et al., 2009). However, in this experiment only the total PDE3A activity was measured, therefore, we were unable to determine whether AKAP disruption specifically affected PDE3A2 or both PDE3A isoforms. We also examined the effect of AKAP disruption upstream of PKA/PDE3A signalling, by measuring cAMP responses. Here, we showed that disruption of AKAP/PKA interactions with HT31 did not significantly alter cAMP responses to PGI<sub>2</sub>. This would suggest that the reduced phosphorylation of PDE3A2 by PGI<sub>2</sub> in the presence of HT31 likely represents reduced access of PKA to its substrate rather than a reduced availability of cAMP. Interestingly, there was a small potentiation of cAMP elevations under AKAP disrupting conditions. This small elevation could be the result of the disruption of PDE containing AKAP complexes in proximity to adenylyl cyclase (Dessauer, 2009).

The disruptor peptide data was suggestive of an AKAP mediated phosphorylation event that could potentially regulate PDE3A activity. The AKAP hypothesis of PKA signalling suggests that PKA, AKAP and substrate are in one complex and we began to explore this. In the first step, we confirmed the association between PKA type II and PDE3A in platelets, using co-immunoprecipitation. With this technique we detected association of PKA type II in PDE3A co-immunoprecipitates with no detectable signal for PKA type I. In other cell types, PDE3A has been shown to interact with both PKA type I and PKA type II, however, it is rare that both isoforms are identified in the same PDE3A containing signalosome (Ahmad et al., 2012). With these data in mind, we wanted to search for the AKAP responsible for

scaffolding the interaction between PKA type II and PDE3A. Of the 16 different AKAPs identified in platelets, we began our search with AKAP7, as the delta splice variant of this particular AKAP has been shown to scaffold PKA type II and PDE3A together in cardiac myocytes (Beca et al., 2013). In addition to AKAP7 $\delta$ , there are three other AKAP7 splice variants expressed from the AKAP7 gene, which are AKAP7 $\alpha$ , AKAP7 $\beta$  and AKAP7 $\gamma$  (Johnson et al., 2012). These splice variants share a conserved PKA regulatory subunit binding site but differ in distinct cellular targeting domains. AKAP7 $\alpha$  and AKAP7 $\beta$  are targeted to the plasma membrane, whereas AKAP7 $\gamma$  and AKAP7 $\delta$  reside in the cytosol (Henn et al., 2004; Trotter et al., 1999). The expression of all four AKAP splice variants was examined in platelets using a polyclonal anti-AKAP7 antibody in conjunction with whole platelet immunoblotting, cAMP pull-down assays and immunoprecipitation experiments. Findings showed that only the AKAP7 $\delta$  at 50kDa was detected in whole cell platelets using standard immunoblotting. A more sensitive detection method for AKAPs in cell lysates is the cAMP pull down assay. The assay purifies all cAMP binding proteins, including PKA and associated AKAPs. Before using this assay to purify AKAP7, we examined all the cAMP binding proteins in platelets using protein staining. Here we observed 11 potential cAMP binding proteins were visualised with the assay, with many additional proteins very faintly stained upon close inspection. These latter bands may represent cAMP binding proteins expressed at low levels or proteins that weakly associate with PKA and, therefore, cannot withstand the mechanics of the assay. Next, we used this assay to confirm the expression of AKAP7 $\delta$  in platelets and to also search for the expression of AKAP7 $\alpha$ , AKAP7 $\beta$  and AKAP7 $\gamma$ . AKAP7 $\delta$  was detected in the cAMP pull down, thus strengthening our initial observations. Interestingly, we also detected the

possible expression of AKAP7 $\gamma$  at very low levels, represented by a faint protein band. This observation could be explained by the fact that AKAP7 $\gamma$  is very closely related to AKAP7 $\delta$ , arising from an internal translation start site present in the AKAP7 $\delta$  cDNA in human cells (Johnson et al., 2012). The final stage in confirming AKAP7 expression in platelets was to cross-reference the commercial AKAP7 antibody with that provided by Professor Enno Klussmann. Using the commercial antibody to immunoprecipitate AKAP7 and the independent antibody to immunoblot AKAP7, we showed that our commercial antibody was indeed specific to AKAP7.

AKAPs function to anchor PKA to discrete cellular locations in proximity to isolated cAMP pools allowing for efficient activation PKAc subunits and accurate substrate selection (Michel and Scott, 2002). We tested the PKA binding ability of AKAP7 by measuring associated PKA activity in AKAP7 immunoprecipitates. Our data showed that immunoprecipitated AKAP7 possessed significant PKA activity when compared to that of an IgG control. These data were important to confirm that AKAP7 was associated with the whole PKA holoenzyme rather simply the regulatory subunit. We wanted to expand on these association experiments and confirm that the proteins were co-localised in whole cells by employing the proximity ligation assay to visualise the specific anchoring of PKA type II by AKAP7 in platelets. The proximity ligation assay is a recent addition to our teams' molecular toolbox, enabling the detection, quantification and visualisation of protein-protein interactions (Gullberg et al., 2003). With this assay, we confirmed the interaction between PKA type II and AKAP7 in platelets. However due to the platelets small size we were unable to pinpoint the precise subcellular location of this event.

Having examined the interactions between PDE3A and PKA type II, and the anchoring of PKA type by AKAP7, we next sought to characterise the entire PDE3A signalosome responsible for PDE3A feedback regulation of PKA. The first step in this process was to co-immunoprecipitate total PDE3A with PKA type II, PKAc and AKAP7. As with other experiments in this chapter, we were unable to specifically immunoprecipitate each PDE3A splice variant due to the lack of splice variant specific antibodies. Our data shows that PKA type II, PKAc and AKAP7 $\delta$  can associate with PDE3A. These interactions were strong enough to withstand the mechanics of the co-immunoprecipitation procedure and did not require the use of over expression systems for investigation. In order to confirm our observations, we performed the reverse of this experiment by co-immunoprecipitating PDE3A with AKAP7 and PKA type II. In line with our previous data, PDE3A co-immunoprecipitated with PKA type II and AKAP7, with a strong association of PDE3A2 and weak association of PDE3A1. In these experiments, we detected a stronger interaction between AKAP7 $\delta$  and PKA type II, when compared to the association of PDE3A to these proteins. This observation may suggest that in the platelet cell there are AKAP7 $\delta$  /PKA type II complexes locally regulated by PDE3A and other complexes devoid of PDE3A regulation. It would be of interest to investigate whether these PDE3A free signalling nodes are instead regulated by PDE2A (Acin-Perez et al., 2011). We next strengthened these data by measuring associated PDE3A activity with PKA type II and AKAP7. Using our PDE activity assay we again showed significant co-association of PDE3A with PKA type II and AKAP7 (Figure 5.11). Together these data describe for the first time a novel platelet signalosome containing PKA type II, AKAP7 $\delta$  and PDE3A.

It was important in this work to characterise the subcellular localisation of this PDE3A signalosome in platelets. In this next experiment, we immunoblotted for PKA type I and II, PDE3A and AKAP7 in both platelet cytosolic and membrane fractions. Additionally, we examined the subcellular localisation of PDE3A regulation by PKA by stimulating platelets with PGI<sub>2</sub> and immunoblotting for PDE3A Ser<sup>312</sup> in platelet fractions. Data from this experiment showed that PKA phosphorylation of PDE3A2 Ser<sup>312</sup> occurred specifically in the cytosol. Furthermore, this observation shows that feedback inhibition of cAMP/PKA signalling in platelets is targeted to specific regions within the platelet.

We also detected cytosolic specific expression of PKA type II and AKAP7. These data are in agreement with studies by Raslan and colleagues who showed using confocal microscopy that PKA type II is localised to the platelet cytosol (Raslan et al., 2015b). Our data is also consistent with studies that describe the cytosolic nature of AKAP7δ (Henn et al., 2004). However, AKAP7δ has also been shown to localise with the membranes of aquaporin 2 bearing vesicles important in the regulation of body water balance (Horner et al., 2012). We detected expression of PDE3A1 specifically in membrane fractions, whereas PDE3A2 was localised primarily to the platelet cytosol, in agreement with our previous data in figure 3.3. As PDE3A1 was specifically localised to the membrane, it could be concluded that cytosolic PDE3A2 is the likely PDE3A splice variant that is scaffolded by AKAP7δ in approximation with PKA type II to form a negative feedback loop of cAMP signalling localised to the platelet cytosol. This model could be further investigated by examining the temporal profile of PGI<sub>2</sub> stimulated PKA signalling events in cells that contain PDE3A Ser<sup>312</sup> specific mutants.

AKAP scaffolded signalosomes often contain functionally important PKA substrates, in which associated PKA, phosphatases and cAMP hydrolyzing PDEs can closely regulate the phosphorylation status of the substrate (Baillie et al., 2005). With this in mind, we searched for the association of PKA substrates with PDE3A by co-immunoprecipitating PDE3A from PGI<sub>2</sub> stimulated platelets and immunoblotting the PDE for associated PKA phosphorylation events. To our surprise, we detected multiple PKA substrates associated with PDE3A, localised to both the platelet cytosol and membrane. In the platelet cytosol, phosphorylation bands at 100kDa, 95kDa, 45kDa and 37kDa were visualised that likely represent PDE3A2, MLCK, G $\alpha$ <sub>13</sub> and LASP, respectively (Aburima et al., 2013; Butt et al., 2003; Manganello et al., 1999). Localised to the platelet membrane were phosphorylation bands 250kDa, 100kDa, 95kDa and 45kDa, which may represent IP<sub>3</sub> receptor, PDE5, MLCK and VASP, respectively (Aburima et al., 2013; Chaloux et al., 2007; Corbin et al., 2000; Jensen et al., 2004). These findings suggest that there are several PKA substrates associated with PDE3A. Moreover, these signalosomes are likely to be PDE3A splice variant specific, localised to distinct regions within the platelet. The association of PKA substrates within PDE3A signalosomes would permit PDE3A to directly regulate local cAMP/PKA responses neighbouring the substrate. It would be of great interest to identify these signalosomes, to uncover new mechanisms of platelet inhibition and potentially fruitful drug targets.

The data in this chapter describes a novel signalling complex localised to platelet cytosol containing PKA type II, PKAc, AKAP $\delta$  and PDE3A2. In this signalling complex PDE3A2 forms a local negative feedback loop of inhibitory cAMP/PKA type II signalling. We have shown that disruption of this signalling complex, and

potentially other PKA type II/AKAP complexes, blunts PDE3A phosphorylation and activation in response to cAMP signalling. This is the first evidence of spatiotemporal regulation of feedback inhibition within the cAMP-signalling pathway in platelets.

## 6 Discussion

Improving our understanding of PDE3A signalling in human platelets holds great value in the development of novel therapeutic strategies for treating arterial thrombosis. PDE3A is a powerful regulator of endogenous platelet inhibition, constantly hydrolysing intracellular cAMP levels to preserve a vital threshold for platelet activation (Feijge et al., 2004). PDE3A inhibitors are already used in antiplatelet therapies with several inhibitors currently undergoing clinical trials for the treatment of atherothrombosis and ischaemic stroke (Maurice et al., 2014). However, the clinical use of current PDE3A inhibitors has been linked to multiple side effects (Gresele et al., 2011). New insights into platelet PDE3A signalling may reveal novel molecular targets that can modify PDE3A activity in a safe and specific manner for the treatment of pathological thrombosis. The aim of this study was to identify novel mechanisms of PDE3A signalling in human platelets using a range of molecular biology techniques. Here, we investigated the characteristics of all three platelet PDE isoforms in platelets with a special focus on the expression of multiple PDE3A splice variants. Furthermore, we examined the regulation of PDE3A by PKA in response to endogenous platelet inhibition and explored the cellular mechanisms that facilitate this interaction.

Ever since Hidaka and colleagues first reported their findings that the PDE3A inhibitor cilostazol inhibited platelet aggregation, PDE3A signalling in platelets has attracted scientific attention (Hidaka et al., 1979). In other cell types, there have been numerous advances in our understanding of PDE3A signalling, particularly in PDE3A regulation of cardiac function (Ahmad et al., 2012; Vandeput et al., 2013). However, these new insights have yet to be translated in platelets. The regulation

of cardiac function in myocyte cells is orchestrated by three PDE3A variants, PDE3A1, PDE3A2 and PDE3A3, which arise from alternative splicing of the PDE3A gene (Choi et al., 2001; Kasuya et al., 1995; Wechsler, 2002). In these cells, PDE3A1 is localised to the myocyte membrane through a unique N-terminal domain, whereas PDE3A2 and PDE3A3 are localised to both the myocyte membrane and cytosol (Hambleton et al., 2005; Vandeput et al., 2013). In our first line of experiments we report that platelets express two of these variants: PDE3A1 and PDE3A2, with PDE3A1 localised to platelet membrane and PDE3A2 primarily expressed in the platelet cytosol (Figure 3.4). This observation adds to the concept of compartmentalised cAMP signalling in platelets, in which cAMP microdomains are differentially regulated in space and time within the cell (Edwards et al., 2012; Raslan et al., 2015a). Unfortunately at this point in time, there are no splice variant-specific antibodies or inhibitors available as research tools; therefore, we were unable to fully dissect the impact of each PDE3A splice variant on platelet function. The full significance of the finding that platelets express two PDE3A splice variants was not recognised until late in the project. Therefore we did not have enough time to fully visualise both PDE3A splice variants in every experiment using an increased gel run time.

In platelets, PDE3A functions as a dynamic negative regulator of cAMP levels. In response to PGI<sub>2</sub>, PDE3A activity increases through PKA-mediated phosphorylation, in turn leading to enhanced cAMP hydrolysis and the preservation of platelet sensitivity to endogenous platelet agonists (Grant et al., 1988; Hunter et al., 2009; Macphee et al., 1988). Additionally, PDE3A activity can be increased via PKC phosphorylation in response to platelet agonist binding, forming a positive feedback loop that lowers intracellular cAMP levels and

heightens the sensitivity of platelets to activatory stimuli (Hunter et al., 2009). At this point in time, there are multiple identified PKC phosphorylation sites on PDE3A with a single PKA phosphorylation identified at site Ser<sup>312</sup> (Pozuelo Rubio et al., 2005). We report for the first time that only PDE3A2 is phosphorylated by PKA in platelets at Ser<sup>312</sup>, and not PDE3A1 (Figure 4.13). Furthermore, we provide evidence that this phosphorylation event is temporal suggesting the presence of regulatory phosphatase (Figure 4.10). The selective regulation of PDE3A2 in platelets indicates that PDE3A1 and PDE3A2 are likely to have distinct roles in the regulation of platelet inhibition. These data raise the possibility of PDE3A variant specific inhibitors inducing alternative effects on endogenous platelet inhibition. Interestingly, cardiac myocytes display a different pattern of PDE3A splice variant regulation with PDE3A1 and PDE3A2 both phosphorylated by PKA (Vandeput et al., 2013). This difference could arise from alternative localisation of PKA isoforms due to different physiological roles cAMP signalling plays between cell types. Recent studies have identified mutations in the PKC phosphorylation sites on PDE3A2 as a driving force behind autosomal dominant hypertension with brachydactyly (Maass et al., 2015; Toka et al., 2015). In these studies, PDE3A2 phosphorylation site mutations result in permanent PDE activation and low cAMP levels in vascular smooth muscle cells (VSCMs), ultimately leading to enhanced cell proliferation and hypertension (Maass et al., 2015; Toka et al., 2015). It is clear that additional studies dissecting differences in PDE3A splice variant signalling and function are of important therapeutic value.

In other cell types, PDE3A often regulates cAMP levels as part of multi-protein signalling complexes, which are tethered to specific regions of the cell to perform a specific physiological function (Ahmad et al., 2012). These signalosomes can

contain PKA isoforms, functional PKA substrates, phosphatases and other regulatory enzymes, scaffolded together and anchored within the cell through the actions of AKAPs (Ahmad et al., 2015; Beca et al., 2013). Within the signalosome, PDE3A can directly regulate the phosphorylation status of the functional substrate through breakdown of local cAMP (Baillie et al., 2005). For instance, PDE3A in HeLa cells has been shown to localise with PKA type I and brefeldin A-inhibited guanine nucleotide-exchange AKAP proteins 1 and 2 (BIG1 and BIG2) to form a signalosome that functions in vesicle transport (Puxeddu et al., 2009). PDE3A in cardiac myocytes localises with PKA type II, AKAP7, PDE3A, PP2A, phospholamban and Serca2a to form a signalosome that regulates heart contractility (Beca et al., 2013). PDE3A in platelets is known to associate with 14-3-3 proteins that regulate protein function through binding to phospho-serine motifs (Hunter et al., 2009). However, at this point in time, the exact function of this interaction is not fully understood. In this study, we provide evidence for the first time of a novel platelet PDE3A signalosome constructed from PDE3A2, PKA type II and AKAP7 $\delta$ , expressed in the platelet cytosol (Figure 5.10 and 5.13). Within this signalosome, PDE3A2 can directly regulate PKA type II activity in response to local cAMP concentrations in a negative feedback manner. It can be hypothesised that AKAP7 $\delta$  functions as a scaffold for PDE3A/PKA type II association, as disruption of PKA type II/AKAP interactions blunts PDE3A2 phosphorylation and activation. It is also likely that this novel signalosome also contains a regulatory phosphatase due to the temporal nature of PDE3A2 phosphorylation. These observations are supported by studies performed by Beca and colleagues that detail the interaction of PDE3A with AKAP7 $\delta$  in cell function (Beca et al., 2013). Moreover, further studies indicated that phosphorylation of PDE3A not only

increases the enzymes activity but also influences the enzymes interaction with associated signalling partners (Ahmad et al., 2015). However, in this study, we did not detect phosphorylation as driving mechanism behind signalosome formation.

A general trend of PDE3A signalosomes is the association of functional substrates that require tight regulation by PKA and PDE3A (Ahmad et al., 2012). Although we did not identify such a substrate regulated within the PDE3A2/PKA type II/AKAP7 $\delta$  signalosome, we did detect promising signs of substrate interaction. Our findings suggest that there are multiple phosphorylated PKA substrates which interact with PDE3A in platelets, within both cytosolic and membrane regions of the cell (Figure 5.14). Yet it is unclear whether these substrates interact with PDE3A through AKAP7 or other scaffolding proteins. Further research is required in platelets to tease apart the spatiotemporal regulation of PKA signalling in platelets and determine the functional outcome of PDE3A-substrate association.

Herein, we provide the first evidence for spatiotemporal regulation of cAMP signalling in blood platelets. Our findings have shown human platelets express two PDE3A splice variants, PDE3A1 and PDE3A2, which are differentially localised and regulated by PKA. Furthermore, our data describes a novel platelet PKA type II containing PDE3A2 signalosome that is scaffolded together by AKAP7 $\delta$  and targeted to the platelet cytosol. Within this signalosome PDE3A2 can directly regulate the inhibitory action of PKA signalling, in a negative feedback manner. Selective inhibition of PDE3A splice variants and/or pharmacological disruption of PDE3A signalosomes may provide new safer ways of specifically controlling the platelet response to endogenous inhibition for the treatment of arterial thrombosis (Tröger et al., 2012).

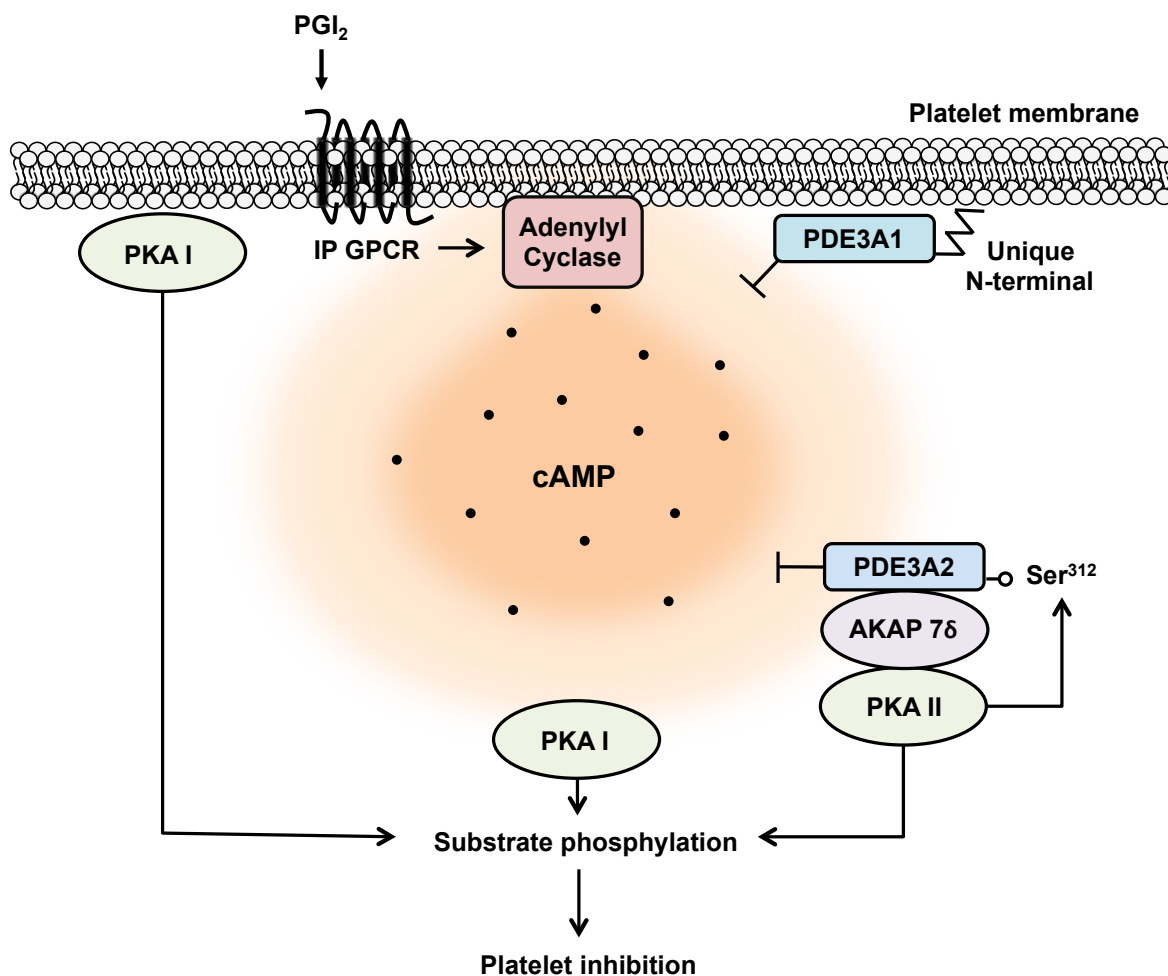


**Figure 6.1 Revised model of PDE3A signalling in platelets as proposed by data in this study.** PGI<sub>2</sub> binds to the IP GPCR and activates AC to synthesise cAMP. Binding of cAMP to PKA type I and type II induces dissociation of PKA catalytic subunits that go on to phosphorylate functionally important proteins that ultimately results in platelet inhibition. At the same time membrane localised PDE3A1 and predominantly cytosolic PDE3A2 regulate the cAMP/PKA response by hydrolysing cAMP into inactive 5'AMP. PDE3A2 is also associated with PKA type II through AKAP7 δ to directly regulate PKA type II activity in a negative feedback manner that is driven by PKA-mediated phosphorylation and activation of PDE3A.

## 6.1 Future direction

This study has shed light on the dynamics of PDE3A signalling in platelets through the identification of differentially regulated PDE3A splice variants and expression of a multiprotein PDE3A signalosome. However, data presented in this study has also given rise to a number of important questions that require answering. Therefore future work could investigate the following:

- **Effect of PDE3A splice variant inhibition on platelet function.** There are numerous studies describing the inhibitory effect of selective PDE3A inhibition on platelet aggregation,  $\text{Ca}^{2+}$  signalling, platelet activation and *in vivo* thrombus formation (Feijge et al., 2004; Manns et al., 2002; Sim et al., 2016; Sun et al., 2007). Our findings indicate that these PDE3A inhibitors are actually targeting two functionally distinct PDE3A splice variants that are likely to have different roles in the regulation of platelet inhibition. In respect to current advancements in PDE3A signalling in other cell types, the development of PDE3A splice variant specific inhibitors can be expected in the near future. It would be of great interest and therapeutic value to evaluate the effect of selective PDE3A splice variant inhibition on platelet function.
- **Identification of PDE3A associated substrates.** Compartmentalisation of cAMP/PKA signalling in platelets is an emerging and exciting area of research in the platelet field (Raslan et al., 2015a). Within cAMP compartments, PDEs can regulate specific physiological processes as components of multiprotein complexes that are targeted to specific

locations within the cell. Data presented in this study suggests that there are multiple PKA substrates associated with PDE3A in platelets, likely through AKAP dependent mechanisms. The identification of these substrates and the PDE3A splice variant they are associated with, using molecular biology techniques may reveal new insights into the mechanisms of cAMP-mediated platelet inhibition.

- **Localisation of PDE regulated cAMP and cGMP pools in platelets.**

Research has shown that stimulation of cGMP-signalling cascades in platelets results in the accumulation of cAMP in platelets, through cGMP-dependant inhibition of PDE3A (Dickinson et al., 1997; Feijge et al., 2004). Under conditions of high cGMP, cGMP-stimulated PDE2A is thought to function as a regulator cAMP elevations (Haslam et al., 1999; Manns et al., 2002). However, the dynamics of these events is unclear, as the current theory of PDE cross talk in platelets is dependent on the ubiquitous access of cAMP and cGMP to all PDE populations within the platelet. The findings in this study along with similar studies in platelets and other cell types instead propose that cAMP and cGMP signalling is a far more organised and complex process (Raslan et al., 2015a, 2015b; Zaccolo and Movsesian, 2007). Analysis of PDE regulated cAMP and cGMP domains within the platelet structure using microscopy techniques may reveal new insights into the mechanism of PDE signalling cross-talk in platelets.

## References

- Aburima, A., Wraith, K.S., Raslan, Z., Law, R., Magwenzi, S., Naseem, K.M., 2013. cAMP signaling regulates platelet myosin light chain (MLC) phosphorylation and shape change through targeting the RhoA-Rho kinase-MLC phosphatase signaling pathway. *Blood* 122, 3533–45.
- Acin-Perez, R., Russwurm, M., Günnewig, K., Gertz, M., Zoidl, G., Ramos, L., Buck, J., Levin, L.R., Rassow, J., Manfredi, G., Steegborn, C., 2011. A phosphodiesterase 2A isoform localized to mitochondria regulates respiration. *J. Biol. Chem.* 286, 30423–32.
- Ahmad, F., Degerman, E., Manganiello, V.C., 2012. Cyclic nucleotide phosphodiesterase 3 signaling complexes. *Horm. Metab. Res.* 44, 776–85.
- Ahmad, F., Murata, T., Shimizu, K., Degerman, E., Maurice, D., Manganiello, V., 2015. Cyclic nucleotide phosphodiesterases: important signaling modulators and therapeutic targets. *Oral Dis.* 21, e25–50.
- Ahmad, F., Shen, W., Vandeput, F., Szabo-Fresnais, N., Krall, J., Degerman, E., Goetz, F., Klusmann, E., Movsesian, M., Manganiello, V., 2015. Regulation of sarcoplasmic reticulum Ca<sup>2+</sup> ATPase 2 (SERCA2) activity by phosphodiesterase 3A (PDE3A) in human myocardium: phosphorylation-dependent interaction of PDE3A1 with SERCA2. *J. Biol. Chem.* 290, 6763–76.
- Antl, M., von Brühl, M.-L., Eiglsperger, C., Werner, M., Konrad, I., Kocher, T., Wilm, M., Hofmann, F., Massberg, S., Schlossmann, J., 2007. IRAG mediates NO/cGMP-dependent inhibition of platelet aggregation and thrombus formation. *Blood* 109, 552–9.
- Armstrong, R.A., 1996. Platelet prostanoid receptors. *Pharmacol. Ther.* 72, 171–91.
- Baillie, G., Scott, J.D., Houslay, M.D., 2005. Compartmentalisation of phosphodiesterases and protein kinase A: Opposites attract. *FEBS Lett.* 579,

3264–3270.

- Baillie, G.S., 2009. Compartmentalized signalling: Spatial regulation of cAMP by the action of compartmentalized phosphodiesterases. *FEBS J.* 276, 1790–1799.
- Battinelli, E., Willoughby, S.R., Foxall, T., Valeri, C.R., Loscalzo, J., 2001. Induction of platelet formation from megakaryocytoid cells by nitric oxide. *Proc. Natl. Acad. Sci. U. S. A.* 98, 14458–63.
- Beca, S., Ahmad, F., Shen, W., Liu, J., Makary, S., Polidovitch, N., Sun, J., Hockman, S., Chung, Y.W., Movsesian, M., Murphy, E., Manganiello, V., Backx, P.H., 2013. Phosphodiesterase type 3A regulates basal myocardial contractility through interacting with sarcoplasmic reticulum calcium ATPase type 2a signaling complexes in mouse heart. *Circ. Res.* 112, 289–97.
- Beck, F., Geiger, J., Gambaryan, S., Veit, J., Vaudel, M., Nollau, P., Kohlbacher, O., Martens, L., Walter, U., Sickmann, A., Zahedi, R.P., 2014. Time-resolved characterization of cAMP/PKA-dependent signaling reveals that platelet inhibition is a concerted process involving multiple signaling pathways. *Blood* 123, 1–11.
- Begonja, A.J., Gambaryan, S., Schulze, H., Patel-Hett, S., Italiano, J.E., Hartwig, J.H., Walter, U., 2013. Differential roles of cAMP and cGMP in megakaryocyte maturation and platelet biogenesis. *Exp. Hematol.* 41, 91–101.e4.
- Bender, A.T., Beavo, J.A., 2006. Cyclic nucleotide phosphodiesterases: molecular regulation to clinical use. *Pharmacol. Rev.* 58, 488–520.
- Berger, G., Massé, J.M., Cramer, E.M., 1996. Alpha-granule membrane mirrors the platelet plasma membrane and contains the glycoproteins Ib, IX, and V. *Blood* 87, 1385–95.
- Bergmeier, W., Chauhan, A.K., Wagner, D.D., 2008. Glycoprotein Iba and von Willebrand factor in primary platelet adhesion and thrombus formation: Lessons from mutant mice. *Thromb. Haemost.*

- Berkels, R., Klotz, T., Sticht, G., Englemann, U., Klaus, W., 2001. Modulation of human platelet aggregation by the phosphodiesterase type 5 inhibitor sildenafil. *J. Cardiovasc. Pharmacol.* 37, 413–21.
- Blair, P., Flaumenhaft, R., 2009. Platelet alpha-granules: basic biology and clinical correlates. *Blood Rev.* 23, 177–89.
- Blair, P., Flaumenhaft, R., 2009. Platelet Alpha–granules: Basic biology and clinical correlates Price. *Blood Rev.* 23, 177–189.
- Bodin, S., Tronchère, H., Payrastre, B., 2003. Lipid rafts are critical membrane domains in blood platelet activation processes. *Biochim. Biophys. Acta - Biomembr.* 1610, 247–257.
- Bodnar, R.J., Xi, X., Li, Z., Berndt, M.C., Du, X., 2002. Regulation of glycoprotein Ib-IX-von Willebrand factor interaction by cAMP-dependent protein kinase-mediated phosphorylation at Ser166 of glycoprotein Ib?? *J. Biol. Chem.* 277, 47080–47087.
- Born, B.Y.G.V.R., Cross, M.J., Fields, I., 1963. THE AGGREGATION OF BLOOD PLATELETS From the Department of Pharmacology , Royal College of Surgeons 178–195.
- Brass, L.F., Zhu, L., Stalker, T.J., 2005. Minding the gaps to promote thrombus growth and stability. *J. Clin. Invest.* 115, 3385–3392.
- Broos, K., Feys, H.B., De Meyer, S.F., Vanhoorelbeke, K., Deckmyn, H., 2011. Platelets at work in primary hemostasis. *Blood Rev.* 25, 155–167.
- Burkhart, J.M., Vaudel, M., Gambaryan, S., Radau, S., Walter, U., Martens, L., Sickmann, A., Zahedi, P., 2012. The first comprehensive and quantitative analysis of human platelet protein composition allows the comparative analysis of structural and functional pathways. *Blood* 120, 73–82.
- Butt, E., Abel, K., Krieger, M., Palm, D., Hoppe, V., Hoppe, J., Walter, U., 1994. cAMP- and cGMP-dependent protein kinase phosphorylation sites of the focal adhesion vasodilator-stimulated phosphoprotein (VASP) in vitro and in intact

- human platelets. *J. Biol. Chem.* 269, 14509–17.
- Butt, E., Gambaryan, S., Göttfert, N., Galler, A., Marcus, K., Meyer, H.E., 2003. Actin binding of human LIM and SH3 protein is regulated by cGMP- and cAMP-dependent protein kinase phosphorylation on serine 146. *J. Biol. Chem.* 278, 15601–15607.
- Butt, E., Immler, D., Meyer, H.E., Kotlyarov, A., Laass, K., Gaestel, M., 2001. Heat shock protein 27 is a substrate of cGMP-dependent protein kinase in intact human platelets: phosphorylation-induced actin polymerization caused by HSP27 mutants. *J. Biol. Chem.* 276, 7108–13.
- Calejo, A.I., Taskén, K., 2015. Targeting protein–protein interactions in complexes organized by A kinase anchoring proteins. *Front. Pharmacol.* 6, 1–13.
- Canobbio, I., Balduini, C., Torti, M., 2004. Signalling through the platelet glycoprotein Ib-V–IX complex. *Cell. Signal.* 16, 1329–1344.
- Carlson, C.R., Lygren, B., Berge, T., Hoshi, N., Wong, W., Tasken, K., Scott, J.D., 2006. Delineation of Type I Protein Kinase A-selective Signaling Events Using an RI Anchoring Disruptor. *J. Biol. Chem.* 281, 21535–21545.
- Carr, D.W., Stofko-Hahn, R.E., Fraser, I.D., Bishop, S.M., Acott, T.S., Brennan, R.G., Scott, J.D., 1991. Interaction of the regulatory subunit (RII) of cAMP-dependent protein kinase with RII-anchoring proteins occurs through an amphipathic helix binding motif. *J. Biol. Chem.* 266, 14188–92.
- Castle, J.D., 2004. Overview of cell fractionation. *Curr. Protoc. Protein Sci.* Chapter 4, Unit 4.1.
- Castro, L.R. V, Verde, I., Cooper, D.M.F., Fischmeister, R., 2006. Cyclic guanosine monophosphate compartmentation in rat cardiac myocytes. *Circulation* 113, 2221–8.
- Cavallini, L., Coassin, M., Borean, A., Alexandre, A., 1996. Prostacyclin and sodium nitroprusside inhibit the activity of the platelet inositol 1,4,5-trisphosphate receptor and promote its phosphorylation. *J. Biol. Chem.* 271,

5545–51.

Chaloux, B., Caron, A.Z., Guillemette, G., 2007. Protein kinase A increases the binding affinity and the Ca<sup>2+</sup> release activity of the inositol 1,4,5-trisphosphate receptor type 3 in RINm5F cells. *Biol. Cell* 99, 379–88.

Chen, J., López, J. a, 2005. Interactions of platelets with subendothelium and endothelium. *Microcirculation* 12, 235–246.

Chen, M., Stracher, a, 1989. In situ phosphorylation of platelet actin-binding protein by cAMP-dependent protein kinase stabilizes it against proteolysis by calpain. *J. Biol. Chem.* 264, 14282–9.

Choi, Y.H., Ekholm, D., Krall, J., Ahmad, F., Degerman, E., Manganiello, V.C., Movsesian, M.A., 2001. Identification of a novel isoform of the cyclic-nucleotide phosphodiesterase PDE3A expressed in vascular smooth-muscle myocytes. *Biochem. J.* 353, 41–50.

Clemetson, K.J., 2012. Platelets and primary haemostasis. *Thromb. Res.* 129, 220–224.

Conti, M., Mika, D., Richter, W., 2013. Perspectives on: Cyclic nucleotide microdomains and signaling specificity: Cyclic AMP compartments and signaling specificity: Role of cyclic nucleotide phosphodiesterases. *J. Gen. Physiol.* 143, 29–38.

Corbin, J.D., Turko, I. V., Beasley, A., Francis, S.H., 2000. Phosphorylation of phosphodiesterase-5 by cyclic nucleotide-dependent protein kinase alters its catalytic and allosteric cGMP-binding activities. *Eur. J. Biochem.* 267, 2760–2767.

Corradini, E., Burgers, P.P., Plank, M., Heck, A.J.R., Scholten, A., 2015. Huntingtin-associated protein 1 (HAP1) is a cGMP-dependent kinase anchoring protein (GKAP) specific for the cGMP-dependent protein kinase I $\beta$  isoform. *J. Biol. Chem.* 290, 7887–96.

Coughlin, S.R., 2000. Thrombin signalling and protease-activated receptors.

Nature 407, 258–264.

- Cristina de Assis, M., Cristina Plotkowski, M., Fierro, I.M., Barja-Fidalgo, C., de Freitas, M.S., 2002. Expression of inducible nitric oxide synthase in human umbilical vein endothelial cells during primary culture. *Nitric Oxide* 7, 254–61.
- Cullen, S.E., Schwartz, B.D., 1976. An improved method for isolation of H-2 and Ia alloantigens with immunoprecipitation induced by protein A-bearing staphylococci. *J. Immunol.* 117, 136–42.
- Dangel, O., Mergia, E., Karlisch, K., Groneberg, D., Koesling, D., Friebe, a, 2010. Nitric oxide-sensitive guanylyl cyclase is the only nitric oxide receptor mediating platelet inhibition. *J. Thromb. Haemost.* 8, 1343–52.
- Dema, A., Perets, E., Schulz, M.S., Deák, V.A., Klussmann, E., 2015. Pharmacological targeting of AKAP-directed compartmentalized cAMP signalling. *Cell. Signal.* 27, 2474–2487.
- Dessauer, C.W., 2009. Adenylyl cyclase--A-kinase anchoring protein complexes: the next dimension in cAMP signaling. *Mol. Pharmacol.* 76, 935–41.
- Dickinson, N.T., Jang, E.K., Haslam, R.J., 1997. Activation of cGMP-stimulated phosphodiesterase by nitroprusside limits cAMP accumulation in human platelets: effects on platelet aggregation. *Biochem. J.* 323 ( Pt 2, 371–7.
- Dopheide, S.M., Maxwell, M.J., Jackson, S.P., 2002. Shear-dependent tether formation during platelet translocation on von Willebrand factor. *Blood* 99, 159–167.
- Dostmann, W.R., 1995. (RP)-cAMPS inhibits the cAMP-dependent protein kinase by blocking the cAMP-induced conformational transition. *FEBS Lett.* 375, 231–234.
- Edwards, H. V., Christian, F., Baillie, G.S., 2012. cAMP: Novel concepts in compartmentalised signalling. *Semin. Cell Dev. Biol.* 23, 181–190.
- Eigentaler, M., Nolte, C., Halbrügge, M., Walter, U., 1992. Concentration and

- regulation of cyclic nucleotides, cyclic-nucleotide-dependent protein kinases and one of their major substrates in human platelets. Estimating the rate of cAMP-regulated and cGMP-regulated protein phosphorylation in intact cells. *Eur. J. Biochem.* 205, 471–81.
- El-Daher, S.S., Eigenthaler, M., Walter, U., Furuichi, T., Miyawaki, A., Mikoshiba, K., Kakkar, V. V, Authi, K.S., 1996. Distribution and activation of cAMP- and cGMP-dependent protein kinases in highly purified human platelet plasma and intracellular membranes. *Thromb. Haemost.* 76, 1063–71.
- El-Daher, S.S., Patel, Y., Siddiqua, A., Hassock, S., Edmunds, S., Maddison, B., Patel, G., Goulding, D., Lupu, F., Wojcikiewicz, R.J., Authi, K.S., 2000. Distinct localization and function of (1,4,5)IP(3) receptor subtypes and the (1,3,4,5)IP(4) receptor GAP1(IP4BP) in highly purified human platelet membranes. *Blood* 95, 3412–22.
- Elbatarny, H.S., Maurice, D.H., 2005. Leptin-mediated activation of human platelets: involvement of a leptin receptor and phosphodiesterase 3A-containing cellular signaling complex. *Am. J. Physiol. Endocrinol. Metab.* 289, E695–702.
- Escolar, G., Krumwiede, M., White, J.G., 1986. Organization of the actin cytoskeleton of resting and activated platelets in suspension. *Am. J. Pathol.* 123, 86–94.
- Escolar, G., White, J.G., 1991. The platelet open canalicular system: a final common pathway. *Blood Cells* 17, 467–85; discussion 486–95.
- Feijge, M.A.H., Ansink, K., Vanschoonbeek, K., Heemskerk, J.W.M., 2004. Control of platelet activation by cyclic AMP turnover and cyclic nucleotide phosphodiesterase type-3. *Biochem. Pharmacol.* 67, 1559–1567.
- Fink, T.L., Francis, S.H., Beasley, A., Grimes, K.A., Corbin, J.D., 1999. Expression of an Active, Monomeric Catalytic Domain of the cGMP-binding cGMP-specific Phosphodiesterase (PDE5). *J. Biol. Chem.* 274, 34613–34620.

- FitzGerald, G. a., Pedersen, a. K., Patrono, C., 1983. Analysis of prostacyclin and thromboxane biosynthesis in cardiovascular disease. *Circulation* 67, 1174–1177.
- Flaumenhaft, R., 2003. Molecular Basis of Platelet Granule Secretion. *Arterioscler. Thromb. Vasc. Biol.* 23, 1152–1160.
- Fox, J.E., Berndt, M.C., 1989. Cyclic AMP-dependent phosphorylation of glycoprotein Ib inhibits collagen-induced polymerization of actin in platelets. *J. Biol. Chem.* 264, 9520–6.
- Francis, S.H., Busch, J.L., Corbin, J.D., 2010. cGMP-Dependent Protein Kinases and cGMP Phosphodiesterases in Nitric Oxide and cGMP Action. *Pharmacol. Rev.* 62, 525–563.
- Francis, S.H., Corbin, J.D., 1999. Cyclic nucleotide-dependent protein kinases: intracellular receptors for cAMP and cGMP action. *Crit. Rev. Clin. Lab. Sci.* 36, 275–328.
- Friebe, A., Koesling, D., 2003. Regulation of Nitric Oxide-Sensitive Guanylyl Cyclase. *Circ. Res.* 93, 96–105.
- Galler, A.B., García Arguinzonis, M.I., Baumgartner, W., Kuhn, M., Smolenski, A., Simm, A., Reinhard, M., 2006. VASP-dependent regulation of actin cytoskeleton rigidity, cell adhesion, and detachment. *Histochem. Cell Biol.* 125, 457–74.
- Gambaryan, S., Friebe, A., Walter, U., 2012. Does the NO/sGC/cGMP/PKG pathway play a stimulatory role in platelets? *Blood* 119, 5335–6; author reply 5336–7.
- Geiger, J., Nolte, C., Walter, U., 1994. Regulation of calcium mobilization and entry in human platelets by endothelium-derived factors. *Am. J. Physiol.* 267, C236–44.
- Gibbins, J.M., 2004. Platelet adhesion signalling and the regulation of thrombus formation. *J. Cell Sci.* 117, 3415–25.

- Gkaliagkousi, E., Ritter, J., Ferro, A., 2007. Platelet-Derived Nitric Oxide Signaling and Regulation. *Circ. Res.* 101, 654–662.
- Gorman, R.R., Bunting, S., Miller, O. V, 1977. Modulation of human platelet adenylate cyclase by prostacyclin (PGX). *Prostaglandins* 13, 377–88.
- Gps, O., Ruggeri, Z.M., 2002. Platelets in atherothrombosis. *Nat. Med.* 8, 1227–1234.
- Gralnick, H.R., Williams, S.B., McKeown, L.P., Krizek, D.M., Shafer, B.C., Rick, M.E., 1985. Platelet von Willebrand factor: comparison with plasma von Willebrand factor. *Thromb. Res.* 38, 623–33.
- Grant, P.G., Mannarino, a F., Colman, R.W., 1988. cAMP-mediated phosphorylation of the low-Km cAMP phosphodiesterase markedly stimulates its catalytic activity. *Proc. Natl. Acad. Sci. U. S. A.* 85, 9071–5.
- Gresele, P., Momi, S., Falcinelli, E., 2011. Anti-platelet therapy: Phosphodiesterase inhibitors. *Br. J. Clin. Pharmacol.* 72, 634–646.
- Gross, S.S., Jaffe, E.A., Levi, R., Kilbourn, R.G., 1991. Cytokine-activated endothelial cells express an isotype of nitric oxide synthase which is tetrahydrobiopterin-dependent, calmodulin-independent and inhibited by arginine analogs with a rank-order of potency characteristic of activated macrophages. *Biochem. Biophys. Res. Commun.* 178, 823–829.
- Gudmundsdóttir, I.J., McRobbie, S.J., Robinson, S.D., Newby, D.E., Megson, I.L., 2005. Sildenafil potentiates nitric oxide mediated inhibition of human platelet aggregation. *Biochem. Biophys. Res. Commun.* 337, 382–5.
- Gullberg, M., Fredriksson, S., Taussig, M., Jarvius, J., Gustafsdottir, S., Landegren, U., 2003. A sense of closeness: Protein detection by proximity ligation. *Curr. Opin. Biotechnol.* 14, 82–86.
- Halcox, J.P.J., Nour, K.R.A., Zalos, G., Mincemoyer, R., Waclawiw, M.A., Rivera, C.E., Willie, G., Ellahham, S., Quyyumi, A.A., 2002. The effect of sildenafil on human vascular function, platelet activation, and myocardial ischemia. *J. Am.*

Coll. Cardiol. 40, 1232–1240.

Hambleton, R., Krall, J., Tikishvili, E., Honeggar, M., Ahmad, F., Manganiello, V.C., Movsesian, M.A., 2005. Isoforms of cyclic nucleotide phosphodiesterase PDE3 and their contribution to cAMP hydrolytic activity in subcellular fractions of human myocardium. *J. Biol. Chem.* 280, 39168–74.

Harbeck, B., Hüttelmaier, S., Schlüter, K., Jockusch, B.M., Illenberger, S., 2000. Phosphorylation of the vasodilator-stimulated phosphoprotein regulates its interaction with actin. *J. Biol. Chem.* 275, 30817–30825.

Harker, L.A., Finch, C.A., 1969. Thrombokinetics in man. *J. Clin. Invest.* 48, 963–974.

Harper, M.T., Poole, a W., 2010. Diverse functions of protein kinase C isoforms in platelet activation and thrombus formation. *J. Thromb. Haemost.* 8, 454–62.

Harteneck, C., Koesling, D., Söling, A., Schultz, G., Böhme, E., 1990. Expression of soluble guanylyl cyclase: catalytic activity requires two enzyme subunits. *FEBS Lett.* 272, 221–223.

Hartwig, J., Italiano, J., 2003. The birth of the platelet. *J. Thromb. Haemost.* 1, 1580–1586.

Hartwig, J.H., 1992. Mechanisms of actin rearrangements mediating platelet activation. *J. Cell Biol.* 118, 1421–42.

Haslam, R.J., Dickinson, N.T., Jang, E.K., 1999. Cyclic nucleotides and phosphodiesterases in platelets. *Thromb. Haemost.* 82, 412–423.

Hassock, S.R., Zhu, M.X., Trost, C., Flockerzi, V., Authi, K.S., 2002. Expression and role of TRPC proteins in human platelets: evidence that TRPC6 forms the store-independent calcium entry channel. *Blood* 100, 2801–11.

Hechler, B., Léon, C., Vial, C., Vigne, P., Frelin, C., Cazenave, J.P., Gachet, C., 1998. The P2Y1 receptor is necessary for adenosine 5'-diphosphate-induced platelet aggregation. *Blood* 92, 152–9.

- Henn, V., Edemir, B., Stefan, E., Wiesner, B., Lorenz, D., Theilig, F., Schmitt, R., Vossebein, L., Tamma, G., Beyermann, M., Krause, E., Herberg, F.W., Valenti, G., Bachmann, S., Rosenthal, W., Klussmann, E., 2004. Identification of a novel A-kinase anchoring protein 18 isoform and evidence for its role in the vasopressin-induced aquaporin-2 shuttle in renal principal cells. *J. Biol. Chem.* 279, 26654–26665.
- Hettasch, J.M., Sellers, J.R., 1991. Caldesmon phosphorylation in intact human platelets by cAMP-dependent protein kinase and protein kinase C. *J. Biol. Chem.* 266, 11876–81.
- Hidaka, H., Asano, T., 1976. Human blood platelet 3' 5'-cyclic nucleotide phosphodiesterase. Isolation of low-Km and high-Km phosphodiesterase. *Biochim. Biophys. Acta* 429, 485–497.
- Hidaka, H., Hayashi, H., Kohri, H., Kimura, Y., Hosokawa, T., Igawa, T., Saitoh, Y., 1979. Selective inhibitor of platelet cyclic adenosine monophosphate phosphodiesterase, cilostamide, inhibits platelet aggregation. *J. Pharmacol. Exp. Ther.* 211, 26–30.
- Hollestelle, M.J., Loots, C.M., Squizzato, A., Renne, T., Bouma, B.J., De Groot, P.G., Lenting, P.J., Meijers, J.C.M., Gerdes, V.E.A., 2011. Decreased active von Willebrand factor level owing to shear stress in aortic stenosis patients. *J. Thromb. Haemost.* 9, 953–958.
- Horner, A., Goetz, F., Tampé, R., Klussmann, E., Pohl, P., 2012. Mechanism for targeting the A-kinase anchoring protein AKAP18δ to the membrane. *J. Biol. Chem.*
- Horstrup, K., Jablonka, B., Hönig-Liedl, P., Just, M., Kochsiek, K., Walter, U., 1994. Phosphorylation of focal adhesion vasodilator-stimulated phosphoprotein at Ser157 in intact human platelets correlates with fibrinogen receptor inhibition. *Eur. J. Biochem.* 225, 21–7.
- Houslay, M.D., 2010. Underpinning compartmentalised cAMP signalling through targeted cAMP breakdown. *Trends Biochem. Sci.* 35, 91–100.

- Hoylaerts, M.F., Yamamoto, H., Nuyts, K., Vreys, I., Deckmyn, H., Vermylen, J., 1997. von Willebrand factor binds to native collagen VI primarily via its A1 domain. *Biochem. J.* 324, 185–191.
- Hunter, R.W., Mackintosh, C., Hers, I., 2009. Protein kinase C-mediated phosphorylation and activation of PDE3A regulate cAMP levels in human platelets. *J. Biol. Chem.* 284, 12339–48.
- Jackson, S.P., 2007. The growing complexity of platelet aggregation. *Blood* 109, 5087–5095.
- Jarnaess, E., Taskén, K., 2007. Spatiotemporal control of cAMP signalling processes by anchored signalling complexes. *Biochem. Soc. Trans.* 35, 931–937.
- Jensen, B.O., Selheim, F., Døskeland, S.O., Gear, a. R.L., Holmsen, H., 2004. Protein kinase A mediates inhibition of the thrombin-induced platelet shape change by nitric oxide. *Blood* 104, 2775–2782.
- Jin, J., Daniel, J.L., Kunapuli, S.P., 1998. Molecular basis for ADP-induced platelet activation. II. The P2Y1 receptor mediates ADP-induced intracellular calcium mobilization and shape change in platelets. *J. Biol. Chem.* 273, 2030–4.
- Johnson, K.R., Nicodemus-Johnson, J., Carnegie, G.K., Danziger, R.S., 2012. Molecular evolution of A-kinase anchoring protein (AKAP)-7: implications in comparative PKA compartmentalization. *BMC Evol. Biol.* 12, 125.
- Jung, S.M., Moroi, M., 2000. Signal-transducing mechanisms involved in activation of the platelet collagen receptor integrin alpha 2 beta 1. *J. Biol. Chem.* 275, 8016–8026.
- Kahn, M.L., Nakanishi-Matsui, M., Shapiro, M.J., Ishihara, H., Coughlin, S.R., 1999. Protease-activated receptors 1 and 4 mediate activation of human platelets by thrombin. *J. Clin. Invest.* 103, 879–87.
- Kase, H., Iwahashi, K., Nakanishi, S., Matsuda, Y., Yamada, K., Takahashi, M., Murakata, C., Sato, A., Kaneko, M., 1987. K-252 compounds, novel and

potent inhibitors of protein kinase C and cyclic nucleotide-dependent protein kinases. *Biochem. Biophys. Res. Commun.* 142, 436–40.

Kasuya, J., Goko, H., Fujita-Yamaguchi, Y., 1995. Multiple transcripts for the human cardiac form of the cGMP-inhibited cAMP phosphodiesterase. *J. Biol. Chem.* 270, 14305–12.

Kaushansky, K., 2006. Lineage-Specific Hematopoietic Growth Factors. *J. Med.* 2034–2045.

Kehrel, B., Wierwille, S., Clemetson, K.J., Anders, O., Steiner, M., Knight, C.G., Farndale, R.W., Okuma, M., Barnes, M.J., 1998. Glycoprotein VI is a major collagen receptor for platelet activation: it recognizes the platelet-activating quaternary structure of collagen, whereas CD36, glycoprotein IIb/IIIa, and von Willebrand factor do not. *Blood* 91, 491–499.

Kim, C., Lau, T.-L., Ulmer, T.S., Ginsberg, M.H., 2009. Interactions of platelet integrin  $\alpha$ IIb and  $\beta$ 3 transmembrane domains in mammalian cell membranes and their role in integrin activation. *Blood* 113, 4747–53.

Kisucka, J., Butterfield, C.E., Duda, D.G., Eichenberger, S.C., Saffaripour, S., Ware, J., Ruggeri, Z.M., Jain, R.K., Folkman, J., Wagner, D.D., 2006. Platelets and platelet adhesion support angiogenesis while preventing excessive hemorrhage. *Proc. Natl. Acad. Sci. U. S. A.* 103, 855–60.

Kopperud, R., Christensen, A.E., Kjirland, E., Viste, K., Kleivdal, H., Diskeland, S.O., 2002. Formation of inactive cAMP-saturated holoenzyme of cAMP-dependent protein kinase under physiological conditions. *J. Biol. Chem.* 277, 13443–13448.

Kulkarni, S., Dopheide, S.M., Yap, C.L., Ravanat, C., Freund, M., Mangin, P., Heel, K.A., Street, A., Harper, I.S., Lanza, F., Jackson, S.P., 2000. A revised model of platelet aggregation. *J. Clin. Invest.* 105, 783–791.

Lacabartz-porret, C., Launay, S., Corvazier, E., Bredoux, R., Papp, B., Enouf, J., 2000. Biogenesis of endoplasmatic reticulum proteins involved in  $Ca^{2+}$

- signalling during megakaryocytic differentiation : an in vitro study. *Biochem J.* 734, 723–734.
- Laemmli, U.K., 1970. Cleavage of structural proteins during the assembly of the head of bacteriophage T4. *Nature* 227, 680–5.
- Lankhof, H., van Hoeij, M., Schiphorst, M.E., Bracke, M., Wu, Y.P., Ijsseldijk, M.J., Vink, T., de Groot, P.G., Sixma, J.J., 1996. A3 domain is essential for interaction of von Willebrand factor with collagen type III. *Thromb. Haemost.* 75, 950–8.
- Lefkimmiatis, K., Zaccolo, M., 2014. cAMP signaling in subcellular compartments. *Pharmacol. Ther.* 143, 295–304.
- Li, Z., Delaney, M.K., O'Brien, K.A., Du, X., 2010. Signaling during platelet adhesion and activation. *Arterioscler. Thromb. Vasc. Biol.* 30, 2341–9.
- Lin, C.-S., Chow, S., Lau, A., Tu, R., Lue, T.F., 2002. Human PDE5A gene encodes three PDE5 isoforms from two alternate promoters. *Int. J. Impot. Res.* 14, 15–24.
- Lugnier, C., 2006. Cyclic nucleotide phosphodiesterase (PDE) superfamily: a new target for the development of specific therapeutic agents. *Pharmacol. Ther.* 109, 366–98.
- Ma, Y.-Q., Qin, J., Plow, E.F., 2007. Platelet integrin alpha(IIb)beta(3): activation mechanisms. *J. Thromb. Haemost.* 5, 1345–1352.
- Maass, P.G., Aydin, A., Luft, F.C., Schächterle, C., Weise, A., Stricker, S., Lindschau, C., Vaegler, M., Qadri, F., Toka, H.R., Schulz, H., Krawitz, P.M., Parkhomchuk, D., Hecht, J., Hollfinger, I., Wefeld-Neuenfeld, Y., Bartels-Klein, E., Mühl, A., Kann, M., Schuster, H., Chitayat, D., Bialer, M.G., Wienker, T.F., Ott, J., Rittscher, K., Liehr, T., Jordan, J., Plessis, G., Tank, J., Mai, K., Naraghi, R., Hodge, R., Hopp, M., Hattenbach, L.O., Busjahn, A., Rauch, A., Vandeput, F., Gong, M., Rüschenhof, F., Hübner, N., Haller, H., Mundlos, S., Bilginturan, N., Movsesian, M. a, Klussmann, E., Toka, O.,

- Bähring, S., 2015. PDE3A mutations cause autosomal dominant hypertension with brachydactyly. *Nat. Genet.* 47, 647–53.
- Macala, L.J., Hayslett, J.P., Smallwood, J.I., 1998. Measurement of cAMP-dependent protein kinase activity using a fluorescent-labeled Kemptide. *Kidney Int.* 54, 1746–1750.
- MacMillan-Crow, L.A., Lincoln, T.M., 1994. High-affinity binding and localization of the cyclic GMP-dependent protein kinase with the intermediate filament protein vimentin. *Biochemistry* 33, 8035–43.
- Macphee, C.H., Reifsnnyder, D.H., Moore, T.A., Lerea, K.M., Beavo, J.A., 1988. Phosphorylation results in activation of a cAMP phosphodiesterase in human platelets. *J Biol Chem* 263, 10353–10358.
- Manganello, J.M., Djellas, Y., Borg, C., Antonakis, K., Le Breton, G.C., 1999. Cyclic AMP-dependent phosphorylation of thromboxane A(2) receptor-associated Galpha(13). *J. Biol. Chem.* 274, 28003–10.
- Manns, J.M., Brenna, K.J., Colman, R.W., Sheth, S.B., 2002. Differential regulation of human platelet responses by cGMP inhibited and stimulated cAMP phosphodiesterases. *Thromb. Haemost.* 87, 873–9.
- Marcus, A.J., Broekman, M.J., Drosopoulos, J.H.F., Islam, N., Alyonycheva, T.N., Safier, L.B., Hajjar, K.A., Posnett, D.N., Schoenborn, M.A., Schooley, K.A., Gayle, R.B., Maliszewski, C.R., 1997. The endothelial cell ecto-ADPase responsible for inhibition of platelet function is CD39. *J. Clin. Invest.* 99, 1351–1360.
- Margarucci, L., Roest, M., Preisinger, C., Bleijerveld, O.B., van Holten, T.C., Heck, A.J.R., Scholten, A., Holten, T.C. Van, Heck, J.R., Scholten, A., 2011. Collagen stimulation of platelets induces a rapid spatial response of cAMP and cGMP signaling scaffolds. *Mol. Biosyst.* 7, 2311–9.
- Martinez, S.E., Wu, A.Y., Glavas, N. a, Tang, X.-B., Turley, S., Hol, W.G.J., Beavo, J. a, 2002. The two GAF domains in phosphodiesterase 2A have

- distinct roles in dimerization and in cGMP binding. *Proc. Natl. Acad. Sci. U. S. A.* 99, 13260–13265.
- Martins, T.J., Mumby, M.C., Beavo, J. a, 1982. Purification and characterization of a cyclic GMP-stimulated cyclic nucleotide phosphodiesterase from bovine tissues. *J. Biol. Chem.* 257, 1973–9.
- Massberg, S., Sausbier, M., Klatt, P., Bauer, M., Pfeifer, A., Siess, W., Fässler, R., Ruth, P., Krombach, F., Hofmann, F., 1999. Increased adhesion and aggregation of platelets lacking cyclic guanosine 3',5'-monophosphate kinase I. *J. Exp. Med.* 189, 1255–64.
- Maurice, D.H., Haslam, R.J., 1990. Molecular basis of the synergistic inhibition of platelet function by nitrovasodilators and activators of adenylate cyclase: inhibition of cyclic AMP breakdown by cyclic GMP. *Mol. Pharmacol.* 37, 671–81.
- Maurice, D.H., Ke, H., Ahmad, F., Wang, Y., Chung, J., Manganiello, V.C., 2014. Advances in targeting cyclic nucleotide phosphodiesterases. *Nat. Rev. Drug Discov.* 13, 290–314.
- McNicol, A., Israels, S.J., 1999. Platelet dense granules: Structure, function and implications for haemostasis. *Thromb. Res.* 95, 1–18.
- Michel, J.J.C., Scott, J.D., 2002. Akap mediated signal transduction. *Annu. Rev. Pharmacol. Toxicol.* 42, 235–257.
- Moroi, M., Jung, S.M., 2004. Platelet glycoprotein VI: Its structure and function. *Thromb. Res.* 114, 221–233.
- Moroi, M., Jung, S.M., Shinmyozu, K., Tomiyama, Y., Ordinas, a, Diaz-Ricart, M., 1996. Analysis of platelet adhesion to a collagen-coated surface under flow conditions: the involvement of glycoprotein VI in the platelet adhesion. *Blood* 88, 2081–2092.
- Mullershausen, F., Friebe, A., Feil, R., Thompson, W.J., Hofmann, F., Koesling, D., 2003. Direct activation of PDE5 by cGMP: Long-term effects within

- NO/cGMP signaling. *J. Cell Biol.* 160, 719–727.
- Mullershausen, F., Russwurm, M., Koesling, D., Friebe, A., 2004. In Vivo Reconstitution of the Negative Feedback in Nitric Oxide/cGMP Signaling: Role of Phosphodiesterase Type 5 Phosphorylation. *Mol. Biol. Cell* 15, 4023–4030.
- Murray, A.J., 2008. Pharmacological PKA inhibition: all may not be what it seems. *Sci. Signal.* 1, re4.
- Mustard, J.F., Kinlough-Rathbone, R.L., Packham, M.A., 1989. Isolation of human platelets from plasma by centrifugation and washing. *Methods Enzymol.* 169, 3–11.
- Naseem, K.M., Riba, R., 2008. Unresolved roles of platelet nitric oxide synthase. *J. Thromb. Haemost.* 6, 10–19.
- Nesbitt, W.S., Westein, E., Tovar-Lopez, F.J., Tolouei, E., Mitchell, A., Fu, J., Carberry, J., Fouras, A., Jackson, S.P., 2009. A shear gradient-dependent platelet aggregation mechanism drives thrombus formation. *Nat. Med.* 15, 665–673.
- Nieswandt, B., Brakebusch, C., Bergmeier, W., Schulte, V., Bouvard, D., Mokhtari-Nejad, R., Lindhout, T., Heemskerk, J.W.M., Zirngibl, H., Fässler, R., 2001. Glycoprotein VI but not  $\alpha 2\beta 1$  integrin is essential for platelet interaction with collagen. *EMBO J.* 20, 2120–2130.
- Nikolaev, V.O., Bünemann, M., Hein, L., Hannawacker, A., Lohse, M.J., 2004. Novel single chain cAMP sensors for receptor-induced signal propagation. *J. Biol. Chem.* 279, 37215–8.
- Nurden, P., Nurden, A.T., 2008. Congenital disorders associated with platelet dysfunctions. *Thromb. Haemost.* 99, 253–63.
- Offermanns, S., 2006. Activation of platelet function through G protein-coupled receptors. *Circ. Res.* 99, 1293–1304.

- Ogura, M., Morishima, Y., Ohno, R., Kato, Y., Hirabayashi, N., Nagura, H., Saito, H., 1985. Establishment of a novel human megakaryoblastic leukemia cell line, MEG-01, with positive Philadelphia chromosome. *Blood* 66, 1384–1392.
- Ogura, M., Morishima, Y., Okumura, M., Hotta, T., Takamoto, S., Ohno, R., Hirabayashi, N., Nagura, H., Saito, H., 1988. Functional Megakaryoblastic Differentiation Induction of a Human Megakaryoblastic Leukemia Cell Line (MEG-01s) by Phorbol Diesters. *Blood* 72, 49–60.
- Ohlmann, P., Laugwitz, K.L., Nürnberg, B., Spicher, K., Schultz, G., Cazenave, J.P., Gachet, C., 1995. The human platelet ADP receptor activates Gi2 proteins. *Biochem. J.* 312 ( Pt 3, 775–9.
- Omori, K., Kotera, J., 2007. Overview of PDEs and their regulation. *Circ. Res.* 100, 309–327.
- Oury, C., Toth-Zsamboki, E., Vermeylen, J., Hoylaerts, M.F., 2006. The platelet ATP and ADP receptors. *Curr. Pharm. Des.* 12, 859–875.
- Palmer, D., Jimmo, S.L., Raymond, D.R., Wilson, L.S., Carter, R.L., Maurice, D.H., 2007. Protein kinase A phosphorylation of human phosphodiesterase 3B promotes 14-3-3 protein binding and inhibits phosphatase-catalyzed inactivation. *J. Biol. Chem.* 282, 9411–9419.
- Palmer, R.M., Ashton, D.S., Moncada, S., 1988. Vascular endothelial cells synthesize nitric oxide from L-arginine. *Nature* 333, 664–6.
- Pandit, J., Forman, M.D., Fennell, K.F., Dillman, K.S., Menniti, F.S., 2009. Mechanism for the allosteric regulation of phosphodiesterase 2A deduced from the X-ray structure of a near full-length construct. *Proc. Natl. Acad. Sci. U. S. A.* 106, 18225–30.
- Pease, D.C., 1956. An electron microscopic study of red bone marrow. *Blood* 11, 501–26.
- Pidoux, G., Taskén, K., 2010. Specificity and spatial dynamics of protein kinase a signaling organized by A-kinase-anchoring proteins. *J. Mol. Endocrinol.* 44,

271–284.

- Pieroni, J.P., Harry, A., Chen, J., Jacobowitz, O., Magnusson, R.P., Iyengar, R., 1995. Distinct Characteristics of the Basal Activities of Adenylyl Cyclases 2 and 6. *J. Biol. Chem.* 270, 21368–21373.
- Pozuelo Rubio, M., Campbell, D.G., Morrice, N. a, Mackintosh, C., 2005. Phosphodiesterase 3A binds to 14-3-3 proteins in response to PMA-induced phosphorylation of Ser428. *Biochem. J.* 392, 163–72.
- Puxeddu, E., Uhart, M., Li, C.-C., Ahmad, F., Pacheco-Rodriguez, G., Manganiello, V.C., Moss, J., Vaughan, M., 2009. Interaction of phosphodiesterase 3A with brefeldin A-inhibited guanine nucleotide-exchange proteins BIG1 and BIG2 and effect on ARF1 activity. *Proc. Natl. Acad. Sci. U. S. A.* 106, 6158–63.
- Radomski, M. W., Palmer, R.M. M., Moncada, S., 1987. Endogenous nitric oxide inhibits human platelet adhesion to vascular endothelium. *Lancet* 330, 1057–1058.
- Radomski, M.W., Palmer, R.M., Moncada, S., 1987a. The anti-aggregating properties of vascular endothelium: interactions between prostacyclin and nitric oxide. *Br. J. Pharmacol.* 92, 639–46.
- Radomski, M.W., Palmer, R.M., Moncada, S., 1987b. Comparative pharmacology of endothelium-derived relaxing factor, nitric oxide and prostacyclin in platelets. *Br. J. Pharmacol.* 92, 181–7.
- Radomski, M.W., Palmer, R.M., Read, N.G., Moncada, S., 1988. Isolation and washing of human platelets with nitric oxide. *Thromb. Res.* 50, 537–46.
- Raslan, Z., Aburima, A., Naseem, K.M., 2015a. The Spatiotemporal Regulation of cAMP Signaling in Blood Platelets—Old Friends and New Players. *Front. Pharmacol.* 6, 1–8.
- Raslan, Z., Magwenzi, S., Aburima, A., Taskén, K., Naseem, K.M., 2015b. Targeting of type I protein kinase A to lipid rafts is required for platelet

- inhibition by the 3',5'-cyclic adenosine monophosphate-signaling pathway. *J. Thromb. Haemost.* 13, 1721–34.
- Raslan, Z., Naseem, K.M., 2014. The control of blood platelets by cAMP signalling. *Biochem. Soc. Trans.* 42, 289–94.
- Reid, H.M., Kinsella, B.T., 2003. The alpha, but not the beta, Isoform of the Human Thromboxane A<sub>2</sub> Receptor Is a Target for Nitric Oxide-mediated Desensitization. *J. Biol. Chem.* 278, 51190–51202.
- Resjö, S., Oknianska, a, Zolnierowicz, S., Manganiello, V., Degerman, E., 1999. Phosphorylation and activation of phosphodiesterase type 3B (PDE3B) in adipocytes in response to serine/threonine phosphatase inhibitors: deactivation of PDE3B in vitro by protein phosphatase type 2A. *Biochem. J.* 341 ( Pt 3, 839–845.
- Roberts, W., Magwenzi, S., Aburima, A., Naseem, K.M., 2010. Thrombospondin-1 induces platelet activation through CD36-dependent inhibition of the cAMP/protein kinase A signaling cascade. *Blood* 116, 4297–4306.
- Rolf, M.G., Brearley, C.A., Mahaut-Smith, M.P., 2001. Platelet shape change evoked by selective activation of P2X<sub>1</sub> purinoceptors with alpha,beta-methylene ATP. *Thromb. Haemost.* 85, 303–8.
- Rosman, G.J., Martins, T.J., Sonnenburg, W.K., Beavo, J. a, Ferguson, K., Loughney, K., 1997. Isolation and characterization of human cDNAs encoding a cGMP-stimulated 3',5'-cyclic nucleotide phosphodiesterase. *Gene* 191, 89–95.
- Rowley, J.W., Oler, A.J., Tolley, N.D., Hunter, B.N., Low, E.N., Nix, D. a., Yost, C.C., Zimmerman, G. a., Weyrich, A.S., 2011. Genome-wide RNA-seq analysis of human and mouse platelet transcriptomes. *Blood* 118, 101–112.
- Ruggeri, Z.M., 2003. Von Willebrand factor, platelets and endothelial cell interactions. *J. Thromb. Haemost.* 1, 1335–42.
- Ruggeri, Z.M., 2007. The role of von Willebrand factor in thrombus formation.

- Thromb. Res. 120 Suppl , S5–9.
- Ruggeri, Z.M., Mendolicchio, G.L., 2007. Adhesion mechanisms in platelet function. *Circ. Res.* 100, 1673–1685.
- Ruggeri, Z.M., Orje, J.N., Habermann, R., Federici, A.B., Reininger, A.J., 2006. Activation-independent platelet adhesion and aggregation under elevated shear stress. *Blood* 108, 1903–10.
- Rukoyatkina, N., Walter, U., Friebe, A., Gambaryan, S., 2011. Differentiation of cGMP-dependent and -independent nitric oxide effects on platelet apoptosis and reactive oxygen species production using platelets lacking soluble guanylyl cyclase. *Thromb. Haemost.* 106, 922–33.
- Sachs, U.J.H., Nieswandt, B., 2007. In vivo thrombus formation in murine models. *Circ. Res.* 100, 979–91.
- Samuelsson, B., Goldyne, M., Granstrom, E., Hamberg, M., Hammarstrom, S., Malmsten, C., 1978. Prostaglandins and Thromboxanes. *Annu. Rev. Biochem.* 47, 997–1029.
- Savage, B., Almus-Jacobs, F., Ruggeri, Z.M., 1998. Specific synergy of multiple substrate-receptor interactions in platelet thrombus formation under flow. *Cell* 94, 657–66.
- Savage, B., Ruggeri, Z.M., 1991. Selective recognition of adhesive sites in surface-bound fibrinogen by glycoprotein IIb-IIIa on nonactivated platelets. *J. Biol. Chem.* 266, 11227–33.
- Schmidt, H.H., Lohmann, S.M., Walter, U., 1993. The nitric oxide and cGMP signal transduction system: regulation and mechanism of action. *Biochim. Biophys. Acta* 1178, 153–75.
- Schultess, J., Danielewski, O., Smolenski, A.P., 2005. Rap1GAP2 is a new GTPase-activating protein of Rap1 expressed in human platelets. *Blood* 105, 3185–3192.

- Schwarz, U.R., Walter, U., Eigenthaler, M., 2001. Taming platelets with cyclic nucleotides. *Biochem. Pharmacol.* 62, 1153–1161.
- Seamon, K.B., Padgett, W., Daly, J.W., 1981. Forskolin: unique diterpene activator of adenylate cyclase in membranes and in intact cells. *Proc. Natl. Acad. Sci. U. S. A.* 78, 3363–3367.
- Sessa, W.C., 2004. eNOS at a glance. *J. Cell Sci.* 117, 2427–2429.
- Shattil, S.J., Newman, P.J., 2004. Integrins: dynamic scaffolds for adhesion and signaling in platelets. *Blood* 104, 1606–15.
- Siegl, A.M., Smith, J.B., Silver, M.J., Nicolaou, K.C., Ahern, D., 1979. Selective binding site for [3H]prostacyclin on platelets. *J. Clin. Invest.* 63, 215–20.
- Siess, W., Winegar, D.A., Lapetina, E.G., 1990. Rap1-B is phosphorylated by protein kinase A in intact human platelets. *Biochem. Biophys. Res. Commun.* 170, 944–50.
- Silverman, M.A., Shoag, J., Wu, J., Koretzky, G.A., 2006. Disruption of SLP-76 interaction with Gads inhibits dynamic clustering of SLP-76 and FcepsilonRI signaling in mast cells. *Mol Cell Biol* 26, 1826–1838.
- Sim, D.S., Merrill-skoloff, G., Furie, B.B.C., Furie, B.B.C., Flaumenhaft, R., 2016. Initial accumulation of platelets during arterial thrombus formation in vivo is inhibited by elevation of basal cAMP levels. *Blood* 103, 2127–2135.
- Skalhegg, B.S., Tasken, K., 2000. Specificity in the cAMP/PKA signaling pathway. Differential expression, regulation, and subcellular localization of subunits of PKA. *Front. Biosci.* 5, D678–93.
- Smolenski, a., 2012. Novel roles of cAMP/cGMP-dependent signaling in platelets. *J. Thromb. Haemost.* 10, 167–176.
- Sopory, S., Balaji, S., Srinivasan, N., Visweswariah, S.S., 2003. Modeling and mutational analysis of the GAF domain of the cGMP-binding, cGMP-specific phosphodiesterase, PDE5. *FEBS Lett.* 539, 161–6.

- Strober, W., 2001. Trypan blue exclusion test of cell viability. *Curr. Protoc. Immunol.* Appendix 3, Appendix 3B.
- Subramanian, H., Zahedi, R.P., Sickmann, a., Walter, U., Gambaryan, S., 2013. Phosphorylation of CalDAG-GEFI by protein kinase A prevents Rap1b activation. *J. Thromb. Haemost.* 11, 1574–1582.
- Sun, B., Li, H., Shakur, Y., Hensley, J., Hockman, S., Kambayashi, J., Manganiello, V.C., Liu, Y., 2007. Role of phosphodiesterase type 3A and 3B in regulating platelet and cardiac function using subtype-selective knockout mice. *Cell. Signal.* 19, 1765–71.
- Tang, W.J., Hurley, J.H., 1998. Catalytic mechanism and regulation of mammalian adenylyl cyclases. *Mol. Pharmacol.* 54, 231–40.
- Taskén, K., Aandahl, E.M., 2004. Localized effects of cAMP mediated by distinct routes of protein kinase A. *Physiol. Rev.* 84, 137–167.
- Tateson, J.E., Moncada, S., Vane, J.R., 1977. Effects of prostacyclin (PGX) on cyclic AMP concentrations in human platelets. *Prostaglandins* 13, 389–97.
- Thomas, D.W., Mannon, R.B., Mannon, P.J., Latour, A., Oliver, J.A., Hoffman, M., Smithies, O., Koller, B.H., Coffman, T.M., 1998. Coagulation defects and altered hemodynamic responses in mice lacking receptors for thromboxane A<sub>2</sub>. *J. Clin. Invest.* 102, 1994–2001.
- Thompson, W.J., Appleman, M.M., 1971. Multiple cyclic nucleotide phosphodiesterase activities from rat brain. *Biochemistry* 10, 311–6.
- Thon, J.N., Italiano, J.E., 2012. Platelets: production, morphology and ultrastructure. *Handb. Exp. Pharmacol.* 3–22.
- Toka, O., Tank, J., Schächterle, C., Aydin, A., Maass, P.G., Elitok, S., Bartels-Klein, E., Hollfänger, I., Lindschau, C., Mai, K., Boschmann, M., Rahn, G., Movsesian, M.A., Müller, T., Doescher, A., Gnoth, S., Mühl, A., Toka, H.R., Wefeld-Neuenfeld, Y., Utz, W., Töpfer, A., Jordan, J., Schulz-Menger, J., Klussmann, E., Bähring, S., Luft, F.C., 2015. Clinical Effects of

- Phosphodiesterase 3A Mutations in Inherited Hypertension With Brachydactyly Novelty and Significance. *Hypertension* 66, 800–808.
- Trepakova, E.S., Cohen, R.A., Bolotina, V.M., 1999. Nitric oxide inhibits capacitative cation influx in human platelets by promoting sarcoplasmic/endoplasmic reticulum Ca<sup>2+</sup>-ATPase-dependent refilling of Ca<sup>2+</sup> stores. *Circ. Res.* 84, 201–9.
- Tröger, J., Moutty, M.C., Skroblin, P., Klussmann, E., 2012. A-kinase anchoring proteins as potential drug targets. *Br. J. Pharmacol.* 166, 420–33.
- Trotter, K.W., Fraser, I.D.C., Scott, G.K., Stutts, M.J., Scott, J.D., Milgram, S.L., 1999. Alternative splicing regulates the subcellular localization of A-kinase anchoring protein 18 isoforms. *J. Cell Biol.* 147, 1481–1492.
- Ubersax, J.A., Ferrell Jr, J.E., 2007. Mechanisms of specificity in protein phosphorylation. *Nat. Rev. Mol. Cell Biol.* 8, 530–541.
- Ulrichs, H., Udvardy, M., Lenting, P.J., Pareyn, I., Vandeputte, N., Vanhoorelbeke, K., Deckmyn, H., 2006. Shielding of the A1 domain by the D'D3 domains of von Willebrand factor modulates its interaction with platelet glycoprotein Ib-IX-V. *J. Biol. Chem.* 281, 4699–707.
- Van Nispen Tot Pannerden, H., De Haas, F., Geerts, W., Posthuma, G., Van Dijk, S., Heijnen, H.F.G., 2010. The platelet interior revisited: Electron tomography reveals tubular  $\alpha$ -granule subtypes. *Blood* 116, 1147–1156.
- Vandeput, F., Szabo-Fresnais, N., Ahmad, F., Kho, C., Lee, A., Krall, J., Dunlop, A., Hazel, M.W., Wohlschlegel, J. a, Hajjar, R.J., Houslay, M.D., Manganiello, V.C., Movsesian, M. a, 2013. Selective regulation of cyclic nucleotide phosphodiesterase PDE3A isoforms. *Proc. Natl. Acad. Sci. U. S. A.* 110, 19778–83.
- Varga-Szabo, D., Braun, a., Nieswandt, B., 2009. Calcium signaling in platelets. *J. Thromb. Haemost.* 7, 1057–1066.
- Varga-Szabo, D., Pleines, I., Nieswandt, B., 2008. Cell adhesion mechanisms in

- platelets. *Arterioscler. Thromb. Vasc. Biol.* 28, 403–413.
- Vargas, J.R., Radomski, M., Moncada, S., 1982. The use of prostacyclin in the separation from plasma and washing of human platelets. *Prostaglandins* 23, 929–45.
- Versteeg, H.H., Heemskerk, J.W.M., Levi, M., Reitsma, P.H., 2013. New Fundamentals in Hemostasis. *Physiol. Rev.* 93, 327–358.
- Vijayaraghavan, S., Goueli, S.A., Davey, M.P., Carr, D.W., 1997. Protein kinase A-anchoring inhibitor peptides arrest mammalian sperm motility. *J. Biol. Chem.* 272, 4747–52.
- Vo, N.K., Gettemy, J.M., Coghlan, V.M., 1998. Identification of cGMP-dependent protein kinase anchoring proteins (GKAPs). *Biochem. Biophys. Res. Commun.* 246, 831–5.
- Von Hundelshausen, P., Weber, C., 2007. Platelets as immune cells: Bridging inflammation and cardiovascular disease. *Circ. Res.* 100, 27–40.
- Vu, T.-K.H., Hung, D.T., Wheaton, V.I., Coughlin, S.R., 1991. Molecular cloning of a functional thrombin receptor reveals a novel proteolytic mechanism of receptor activation. *Cell* 64, 1057–1068.
- Walsh, M.T., Foley, J.F., Kinsella, B.T., 2000. The alpha, but not the beta, isoform of the human thromboxane A2 receptor is a target for prostacyclin-mediated desensitization. *J. Biol. Chem.* 275, 20412–23.
- Wang, L., Sunahara, R.K., Krumin, A., Perkins, G., Crochiere, M.L., Mackey, M., Bell, S., Ellisman, M.H., Taylor, S.S., 2001. Cloning and mitochondrial localization of full-length D-AKAP2, a protein kinase A anchoring protein. *Proc. Natl. Acad. Sci. U. S. A.* 98, 3220–5.
- Wang, Y., Chen, Y., Chen, M., Xu, W., 2006. AKAPs competing peptide HT31 disrupts the inhibitory effect of PKA on RhoA activity. *Oncol. Rep.* 16, 755–761.

- Watson, S.P., Auger, J.M., McCarty, O.J.T., Pearce, a C., 2005. GPVI and integrin alphaIIb beta3 signaling in platelets. *J. Thromb. Haemost.* 3, 1752–1762.
- Wechsler, J., 2002. Isoforms of Cyclic Nucleotide Phosphodiesterase PDE3A in Cardiac Myocytes. *J. Biol. Chem.* 277, 38072–38078.
- Weiss, H.J., Turitto, V.T., 1979. Prostacyclin (prostaglandin I<sub>2</sub>, PGI<sub>2</sub>) inhibits platelet adhesion and thrombus formation on subendothelium. *Blood* 53, 244–50.
- Weksler, B.B., Marcus, A.J., Jaffe, E.A., 1977. Synthesis of prostaglandin I<sub>2</sub> (prostacyclin) by cultured human and bovine endothelial cells. *Proc. Natl. Acad. Sci. U. S. A.* 74, 3922–6.
- White, C.D., Toker, A., 2013. Using phospho-motif antibodies to determine kinase substrates. *Curr. Protoc. Mol. Biol.* Chapter 18, Unit 18.20.
- White, J., 2007. Platelet structure. In: *Platelets*. Elsevier, pp. 45–73.
- Wilson, L.S., Elbatarny, H.S., Crawley, S.W., Bennett, B.M., Maurice, D.H., 2008. Compartmentation and compartment-specific regulation of PDE5 by protein kinase G allows selective cGMP-mediated regulation of platelet functions. *Proc Natl Acad Sci U S A* 105, 13650–13655.
- Zaccolo, M., 2009. cAMP signal transduction in the heart: understanding spatial control for the development of novel therapeutic strategies. *Br. J. Pharmacol.* 158, 50–60.
- Zaccolo, M., Movsesian, M. a, 2007. cAMP and cGMP signaling cross-talk: role of phosphodiesterases and implications for cardiac pathophysiology. *Circ. Res.* 100, 1569–78.
- Zaccolo, M., Pozzan, T., 2002. Discrete microdomains with high concentration of cAMP in stimulated rat neonatal cardiac myocytes. *Science* 295, 1711–1715.
- Zhang, G., Xiang, B., Dong, A., Skoda, R.C., Daugherty, A., Smyth, S.S., Du, X.,

Li, Z., 2011. Biphasic roles for soluble guanylyl cyclase (sGC) in platelet activation. *Blood* 118, 3670–9.

Zhang, W., Colman, R.W., 2007. Thrombin regulates intracellular cyclic AMP concentration in human platelets through phosphorylation/activation of phosphodiesterase 3A. *Blood* 110, 1475–82.

Zoraghi, R., Bessay, E.P., Corbin, J.D., Francis, S.H., 2005. Structural and Functional Features in Human PDE5A1 Regulatory Domain That Provide for Allosteric cGMP Binding, Dimerization, and Regulation. *J. Biol. Chem.* 280, 12051–12063.